QUANTIFICATION OF MODELLING UNCERTAINTIES IN CLIMATE CHANGE IMPACT STUDIES ON WATER RESOURCES: APPLICATION TO A GLACIER-FED HYDROPOWER PRODUCTION SYSTEM IN THE SWISS ALPS

THÈSE N^{O} 3225 (2005)

PRÉSENTÉE À LA FACULTÉ ENVIRONNEMENT NATUREL, ARCHITECTURAL ET CONSTRUIT

Institut des sciences et technologies de l'environnement

SECTION DES SCIENCES ET INGÉNIERIE DE L'ENVIRONNEMNT

ÉCOLE POLYTECHNIQUE FÉDÉRALE DE LAUSANNE

POUR L'OBTENTION DU GRADE DE DOCTEUR ÈS SCIENCES

PAR

Bettina SCHÄFLI

ingénieure du génie rural diplômée EPF
de nationalité suisse et originaire de Homburg (TG)

acceptée sur proposition du jury:

Prof. A. Musy, directeur de thèse
Prof. A. Bárdossy, rapporteur
Dr D. Duband, rapporteur
Dr B. Hingray, rapporteur
Prof. M. Parlange, rapporteur

Lausanne, EPFL
2005

Abstract

This PhD thesis presents the development of a methodological framework to analyse potential climate change impacts on a high mountainous water resources system and to quantify the associated modelling uncertainties. The main objective is to show whether state-of-the-art hydrological modelling techniques driven by currently available climate change scenarios enable a prediction of the long-term evolution of the analysed system. The case study is a highly glacierized catchment feeding a hydropower plant located in the Swiss Alps. The climate change impact analysis is based on a classical simulation approach: The system behaviour is modelled for an observed control period (1961 to 1990) and for a future period (2070 to 2099) characterised by a modified (predicted) climate. The climate change impact on the studied system is assessed through the comparison of some key characteristics of the system for the two periods (e.g. the mean annual discharge or the hydropower production).

The system simulation is completed through a set of four models, a water management model, a hydrological discharge model, a glacier surface evolution model and a model for the production of local scale meteorological time series (precipitation and temperature) based on global and regional climate model outputs. The local scale models have been specifically developed for the purposes of this thesis. For each of them, an appropriate statistical method for the quantification of the inherent modelling uncertainties has been developed. A special emphasis is given to the modelling uncertainties induced by the conceptual hydrological model. A method has been developed to quantify the statistical and the multi-objective modelling uncertainty in a multi-model framework including several equivalent model structures. This method has been specially designed for the quantification of the prediction uncertainty in climate change impact studies but it is transposable to other hydrological modelling contexts.

The overall prediction uncertainty and the contribution of each source of modelling uncertainty is quantified through Monte Carlo simulations of the system behaviour combining successively the different sources of modelling uncertainty. It is shown that the uncertainties induced by the prediction of the climate evolution are much higher than the ones induced by the local scale models of the system behaviour. The uncertainty related to the use of different regional climate models is however nearly as important as the one due to the choice of the underlying global climate model and the green house gas emission scenario.

Using a fixed hydrological model structure, the predicted climate evolution induces a significant reduction of the hydropower production performance due to a considerable hydrological regime modification. The available data, the current discharge modelling techniques and the knowledge about the underlying processes are however not sufficient to chose an objectively best model structure. Considering the multi-model approach (including different hydrological model structures), an unambiguous prediction of the hydrological reaction to the analysed climate change reveals impossible at the given temporal horizon.

Résumé

Cette thèse de doctorat présente le développement d'un cadre méthodologique pour l'analyse des impacts potentiels d'un changement climatique sur un système de ressources en eau de haute montagne et pour la quantification des incertitudes associées. L'objectif principal est de déterminer si les méthodes actuelles de modélisation hydrologique et les scénarios de changement climatique disponibles permettent de prédire l'évolution à long terme du système analysé. Le cas d'étude est un bassin versant des Alpes suisses à forte couverture glaciaire, exploité pour la production hydroélectrique. L'analyse du changement climatique y est effectuée selon une approche de simulation classique : le comportement du système est modélisé pour une période de contrôle observée (1961 à 1990) et pour une période future (2070 à 2099) caractérisée par une modification (projetée) du climat. L'impact résultant du changement climatique est quantifié à travers d'un ensemble de caractéristiques clé du système (p. ex. la production hydroélectrique annuelle) simulés pour les deux périodes.

La simulation s'effectue à l'aide de quatre modèles, un modèle de gestion de l'eau, un modèle hydrologique, un modèle d'évolution de la surface glaciaire et un modèle de génération de séries temporelles locales de précipitations et de température à partir de résultats de modèles climatiques globaux et régionaux. Les modèles à l'échelle locale ont été développés spécifiquement pour ce travail de recherche. Ils sont accompagnés chacun d'une méthode statistique de quantification des incertitudes de modélisation inhérentes. Les incertitudes liées au modèle hydrologique conceptuel sont étudiées plus en détail. Une méthode a été développée pour quantifier l'incertitude statistique et multi-objective dans une approche multi-modèles analysant simultanément différentes structures équivalentes du modèle. Développée spécifiquement pour une application aux études de changements climatiques, cette méthode peut être transposée à d'autres problèmes de modélisation hydrologique.

L'incertitude liée à chaque modèle et l'incertitude totale sont quantifiées par des simulations Monte Carlo du comportement du système en combinant successivement les différentes sources d'incertitudes. Cette évaluation permet de montrer que l'incertitude issue de la prévision de l'évolution climatique est considérablement plus importante que celle liée aux modèles décrivant la réaction du système étudié. La modélisation de la réponse du climat régional à un changement climatique global introduit par contre autant d'incertitude dans la réponse du régime hydrologique que ce seul changement climatique global.

Simulant le comportement du système avec un modèle hydrologique prédéfini, les scénarios climatiques étudiés montrent une évolution vers une réduction importante de la performance de la production hydroélectrique. Les données disponibles, les techniques de modélisation actuelles et la connaissance des processus hydrologiques ne permettent cependant pas de déterminer objectivement la meilleure structure de modèle. Dans le cadre d'une approche multi-modèles (incluant différentes structures de modèle hydrologique), on peut montrer qu'il n'est pas possible d'effectuer une prévision univoque de la réaction du système hydrologique à un changement climatique pour l'horizon temporel retenu.

Acknowledgements

My first thanks go to Prof. André Musy who proposed me to join his research group and followed my work on the PhD-thesis. I very much appreciated the liberty he gave me to develop my ideas and the excellent and motivating working conditions he offered in his laboratory. A special thank goes to Dr. Benoît Hingray from whom I learnt a lot and who followed closely my research. I greatly appreciated our scientific discussions and his remarks on all my manuscripts he reviewed. The work on my PhD-thesis also greatly benefited from the numerous internationally renowned researchers who stayed in our lab for short periods, especially Prof. Roman Krzysztofowicz, Prof. Peter Rasmussen and Dr. Eric Parent whom I thank for their precious contribution to my developments.

The work on the case study would not have been possible without the help of Kurt Seiler from the Forces Motrices de Mauvoisin whom I would like to thank for his availability and his explanations about hydropower management.

The major part of this thesis has been funded through the European project SWURVE (Sustainable Water, Uncertainty, Risk and Vulnerability in Europe), funded under the EU Environment and Sustainable Development programme. The Swiss part of this project was funded by the Federal Office for Education and Science. Thanks for funding are also due to the Swiss National Science Foundation for the promotion of scientific research who funded my 6 months research stay at the Hydraulic Institute of the University of Stuttgart in the group of Prof. András Bárdossy. This research stay has given me a lot of new inputs during the last part of my research. I would like to thank Prof. András Bárdossy for having welcomed me in his group and for his invaluable comments and ideas.

I would also like to thank the other members of the jury, Prof. Marc Parlange and Dr. Daniel Duband, who have accepted to evaluate this work and made a lot of interesting remarks.

The people working at the Laboratory of Hydrology and Land Improvement (Hydram) deserve a lot of thanks, especially Dr. Séverine Vuilleumier who shared my office during three years and who gave me a lot of essential hints about the scientific world and about how to manage to do a PhD-thesis. Thanks also to Dr. Daniela Balin Talamba who helped me with the development of some of the statistical methods and Dr. Markus Niggli who passed on to me his experience in the area of conceptual hydrological modelling. I also wish to thank Dr. Cécile Picouet who always had an ear for any kind of questions and problems and Colin Schenk for having made the work at Hydram much funnier and having always been available to help in any computer related problems. And of course, I will never forget the evenings and weekends I spent together with Séverine, Cécile, Benoît, Alain, Frédéric, Flavio and Richard. Grâce à vous, c'était un vrai plaisir de travailler à l'Hydram!

I would also like to thank Pascal Horton who has joined our research group recently and who continued my work on other case studies. He has managed to read all my programs (incredible!) and contributed to improve them.

The last and perhaps most difficult phase of completion of this PhD-thesis has greatly benefited from my colleagues of the Hydraulic Institute of the University of Stuttgart), with whom I worked during 6 months. Thanks to Jürgen Brommundt and Jens Götzinger who introduced me to the new research environment and to Jan, Ferdi, Christian and Arne for the inspiring working conditions.

I would also like to thank the people working at the Laboratory for Industrial Energy Systems (Laboratoire d'Energie Industrielle – LENI). This exchange with researchers working on quite different modelling problems has given me a lot of new ideas. Thanks to Dr. François Maréchal for having made available the source code of their optimisation algorithm and to Dr. Geoff Leyland for his help on the algorithm application and on multi-objective optimisation in general and for having been a good friend during his stay in Lausanne. Thanks also to Dr. Xavier Pelet with whom I have visited a lot of snow and glacier covered catchments in the Swiss Alps and to all the others who were always available when my own colleagues did not want to go for a beer at Satellite. Merci au passage à tous les gens qui contribuent à faire vivre ce lieu sans lequel le travail à l'EPFL serait beaucoup plus difficile!

Thanks also to the family Larrain for having been like a second family for me and to my friends for having accompanied me during all my years in Lausanne and made my studies and research much more enjoyable. I especially would like to thank Sara, Séverine, Yariv, Mathieu and Delphine and all my friends from the Lausanne Sports rowing club, especially Elena. Rowing on lake Geneva during sunrise is perhaps the best preparation you can get for a working day. Handling the nervosity before a scientific talk becomes trivial if you once have been on a regatta starting line!

An important thank goes to my parents who encouraged me in all my decisions and made my studies possible. Without their support and the convictions they passed on to me, I would perhaps never have made my way into a technical institute and a scientific doctoral degree. Dank Euch haben mir im Leben immer alle Möglichkeiten offengestanden! Danke für alles!

I finally would like to thank Diego, who always stood by my side, who shared not only the pleasing but also the difficult moments and without whom I would never have been able to get through all this. Merci beaucoup, Diego, d'avoir été là pour moi pendant tout ce temps !

Content

Chapter 1

Introduction

Abstract

The present PhD thesis is composed of several papers either published or submitted to publication. This introductory section, a detailed description of the principal case study and the overall conclusions, completes them. The present section introduces first the general research context. The fundamental scientific questions in the area of climate change research are briefly presented before discussing the implications for water resources management, in particular in high mountainous catchments, on which this thesis is focused. A short introduction to hydrological modelling uncertainty is given. This overview of the research context is followed by the scientific questions that motivated this PhD research and an introduction to the methodological framework developed to answer them. Finally, the content of the different papers composing this thesis is set out with a special emphasis on how they integrate into the methodological framework and how they contribute to answer the main underlying scientific questions.

1.1 Research context

1.1.1 Climate change: fundamental questions

Climate changes are induced by the internal variability within the climate system and external factors that are either natural or anthropogenic. Current climate change research still tries to answer the fundamental questions whether the currently observed global warming is a real trend or due to the internal variability and whether this global warming is induced by anthropogenic forcing.

The Third Assessment Report of the Intergovernmental Panel on Climate Change – the most up-to-date scientific assessment of past, present and potential future climates (IPCC, 2001) - resumes the current findings of the scientific community as follows: "There is new and stronger evidence that most of the warming observed over the last 50 years is attributable to human activities" (IPCC, 2001).

The global average Earth surface temperature has increased by about 0.6°C over the 20th century (Folland et al., 2001). This temperature increase is likely to have been the largest of any century during the past 1000 years and is unlikely to be either due to the internal variability alone or entirely natural in origin (Folland et al., 2001). The observed concentrations of atmospheric greenhouse gases have increased as a result of human activities. The concentration of carbon dioxide (CO_2) has increased by 31% since 1750 and the present CO_2 concentration has not been exceeded during the past 420'000 years (Prentice et al., 2001). This increase in greenhouse gas concentrations is likely to have induced most of the observed warming over the last 50 years (Mitchell et al., 2001).

Today, the scientific community agrees that human activities do interact with the climate. This immediately raises the questions whether we can model and predict these activities, their interaction with the climate and the resulting climate evolution. And what is the impact of a potential climate change on human activities and on life on Earth in general?

The modelling of the climate system requires complex physically based models and a large amount of input data to define initial and limiting conditions. Despite this highly complex task, "confidence in the ability of models to project future climate has increased" (IPCC, 2001). Regardless of this fundamental question whether actual scientific knowledge enables us to predict the climate evolution, we can affirm that any modification of the climate will indeed have an important impact on the natural and man-made environment. But are we able to predict this impact? Can we predict these climate change induced impacts on water resources systems and how uncertain are these predictions? These essential questions have motivated the research of the present PhD thesis.

1.1.2 Mountainous water resources and climate change

The climate system is closely interconnected with the water cycle. Any perturbation of the system will temporarily or permanently modify the hydrological cycle and have an impact on water resources and related water uses. Accordingly, the number of climate change impact studies in water related literature has rapidly increased in the last years (see, e.g. Lettenmaier et al., 1999; Bergstrom et al., 2001; Shabalova et al., 2003; Payne et al., 2004).

Potential climate change impacts on hydrological systems strongly depend on the studied hydro-climatic area (see, e.g., Skiles and Hanson, 1994; Mohseni and Stefan, 2001; Singh and Bengtsson, 2005; Zierl and Bugmann, 2005). In the present PhD research, we focus on high-mountainous water resources systems in the Alpine area. Mountains are a key element of the hydrological cycle; they are the source of many of the world's major river systems. High mountainous water resource systems are particularly sensitive to potential climate change impacts. The hydrological regime of such environments is strongly influenced by water accumulation in form of snow and ice and the corresponding melt processes. A modification of the prevalent climate and especially of the temperature can therefore considerably affect the hydrological regime and induce important impacts on the water management (see, e.g., Burlando et al., 2002; Jasper et al., 2004). This could have a significant impact on water uses highly dependent on the hydrological regime, such as hydropower production or irrigation, but also increase water related risks such as flood and droughts (see, e.g. Willis and Bonvin, 1995; Loukas et al., 2002). The prediction of climate change impacts has consequently an evident socio-economic interest.

In the Swiss Alps, a major concern is currently focused on climate change induced reduction of the glacier surfaces (see, e.g., Haeberli and Beniston, 1998; Paul et al., 2004). A decrease of the glacier surface due to global-mean warming has potentially a major impact, especially on hydropower production. A total glacier surface reduction decreases the future ice melt discharge feeding the hydropower plants that produce in Switzerland up to 75 % of the consumed electricity of which around 60 % are produced by accumulation (Swiss Federal Office for Energy, 2003). It could also have a direct impact on the sediment load of the discharged water – a concern for lake sedimentation and turbine abrasion. These problems are potentially enhanced by a climate change induced modification of the frequency and intensity of heavy rainfall events.

1.1.3 Climate change predictions in high mountainous catchments

The simulation of components of the hydrological cycle in high mountainous areas is particularly difficult. The topographically induced heterogeneity of the landscape conditions a high spatial variability of meteorological and hydrological processes. Additionally, the available meteorological and hydrological data is scarce – at high altitudes nearly inexistent - and - due to the extreme weather conditions - highly error prone. A good spatial interpolation of the meteorological conditions is therefore difficult. This problem represents a considerable

source of uncertainty for runoff and water balance simulation, especially in the presence of glaciers: They constitute an important water storage reservoir and for water balance simulation, any under- or overestimation of the precipitation can be compensated by simulated ice melt.

The simulation of observed conditions being a complex task, the simulation of hypothetic future climate conditions becomes a challenge in such environments. This difficulty is enhanced by the classical scale incompatibility problem between future climate predictions and local scale hydrological models: The climate predictions are the result of climate models that have typically a spatial resolution of around 2.5° of latitude and 3.75° of longitude for global models (modelling the entire climate system) and of 50 km by 50 km for regional climate models. This resolution is generally far too coarse for a direct use of the model outputs, namely precipitation and temperature, in hydrological models (see, e.g., Hay et al., 2002; Wood et al., 2004), especially in the present context where the studied catchments are smaller than 200 km^2. For a further discussion of this problem, refer to Section 4.3.

A modification of the climate system potentially affects the hydrological regime but also the frequency and intensity of extreme events. In the present research context, the models have been developed with a focus on the prediction of hydrological regimes (see Section 3.1 and Section 4.3) rather than of extreme hydrological events (see, e.g., Katz et al., 2002; Kim, 2005).

1.1.4 Uncertainty in hydrological modelling

In this thesis, a special emphasis is given to the hydrological modelling uncertainties. Their quantification is currently one of the key issues in hydrological research (see, e.g., Kuczera and Parent, 1998; Beven and Freer, 2001; Vrugt et al., 2003). If the simulation results are used in management or planning decisions, the estimation of the precision and the exactitude of the obtained results is fundamental for the decision maker to judge his confidence in the results. In the context of climate change impact studies, the quantification of the modelling uncertainties is essential to assess whether the system modification is induced by climate change or by model errors.

The hydrological modelling uncertainties are caused by four different sources (Refsgaard and Storm, 1996): i) errors in the input data, especially in the meteorological data; ii) errors in the recorded observations of the phenomenon to be modelled; iii) errors and simplifications inherent in the model structure; iv) uncertainty due to the values of the model parameters.

The observational errors of input or output data hide two different sources of modelling uncertainty: the measurement uncertainty that is directly linked to the used method and the uncertainty induced by the fact that the observed phenomenon does not correspond to the type of inputs (respectively outputs) that the model requires. The classical example is the use of a series of point precipitation whereas the model would require an area-average time series.

A model is a simplified representation of a natural phenomenon and is therefore imperfect. Even if the input and output data were exact, the model would not be able to match the observed output perfectly. We refer to this source of modelling uncertainty as the model structure uncertainty. The fourth source of uncertainty is perhaps the most extensively studied in hydrological literature. The type of errors induced by the parameters depends on how they are estimated. Physical parameters are assumed to represent a measurable property of the studied system. The related uncertainties are the same as for the observed input and output variables. Many hydrological models have parameters that cannot be estimated from some observed system characteristics – either because the underlying mathematical equations are not physically-based but purely conceptual or because the necessary system characteristics have not been or cannot be observed. These parameters have to be calibrated, i.e. the best parameter values are estimated so that the model output matches as closely as possible the observed data. This best parameter set – if it exists – is difficult to find and several different parameter sets can yield equally good results for the model calibration (see, e.g., Beven and Binley, 1992; Gupta et al., 1998).

In the past, the determination of the best or the most probable parameter set has been subject to intense research (see, e. g., Duan et al., 1992; Yapo et al., 1998; Madsen, 2000) whereas current research concentrates on the estimation of the entire probability distribution of the parameters (see, e. g., Kuczera and Parent, 1998; Vrugt et al., 2003).

1.2 Fundamental questions of this PhD research

Most climate change impact studies are based on the paradigm that if we were able to predict the climate evolution, we could predict the resulting impact on the considered system. Accordingly, most studies suffer from an important drawback: They lack to quantify the uncertainty associated with the impact prediction. The present PhD thesis faces this major challenge in the field of climate change impact research: to show whether this paradigm holds for water resources systems in high mountainous areas.

The research concentrated on the quantification of the impact prediction uncertainty associated with the modelling of the hydrological system. The obtained results are compared to the uncertainty inherent in the climate evolution prediction itself. Ultimately, the developed methodology should give the answer to the following main question: If we were able to predict the evolution of the climate, could we predict its impact on water resources systems and if yes, how precise are these predictions? And compared to the uncertainty associated with the prediction of the climate evolution itself, how uncertain is the evolution of the hydrological system?

1.3 Methodological framework

We use the classical simulation approach for climate change impact analysis that is based on a set of interacting models to simulate the considered system behaviour under different situations and for different time periods (see, e.g., Bergstrom et al., 2001; Fowler et al., 2003; Payne et al., 2004). The system behaviour is modelled for a known (observed) control period and for a future period characterised by a modified (predicted) climate. Classically, the control period is the 30-year period from 1961 to 1990 for which the climate is assumed not to be influenced by anthropogenic forcing. The future period depends on the type of application but is generally a 30-year period distanced of between 20 to 110 years from the control period. The climate change impact is assessed by comparing some key characteristics of the system for the two periods.

The analysis of potential climate change impacts on the management of a water resources system requires at least 4 model types: a water management model, a hydrological model, a land cover evolution model and a climate model. Due to the mentioned scale problems, a global scale and a regional scale climate model are generally necessary, possibly completed by a model for the production of local scale meteorological time series (precipitation, temperature). Figure 1 shows the model types used in this thesis for the simulation of climate change impacts on hydropower production in a high mountainous area. The local scale models have been developed for the purposes of this thesis. The global and regional scale model outputs have been made available by other research teams (see Chapter 4).

The integrated simulation tool based on the models presented in Figure 1 is used to simulate the system behaviour under the observed climate for the control period 1961 - 1990 and under future climate scenarios for the period 2070 – 2099. A case study-specific indicator set is elaborated to evaluate the system performance and to compare the control period and the future scenarios.

The main objective of the present research is to quantify the modelling uncertainties associated with the different modelling steps. This objective considerably influenced the design choices during the development of the local scale models. For each of them, the inherent sources of modelling uncertainty are quantified through Monte Carlo simulations of the model output: The model output is simulated an important number of times drawing for each simulation the relevant model parameters (the ones that are uncertain) randomly in a predefined probability distribution. These probability distributions are obtained for each source of uncertainty through appropriate statistical methods.

The overall prediction uncertainty is quantified through Monte Carlo simulations considering successive combinations of the different sources of modelling uncertainties. The relative contribution of the different models to the overall uncertainty is assessed. The predicted climate change impact is judged by comparing the obtained distributions of the system performance indicators for the control and the future period, answering namely the question whether these impacts are statistically significant given the different levels of modelling uncertainty.

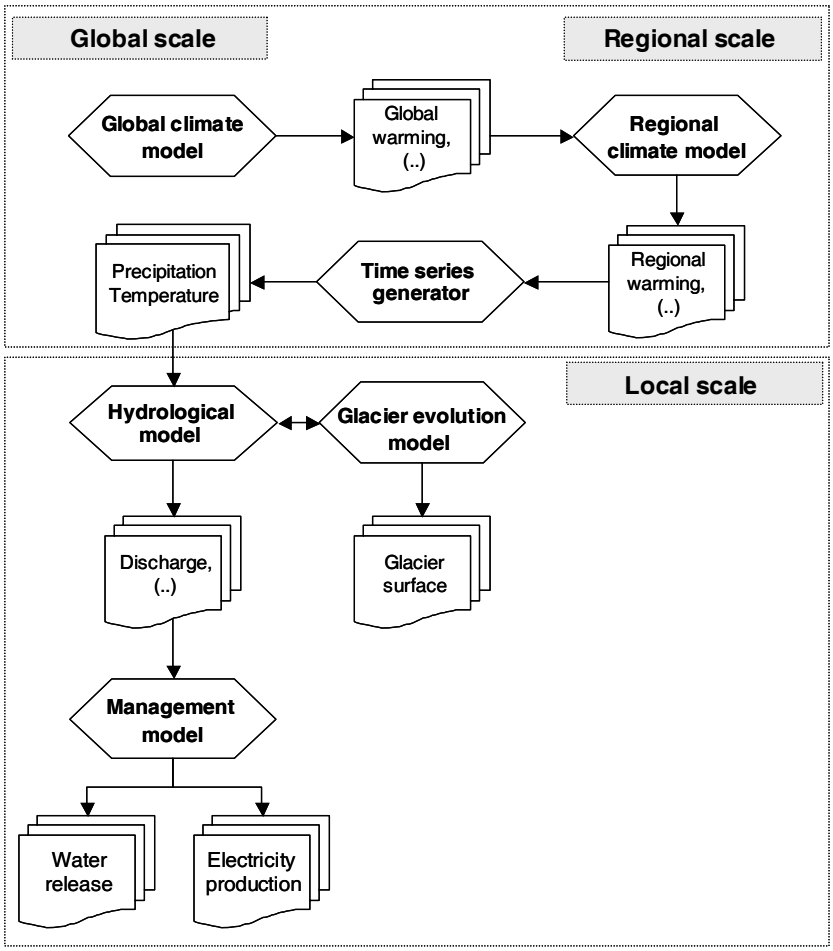

Figure 1: Flowchart of the models used for the simulation of climate change impacts on a hydropower production system in a high mountainous area

1.4 Outline of the thesis

During the work on this thesis, the obtained results have been submitted to publication in international relevant journals and presented during different conferences. The resulting final document is therefore a collection of papers (published or submitted for publication[1]) completed by the present introductory chapter, a chapter presenting the main case study (Chapter 2) and the general conclusions (Chapter 9).

Each of the papers corresponds to a chapter of this final manuscript but forms an independent unit that can be understood without the context of the entire manuscript. This results in inevitable repetitions, for which we apologise. The main features of the case study and of the

[1] Due to the sometimes considerably time-consuming reviewing process, only one paper is published (Chapter 7) and one paper is accepted for publication (Chapter 6). The paper corresponding to Chapter 3 has undergone the first publication phase; it is published on the Internet and the referees recommend the publication of the paper. Two other chapters (Chapter 4 and 5) have been submitted and the editor's answer is outstanding. Chapter 8 will be submitted to publication after finishing the work on this final manuscript.

hydrological model are shortly presented in each chapter as far as they are necessary for the understanding of the corresponding paper. The acknowledgements at the end of each chapter are redundant but formally required for the publication of the individual papers.

The chapter titles correspond to the ones retained for the paper publication. A footnote on the front page of each chapter specifies where it has been submitted or published. Note that the chronological order of submission of these papers does not correspond to the order of appearance in this manuscript. In the following, the content of the 9 chapters composing this thesis is briefly outlined.

Chapter 2 introduces the main case study, the hydropower production system called Mauvoisin and the water management model developed to analyse potential climate change impacts on this water resources system. The Mauvoisin power plant is located in the southern Swiss Alps and produces hydropower by accumulation. The catchment feeding the accumulation lake is strongly influenced by snow- and ice melt. As for most such hydropower production systems in the Alps, the accumulation lake acts like a buffer for shifting the electricity production from periods of high water inflow (summer) to periods of high electricity consumption (winter).

Note that some of the presented models have been developed and tested for another case study[2], the so-called Rhone catchment measured at Gletsch. This catchment is representative of the hydrological regime of the Mauvoisin catchment but is smaller and has a better data availability for model calibration and validation. For the main glacier of the Rhone catchment, detailed observations are available, in particular glacier mass balance data. Namely Chapter 3, Chapter 4 and Chapter 7 present results referring to this case study.

Chapter 3 presents the hydrological model developed for the purpose of this thesis for the simulation of the daily discharge in a high mountainous catchment. Given the research context, the model development was based on the following constraints: It has to be applicable in glacierized catchments that are data scarce. The necessary input data for simulation has to be derivable from current climate model outputs and the discharge simulation uncertainty has to be quantifiable. Accordingly, the model had to be parsimonious: The number of meteorological input variables and calibrated parameters has been reduced to the strict minimum. Another important aspect had to be considered during the model development: Climate change studies over long time periods have to analyse potential land cover change. In high mountainous catchments, the most important expected land cover change is the modification of the glacier surface. The hydrological model has to be able to react to such a land cover change.

The present chapter discusses the model, its calibration and its ability to simulate discharge from high mountainous catchments. It is calibrated and validated for three case studies. Note

[2] The analysis of a managed water resources system such as the catchment of Mauvoisin is highly interesting as the resulting conclusions are of direct use for water management. This comes however with the cost of data scarcity and a time-consuming data collection process.

that the quantification of the modelling uncertainties inherent in this hydrological model is presented in Chapter 5.

Chapter 4 presents how the land cover change – the glacier surface evolution – can be predicted. The underlying glacier surface model is closely connected to the hydrological model as it uses the simulated snow and ice accumulation and melting as an input for the estimation of the glacier surface. The model has been developed for an application in probabilistic climate change impact studies considering a range of potential global-mean warming. The prediction uncertainty can be quantified as illustrated in this paper for several global-mean warming scenarios. This chapter analyses the Rhone case study. The model application to the Mauvoisin catchment is discussed in Chapter 6.

Note that the present chapter explains how the local scale climate change scenarios are generated. The underlying methodology has been developed by Hingray et al. (submitted manuscript)[3].

Chapter 5 addresses the quantification of the hydrological modelling uncertainties. In the context of this doctoral thesis, a Markov Chain Monte Carlo (MCMC) method, the so-called Metropolis-Hastings algorithm has been implemented for the quantification of the hydrological modelling uncertainties for a given model structure. This algorithm has become increasingly popular in hydrological modelling. Its application in the context of climate change impact studies poses however a few problems.

This algorithm carries out a Bayesian inference of the posterior parameter distributions and requires therefore the definition of an appropriate statistical model. This model classically assumes a Gaussian modelling error with zero mean and a given variance. Hydrological residuals rarely respect this basic assumption but could be normalised through data transformations. In the present context, the variable to be modelled is the discharge. The modelling error could by normalised by a logarithmic transformation. Since the discharge is used as an input into the water management model, the retransformation has to be carried out after modelling error estimation. This step introduces however a bias, a so-called retransformation bias. This problem has been solved by using a statistical error model composed of a mixture of two normal models instead of applying a data transformation. This solution is new in this context.

Chapter 6 applies the so-far presented methods to the Mauvoisin case study. The resulting prediction of potential climate change impacts includes the largest possible range of potential climate change scenarios and quantifies the modelling uncertainties related to the different modelling steps. The climate change induced impacts on the water management are quantified through a set of performance indicators developed for this case study and presented in this

[3] Hingray, B., Mouhous, N., Mezghani, A., Bogner, K., Schaefli, B. and Musy, A.: Accounting for global warming and scaling uncertainties in climate change impact studies: application to a regulated lakes system. Submitted to Hydrology and Earth System Sciences; hereinafter referred to as Hingray et al., submitted manuscript

chapter. The impact is judged in terms of system performance modification between the control period (1961 – 1990) and the future period (2070 – 2099). Beside the predicted climate change impacts, a main result of this chapter is the comparison of the different sources of modelling uncertainties included in the analysis, namely the one due to the global-mean warming, the regional climate response, the hydrological model, the glacier surface evolution model and the management model.

This paper has been accepted for publication in a special edition of Hydrology and Earth System Sciences dedicated to the results of the European research project SWURVE (Sustainable Water: Uncertainty, Risk and Vulnerability in Europe) in the context of which most research of the present thesis has been carried out. It is in close connection to the work of Hingray et al. (submitted manuscript) submitted as an accompanying paper. An extract of this paper is included in Chapter 4 (see Section 4.3 and Appendix 2 and 3 of Chapter 4).

Chapter 7 analyses the potential prediction uncertainties induced by the hydrological model structure – an aspect that has not been considered in the previous chapters but that may considerably modify the conclusions of Chapter 6. Based on the basic structure of the hydrological model, different equivalent model structures are identified through the application of a multi-objective evolutionary algorithm that has been developed for industrial design problems at the Laboratory of Industrial Energy Systems of the Swiss Institute of Technology in Lausanne. Using this multi-objective optimisation algorithm, decision variables referring to the model design can be included in the model optimisation process and accordingly several equivalent model structures can be identified. Although being equivalent for the calibration and validation period, the different model structures yield different results for a future climate.

This chapter highlights that the model structure is a considerable source of uncertainty in climate change impact studies on water resources. Note that the results are based on the Rhone case study. The application of the presented method to the Mauvoisin catchment is discussed in Chapter 8.

Chapter 8 presents a methodology to quantify the uncertainty induced by the so-called multi-objective equivalence of different models (having different structures or different parameter sets) that has been highlighted in the previous chapter. The resulting uncertainty is compared to the one induced by the statistical concept of posterior model output distribution presented previously (Chapter 5). In order to quantify the total modelling uncertainty associated with hydrological modelling in the context of climate change impact studies, the relative importance of each of the two sources is assessed for different observed periods and for a future period characterised by a climate change.

Chapter 9 contains a summary of the main results, the overall conclusions and an overview over the questions that remain unanswered or that have been raised through this research. Based on all presented results, this chapter tries to answer the main question motivating this PhD research: *Can we predict climate change impacts on water resources by current state-of-*

the-art modelling techniques incorporating current hydrological process knowledge and statistical methods of modelling uncertainty estimation?

References

Bergstrom, S., Carlsson, B., Gardelin, M., Lindstrom, G., Pettersson, A. and Rummukainen, M., 2001. Climate change impacts on runoff in Sweden - assessments by global climate models, dynamical downscaling and hydrological modelling. Climate Research, 16(2): 101-112.

Beven, K. and Binley, A., 1992. The future of distributed models: model calibration and uncertainty prediction. Hydrological Processes, 6(3): 279-298.

Beven, K. and Freer, J., 2001. Equifinality, data assimilation, and uncertainty estimation in mechanistic modelling of complex environmental systems using the GLUE methodology. Journal of Hydrology, 249(1-4).

Burlando, P., Pellicciotti, F. and Strasser, U., 2002. Modelling mountainous water systems between learning and speculating looking for challenges. Nordic Hydrology, 33(1): 47-74.

Duan, Q., Sorooshian, S. and Gupta, V., 1992. Effective and efficient global optimization for conceptual rainfall-runoff models. Water Resources Research, 28(4): 1015-1031.

Folland, C.K. et al., 2001. Observed Climate Variability and Change. In: C.A. Johnson (Editor), Climate Change 2001: The Scientific Basis. Contribution of Working Group I to the Third Assessment Report of the Intergovernmental Panel on Climate Change. Cambridge University Press, Cambridge, UK, pp. 99-181.

Fowler, H.J., Kilsby, C.G. and O'Connell, P.E., 2003. Modeling the impacts of climatic change and variability on the reliability, resilience, and vulnerability of a water resource system. Water Resources Research, 39(8).

Gupta, H.V., Sorooshian, S. and Yapo, P.O., 1998. Toward improved calibration of hydrologic models: Multiple and noncommensurable measures of information. Water Resources Research, 34(4): 751-763.

Haeberli, W. and Beniston, M., 1998. Climate change and its impacts on glaciers and permafrost in the Alps. Ambio, 27(4): 258-265.

Hay, L.E., Clark, M.P., Wilby, R.L., Gutowski, W.J., Leavesley, G.H., Pan, Z., Arritt, R.W. and Takle, E.S., 2002. Use of regional climate model output for hydrologic simulations. Journal of Hydrometeorology, 3(5), 571-590.

IPCC, 2001. Climate Change 2001: the Scientific Basis. A Contribution of Working Group I to the Third Assessment Report of the Intergovernmental Panel on Climate Change. In: C.A. Johnson (Editor). Cambridge University Press, Cambridge, UK, pp. 881.

Jasper, K., Calanca, P., Gyalistras, D. and Fuhrer, J., 2004. Differential impacts of climate change on the hydrology of two alpine river basins. Climate Research, 26(2): 113-129.

Katz, R.W., Parlange, M.B. and Naveau, P., 2002. Statistics of extremes in hydrology. Advances in Water Resources, 25(8-12), 1287-1304.

Kim, J., 2005. A projection of the effects of the climate change induced by increased CO2 on extreme hydrologic events in the western US. Climatic Change, 68(1-2), 153-168.

Kuczera, G. and Parent, E., 1998. Monte Carlo assessment of parameter uncertainty in conceptual catchment models: the Metropolis algorithm. Journal of Hydrology, 211(1-4): 69-85.

Lettenmaier, D.P., Wood, A.W., Palmer, R.N., Wood, E.F. and Stakhiv, E.Z., 1999. Water resources implications of global warming: An U.S. regional perspective. Climatic Change, 43(3): 537-579.

Loukas, A., Vasiliades, L. and Dalezios, N.R., 2002. Potential climate change impacts on flood producing mechanisms in southern British Columbia, Canada using the CGCMA1 simulation results. Journal of Hydrology, 259(1-4): 163-188.

Madsen, H., 2000. Automatic calibration of a conceptual rainfall-runoff model using multiple objectives. Journal of Hydrology, 235(3-4): 276-288.

Mitchell, J.F.B., Karoly, D.J., Hegerl, G.C., Zwiers, F.W., Allen, M.R. and Marengo, J., 2001. Detection of Climate Change and Attribution of Causes. In: C.A. Johnson (Editor), Climate Change 2001: The Scientific Basis. Contribution of Working Group I to the Third Assessment Report of the Intergovernmental Panel on Climate Change. Cambridge University Press, Cambridge, UK, pp. 695-738.

Mohseni, O. and Stefan, H.G., 2001. Water budgets of two watersheds in different climatic zones under projected climate warming. Climatic Change, 49(1-2), 77-104.

Paul, F., Kääb, A., Maisch, M., Kellenberger, T. and Haeberli, W., 2004. Rapid disintegration of Alpine glaciers observed with satellite data. Geophysical Research Letters, 31(21): Art. No. L21402.

Payne, J.T., Wood, A.W., Hamlet, A.F., Palmer, R.N. and Lettenmaier, D.P., 2004. Mitigating the effects of climate change on the water resources of the Columbia river basin. Climatic Change, 62(1-3): 233-256.

Prentice, I.C. et al., 2001. The Carbon Cycle and Atmospheric Carbon Dioxide. In: C.A. Johnson (Editor), Climate Change 2001: The Scientific Basis. Contribution of Working Group I to the Third Assessment Report of the Intergovernmental Panel on Climate Change. Cambridge University Press, Cambridge, UK, pp. 183-237.

Refsgaard, J.C. and Storm, B., 1996. Construction, calibration and validation of hydrological models. In: J.C. Refsgaard (Editor), Distributed hydrological modelling. Kluwer Academic Press, Dordrecht, Netherlands, pp. 41-54.

Shabalova, M.V., Van Deursen, W.P.A. and Buishand, T.A., 2003. Assessing future discharge of the river Rhine using regional climate model integrations and a hydrological model. Climate Research, 23: 223-246.

Singh, P. and Bengtsson, L., 2005. Impact of warmer climate on melt and evaporation for the rainfed, snowfed and glacierfed basins in the Himalayan region. Journal of Hydrology, 300(1-4), 140-154, doi.

Skiles, J.W. and Hanson, J.D., 1994. Responses of arid and semiarid watersheds to increasing carbon-dioxide and climate-change as shown by simulation studies. Climatic Change, 26(4), 377-397.

Swiss Federal Office for Energy, 2003. Statistique suisse de l'électricité 2002, Bern.

Vrugt, J.A., Gupta, H.V., Bouten, W. and Sorooshian, S., 2003. A shuffled complexe evolution Metropolis algorithm for optimization and uncertainty assessment of hydrologic models. Water Resources Research, 39(8): 1201.

Willis, I. and Bonvin, J.-M., 1995. Climate change in mountain environments: hydrological and water resource implications. Geography, 80(3): 247-261.

Wood, A.W., Leung, L.R., Sridhar, V. and Lettenmaier, D.P., 2004. Hydrologic implications of dynamical and statistical approaches to downscaling climate model outputs. Climate Change, 62(1-3): 189-216.

Yapo, P.O., Gupta, H.V. and Sorooshian, S., 1998. Multi-objective global optimization for hydrologic models. Journal of Hydrology, 204(1-4): 83-97.

Zierl, B. and Bugmann, H., 2005. Global change impacts on hydrological processes in Alpine catchments. Water Resources Research, 41, W02028, doi: 10.1029/2004WR003447.

Chapter 2

Case study: Mauvoisin hydropower plant[1]

Abstract

This chapter presents the main case study, the Mauvoisin hydropower plant, and the water management model developed to analyse potential climate change impacts on this water resources system. The Mauvoisin accumulation hydropower plant is located in the southern Swiss Alps, the catchment feeding the accumulation lake has a size of 169 km^2 and its hydrological regime is strongly influenced by snow- and ice melt. The hydropower production is dependent on the resulting annual water cycle and on the electricity market. Accordingly, no explicit management rules exist and an empiric water management model has been designed to reproduce the observed water release management in the past. The developed model is semi-deterministic: The deterministic part models the seasonal and weekly water release variations whereas the stochastic part models the day-to-day variations due to the fluctuations of the electricity demand and of the price on the electricity market. Using observed lake inflows as input, the management model reproduces well the observed lake level evolution throughout the year and the monthly electricity production.

[1] This chapter corresponds to an unpublished annual report: Schaefli B, Hingray B., Musy A., 2002. Dam of Mauvoisin: Modelling of the water management. Annual report of the SWURVE (Sustainable Water: Uncertainty, Risk and Vulnerability in Europe) project, Swiss Institute of Technology, Lausanne, 27 pp.

2.1 Introduction

The analysis of potential climate change impacts on a water resources system is classically carried out by simulating the system behaviour for a control period and for a future period characterised by a predicted climate change. The simulation of the system behaviour for these periods requires three types of models: a climate model to simulate meteorological time series such as precipitation and temperature, a hydrological model to simulate the transformation of these time series into river discharge and a management model to simulate the water management. The aim of the present study is to develop such a water management model for an accumulation hydropower plant in the Swiss Alps called Mauvoisin.

The management model simulates the water release from the accumulation lake having as input the water inflow into the lake. The time series of water inflow are either observed (for past and present situations) or simulated through a hydrological model. For the present application, the observed and the simulated discharge series have a daily time step. Accordingly, the water management model has to be able to simulate daily water releases and the corresponding daily storage evolution. The analysis of potential climate change impacts on water release and hydropower production is however analysed for larger time periods, typically in terms of monthly or annual mean production. Consequently, the management model has to reproduce the observed mean water releases at different aggregated time steps.

The development of the management model starts with a description of the system and a detailed analysis of the available data of hydropower production in the past. Based on the conclusion of this analysis, a mixed deterministic and stochastic modelling approach of the water release is developed. Finally, the application of the model, results and further developments are discussed.

2.2 Hydropower plant of Mauvoisin

2.2.1 General description of the system

The hydropower plant of Mauvoisin is located in the southern Swiss Alps (Figure 1). It is composed of an accumulation lake and three hydropower production levels. The 250 m high arched dam wall is the second highest in the world of its type today. The owner and manager of the dam is the stock corporation Forces Motrices de Mauvoisin (FMM). The accumulation lake was filled for the first time in 1958. A total volume of $204 \cdot 10^6 m^3$ of water, corresponding to 660 GWh, can be stored to ensure a flexible power generation. The catchment of the dam has a size of 169 km^2 and an elevation range between 1975 m and 4314 m a.s.l. Around 40 % of the surface is covered by glacier and 43 % by rock (Spreafico et al., 1992). The maximum daily inflow into the lake is about $6 \cdot 10^6 m^3$ and the mean annual inflow $265 \cdot 10^6 m^3$. The hydrological regime is strongly influenced by glacier and snowmelt. It is of the so-called a-

glacier type (Spreafico et al., 1992): The maximum monthly discharge takes place in July and August and the minimum monthly discharge (around 100 times less!) in February and March.

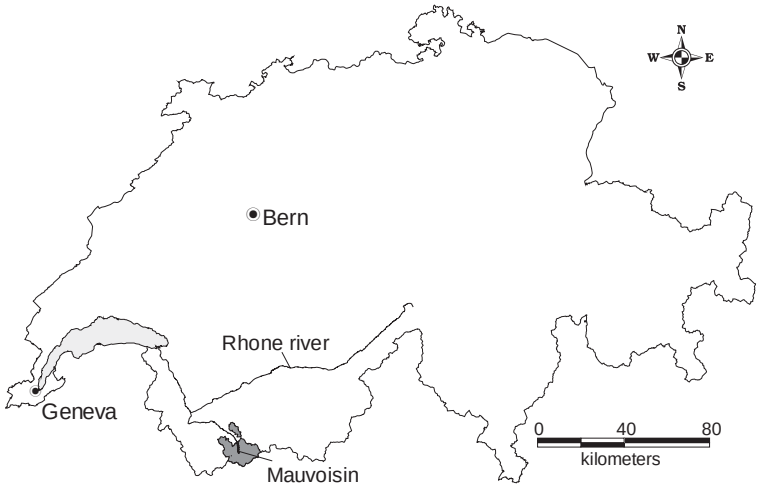

Figure 1: Location of the Mauvoisin catchment in the Swiss Alps (SwissTopo, 1997)

The hydropower production uses the water of the accumulation lake in three levels corresponding to a power of 381 MW. The plant does not use any pump system for water recirculation. For the purposes of this study, the main interest is focused on the release management of the water accumulated by the dam. Only one of the three levels uses the water directly released from the dam, the other two levels use the water released from this first level and from some additional water intakes. Accordingly, only the first production level is taken into account for the model development. It consists of three turbines Francis with vertical-axis that correspond to a maximal installed power of 127.5 MW and a maximal total discharge of 34.5 m^3/s. The hydraulic head varies between 320 m and 490 m.

2.2.2 Water release management

The hydropower plant belongs to a stock corporation formed by 6 shareholders. Each shareholder exploits its part of the accumulated energy according to its own strategy that is strongly influenced by the electricity demand but also by the annual water inflow into the lake. This type of water management is known as capacity sharing (Dudley, 1992). There is one person – the exploitation manager - who is responsible for surveying the evolution of the dam lake level. He guides the electricity production of the different shareholders and surveys the inflow into the lake in order to ensure the safety of the hydropower plant and an optimal filling by the end of the snow- and glacier melt season (around end of August).

The inflow can be reduced during critic situations by disconnecting some of the 12 water intakes. Such critic situations occur if the water level comes close to 97.7 % of the maximal acceptable fill. If the water level reaches the maximal acceptable level, an emergency management plan defines the actions to be undertaken that include water release through the

spillway (up to 347 m^3/s). The spillway has never been activated in the past, but in case, its activation could lead to important inundations in the downstream inhabited areas: The maximal spillway discharge corresponds to more than 1.5 times the estimated flood event with a return period of 1000 years[2].

The only other management constraint to be respected refers to the maximal discharge in the Rhone river (Figure 1) that receives the water released through the turbines: The hydropower production has to be stopped if the discharge reaches 930 m^3/s. There are no minimum discharge constraints that affect the hydropower management as the minimum discharge in the accumulated river is ensured by a diverted spring.

This leads to the conclusion that - except for extreme situations - there are no clearly defined water management or hydropower production rules. The evolution of the lake level is dependent on the electricity production strategy of the different shareholders and the hydrological regime.

2.3 Analysis of inflow, storage and water release

The water management decision system under regular conditions is not known. Accordingly, it is difficult to determine a priori, which factors influence the hydropower production. For the shareholders, economic interests are prevailing, i.e. hydropower production is strongly influenced by the electricity price on the electricity market. We can strongly believe that this explains almost all daily variation of the electricity production (production during peak demand). On the other hand, the long term production mean and variation can only be explained by analysing demand (electricity consumption) and offer (available hydropower) simultaneously.

In the context of the present study, the development of a management model has to be based on data that is known for past and present situations and that can be obtained for future situations through simulation. Climatic data such as rainfall or temperature – influencing the hydrological regime - can be obtained for future climate situations from appropriate climate models. Such future climate scenarios are available in the context of the underlying climate change impact study. In return, the use of socio-economic data has to be restricted. Either the factors acting on a hydropower decision system are not easily identified or their values are difficult to estimate for future situations. The electricity demand and its price on the market

[2] For the dam construction project, the discharge with a return period of 1000 years has been estimated to 200 m^3/s. The design flood discharge for the spillway has been fixed equal to 1.5 times this value. The spillways where however redesigned during a dam raising carried out between 1989 and 1992 (before the raising, the dam had a height of 237 m).

for example can be known for the past but their estimation for future situations exceeds the context of the present study.

Consequently, the objective of the management model development is not to identify a hypothetic decision system but to determine the empiric relationship between the system input (water inflow), the state variable (storage) and the output (water release).

2.3.1 Available data

For the period from April 1987 to September 2000 the following data is available: daily data of water release through the turbines at each production level, of other releases (spillway) and of the lake level measured at the end of the day. The lake level measurements, which are the result of a reading by binoculars on a levelling rod, have an approximate precision of 5 cm that - according to the filling degree of the lake - corresponds to between 27'000 m^3 and 113'000 m^3. The precision of the water release measurement is more difficult to quantify. It is not measured directly but estimated based on the electricity production (measurement precision 500 kWh/d) and the electricity production factor that expresses the relationship between the produced electricity and the amount of water released through the turbines. The exact value of the electricity production factor is depending on the hydraulic head and on the regime of the turbines. For the available data, the electricity production factor is estimated as a linear function of the hydraulic head, i.e. of the lake level. The exact water release measurement precision is therefore impossible to quantify (the instantaneous regime of the turbines is unknown). Assuming that the precision of the production factor estimation is around +/- 0.1 kWh/m^3, the measurement precision can be estimated at 5000 m^3/d. It can be easily seen that this measurement uncertainty is much smaller than the one resulting directly from the lake level measurement.

As the relationship between the lake level and the accumulated water volume is known, the available data can be used to calculate the water inflow according to the continuity equation (Equation 1).

$$\Delta V_t = V_t - V_{t-\Delta t} = Q_{t,in} \bullet \Delta t - Q_{t,out} \bullet \Delta t \qquad (1)$$

where V_t is the storage at the end of day t, Δt the time step (1 day), $Q_{t,in}$ the mean daily inflow (1000 m^3/d) and $Q_{t,out}$ (1000 m^3/d) the mean daily outflow on day t.

2.3.2 Temporal evolution of storage, release and inflow

Annual and monthly evolution

The artificial accumulation lake of the Mauvoisin hydropower plant acts like a buffer system to shift the natural hydropower offer (water inflow) to periods of maximum electricity demand (Figure 2). This ensures a flexible electricity production during the whole year and especially during the winter when electricity consumption is particularly high in central Europe. This basic management principle underpins the management of most accumulation hydropower plants in the European Alps where the inflow is high during the summer whereas the electricity consumption is high during the winter.

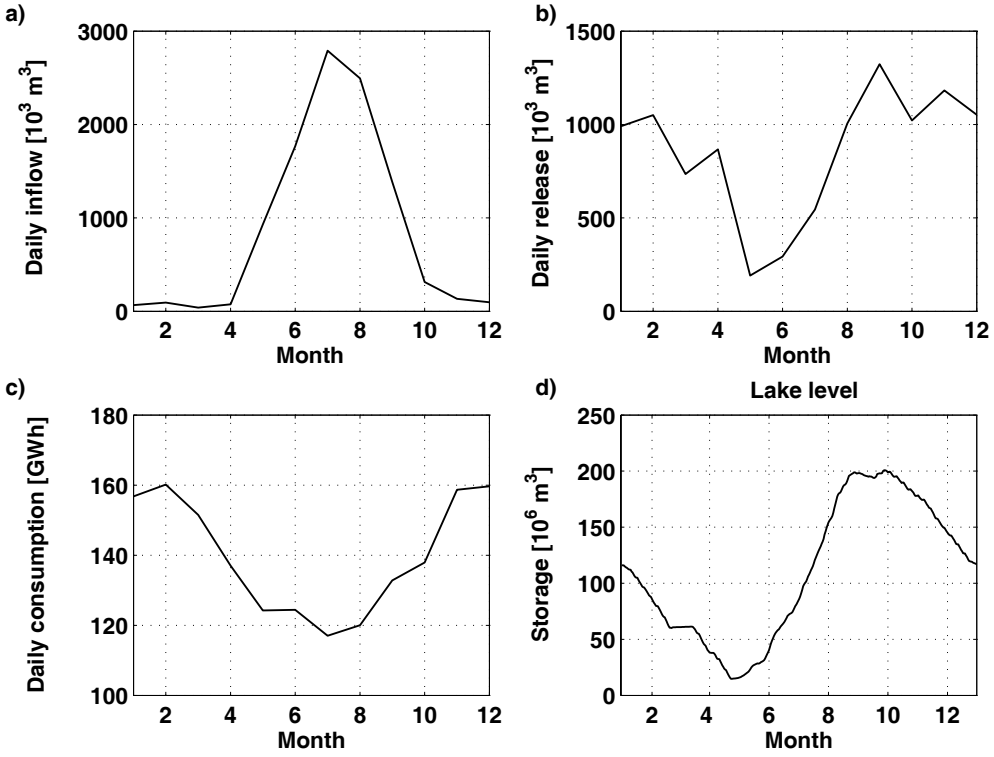

Figure 2: a) Mean monthly inflow into the lake of Mauvoisin; b) mean monthly water release through the turbines, c) mean monthly electricity consumption in Switzerland (Swiss Federal Office for Energy, 1999); d) evolution of the daily water storage of the lake of Mauvoisin; all figures for the same year of the observed period[3]

[3] For reasons of confidentiality, the exact temporal reference is not indicated in any of the figures.

The analysis of the standard deviation of the daily storage helps to identify the periods of minimum variation. For the period 1987 to 2000, the absolute minimum is located around the end of August (Figure 3). This corresponds to the basic management objective: maximum lake filling by the end of the snow and glacier melt season. The period of local minimum variation at mid-May corresponds to the period when the lake is almost empty at the start of the melt season.

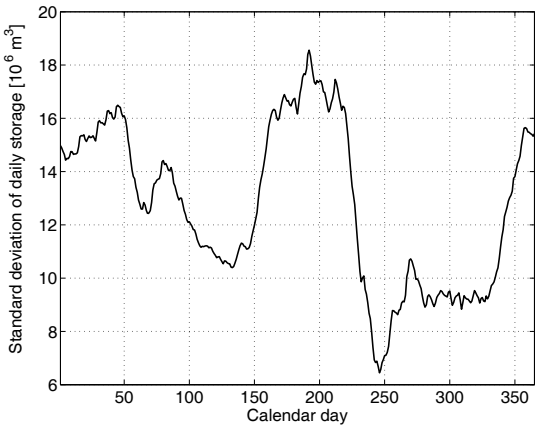

Figure 3: Interannual standard deviation of daily water storage

Defining a water management year that starts by the end of August, the initial and final storage are more or less the same and there is a high correlation between total annual inflow and outflow (linear correlation of 0.95, see Table 1). Given this starting date, almost all management years suggest the existence of two distinctive seasons of more or less constant release (Figure 4). The transition between the two seasons corresponds to the beginning of high inflow in spring (around mid-May). Around this period of the year, the lake level reaches its minimum annual level. This minimum level is generally kept above zero, except if some maintenance work has to be carried out. This management principle can be illustrated through the joint analysis of the cumulative inflow (having as initial value the initial storage at the beginning of the management year) and the cumulative release (Figure 4). The minimum distance between the two curves occurs around mid-May. Based on these considerations, two different management seasons are defined, season 1 (S_1) and season 2 (S_2) (Equation 2).

$$n \in \begin{cases} S_2 & \text{if } 16\ May \le n \le 31\ August \\ S_1 & \text{otherwise} \end{cases} \tag{2}$$

where n is a given day of the year.

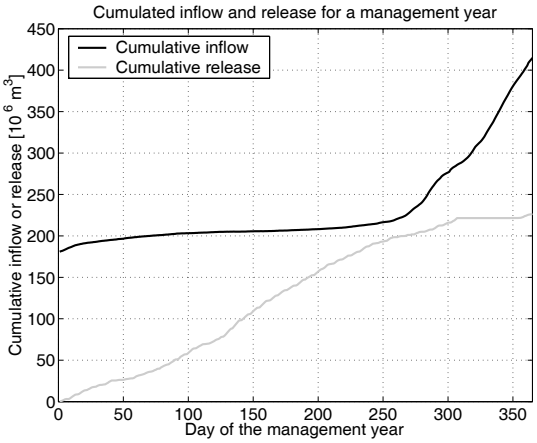

Figure 4: Cumulative inflow and release for one management year (starting at the 1 September) of the observed period; the cumulative inflow starts at the initial volume in the accumulation lake

It would be interesting to relate the slope of the cumulative release during each of the two seasons to other observable data such as the water inflow or the storage. The manager and the electricity producers use some short-term meteorological predictions (a few days) for decision making but no mid-term (seasonal) inflow forecasts. In return, some of the electricity production decisions rely on the historical production experience and on the interannual inflow variability throughout the seasons. This could lead to the assumption that there is a relationship between the available water and the mean daily release of the management seasons. The linear correlations between the mean inflow and the mean release over the two seasons and the initial storages are however small (Table 1). The only significant correlation is the one between the water inflow and the release over season 1 (Table 1). The inflow during this period is generally low (winter season), but the higher it is, the higher is the hydropower production. For the summer seasons, the water availability is not sufficient to explain the mean water release.

Table 1: Linear correlations between the mean release of the two seasons, the inflow and release at annual and seasonal scale and the initial storages (correlation between total release S_1 and total release S_2 = 0.15)

	Annual inflow	Annual release	Inflow S_1	Inflow S_2	Initial storage S_1	Initial storage S_2
Release S_1	0.80	0.87	0.86	0.49	0.49	-0.35
Release S_2	0.63	0.60	0.54	0.69	-0.17	0.32

Weekly and daily evolution

The analysis of the daily release shows that there is a weekly cycle with a minimum during the weekend (Figure 5a and Table 2). This weekly cycle is conditioned by the electricity

demand that varies during the week and is minimal during the weekend. There is a high correlation between the mean weekly release on weekdays and on weekend days (linear correlation of 0.82). Throughout the year, the variability of the daily release on weekdays is slightly higher than on weekend days (Table 2).

Table 2: Mean daily release and standard deviation of daily release for the observed period (independent on the type of day respectively dependent on the type of day, unit 1000 m^3)

Day type	Mean daily release	Standard deviation
Unconditioned	717	604
Release on week days	765	615
Release on weekend days	596	559

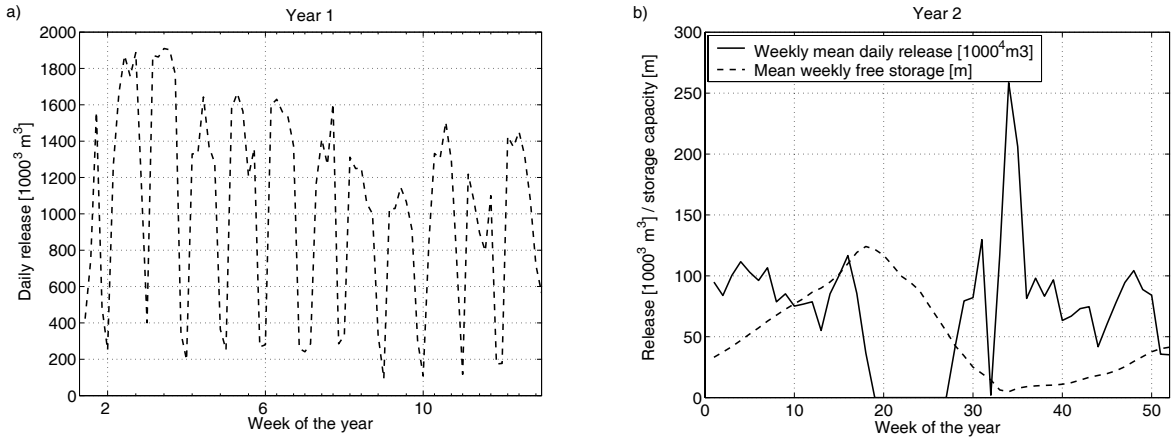

Figure 5: a) Daily release for one year of the observed period (first day of the week is Monday); b) weekly mean daily release and free storage capacity for another year (the free storage capacity corresponds to the difference of actual lake level and maximum admissible lake level)

During several years, weeks with zero release are observed. This can be due to water shortage and related economic considerations or to some technical reasons (maintenance work). There are also a few weeks with high release that is due to overfill conditions of the lake. Joint analysis of the daily release and the storage data helps identifying such situations where the daily release is presumably conditioned by management constraints rather than economic considerations. Figure 5b illustrates such a situation where the lake filling conditions a high mean daily release (week 34 in Figure 5b).

2.4 Management model

As mentioned before, the daily water release through the turbines is not only the result of the hydropower production strategy but takes into account some additional constraints such as the security plan or technical constraints. Accordingly, over some periods the water release is not directly determined by economic considerations. Therefore, the simulation model should account for a planned and an actual - possible or necessary – daily release. The development of a management model for the planned release has to be based on days where the release is not influenced by exceptional situations. The corresponding days are removed from the observed series through an appropriate data filtering.

2.4.1 Data filtering

The two types of situations where the water release is presumably not determined by economic considerations are the following: i) days where the water level in the lake is close to the maximum level and ii) days of zero release.

Critical high-level situations

A critical high-level situation occurs if the storage is close to its maximum level. This can lead to a forced release that is higher than interesting from an economic point of view. Such situations can be identified by joint analysis of storage and release (see section 2.1.2). This identification cannot follow any strictly objective criteria as the release in such situations is subject to the judgement of the dam manager. For the model development, we remove all days on which the release is significantly higher than the mean release, provided that the lake level at these days is close (within in a range of 2 m) to the maximum possible lake level (1975 m a.s.l.). The observed release on a given day is considered being significantly higher than the average value if the condition in Equation 3 is satisfied.

$$r_{n,obs} \in R_{except} \quad if\ r_{obs} > M_s + 2.5 * \sigma_s \tag{3}$$

where $r_{n,obs}$ is the observed release on day n, R_{except} is the set of filtered exceptional releases, M_s the mean observed release over season s ($s = S_1, S_2$) and σ_s the standard deviation of the observed daily release during season s. Applying this filtering, 30 days are removed from the observed data series.

Days with zero release

The objective of the filter process is to remove days with zero release that are not due to economic interests. The first step is to identify days of joint zero release and low lake level

(i.e. lower than 10 m of relative storage): In this case, the empty lake presumably determines the zero release. During normal management situations, the lake is never emptied completely in order to ensure a minimum electricity production[4]. Periods of zero storage are due to technical interventions. Such interventions can occur at any period of the year and induce a stop of hydropower production. These periods are however impossible to identify through an exclusively databased approach. A detailed investigation of historical management situations would be necessary. For the present study context, corresponding information was not available and the management model is developed filtering all days with zero release.

2.4.2 Simulation of planned release

Based on the results of the data analysis, a mixed deterministic-stochastic modelling approach is adopted: The deterministic part models the mean daily release, its seasonal variation and the mean weekly cycle.

The planned mean daily release is modelled separately for the two different seasons of the year. A daily mean distribution factor ϕ is introduced to model the weekly cycle. The stochastic component θ enables the reproduction of the variation of the observed daily release. The basic model can be expressed as follows (Equation 4 and 5).

$$r_n = M_s \phi_{s,j} + \theta_{n,s,j} \tag{4}$$

where r_n is the planned release through the turbines on day n, M_s the mean daily release during season s, $\phi_{s,j}$ the daily mean distribution factor where $j = 1$ if n is a weekend day and $j = 2$ if n is a weekday. $\theta_{n,s,j}$ is the residual of day n given season s and day type j.

At each time step, the corresponding planned storage ξ_n is calculated based on the continuity equation given the actual storage at the end of the day before (Equation 5).

$$\xi_n = v_{n-1} + x_n - r_n \tag{5}$$

where ξ_n is the planned storage at the end of day n, v_{n-1} the actual storage at the end of the day $n-1$ and x_n the net inflow during the day n (equal to inflow minus loss through evaporation and infiltration).

[4] Economic interests condition this management principle. The periods during which the accumulation lake is almost empty correspond to periods where only little hydropower is available in the European Alps (just before the start of the melt season in spring). Accordingly, these periods are the most interesting ones from an economic point of view (electricity demand is high but the offer is low).

Parameter estimation

All the model parameters are calculated based on the filtered observed data and conditional on days with release ($r_{n,obs} > 0$). The seasonal mean daily release is calculated for each of the two seasons (Equation 2).

The release is significantly lower during weekend days than during weekdays. The daily mean release distribution factor $\phi_{s,j}$ expresses the relationship between these two types of days and is calculated according to Equation 6.

$$\phi_{s,j} = \frac{m_{s,j}}{M_s} \tag{6}$$

where $m_{s,j}$ is the mean daily release given seasons s and day type j. We define $\sigma_{s,j}$ as the standard deviation of the corresponding daily releases and σ_s the standard deviation given season s. Based on the above definitions, M_s and σ_s have to meet the following conditions (Equation 7 and 8).

$$M_s = \frac{2}{7} m_{s,1} + \frac{5}{7} m_{s,2} \tag{7}$$

$$\sigma_s^{\,2} = \frac{2}{7}(\sigma_{s,1}^2 + m_{s,1}^2) + \frac{5}{7}(\sigma_{s,2}^2 + m_{s,2}^2) - (\frac{2}{7} m_{s,1} + \frac{5}{7} m_{s,2})^2 \tag{8}$$

The analytical development of Equation 8 is detailed in Appendix 1.

The choice of constant $\phi_{s,j}$ throughout each season has been based on a preliminary analysis that showed these values are approximately constant for each season (Figure 6).

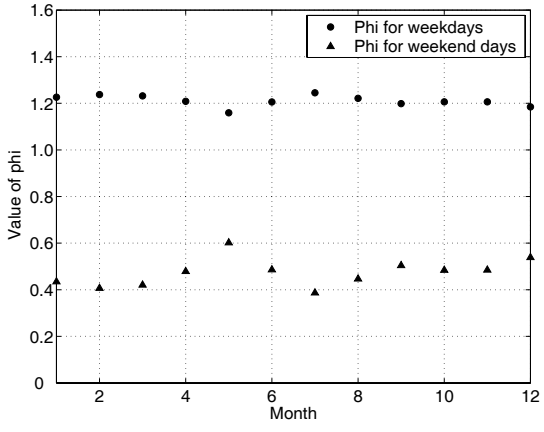

Figure 6: Monthly values of release distribution factors $\phi_{k,j}$ where k = 1,2, .., 12 is a given month

Estimation of daily residuals

The daily release residuals are modelled by random variables, the distributions of which depend on the season *s* and the type of day *j*. The empirical residuals are calculated based on Equation 4, replacing the planned release r_n by the observed release $r_{n,obs}$. The analysis of the observed residuals shows that the empirical distributions are left skewed.

These empirical distributions are modelled with a Log-Weibull distribution of type II (Equation 9). This theoretic distribution enables the reproduction of the left skew and is bounded. This last condition is necessary to avoid extreme residual values for the simulation of the daily planned release according to Equation 4.

$$H(\theta) = 1 - \exp\{-\left[-\ln(1-\theta)/a\right]^b\}, \quad 0 < \theta < 1 \tag{9}$$

where $H(\theta)$ is the distribution function of the random variable θ. This distribution has two parameters: $a > 0$ is the scale parameter and $b > 0$ the shape parameter. The estimation of these two parameters is presented in Appendix 2. The estimated Log-Weibull distributions fit well the observed residuals for all seasons and day types (see Table 3 and Figure 7).

Table 3: Estimated parameter values of the Log-Weibull distribution and the coefficient of determination R^2 of the empiric frequency versus theoretic frequency

Period	a	b	R^2
S_1, weekend	0.38	1.37	0.993
S_1, week days	0.84	1.44	0.996
S_2, weekend	0.31	1.04	0.959
S_2, week days	0.40	1.17	0.998

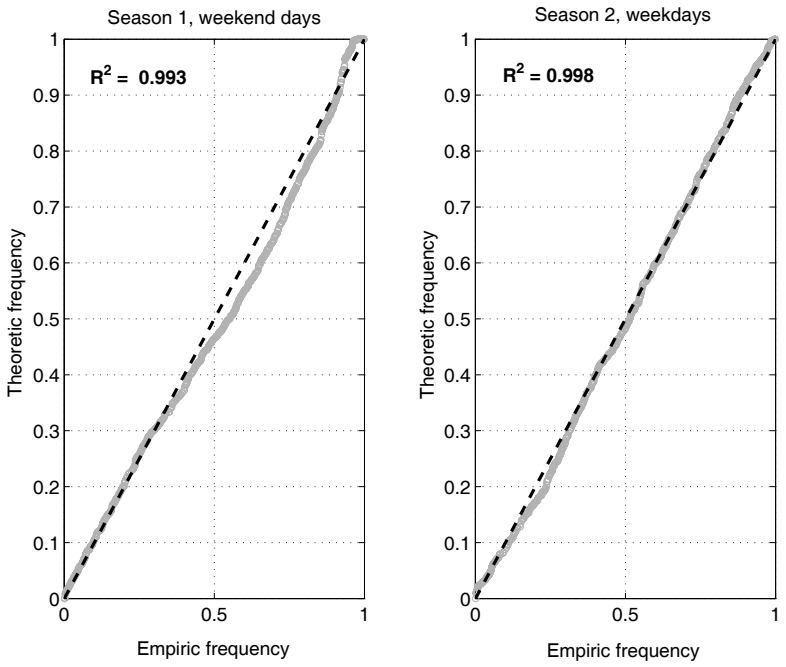

Figure 7: Plot of empirical distributions versus fitted distributions for season 1 and weekend days and season 2 and weekdays

2.4.3 Simulation of actual release

Management constraints

The simulated planned release and storage are compared to the management constraints in order to determine the actual possible or necessary release and the corresponding storage. Three types of constraints and objectives have to be considered:

- Maximum release capacity
- Dam security: highest acceptable water level
- Water storage objective: upper and lower daily storage objectives

The maximum release is conditioned by the hydropower production system and is currently fixed at 34.5 m^3/s. This corresponds to the maximum possible release through the turbines at the first production level. The highest acceptable water level for normal water storage is 1975 m a.s.l. and corresponds to a water level that is 1 m lower than the absolute height of the dam crown (1976 m a.s.l.). The water storage should never be higher than this maximum level. For every day management situations the maximum objective water level is fixed to 1973 m a.s.l. This level is 2 m lower than the highest acceptable level representing therefore a management margin of around $4 \cdot 10^6 m^3$ (the maximum daily inflow is about $6 \cdot 10^6 m^3$ and the maximum daily outflow through the turbines is about $3 \cdot 10^6 m^3$).

If the water storage reaches a level of 1975.1 m a.s.l. (the so-called emergency level), the emergency plan is launched for controlled spillway activation (see Figure 8).

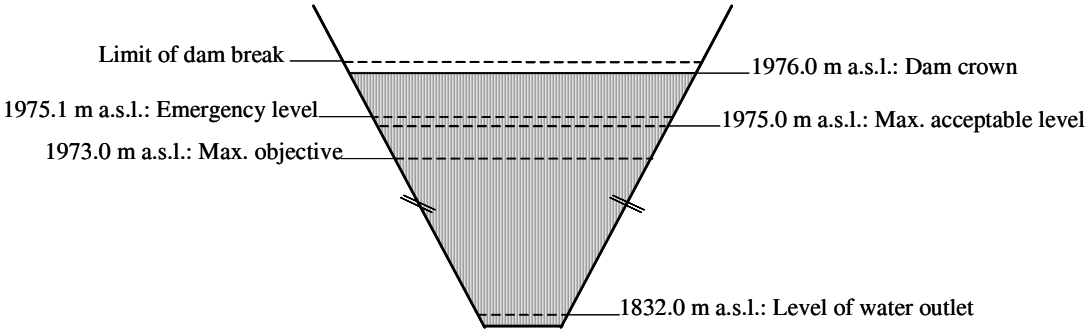

Figure 8: Critical lake levels

The water management throughout the year is guided by the water level target curves that correspond to the daily minimum and maximum water level observed in all management years since the dam construction. The observed variation of the storage in the past is the result of the underlying management strategies. These strategies are the outcome of a long management experience and we can assume that they represent the optimal lake filling strategy for the given hydro-climatic and socio-economic context. This assumption is enhanced by the fact that the lake filling degree of the Mauvoisin hydropower plant is strongly correlated to the filling degree of all accumulation lakes for hydropower production in the Swiss Alps. For the years 1996 to 1999 the linear correlation between the mean monthly filling degree of the Mauvoisin lake and all Swiss lakes (Swiss Federal Office for Energy, 1999) is 0.97.

Actual release: outflow and storage operator

The actual release through the turbines on day n, r_{na}, is a function of the planned release, the available water, the storage target curves and the actual release through the spillway (Equation 10).

$$r_{na} = f(x_n, r_n, r_{nspill}, v_{n-1}, VU_n, VL_n)$$

Constraints:

$$r_{na} \in [0, r_{max}]$$
$$r_{nspill} \in [0, r_{spillmax}] \qquad (10)$$
$$v_n \in [0, v_{max}]$$

where r_{max} is the maximum daily release through the turbines that equals $2.981 \cdot 10^6 m^3$, v_{max} the maximum acceptable storage that equals $204.440 \cdot 10^6 m^3$ and r_{nspill} is the daily release through the spillway. VU_n (1000 m^3) respectively VL_n (1000 m^3) are the upper respectively the lower storage objectives on day n. The spillway is only activated if the planned storage for a given day is higher than the storage corresponding to the emergency level V_{emerg} that equals $204.779 \cdot 10^6 m^3$. The exact value of the r_{nspill} is fixed in the emergency plan.

Based on the management constraints, the actual release and storage can be calculated according to the following outflow and storage operators (Equation 11 and 12).

$$r_{na} = \begin{cases} 0 & if\ \ v_{n-1} + x_n \le VL_n \\ v_{n-1} + x_n - VL_n & if\ \ \xi_n \le VL_n < v_{n-1} + x_n \\ r_n & if\ \ VL_n < \xi_n < VU_n \\ v_{n-1} + x_n - VU_n & if\ \ VU_n \le \xi_n < V_{emerg}\ \ and\ \ v_{n-1} + x_n - VU_n \le r_{\max} \\ r_{\max} & if\ \ V_{emerg} \le \xi_n \end{cases} \tag{11}$$

$$v_n = \begin{cases} v_{n-1} + x_n & if\ \ v_{n-1} + x_n \le VL_n \\ VL_n & if\ \ \xi_n \le VL_n < v_{n-1} + x_n \\ \xi_n & if\ \ VL_n < \xi_n < VU_n \\ VU_n & if\ \ VU_n \le \xi_n < V_{emerg}\ ,\ v_{n-1} + x_n - VU_n \le r_{max} \\ v_{n-1} + x_n - r_{max} - r_{nspill} & if\ \ V_{emerg} < \xi_n \end{cases} \tag{12}$$

2.5 Results

A continuous simulation is carried out for the available inflow data. The initial storage is set to the measured storage on 1 April 1987. The resulting series of daily water release and lake level are compared to the observed values in order to judge de simulation quality. As the model has a stochastic component, 1000 simulation runs are carried out in order to compare the obtained distributions of release and storage to the observed data. Based on the daily values of release and storage, the 80 % and 90 % confidence intervals are estimated. 80 % respectively 90 % of the corresponding observed values should lie inside these confidence intervals.

The estimated confidence intervals of the daily water release predict well the observed data (Table 4). The observed storage evolution is poorly covered by the simulated confidence intervals; only 27 % of all observed values lie inside the predicted 80 % confidence interval (Table 4). This apparently meagre simulation quality is essentially due to the model inability to reproduce special management situations resulting for example in exceptional emptying of the lake. The induced difference in observed and simulated water storage is propagated

throughout the management year until the management returns to the long-term management strategy (see an example in Figure 9b). Such an exceptional emptying occurred four times over the simulation period in the summers 1990, 1991, 1995 and 1998. For classical management years, the model predicts well the observed lake level evolution (Figure 9a).

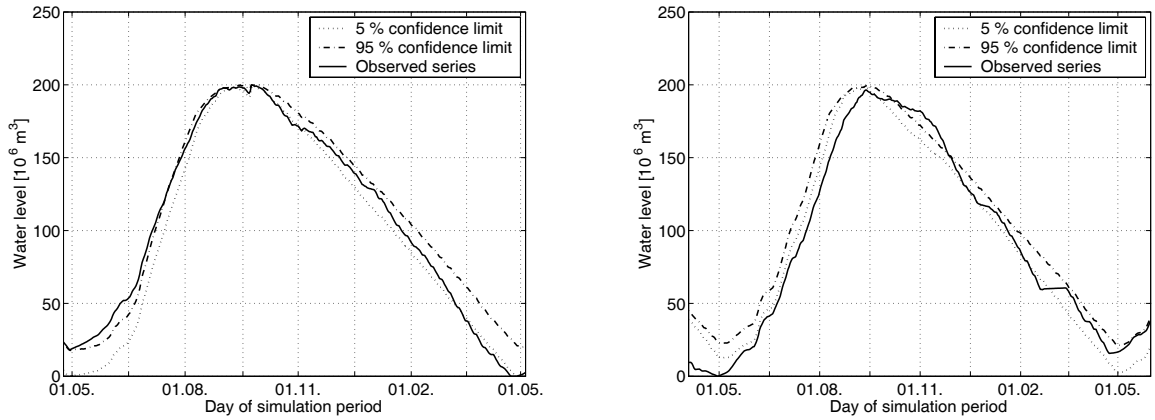

Figure 9: Observed storage and simulated 5 % respectively 95 % confidence limits; left: year with good simulation quality; right: year with exceptional lake emptying (as a result the observed storage lies outside the confidence interval over the first 6 months)

We also apply two formal simulation quality criteria classically used in hydrological modelling, the so-called Nash value (Nash and Sutcliffe, 1970) R^2_N (Equation 13) and the bias B_N (Equation 14).

$$R_N^2 = 1 - \sum_{n=1}^{N} (y_n - x_n)^2 \cdot [\sum_{n=1}^{N} (y_n - \overline{y_n})^2]^{-1} \tag{13}$$

$$B_N = \sum_{n=1}^{N} (x_n - y_n) \cdot (\sum_{n=1}^{N} y_n)^{-1} \tag{14}$$

where y_n is the observed and x_n the simulated quantity on day n, n = 1, .., N. $\overline{y_n}$ is the mean value of y_n.

The bias measures the total difference between the observed and the simulated quantity. The Nash value compares the error of the used model to the one resulting from the simplest possible model that is the mean value $\overline{y_n}$. If the used model is significantly better, the R^2_N value is close to 1. The value of this criterion strongly depends on the highest observed respectively simulated quantities – overemphasizing therefore certain periods of the year. Using the log value of the y_n and x_n avoids this problem. The corresponding criterion value is called R^2_{Nlog}. Because of the stochastic component of the daily release, the R^2_N and R^2_{Nlog} are calculated for the corresponding cumulated series starting at the beginning of each management year (see an example in Figure 10).

Table 4: Percentage of observed values contained in the 80 % respectively the 90 % confidence intervals

	Mean criteria value			Confidence intervals	
	R^2_N	R^2_{Nlog}	B_N	80 %	90 %
Daily actual release	0.96	0.91	0.00	85.3	91.0
Daily actual storage	0.93	0.72	-0.07	27.2	33.2

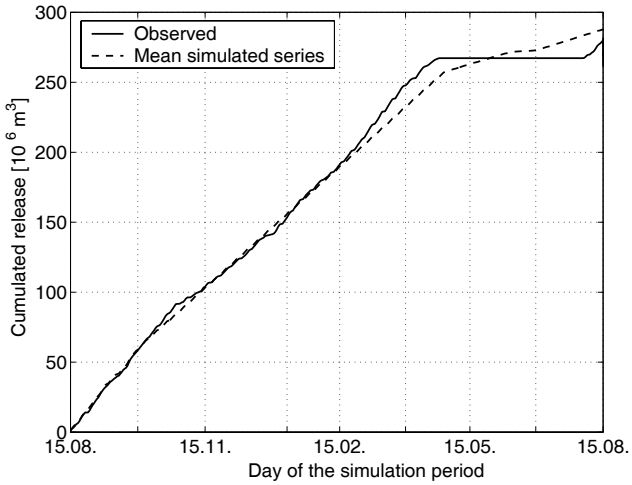

Figure 10: Cumulated daily mean release, observed and mean simulated series for one management year

The water release has been designed to reproduce the observed mean and variance of the daily release at annual and seasonal resolution for weekdays and weekend days. These conditions are however assigned to the planned release. As lake level target-curves are introduced in the simulation model, the mean and standard deviations of the actual release slightly differ (Table 5). Note that the bias of the simulated actual release for the different temporal resolutions does not exceed 1 % and that the observed standard deviations are reasonably well respected by the simulated series.

Table 5: Mean and standard deviation of the daily release at different aggregation levels for the observed and the simulated series; the simulated values correspond to the mean of 1000 simulations (unit: 1000 m^3)

	Mean daily release			Daily standard deviation	
	Observed	Simulated	Bias	Observed	Simulated
Annual mean release	717	720	0.00	604	630
Season 1	901	907	0.01	589	630
Season 2	295	291	-0.01	389	367
Weekend days	596	602	0.01	559	583
Weekdays	765	767	0.00	615	642

The R^2_N and R^2_{Nlog} values of the water level (Table 4) show that the model has a good overall performance but is deficient during low-level situations (R^2_{Nlo} = 0.72). During high-level situations, the water management is strongly dependent on the water cycle, whereas during low-level situations, economic interests and technical requirements induce a difficult-to-predict water release management. Further investigation about the management strategies during these periods could improve the simulation. The high R^2_N and R^2_{Nlog} values of the simulated actual water release confirm the overall model ability to simulate the daily release (Table 4). For a few years, the total annual release is however completely over- or underestimated resulting in a low R^2_N if calculated on the series of total annual release (mean R^2_N = 0.55 for annual observed and simulated release).

2.6 Conclusion

The simulation of the water management of an alpine hydropower plant is confronted with the major problem that the management of such systems does generally not follow some deterministic rules. The daily hydropower production depends on the electricity market and accordingly the water release is a function of difficult to determine factors of demand and offer depending on the physical system and on the socio-economic context. A detailed analysis of the available hydropower production data showed however that the system evolution can be simulated considering essentially the mean seasonal hydropower offer (the water availability) and assembling all other factors in a stochastic component of the daily release.

The resulting mixed deterministic-stochastic modelling approach enables the simulation of daily water releases without considering explicit management rules. The simulation shows a good reproduction of the current water management strategies for the Mauvoisin hydropower plant.

The long-term management experience is taken into account through the inclusion of explicit management constraints in the simulation model. These constraints are essentially related to

the target lake level at a given calendar day. They could be refined in collaboration with the end user (i.e. the hydropower production company) and possibly be parameterised.

It should be kept in mind that although the developed simulation tool is highly case study specific, it could potentially be transferred to other hydropower plants in the Alps. The underlying management strategies can be supposed to be comparable for most accumulation hydropower plants fed by highly glacierized catchments: All hydropower production companies sell the electricity on the same European electricity market and the high mountainous catchments in this area can be supposed to have a similar hydrological regime.

Acknowledgements

We wish to thank the Forces Motrices de Mauvoisin for having made available the hydropower production data. We also wish to thank Prof. R. Krzysztofowicz from the University of Virginia for his help in the model development. This work is part of the SWURVE (Sustainable Water: Uncertainty, Risk and Vulnerability in Europe) project, funded under the EU Environment and Sustainable Development programme, grant number EVK1-2000-00075. The Swiss part of this project was funded by the Federal Office for Education and Science, contract number 00.0117.

References

Dudley, N.J., 1992. Water allocation by markets, common property and capacity sharing - companions or competitors? Natural Resources Journal, 32(4): 757-778.

Nash, J.E. and Sutcliffe, J.V., 1970. River flow forecasting through conceptual models. Part I, a discussion of principles. Journal of Hydrology, 10(3): 282-290.

Spreafico, M., Weingartner, R. and Leibundgut, C., 1992. Atlas hydrologique de la Suisse. Service Hydrologique et Géologique National (SHGN), Bern.

Swiss Federal Office for Energy, 1999. Statistique suisse de l'électricité 1999, Bern.

SwissTopo, 1997. Digital National Maps of Switzerland - PM25, Waber, Switzerland.

Appendix 1: Calculation of the seasonal standard deviation σ_s

The variance σ_s of the daily mean release during season s can be written as:

$$\sigma_s^2 = Var(r_n \mid n \in s) = E(r_n^2 \mid n \in s) - E^2(r_n \mid n \in s) \tag{A1.1}$$

where r_n is the daily mean release on a given day n belonging to season s.

The second part of the right hand side of Equation A1.1 corresponds the square of the seasonal mean release M_s that can be written as:

$$E(r_n \mid n \in s) = M_s = \frac{2}{7} m_{s,1} + \frac{5}{7} m_{s,2} \tag{A1.2}$$

The first part of the right hand side of Equation A1.1 can be written as:

$$\begin{aligned} E(r_n^2 \mid n \in s) &= \frac{1}{N} \sum_{n=1}^{N} r_n^2 \\ &= \sum_{j=1}^{2} [\frac{N_j}{N} E(r_n^2 \mid n \in s, n \in j)] \end{aligned} \tag{A.1.3}$$

Based on the definition of the variance, Equation A1.3 can be written as:

$$E(r_n^2 \mid n \in s) = \sum_{j=1}^{2} \{\frac{N_j}{N} [Var(r_n \mid n \in s, n \in j) + E^2(r_n \mid n \in s, n \in j)\} \tag{A1.4}$$

Defining $\sigma_{s,j}$ as the variance of the daily release during season s and for day type j and $m_{s,j}$ the corresponding mean value, Equation A1.4 can be written as:

$$\sigma_s^2 = \frac{N_1}{N} (\sigma_{s,1}^2 + m_{s,1}^2) + \frac{N_2}{N} (\sigma_{s,2}^2 + m_{s,2}^2) \tag{A1.5}$$

Approximating N_1/N by $2/7$ and N_2/N by $5/7$, it follows from Equations A1.1 to A1.5:

$$\sigma_s^2 = \frac{2}{7} (\sigma_{s,1}^2 + m_{s,1}^2) + \frac{5}{7} (\sigma_{s,2}^2 + m_{s,2}^2) - (\frac{2}{7} m_{s,1} + \frac{5}{7} m_{s,2})^2 \tag{A1.6}$$

Appendix 2: Estimation of the parameters of a Log-Weibull distribution

Let W be a random variable with the distribution function $G(w)$ where w is a realisation of the random variable W. Let $G(w)$ be a member of the family of Weibull distributions (Equation A2.1):

$$G(w) = p(W \le w) = 1 - \exp[-(w/\alpha)^{\beta}\ ], \qquad w \ge 0 \tag{A2.1}$$

where $p(W \le w)$ is the probability that W does not exceed w. $\alpha > 0$ is the scale parameter and $\beta > 0$ is the shape parameter of the distribution function.

There is a closed form inverse of $G(w)$, for any probability p the equation $p = G(w)$ can be solved for $w = G^{-1}(p)$:

$$G^{-1}(p) = \alpha \cdot [-\ln(1-p)]^{1/\beta}, \quad 0 < p < 1 \tag{A2.2}$$

The parameters α and β of the Weibull distribution can be estimated through a linear regression as illustrated through Equation A2.3 and A2.4:

$$y = G^{-1}(p) \tag{A2.3}$$

$$\ln(y) = \ln(\alpha) + 1/\beta \cdot \ln[-\ln(1-p)] \tag{A2.4}$$

where p is estimated by the empiric probability.

In the presented application, the empiric distributions are negatively skewed. We therefore use a Log-Weibull distribution of the type II. Let Z be a random variable that follows a Weibull distribution with the parameters α and β. Let θ be a random variable that is a function of Z (Equation A2.5).

$$Z = -\ln(1-\theta) \tag{A2.5}$$

In this case, the distribution $H(\theta)$ is a Log-Weibull distribution of the type II (Equation A2.6).

$$H(\theta) = 1 - \exp\{-[-\ln(1-\theta)/a]^{b}\}, \quad 0 < \theta < 1 \tag{A2.6}$$

There is a closed form inverse of $H(\theta)$ (Equation A2.7) and the parameters a and b can be estimated as for the Weibull distribution.

$$\theta = H^{-1}(p) = 1 - \exp\{-a \cdot [-\ln(1-p)]^{1/b}\}, \quad 0 < p < 1 \tag{A2.7}$$

Chapter 3

A conceptual glacio-hydrological model for high mountainous catchments[1]

Abstract

In high mountainous catchments, the spatial precipitation and therefore the overall water balance is generally difficult to estimate. The present paper describes the structure and calibration of a semi-lumped conceptual glacio-hydrological model for the joint simulation of daily discharge and annual glacier mass balance that represents a better integrator of the water balance. The model has been developed for climate change impact studies and has therefore a parsimonious structure; it requires three input times series - precipitation, temperature and potential evapotranspiration – and has 7 parameters to calibrate. A multi-signal approach considering daily discharge and – if available - annual glacier mass balance has been developed for the calibration of these parameters. The model has been calibrated for three different catchments in the Swiss Alps having glaciation rates between 37 % and 52 %. It simulates well the observed daily discharge, the hydrological regime and some basic glaciological features, such as the annual mass balance.

[1] This chapter has been submitted for publication to Hydrology and Earth System Sciences: Schaefli, B., Hingray, B. and Musy, A., 2004. A conceptual glacio-hydrological model for high mountainous catchments.

3.1 Introduction

Discharge estimation from highly glacierized catchments has always been a key hydrological issue in the Swiss Alps, especially for the design and management of hydropower plants and for flood risk studies. However, the interest of scientists and civil engineers in this issue drastically decreased after the main period of dam construction in the middle of the last century. Catchments subject to a glacier regime show a very constant annual hydrological cycle, the start and the end of the melting season varying little from year to year. For hydroelectricity production, the water management therefore rather relies on the long-term experience than on discharge simulations. In the nineties, land managers started asking for hydrological models able to simulate runoff from these snow- and ice melt affected catchments for flood risk studies. In this context, the main interest was focused on rainfall and snowmelt induced processes and on event-based discharge simulation (e.g. Consuegra et al., 1998). Recently, continuous runoff simulation from glacierized catchments has experienced a regain of interest among scientists, hydropower and land managers, in particular in the context of climate change impact studies (see, e.g., Willis and Bonvin, 1995; Singh and Kumar, 1997; Braun et al., 2000).

In high mountainous catchments, discharge simulation is confronted with a major challenge: the available meteorological data is scarce – at high altitudes nearly inexistent - and the spatial variability of the meteorological phenomena very strong. A good spatial interpolation of corresponding data series is therefore difficult and the prevailing extreme conditions imply an important measurement uncertainty. The objective of the present study was to develop a hydrological model that can be applied to these data scarce catchments - given that discharge data is available for calibration - and that can be used for climate change impact studies (see Schaefli et al., 2005). This context imposes a set of modelling constraints, the most important being that the model input variables have to be derivable from current GCMs (Global Circulation Models) outputs. This means that the model should be parsimonious in order to reduce the number of meteorological input variables to the strict minimum.

The mentioned difficulties in spatial interpolation of the meteorological time series are not easy to overcome and especially area-average precipitation is an important source of uncertainty for runoff and water balance simulation. In high mountainous catchments, the glaciers represent the most important water storage reservoir and for water balance simulation, any under- or overestimation of the area-average precipitation can be compensated by simulated ice melt. Glacier mass balance estimated over long time periods is thus a good integrator of the overall water balance of the catchment. Corresponding observed data can be obtained for glaciers in all ice-covered regions of the world (Haeberli et al., 2003). Accordingly, the structure of the developed hydrological model has been chosen in order to enable a multi-signal calibration based on observed discharge and glacier mass balance data.

This paper presents the hydrological model that has been developed based on the above considerations. The need for a parsimonious structure led us to the development of a

conceptual, reservoir-based model having as input variables temperature, precipitation and potential evapotranspiration. The model simulates well the daily discharge, the hydrological cycle and some basic glaciological features as illustrated through the application to three glacierized catchments in the Swiss Alps representing different glaciation rates and hydro-climatic areas. Based on one of these case studies, the calibration of the model and its behaviour is presented in detail. The integration of glacier mass balance data in the calibration process is discussed and corresponding results for the simulation of the mass balance as well as of other glaciological characteristics is illustrated. All these results are directly dependant on the estimated area-average precipitation. Its relationship with the simulated discharge and mass balance is therefore investigated before presenting the main conclusions of this study.

3.2 Model description

The hydrological discharge simulation is carried out at a daily time step through a conceptual, semi-lumped model called GSM-SOCONT (Glacier and SnowMelt – SOil CONTribution model). The catchment is represented as a set of spatial units, each of which is assumed to have a homogeneous hydrological behaviour. For each unit, meteorological data series are computed from data observed at neighbouring meteorological stations. Based on these series, snow accumulation and snow- and ice melt are simulated. A reservoir based modelling approach is used to simulate the hydrological response, i.e. the rainfall and melt water – runoff transformation of each unit (Figure 1). The runoff contributions of all units are added to provide the total discharge at the outlet of the entire catchment. No routing between the spatial units and the river outlet is carried out. In the present modelling context, this simplification is justified by the fact that the studied catchments are relatively small and have rather steep slopes, the runoff delay due to routing in the river network is thus much smaller than the given time step of one day.

In the following, the different modelling steps are described in detail. Additionally, the glacier mass balance computation based on the output of the snow accumulation and snow- and ice melt submodel is presented.

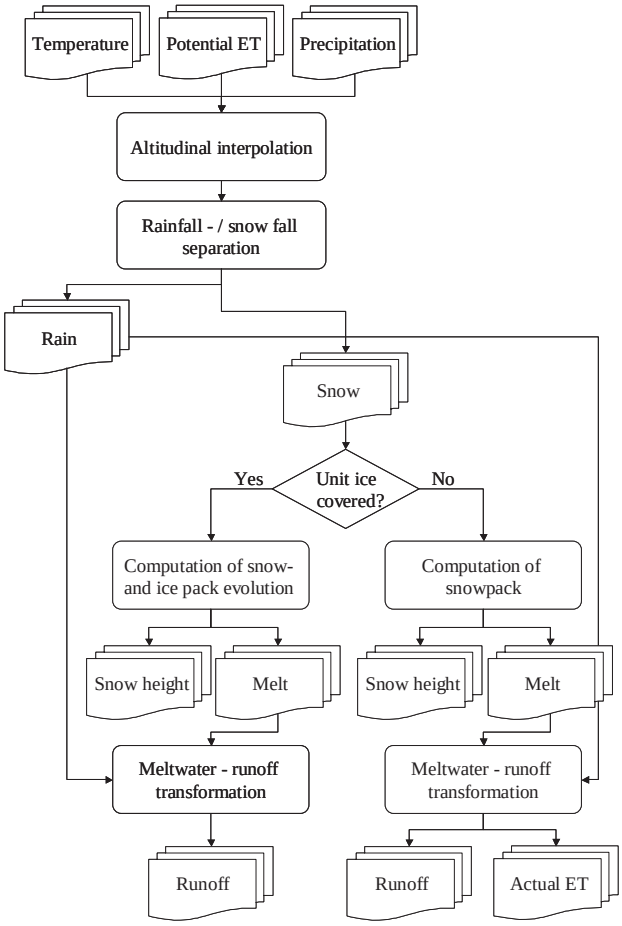

Figure 1: Hydrological model structure for one spatial unit (ET = evapotranspiration)

3.2.1 Catchment discretization

The model has two levels of discretization. The first level corresponds to the separation between the ice-covered part of the catchment and the not ice-covered part. This separation is completed based on a topographic map at the scale 1: 25'000, (SwissTopo, 1997). Each of the two areas is characterised by its surface and its hypsometric curve. The surface area of the ice-covered part is supposed to be constant throughout a given short-term simulation period (a few years). Even for short simulation periods (several years), this assumption is a rough approximation; the ice-covered area varies throughout the year and from year to year. In extreme years, glacier snouts can retire or advance considerably. In the Swiss Alps more than 100 m of length change within single years have been observed (e.g. Herren et al., 2001). Such an extreme variation of the snout position concerns however only a small fraction of the total area of a glacier.

The second level of discretization consists in dividing each part of the catchment in a set of elevation bands. Precipitation and temperature time series and the corresponding runoff discharge are computed separately for each of the bands. The runoff model depends on

whether the band forms part of the ice-covered area or not. For the total catchment, the mean specific runoff Q (mm d^{-1}) on a given day is therefore:

$$Q = \frac{1}{a_c} \sum_{i=1}^{2} \sum_{j=1}^{n_i} a_{i,j} \cdot Q_{i,j} \tag{1}$$

where i is an index for each of the two parts of the catchment and j an index for each of the n_i elevation bands in part i. $a_{i,j}$ (km^2) is the area of an elevation band j belonging to the catchment part i and the $Q_{i,j}$ (mm d^{-1}) the mean daily specific runoff from this spatial unit. a_c (km^2) is the area of the entire catchment.

3.2.2 Meteorological data pre-processing

The precipitation and temperature time series are interpolated for each elevation band according to its mean elevation. The interpolation is based on an altitude dependent regression of the observations at meteorological measurement stations located in or nearby the study catchments. For the temperature time series a constant lapse rate is applied to the temperature series measured at the closest meteorological station. This lapse rate is fixed to –0.65 °C per 100 m of altitude increase (the mean gradient of observed temperature series in the studied area). The precipitation increase with altitude is set to a fixed percentage of the amount observed at the used measurement station. For a given catchment, this constant is estimated based on regressions between the mean annual precipitation amounts observed at several precipitation measurement stations located around the catchment.

3.2.3 Snow accumulation, snow- and ice melt

For each elevation band of the catchment, the temporal evolution of the snowpack is computed through an accumulation and a melt model. The aggregation state of precipitation is determined based on a simple temperature threshold.

$$\begin{aligned} P_{snow} &= P_{tot}\,, \quad P_{liq} = 0 \qquad T \le T_0 \\ P_{snow} &= 0, \qquad P_{liq} = P_{tot} \qquad T > T_0 \end{aligned} \tag{2}$$

where P_{tot} (mm d^{-1}) is the total precipitation on a given day, P_{snow} (mm d^{-1}) the solid and P_{liq} (mm d^{-1}) the liquid precipitation. T (°C) is the mean daily air temperature and T_0 is the threshold temperature that is set to 0 °C.

This threshold temperature could be calibrated using joint precipitation and temperature measurements and corresponding aggregation state observations. At the automatic weather stations of the Swiss Meteorological Institute, the instantaneous form of precipitation (liquid/ solid or mixed) is recorded. This data could be used to determine for each measurement

station a threshold temperature below which precipitation is almost always solid. It is noteworthy that this empiric threshold can be different from the threshold temperature above which precipitation is almost always liquid. Rohrer et al.(1994) indicate that for example for the Davos station (located at 1590 m a.s.l.) these two thresholds are respectively 0°C and 1°C. Considering a unique threshold, Rohrer et al.(1994) have estimated its value for the different Swiss stations and found values between 0.0°C and 1.5°C for hourly precipitation and temperature data. These thresholds cannot be directly used for snow-/ rainfall separation at a different time step. Rohrer et al.(1994) found for the Davos station that using mean daily data leads to a misclassification of 13.8 % of all events. An additional difficulty arises if these thresholds have to be interpolated spatially for a given spatial aggregation level.

The threshold temperature could also be calibrated together with all other hydrological parameters (see Section 4). In a semi-automatic approach as the one proposed in the present paper, such a calibration is however made difficult by the fact that the model clearly suffers from over-parameterisation as any lack of rainfall or of accumulated snow can be equilibrated by ice melt. We have tested its calibration in other model applications using an automatic optimisation method (e.g., Schaefli et al., 2004) but could not find any unique best value. Based on these considerations, the temperature threshold has been set to 0 °C.

The potential snowmelt $M_{p,snow}$ (mm d^{-1}) is computed according to a degree-day approach:

$$M_{p,snow} = \begin{cases} a_{snow}(T - T_m) & T > T_m \\ 0 & T < T_m \end{cases} \quad (3)$$

where a_{snow} is the degree-day factor for snowmelt (mm°$C^{-1}d^{-1}$) and T_m the threshold temperature for melting that is set to 0 °C. The actual snowmelt M_{snow} (mm d^{-1}) is computed depending on the available snow height H_s (mm water equivalent).

In the past, comparisons of snowmelt models showed that this simple, empirical approach has an accuracy comparable to more complex energy budget formulations (WMO, 1986). At a small time step, such as a daily time step, it should however only be used in connection with an adequate snowmelt-runoff transformation model (Rango and Martinec, 1995) rather than considering the catchment runoff being directly equal to the computed snowmelt.

Recent work shows that the use of the degree-day method is justified more on physical grounds than previously has been assumed (Ohmura, 2001). The incorporation of radiation data into the basic degree-day equation has been shown to give better results for snowmelt estimations (Kustas and Rango, 1994). However, data scarcity in high mountainous catchments and the need of a parsimonious model structure imposed by the presented modelling context prevented us from applying such a more complex approach.

For the ice-covered spatial units, the same degree-day approach is used for the ice melt computation, replacing all subscripts *snow* of Equation 3 by the subscript *ice*. For each elevation band, the actual ice melt M_{ice} (mm d^{-1}) is calculated depending on the snowpack, assuming that there is no ice melt if the glacier surface is covered by snow. As mentioned

before, the ice storage is assumed to be infinite. The snow accumulation and snow- and ice melt computation submodel has 2 parameters to calibrate, the degree-day factors for snow a_{snow} and for ice a_{ice}.

In comparable models, several authors use three different aggregation states of accumulated water, i.e. snow, ice and firn, a transition state between the two previous (see, e.g., Baker et al., 1982; Klok et al., 2001). We have shown that for the analysed hydro-climatic area, the use of firn does not improve neither the discharge nor the mass balance simulation (Schaefli et al., 2004; Schaefli, 2005). For these studies, the firn evolution was modelled as follows: At the end of each hydrological year (30th September), the snow that has fallen during the year but not melted is added to the firn pack. On a given spatial unit, firn melt only occurs if the snow pack has disappeared and ice melt occurs if the snow and firn packs have disappeared. Using a powerful global optimisation method (Schaefli et al., 2004), the calibration results obtained using only two aggregation states are generally better than for models that use the additional firn type. This result is obtained if the model is calibrated based only on discharge data or based on discharge and mass balance data (Schaefli et al., 2004; Schaefli, 2005). We assume that this result is due to the over-parameterisation of the model with respect to the available data.

3.2.4 Runoff model

Ice-covered area

For the part of the catchment that is covered by glacier or isolated ice patches, the runoff model consists of a simple linear reservoir approach inspired by the model presented by (Baker et al., 1982) who proposed to simulate glacier runoff through three different linear reservoirs representing snow, firn and ice. The present model considers only two different aggregation states of accumulated water (see previous section) and accordingly, only two linear reservoirs are used, one for snow and one for ice.

The general linear reservoir equation for the snow reservoir can be written as follows (Equation 4). For the ice reservoir, all subscripts *snow* of Equation 4 are replaced by the subscript *ice*.

$$Q_{snow}(t_{i+1}) = Q_{snow}(t_i) \cdot e^{-\frac{t_{i+1}-t_i}{k_{snow}}} + [P_{liq,snow}(t_{i+1}) + M_{snow}(t_{i+1})] \cdot (1 - e^{-\frac{t_{i+1}-t_i}{k_{snow}}}) \quad (4)$$

where $Q_{snow}(t_i)$ (mm d^{-1}) is the discharge from the snow reservoir at time step t_i and $Q_{snow}(t_{i+1})$ the discharge at the subsequent time step. k_{snow} (d) is the time constant of the reservoir. $P_{liq,snow}$ (mm d^{-1}) is the liquid precipitation falling on snow.

The total runoff from the ice-covered catchment area corresponds to the sum of the ice and snowmelt runoff components. The runoff model for the ice-covered area has 2 parameters to calibrate, namely k_{ice} and k_{snow}.

Area not covered by ice

For each elevation band of this part of the catchment, an equivalent rainfall P_{eq} (mm d^{-1}) corresponding to the sum of liquid precipitation and snowmelt is computed (Equation 5).

$$P_{eq} = P_{liq} + M_{snow} \tag{5}$$

The equivalent rainfall-runoff transformation in this part of the catchment has to take into account soil infiltration processes and direct runoff. It is carried out through a conceptual reservoir-based model named SOCONT developed by Bérod (1994) and similar to the GR-models (Edijatno and Michel, 1989). It is composed of two reservoirs, a linear reservoir for the slow contribution of soil and underground water and a non-linear reservoir for direct runoff. The equivalent rainfall is divided into infiltrated and effective rainfall, supplying water to the slow respectively the direct runoff reservoir.

The slow reservoir has two possible outflows, the base flow Q_{base} and actual evapotranspiration ET. The effective rainfall as well as the actual evapotranspiration is conditioned by the filling rate S_{slow}/A of the slow reservoir according to the following equations.

$$P_{eff} = P_{tot} \cdot (S_{slow} / A)^{y} \tag{6}$$

$$ET = ET_0 \cdot (S_{slow} / A)^{x} \tag{7}$$

where ET (mm d^{-1}), ET_0 (mm d^{-1}), P_{eff} (mm d^{-1}) and P_{tot} (mm d^{-1}) are the actual and potential evapotranspiration, the effective and total rainfall respectively. In the present application, the total rainfall corresponds to the equivalent rainfall. x and y are exponents to be calibrated. A (mm) is the maximum storage capacity of the reservoir and S_{slow} (mm) the actual storage. The base flow Q_{base} (m^3/s) is related linearly to the actual storage through the reservoir coefficient k_{slow} (Equation 8).

$$Q_{base} = k_{slow} \cdot S_{slow} \cdot a_c \tag{8}$$

where a_c (m^2) is the catchment area.

The quick flow component Q_{quick} (m^3/s) is modelled by a non-linear storage-discharge relationship (Equation 9):

$$Q_{quick} = \beta \cdot J^{1/2} \cdot H^{5/3} \tag{9}$$

where J is the slope of the catchment, H (mm) the actual storage and β a parameter to calibrate.

The total runoff from the non ice-covered part of the catchment corresponds to the sum of the quick and the base flow. The runoff model for the non ice-covered part has 5 parameters *A, k,*

x, y and β. According to previous studies (Consuegra and Vez, 1996), the exponent x and y can be set to 0.5 and 2, respectively. The parameters A, k and β have to be calibrated. Several applications of the SOCONT model to non-glacierized catchments (Consuegra et al., 1998; Guex et al., 2002) have shown that this model is able to reproduce all the major characteristics of the discharge such as floods, flow-duration-curves or the hydrological regime.

3.2.5 Annual mass balance computation

The annual mass balance at a given point of a glacier is defined as the sum of water accumulation in form of snow and ice minus the corresponding ablation over the whole year (Paterson, 1994):

$$b_a = a_a + c_a = \int_{t_0}^{t_1} [c(t) + a(t)]dt \tag{10}$$

where b_a (m) is the annual mass balance at a given point, c_a (m) the annual accumulation, a_a (m) the annual ablation, $c(t)$ (m/d) the accumulation rate at time t, $a(t)$ (m/d) the ablation rate at time t, t_o the start date of the measurement year (here the 1 October) and t_1 the end of the measurement year (30 September the following year). The annual mass balance B_a (m^3) of the entire glacier corresponds to the integration of the point balance over the whole glacier area.

Different methods exist to determine the annual mass balance of a glacier. The data used in the present study has been obtained through the so-called direct glaciological method (Paterson, 1994): The annual mass balance is measured at a representative set of points in the accumulation area and the ablation area. The resulting data are spatially interpolated and superimposed to topographic information in order to obtain the total annual mass balance of the entire glacier.

The presented hydrological model enables the estimation of the annual mass balance based on the hydrological simulation outputs. For each elevation band, the mean annual mass balance is calculated based on the simulated snow accumulation and the simulated snow- and ice melt (Equation 11).

$$b_{a,i} = \int_{t_0}^{t_1} [P_{snow}(t) - M_{snow}(t) - M_{ice}(t)]dt \tag{11}$$

where $b_{a,i}$ (m) is the annual mass balance of the elevation band i. The annual mass balance of the entire glacier is estimated as the area-weighted sum of the mass balance of all elevation bands (Equation 12).

$$B'_a = \frac{1}{s_g} \sum_{i=1}^{n} (b_{a,i} \cdot s_i) \tag{12}$$

where B'_a (m) is the simulated total annual mass balance of the glacier and s_i (m^2) is the area of elevation band i.

3.3 Case studies: Site description and data collection

In the present study, GSM-SOCONT has been applied to three different gauged catchments situated in the Southern Swiss Alps: the Lonza at Blatten, the Rhone at Gletsch and the Drance at the inflow into the dam of Mauvoisin (Figure 2). The hydrological regime of these rivers is strongly influenced by glacier and snowmelt. It is of the so-called a-glacier type (Spreafico et al., 1992): the maximum monthly discharge takes place in July and August and the minimum monthly discharge (up to 100 times less) in February and March.

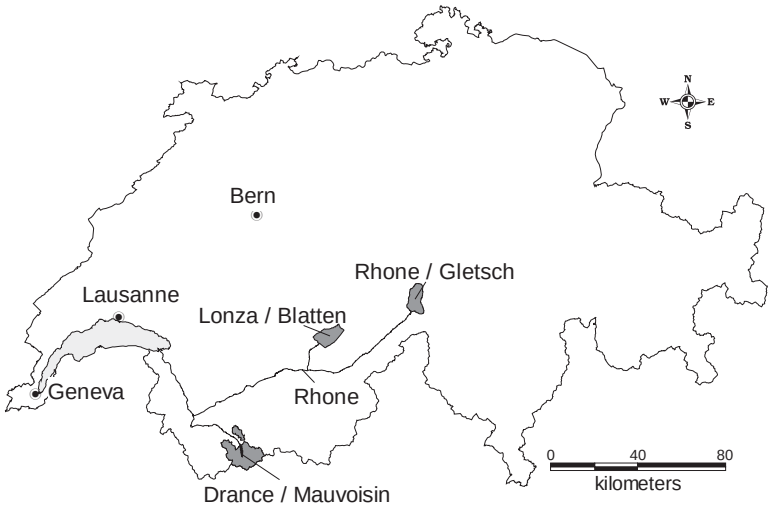

Figure 2: Location of the case study catchments in the Swiss Alps (SwissTopo, 1997)

These three catchments have been chosen because they represent different catchment sizes and have different glaciation ratios (Table 1). Additionally, even though they are all located in the same relatively small geographic area, the meteorological conditions vary considerably (Table 2).

Table 1: Main physiographic characteristics of the three catchments (reference year for glaciation: 1985) and the estimated precipitation increase with altitude (c_{precip})

River	Area (km^2)	Glaciation (%)	Mean altitude (m a.s.l.)	Altitude range (m a.s.l.)	Mean slope (°)	c_{precip} (%100^{-1} m^{-1})
Rhone	38.9	52.2	2713	1755 – 3612	22.9	3.1
Lonza	77.8	36.5	2601	1520 – 3890	30.0	7.9
Drance	169.3	41.4	2940	1961 – 4305	26.7	2.2

Table 2: Estimated meteorological conditions of the three catchments (reference altitude 2800 m. a. s. l., reference period 1974 - 1994) and time periods used for the model calibration and validation

River	Mean annual precipitation (mm)	Daily mean temperature (°C)	Discharge calibration	Discharge validation	Mass balance calibration
Rhône	2005	-5.9	1981 – 1990	1991 – 1999	1979 – 1982
Lonza	2304	-3.9	1974 – 1984	1985 – 1994	-
Drance	1449	-3.2	1995 – 1999	1990 – 1994	-

3.3.1 Data collection

The spatial discretization of the catchment is carried out based on a digital elevation model with a resolution of 25 m (SwissTopo, 1995) and on topographic maps with a scale of 1: 25'000 (SwissTopo, 1997). The hydrological model needs daily mean values of temperature, precipitation and potential evapotranspiration as meteorological input and daily mean discharge measurements for the model calibration. The precipitation and temperature time series are obtained from the Swiss Meteorological Institute at measurement stations located within a few kilometres distance of the catchments (Table 3). The potential evapotranspiration time series are calculated based on the Penman-Monteith version given by (Burman and Pochop, 1994).

Table 3: Meteorological measurement stations used for precipitation (P) and temperature (T) time series and their spatial situation compared to the studied catchments

River	Station name	Measured variable	Station altitude (m a.s.l.)	Distance to catchment centroid (km)	Distance to nearest, farthest catchment point (km)
Rhone	Oberwald	P	1375	8.1	[3.0, 14.2]
Rhone	Ulrichen	T	1345	12.3	[7.4, 18.4]
Lonza	Ried	P, T	1480	6.8	[1.0, 13.7]
Drance	Mauvoisin	P, T	1841	5.1	[0.7, 12.7]

The Swiss Federal Office provided daily discharge data for the Rhone and the Lonza catchments for Water and Geology (see Table 2 for the used time periods). For the Drance catchment, the reference daily discharges are the daily inflows into the accumulation lake of Mauvoisin (used for hydropower production since 1959). These daily inflows are recalculated based on the observed lake level and outflow, both obtained from the Forces Motrices de Mauvoisin. The measurement uncertainty inherent in the inflow estimation is difficult to quantify but it is known to be higher for the validation period than for the calibration period due to a modification of the measurement method. We nevertheless include this catchment in the present study, as the relative uncertainty on observed discharges is not significant during

high-flow periods and no undisturbed gauged catchment is available in this particular area of the Swiss Alps.

The calibration procedure for the Rhone catchment uses a second data set, the observed annual mass balance of the Rhone glacier given for the hydrological years 1979/80 to 1981/82 by Funk (1985). This data set is based on direct glaciological measurements.

3.4 Model set-up and calibration

The model has 7 parameters to calibrate: two degree-day factors (a_{ice}, a_{snow}), three linear reservoir coefficients (k_{slow}, k_{ice}, k_{snow}), the maximum storage capacity of the slow reservoir (A) and one non-linear reservoir coefficient for the direct runoff (β). Note that in the present study, these parameters do not vary in space. The calibration procedure is based on the assumption that during certain periods, some parameters have a much stronger influence on the discharge signal than others and that accordingly, it is possible to define appropriate discriminant calibration criteria.

The overall water balance of the system is conditioned by the timing and intensity of snow- and ice melt, i.e. by the degree-day factors for snow and ice. The slow reservoir parameters (A, k_{slow}) are the determinant parameters for reproduction of the base flow during winter months. The reservoir coefficients k_{snow} and k_{ice} have a major influence on the simulation quality during summer months, whereas the direct runoff coefficient β acts on the model ability to simulate discharge during precipitation events. Based on these considerations, we have developed a multi-signal / multi-objective calibration procedure based on random generation and stepwise local parameter refinement.

The simulation quality is also highly dependent on the used spatial discretization. The number of elevation bands is proportionally distributed between the two types of land cover (ice- and not ice-cover) in accordance to their percentage of the total catchment area. The total number determines the altitudinal resolution of the meteorological time series and of the corresponding simulated snow cover evolution. It has therefore a strong influence on the model performance. It can be shown through simulation, that there is a threshold value beyond which an increase in the number of elevation bands does not result in a model performance increase (Figure 3). For all 3 catchments, the threshold corresponds to around 10 elevation bands (Figure 3). The corresponding mean altitudinal intervals vary between 192 m (Rhone catchment) and 242 m (Drance catchment). Consequently, only 10 elevation bands are used for the simulations presented in this paper.

For all simulations, the first two years are assumed to initialise the system and are therefore discarded before the calibration criteria computation. Note that in the following, if nothing else is stated, the numerical examples and illustrations refer to the Rhone catchment.

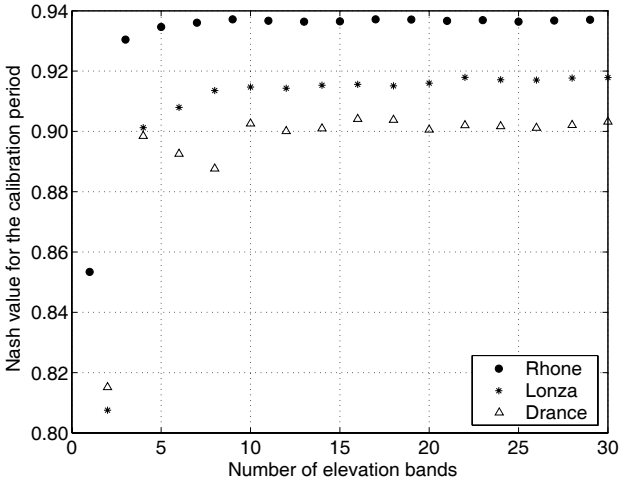

Figure 3: Nash value for the calibration period as a function of the total number of elevation bands (model parameters are fixed to their calibrated values)

3.4.1 Selection of an initial parameter set by random generation

An initial "good" parameter set is chosen among 10'000 randomly generated parameter sets. The underlying criteria are the bias between simulated and observed discharge (Equation 13) and the classical Nash criterion (Nash and Sutcliffe, 1970).

$$Bias_D = \sum_{t=1}^{n}(Q_{obs,t} - Q_{sim,t}) \cdot (\sum_{t=1}^{n} Q_{obs,t})^{-1} \tag{13}$$

where $Q_{obs,t}$ is the observed discharge and $Q_{sim,t}$ the simulated discharge on day t and n the number of days of the simulation period.

For the random generation, the parameters are supposed to be uniformly distributed within an interval that can be defined based on some theoretical considerations and on the results of other case studies reported in the literature (Table 4).

Table 4: Parameter intervals used for random generation and reference case studies

Parameter	Unit	Min. value	Max. value	Reference
a_{ice}	$mm°C^{-1}d^{-1}$	5.0	20.0	Rango and Martinec, 1995;
a_{snow}	$mm°C^{-1}d^{-1}$	1.3	11.6	Singh et al., 2000; Hock, 2003
k_{ice}	d	0.2	15.0	Baker et al., 1982;
k_{snow}	d	4.0	18.0	Klok et al., 2001
A	mm	10	3000	Consuegra et al., 1998; Guex et al., 2002
$log(k)$	$log(h^{-1})$	-12	-2	
β	$m^{4/3}s^{-1}$	100	30'000	

Note that the value of the degree-day factor depends on the calculation procedure and especially on the time step chosen (see Braithwaite and Olesen, 1989 for a numerical example). The above ranges must therefore be considered with care. The degree-day factor for ice can be assumed to be higher than for snow because of a higher albedo, meaning that the utilisation of the available energy is lower for snow than for ice (see, e.g., Braithwaite and Olesen, 1989; Rango and Martinec, 1995) This theoretical consideration has been confirmed by hydro-glaciological studies (Singh et al., 2000).

The random generation within these intervals leads to Nash values higher than 0.9. For highly glacierized catchments, such high Nash values are easy to achieve as long as the model reproduces the strong seasonality of the discharge. A very simple model corresponding just to the mean observed discharge for each calendar day would yield a Nash value of 0.85 for the calibration period (1981-1990) and a value of 0.81 for the validation period (1991-1999). This means that the classical Nash criterion calculated over the entire calibration period is not sensitive enough for further calibration.

3.4.2 Local refinement

Based on this first good parameter set, all the parameters are optimised by varying one or two of them and keeping the others constant. For each parameter or couple of parameters an appropriate optimisation criterion is defined. The order of fine-tuning is motivated by the model sensitivity to the 7 model parameters. An initial sensitivity analysis showed that the model performance is the most sensitive to the values of the degree-day factors and the time constant k of the base flow component of the discharge. Accordingly, the degree-day factors are the first parameter couple to optimise. The higher the a_{ice} value is, the higher is the simulated ice melt contribution to the total runoff. On the other hand, ice melt only occurs when the ice surfaces are not snow covered. The length of these time periods is directly dependent on the a_{snow} value. The higher it is, the faster the snow cover disappears. It follows that the overall water balance - and consequently the bias between simulated and observed discharge and between simulated and observed annual mass balance of the glaciers - mainly depend on these two parameters. Accordingly, the mean annual discharge bias ($Bias_D$, Equation 13) is used as an objective function for their fine-tuning. If data is available, the bias between simulated and observed annual mass balance ($Bias_M$) is used as a second objective function (Equation 14).

$$Bias_M = \frac{1}{n_y}\sum_{y=1}^{n_y}[abs(B_{a,y} - B'_{a,y}) \cdot abs(B_{a,y})^{-1}] \qquad (14)$$

where $B_{a,y}$ (m) is the observed and $B'_{a,y}$ (m) the estimated annual mass balance of year y and n_y the number of simulated years.

For each of these functions, a response surface is generated by varying the two degree-day parameters. For the Rhone catchment, both surfaces show a strong correlation between the

two parameters (Figure 4), the local optima describing a power function of the type $a_{snow} = \alpha * a_{ice}^{\beta} + \gamma$ where α, β and γ are constants. Hock (1999) found a similar relationship between these two parameters. The curves described by the local optima of both response surfaces have one intersection point. This result has an important implication: By choosing this intersection point for the calibrated values of a_{snow} and a_{ice}, the model yields good results for the mean annual discharge of the catchment and for the mass balance of the glacier. This ensures that the overall water balance of the system is respected and that the estimated precipitation time series represents well the area-average precipitation. The estimation of this area-average precipitation in high mountainous catchments remains a very difficult task. Aellen and Funk (1990) and Kuhn (2003) pointed out that the total annual snow and ice storage change has about the same order of magnitude as the error committed on area-average precipitation estimation.

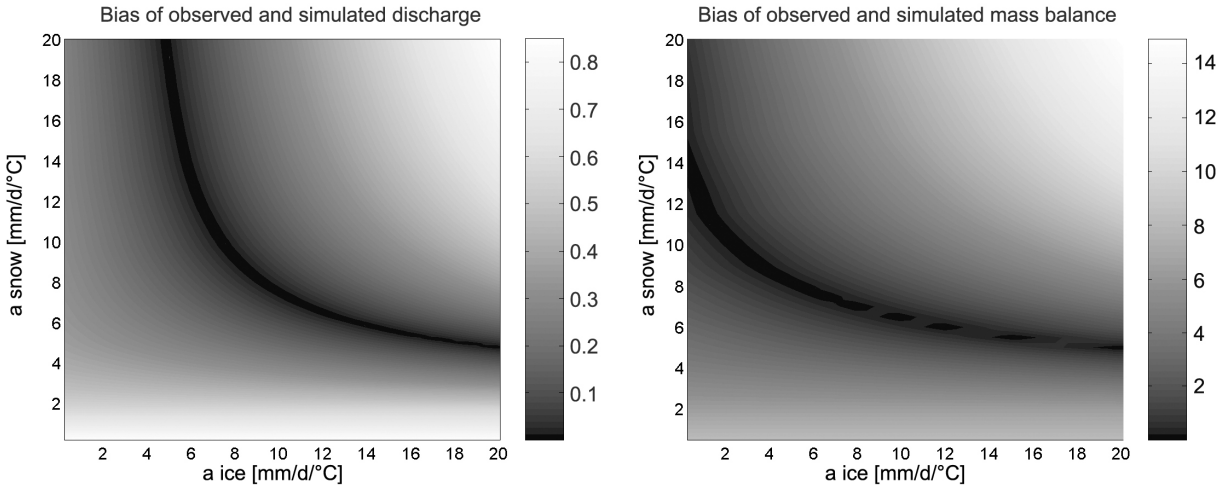

Figure 4: Response surface of the bias of simulated and observed mean annual discharge (left) and mass balance (right) as a function of snow and ice degree-day factors (Rhone catchment)

We could not find any study in the literature that uses glacier mass balance data for rigorous parameter estimation of a hydrological model for discharge simulation. Such a cross-calibration for river discharge and glacier mass balance has been proposed in the past by Braun and Renner (1992) but for subjective manual calibration of the hydrological model: The mass balance data helped rejecting unrealistic parameter values. Verbunt et al. (2003) used some long-term glacier mass balance aspects for a qualitative model validation.

If no glacier mass balance data is available, the choice of the parameter couple a_{ice} and a_{snow} has to be based on an additional calibration criterion for simulated daily discharge. We use the classical Nash criterion that – if computed for all local optima of the bias response surface - has a global optimum.

All other parameters are optimised following a similar approach. For the slow reservoir constants *A* and *k*, the objective function corresponds to the Nash-log criterion (Equation 15) as these two parameters have the most important influence on the base flow.

$$R^2_{\ln} = 1 - \sum_{t=1}^{n} [\ln(Q_{obs,t}) - \ln(Q_{sim,t})]^2 \cdot (\sum_{t=1}^{n} [\ln(Q_{obs,t}) - \frac{1}{n} \sum_{j=1}^{n} \ln(Q_{obs,j})]^2)^{-1} \quad (15)$$

The response surface shows also a strong correlation between the local optima (Figure 5). This correlation between *A* and *k* has already been highlighted in previous studies (Niggli et al., 2001; Guex et al., 2002) for catchments located at much lower elevations. The choice of a parameter couple is not unambiguous, for further calibration, the global optimum is retained. The identified relationship between the two parameters could be useful for further sensitivity analysis.

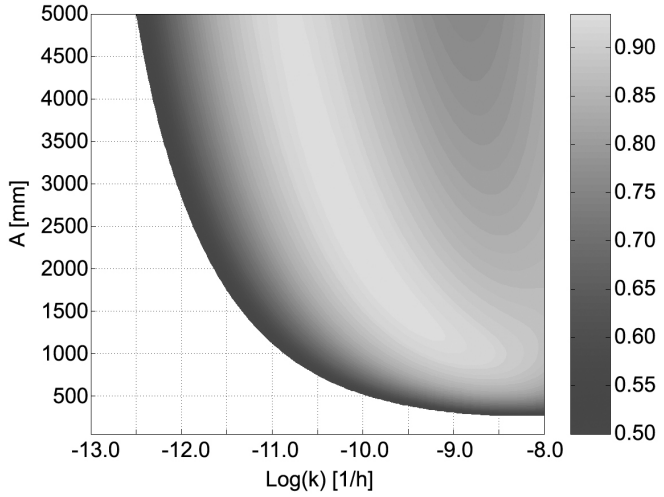

Figure 5: Variation of Nash-log value as a function of *A* and log(*k*); for better readability, values < 0.5 are not plotted (Rhone catchment)

The reservoirs coefficients k_{snow} and k_{ice} are optimised using the Nash criterion calculated for the period of snow- and ice melt (called hereafter Nash-melt criterion). This period has been fixed to the days between i.e. 15 July and 15 September. This objective function has a global optimum. The values of these two parameters can be interpreted as the elapsed time between the moment when melt takes place and the moment when the corresponding water volume reaches the outlet of the catchment. The ice melt water can be assumed to arrive quicker at the outlet, as the internal drainage systems of the glaciers are well developed when ice melt starts taking place. The snowmelt water in contrast can be stored within the snowpack leading to high time intervals between melt and arrival at the outlet.

The remaining model parameter β influences the model quality during precipitation events that involve direct runoff in the not ice-covered part of the catchment. These events are generally characterised by a sudden increase of the mean daily discharge. The chosen

objective function corresponds therefore to the classical Nash criterion calculated over all days that satisfy the following condition: The ratio between the maximum discharge and the minimum discharge observed during the 3 day period including the preceding, the current and the following day is higher than 1.5 and the total spatial rainfall over the same period is higher than 10 mm. Note that the so identified days can also include runoff events caused by other phenomena than direct runoff. This objective function is called Nash peak and its response curve has a global optimum.

The elaborated parameter optimisation procedure represents a rapid and consistent calibration tool for the glacio-hydrological model in use. Its application is subject to the constraint that an initial, good parameter set has been previously identified.

3.5 Calibration and simulation results

3.5.1 Simulation of daily discharge and the hydrological regime

The model has been calibrated and validated for the three catchments Rhone, Lonza and Drance. For the last two, only discharge data was available for calibration. For the model validation, the glaciation rates of the catchments had to be updated (Table 5). This update is based on available topographic data. For the Drance catchment, no estimate of the glacier surface evolution was available; the used value corresponds to the year 1995 for both periods.

Table 5: Calibration criteria values (Nash, Nash-log and bias) for the 3 catchments for the calibration and the validation period; for both periods, the used glaciation rates are indicated

Criterion	Period	Rhone	Lonza	Drance
Nash	Calibration	0.94	0.92	0.90
Nash	Validation	0.92	0.91	0.84
Nash-log	Calibration	0.93	0.88	0.83
Nash-log	Validation	0.93	0.93	0.79
Bias	Calibration	-0.03	-0.02	0.00
Bias	Validation	-0.00	0.03	0.05
Glaciation	Calibration	0.52	0.38	0.41
Glaciation	Validation	0.50	0.36	0.41

The calibrated model parameters for all 3 catchments respect the theoretic considerations stated in Section 4, namely $a_{ice} > a_{snow}$ and $k_{ice} < k_{snow}$ (Table 6). Despite its parsimonious structure, the model shows a good overall performance for the daily discharge simulation over the calibration and the validation periods (Table 5). The model performs particularly well for low flow situations during the winter months (Figure 6) but also for the periods of snowmelt

in late spring and for snow- and ice melt induced high flow situations during the summer months (see the following section for further discussion of high flow simulation). Accordingly, the model reproduces well the observed flow-duration curves (Figure 6d).

Table 6: Calibrated parameter values

Parameter	Unit	Rhone	Lonza	Drance
a_{ice}	$mm°C^{-1}d^{-1}$	11.5	7.1	8.0
a_{snow}	$mm°C^{-1}d^{-1}$	6.6	6.1	4.5
A	mm	2147	710	1464
$log(k)$	$log(h^{-1})$	-9.9	-7.4	-10.8
k_{ice}	d	4.7	1.7	4.6
k_{snow}	d	5.2	4.0	5.9
β	$m^{4/3}s^{-1}$	301	2342	1213

For the Rhone and the Lonza catchment, the model performs equally well for the validation period as for the calibration period (Table 5). This implies in particular that the estimated mean ice-covered areas reflect sufficiently well their contribution to the total runoff during both periods. The Drance catchment has to be considered separately. As mentioned before (Section 3), the quality of the observed discharge is considerably lower than for the other two catchments, (especially during low flow situations) and the measurement uncertainty is higher for the validation period than for the calibration period, explaining partly the difference of the model performance for the two periods.

In the considered hydro-climatic region, water managers are especially interested in the simulation of high discharge events as they lead regularly to flood situations. The water management implications of these high flow situations depend on to the seasonal timing of their appearance. High flow situations can occur during the snow- and ice melt season when the highest annual discharges occur. These high flow events are well simulated by the presented discharge model (Figure 6). At this time of the year, potential flood situations are generally easily managed especially through the numerous accumulation lakes that have been built for hydropower production all over the Swiss Alps. High discharge events occurring between mid-September and mid-October (Figure 6b) can induce more critical situations as at this season the accumulation lakes are usually filled up and cannot mitigate the floods. These situations are generally caused by important rainfall events. In high mountainous catchments, such events can be extremely localised and consequently, the simulation of the corresponding discharge is strongly dependant on the representativeness of the precipitation recorded at the measurement station (see, e.g., the high flow event in Figure 6c, for which no rainfall was recorded). A further discussion of the problem of spatial representativeness of the precipitation follows hereafter.

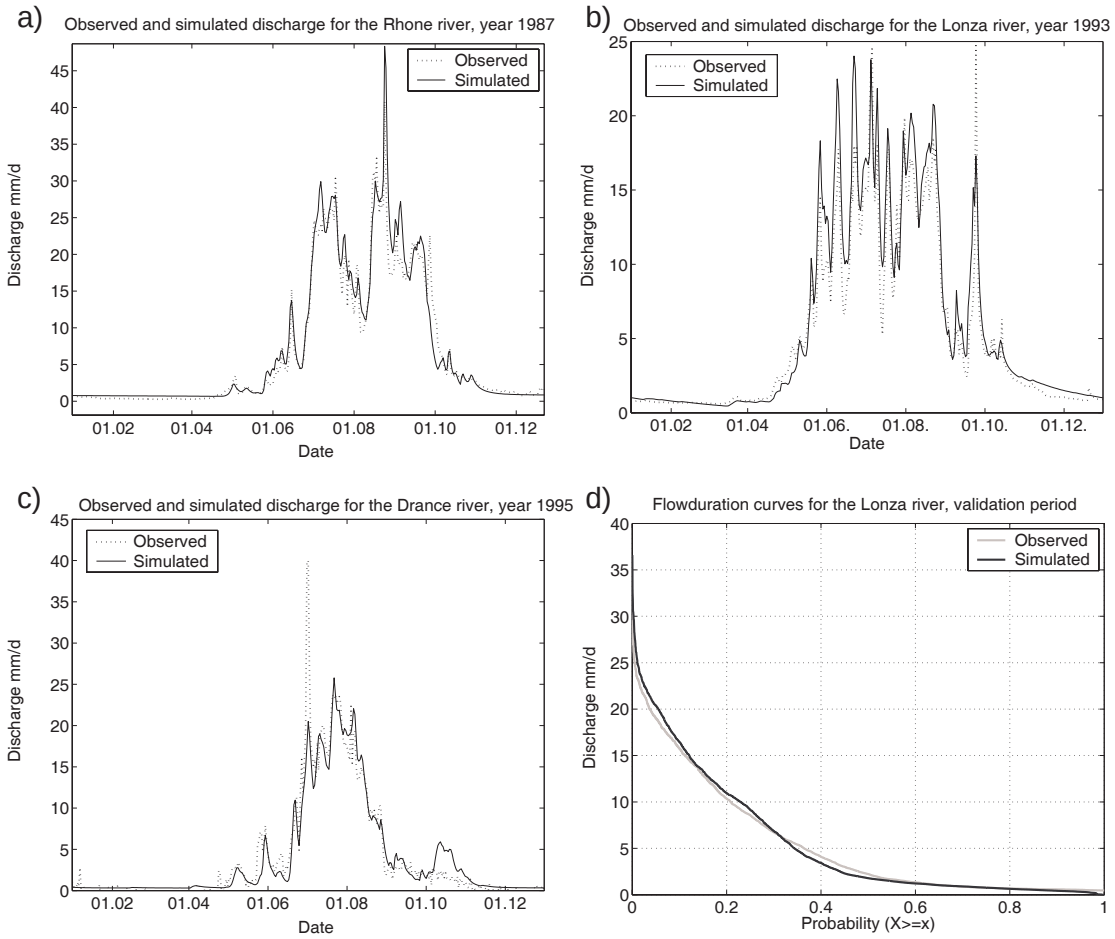

Figure 6: Observed and simulated discharge: a) for the Rhone catchment (year 1987); b) for the Lonza catchment (year 1993); c) for the Drance catchment (year 1995); d) observed and simulated flow-duration curves of the Lonza river for the validation period

3.5.2 Simulation of glacier characteristics for the Rhone glacier

In catchments where glacier mass balance data is available, the GSM-SOCONT can be calibrated on this data. For the Rhone catchment, the mean annual mass balance of the Rhone glacier has been used for the calibration of the degree-day factors. Accordingly, its total annual mass balance is well simulated (Table 7), except for the winter 1981/82, where it is considerably underestimated (see further discussion hereafter). Note that if the model is calibrated without considering the mass balance data, the retained parameter set would be a_{ice} = 10.4 mm°C^{-1}d^{-1} and a_{snow} = 7.2 mm°C^{-1}d^{-1} leading to a less accurate estimate of the annual glacier mass balance (respectively 753 mm, 38 mm and –1147 mm for the considered period 1979/80 to 1981/82).

The presented glacio-hydrological model reproduces also well the observed altitudinal distribution of the mean annual glacier mass balance (Figure 7). This result shows that for the studied system, the processes of snow- and ice accumulation and ablation are sufficiently well simulated through the chosen modelling approach considering only precipitation and

temperature as underlying driving forces. In other climatic and topographic conditions, snow redistribution by wind and avalanches could also strongly influence the snow accumulation - and consequently the mass balance - at a given point (see, e.g., Hartman et al., 1999; Kuhn, 2003 for an attempt to include this redistribution in a hydrological model).

Table 7: Simulated and observed total annual mass balance, AAR and ELA

	Mass balance (mm yr^{-1})		AAR (%)		ELA (m a.s.l.)	
Year	Observed	Simulated	Obs.	Sim.	Obs.	Sim.
1979/80	890	835	64	75	2764	2682
1980/81	90	115	53	60	2875	2831
1981/82	-380	-1110	45	36	3035	3023

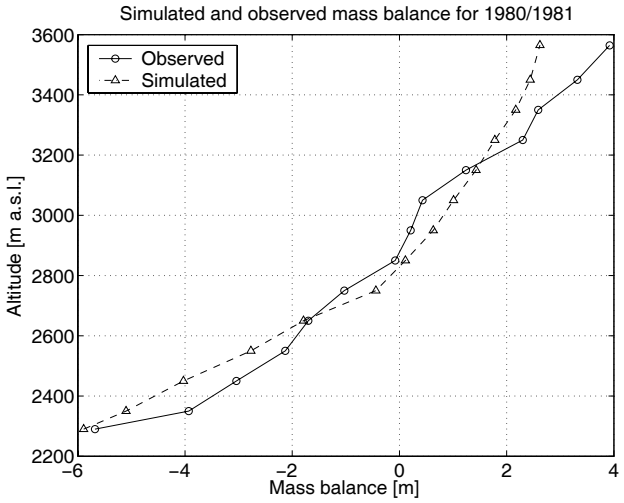

Figure 7: Observed and simulated mean annual mass balance of the Rhone glacier as a function of altitude for the winter 1980/81 (the altitudinal discretization and the observed data are drawn from (Funk, 1985))

A good simulation of the altitudinal distribution of the mean annual mass balance indicates that the applied spatial interpolation of the meteorological time series can be assumed to be representative of the real conditions. Note however that the model is not able to reproduce the observed high accumulation in the uppermost parts of the glacier (Fig. 7). Further research into the exact altitudinal distribution of precipitation could help solving this problem.

This underestimation in the highest glacier area partly explains the mass balance underestimation during the year 1981/82. In this mass balance year, only the highest spatial units experience accumulation and for these units the accumulation is underestimated. The most important part of the mass balance underestimation is however due to an important overestimation of the ablation increase with altitude decrease in the ablation area of the

glacier. The mean value obtained based on the glaciological measurements of Funk (1985) is 91 cm of ablation increase per 100 m of altitude decrease, whereas the mean simulated value is 111 cm per 100 m. This results in an ablation simulation of up to -9 m. This unrealistic value results from the model assumption that the available stock of ice in a given point is infinite whereas in reality the ice in the considered part would disappear. This problem however only concerns the lowest glacier parts. Further research into the particular ablation conditions of this mass balance year is necessary to determine the cause of the general ablation overestimation.

Two other important descriptors are usually used to characterise a glacier: the equilibrium line altitude (ELA) and the accumulation area ratio (AAR). The ELA is the line connecting all points with zero balance at the end of a fixed year (Anonymous, 1969). It separates the ablation area from the accumulation area. The AAR is the ratio between the accumulation area and the entire glacier surface. According to Ohmura et al., (1992), the equilibrium line represents the lowest boundary of the climatic glacierization, i.e. the climatic conditions which prevail at the glacier equilibrium line are considered to be just sufficient to maintain the existence of ice. Ohmura et al. (1992) also point out that knowledge about the ELA is essential for understanding the relationship between climatic changes and glacier variations. The correct simulation of the ELA (respectively the AAR values) is therefore a major objective for the present hydrological model that has been developed for an application in climate change impact studies. The observed ELA and AAR values are well reproduced by the hydrological model (Table 7). For the winter 1981/82 – even though the total annual mass balance is considerably underestimated – the ELA is very well simulated. The model also reproduces the typical linear relationship between the ELA and the total annual mass balance (Figure 8) that is characteristic for a given glacier (see, e.g., Aellen and Funk, 1990; Kulkarni, 1992; Herren et al., 2002). The simulated slope is close to the one observed in the past.

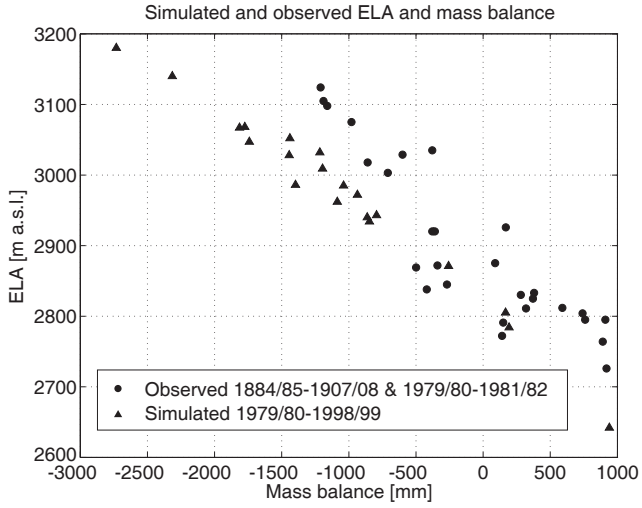

Figure 8: ELA versus annual mass balance: observed values for 1884/85-1908/9 and 1979/80-1981/82 (Chen and Funk, 1990) and simulated values for 1979/80-1998/99

This model feature enables its use for a glacier surface evolution model based on the AAR concept. This concept is classically used to reconstruct paleoclimatic glacier surfaces (see, e.g., Porter, 1975; Torsnes et al., 1993). As shown by Schaefli et al. (2005a, submitted manuscript)[2] it can be used – in an extended form - for the prediction of the glacier surface for future climate conditions.

A consequent modelling approach would ask for a validation of the obtained mass balance simulations for another period. Long series of mass balance observations are however difficult to obtain. Its noteworthy that many published series of mass balance data are in fact the result of a hydrological water balance estimation (see, e.g. Spreafico et al., 1992). Accordingly, they do not encode an additional source of information as they are directly related to the discharge measurement.

3.5.3 Simulation results and area-average precipitation

As mentioned earlier in this paper, the estimation of area-average precipitation for high mountainous catchments is a considerable source of modelling uncertainty. Due to the high spatial variability of precipitation in such catchments, two main problems arise: i) The precipitation events recorded at the measurement station(s) are not necessarily representative for the events effectively occurred in the catchment and ii) the amount of precipitation at a given catchment point based on the precipitation records is difficult to estimate.

In the present modelling context, the first problem can be assumed to have an important influence on the daily discharge simulation for rainfall-induced high-flow events. A detailed analysis would require more spatially distributed precipitation data (e.g. based on radar measurements) and is therefore beyond the study context. The second problem is taken into account by the interpolation of the precipitation for each elevation band based on a constant altitudinal increase (c_{precip}) of the precipitation observed at the measurement station. In high mountainous areas, the value of c_{precip} is highly difficult to estimate and it could even be justifiable to calibrate this parameter as it is frequently done in hydro-glaciological studies (e.g., Kuhn, 2000). Its calibration based on discharge and glacier mass balance data would however clearly suffer from overparametrisation as the two degree-day factors and c_{precip} are mutually interdependent. The curve of optimal values of a_{ice} and a_{snow} in terms of discharge or mass balance bias undergoes a shift when varying c_{precip} (Figure 9a). This shift is in the opposite direction for the discharge bias than for the mass balance bias and consequently the intersection points between these two curves also describe a power function (Figure 9a). If

[2] Schaefli, B., Hingray, B. and Musy, A.: Uncertain glacier surface evolution under changing climate. Submitted to Journal of Geophysical Research - Atmospheres; hereinafter referred to as Schaefli et al, 2005a, submitted manuscript.

c_{precip} is higher than 3.6 %100^{-1}m^{-1}, the value of a_{ice} of the intersection point is lower than the value of a_{snow}. Such couples of degree-day factors are contrary to the basic theoretic considerations stated in Section 4. The smaller c_{precip} is, the closer are the two curves at their right-hand tails and the less well defined is the best parameter couple a_{ice}/a_{snow} (Figure 9b). For small values of c_{precip} the intersection point corresponds to unreasonable a_{ice} values (higher than 20 mm°C^{-1}d^{-1}) or does not exist.

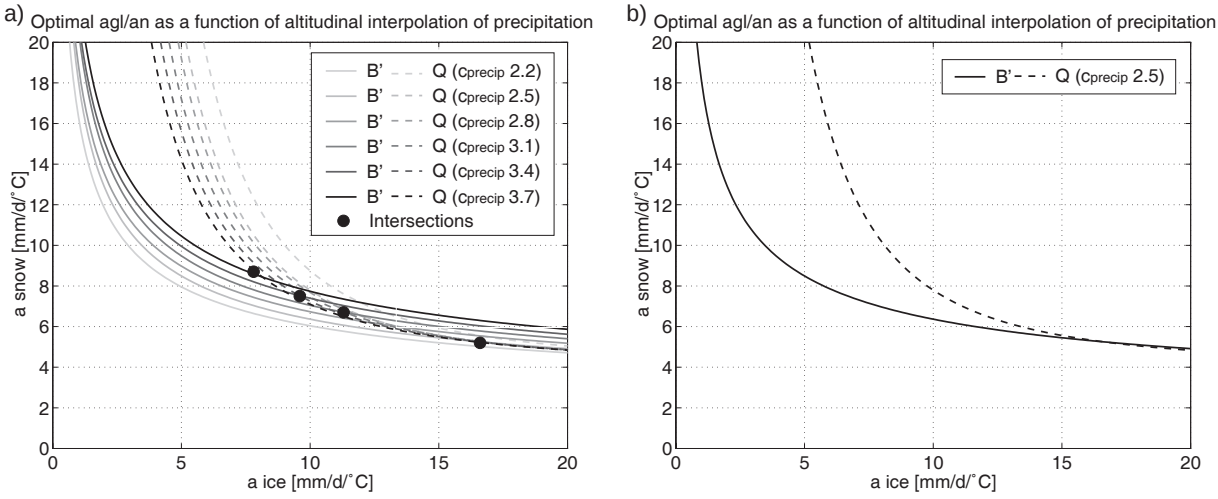

Figure 9: Optimal curves of mass balance and discharge bias as a function of a_{ice}, a_{snow} and c_{precip}

This leads to the conclusion that it is not possible to fix a unique best value for c_{precip}. The multiresponse calibration through the joint use of discharge and glacier mass balance data enables however the definition of an interval of possible values for c_{precip} that for the Rhone catchment corresponds to (2.3 %100^{-1}m^{-1}, 3.8 %100^{-1}m^{-1}). A detailed analysis of the influence of c_{precip} on the model ability to simulate the presented glaciological characteristics (AAR, ELA and altitudinal mass balance distribution) could possibly lead to some further conclusions.

3.6 Conclusions

The presented hydrological model is based on a simple reservoir approach that includes the basic glacio-hydrological features, namely soil infiltration and melt water storage in the snow cover and the glacier. The model gives good results for mean daily discharge simulation from highly glacierized catchments as illustrated through its application to three catchments in the Swiss Alps. It simulates well the hydrological regime and reproduces some basic glaciological features such as the total annual glacier mass balance or the accumulation area ratio. This characteristic makes the model particularly interesting for applications in climate change impact studies as the simulation results can be used for glacier surface evolution

studies (Schaefli et al., 2005a, submitted manuscript). The parsimonious model structure is also adapted to such applications: All required climatic input variables can be obtained from current climate models. Given the simplicity of the model structure and its effectiveness for discharge and mass balance simulations, the model represents also an easy to use simulation tool to study highly glacierized alpine catchments in other contexts, such as water resources management.

The elaborated procedure of parameter calibration represents a rapid and consistent calibration tool for the model. The presented multi-signal calibration of the river discharge and the glacier mass balance constitutes an interesting approach for the estimation of the total water balance of highly glacierized catchments. In mountainous areas, the spatial distribution of precipitation represents an important source of uncertainty. Calibrated rainfall-runoff models can give good estimates of the discharge even if the spatial precipitation is estimated poorly. Differences between simulated and real precipitation can typically be compensated by simulated evapotranspiration or as in the present model by simulated ice melt. This does not represent a real problem for applications where the main interest lies in short-term prediction of the daily discharge. In long-term projections however, a wrong overall water balance simulation can be significantly misleading, especially in the present context where the ice melt contribution to the runoff could be completely under- or overestimated.

The model does not account for seasonal variations of the physical system even if the subglacial drainage system is known to undergo a strong evolution throughout the melt season. The drainage network as well as the channel sizes vary in response to changing water inputs (see, e.g., Röthlisberger, 1972; Hubbard and Nienow, 1997). This evolution of the internal drainage system can be assumed to have a notable influence on the discharge. In order to improve the discharge simulations, further investigation in the time-dependency of the parameters could be interesting, considering especially potential links between the parameters and climate variables.

It should be kept in mind that the proposed parameter calibration approach – random search completed by local refinement – guarantees neither that the globally best parameter set nor that all possibly good parameter sets are found. A quantitative parameter and model uncertainty analysis such as the one presented by Kuczera and Parent (1998) would complete the current results (see Schaefli et al., 2005b, submitted manuscript)[3]. Such an uncertainty analysis could in particular make use of the identified relationships between some of the model parameters and produce confidence intervals on the simulated daily discharge and annual glacier mass balance.

[3] Schaefli, B., Balin Talamba, D. and Musy, A., 2005. Quantifying hydrological modeling errors through finite mixture distributions. Submitted to Journal of Hydrology

Acknowledgements

We wish to thank the Forces Motrices de Mauvoisin and the Swiss Federal Office for Water and Geology for providing the discharge data and the national weather service MeteoSwiss for providing the meteorological time series. The model was developed in the context of the European project SWURVE (Sustainable Water: Uncertainty, Risk and Vulnerability in Europe, funded under the EU Environment and Sustainable Development programme, grant number EVK1-2000-00075) that analyses climate change impacts on water resources systems in Europe. The Swiss part of this project was funded by the Federal Office for Education and Science, contract number 00.0117.

References

Aellen, M. and Funk, M., 1990. Bilan hydrologique du bassin versant de la Massa et bilan de masse des glaciers d'Aletsch (Alpes Bernoises, Suisse). In: Lang H. and Musy A. (Editors), Hydrology in Mountainous Regions I: Hydrological Measurements; the Water Cycle,. IAHS Publ. No. 193, Wallingford, Oxfordshire UK, pp. 89-98.

Anonymous, 1969. Mass-balance terms. Journal of Glaciology, 8(52): 3-7.

Baker, D., Escher-Vetter, H., Moser, H., Oerter, H. and Reinwarth, O., 1982. A glacier discharge model based on results from field studies of energy balance, water storage and flow. In: J.W. Glen (Editor), Hydrological Aspects of Alpine and High-Mountain Areas. IAHS Publ. no. 138, Wallingford, Oxfordshire UK, pp. 103-112.

Bérod, D., 1994. Contribution à l'estimation des crues rares à l'aide de méthodes déterministes - apport de la description géomorphologique pour la simulation des processus d'écoulement. Doctoral Thesis, Swiss Federal Institute of Technology, Lausanne.

Braithwaite, R.J. and Olesen, O.B., 1989. Calculation of glacier ablation from air temperature, West Greenland. In: Oerlemans J. (Editor), Glacier fluctuations and climatic change. Proceedings of the Symposium on Glacier Fluctuations and Climatic Change, held in Amsterdam, 1-5 June 1987. Glaciology and quaternary geology. Kluwer Academic Publishers, Dordrecht, pp. 219-233.

Braun, L.N. and Renner, C.B., 1992. Application of a conceptual runoff model in different physiographic regions of Switzerland. Hydrological Sciences Journal, 37(3): 217-231.

Braun, L.N., Weber, M. and Schulz, M., 2000. Consequences of climate change for runoff from Alpine regions. Annals of Glaciology, 31: 19-25.

Burman, R. and Pochop, L.O., 1994. Evaporation, evapotranspiration and climatic data. Elsevier, Amsterdam, 278 pp.

Chen, J. and Funk, M., 1990. Mass balance of Rhonegletscher during 1882/83 - 1986/87. Journal of Glaciology, 36(123): 199-209.

Consuegra, D., Niggli, M. and Musy, A., 1998. Concepts méthodologiques pour le calcul des crues, application au bassin versant supérieur du Rhône. Eau, énergie, air, 9/10(90): 223-231.

Consuegra, D. and Vez, E., 1996. AMIE: Analyse et Modélisation Intégrées du cheminement des Eaux en zones habitées, modélisation hydrologique, Application au bassin versant de la Haute Broye, IATE/HYDRAM, Swiss Institute of Technology, Lausanne, Lausanne.

Edijatno and Michel, C., 1989. Un modèle pluie-débit journalier à trois paramètres. La Houille Blanche, 2: 113-121.

Funk, M., 1985. Räumliche Verteilung der Massenbilanz auf dem Rhonegletscher und ihre Beziehung zu Klimaelementen. Doctoral Thesis, Eidgenössische Technische Hochschule Zürich, Zürich, 183 pp.

Guex, D., Guex, F., Pugin, S., Hingray, B. and Musy, A., 2002. Regionalisation of hydrological processes in view of improving model transposability. WP3 Final Report of the Pan-European FRHYMAP Project (Flood Risk scenarios and Hydrological MAPping), N° Contract CE : 3/NL/1/164/99 15 183 01., Swiss Institute of Technology, Lausanne, Lausanne.

Haeberli, W., Frauenfelder, R. and Hoelzle, M. (Editors), 2003. Glacier mass balance bulletin no. 7 (2000 - 2001). IAHS - UNEP - UNESCO - WMO, Zürich, Switzerland, 87 pp.

Hartman, M.D., Baron, J.S., Lammers, R.B., Cline, D.W., Band, L.E., Liston, G.E. and Tague, C., 1999. Simulations of snow distribution and hydrology in a mountain basin. Water Resources Research, 35(5): 1587-1603.

Herren, E.R., Bauder, A., Hoelzle, M. and Maisch, M., 2002. The Swiss Glaciers 1999/2000 and 2001/2002. 121/122, Glaciological Commission of the Swiss Academy of Sciences, Zürich.

Herren, E.R., Hoelzle, M. and Maisch, M., 2001. The Swiss Glaciers 1997/98 and 1998/99. 119/120, Glaciological Commission of the Swiss Academy of Sciences, Zürich.

Hock, R., 1999. A distributed temperature-index ice- and snowmelt model including potential direct solar radiation. Journal of Glaciology, 45(149): 101-111.

Hock, R., 2003. Temperature index melt modelling in mountain areas. Journal of Hydrology, 282(1-4): 104-115.

Hubbard, B. and Nienow, P., 1997. Alpine subglacial hydrology. Quaternary Science Reviews, 16(9): 939-955.

Klok, E.J., Jasper, K., Roelofsma, K.P., Gurtz, J. and Badoux, A., 2001. Distributed hydrological modelling of a heavily glaciated Alpine river basin. Hydrological Sciences Journal, 46(4): 553-570.

Kuczera, G. and Parent, E., 1998. Monte Carlo assessment of parameter uncertainty in conceptual catchment models: the Metropolis algorithm. Journal of Hydrology, 211(1-4): 69-85.

Kuhn, M., 2000. Verification of a hydrometeorological model of glacierized basins. Annals of Glaciology, 31: 15-18.

Kuhn, M., 2003. Redistribution of snow and glacier mass balance from a hydrometeorological model. Journal of Hydrology, 282(1-4): 95-103.

Kulkarni, A.V., 1992. Mass balance of Himalayan glaciers using AAR and ELA methods. Journal of Glaciology, 38: 101-104.

Kustas, W.P. and Rango, A., 1994. A simple energy budget algorithm for the snowmelt runoff model. Water Resources Research, 30(5): 1515-1527.

Nash, J.E. and Sutcliffe, J.V., 1970. River flow forecasting through conceptual models. Part I, a discussion of principles. Journal of Hydrology, 10(3): 282-290.

Niggli, M., Hingray, B. and Musy, A., 2001. A Methodology for Producing Runoff Maps and Assessing the Influence of Climat Change in Europe in WRINCLE (Water Resources: Influence of Climate Change in Europe), Swiss Federal Institute of Technology Lausanne, Lausanne.

Ohmura, A., 2001. Physical basis for the temperature-based melt-index method. Journal of applied meteorology, 40(4): 753-761.

Ohmura, A., Kasser, P. and Funk, M., 1992. Climate at the equilibrium line of glaciers. Journal of Glaciology, 38(130): 397-411.

Paterson, W.S.B., 1994. The Physics of Glaciers. Pergamon, Oxford, 480 pp.

Porter, S.C., 1975. Equilibrium-line altitudes of late quaternary glaciers in southern alps, New Zealand. Quaternary Research, 5(1): 27-47.

Rango, A. and Martinec, J., 1995. Revisiting the degree-day method for snowmelt computations. Water Resources Bulletin, 31(4): 657-669.

Rohrer, M.B., Braun, L.N. and Lang, H., 1994. Long-term records of snow cover water equivalent in the Swiss Alps. 2. Simulations. Nordic Hydrology, 25(1-2), 65-78, doi.

Röthlisberger, H., 1972. Water pressure in intra- and subglacial channels. Journal of Glaciology, 11(62): 177–203.

Schaefli, B., Hingray, B. and Musy, A., 2004. Improved calibration of hydrological models: use of a multi-objective evolutionary algorithm for parameter and model structure uncertainty estimation. In: B. Webb (Editor), Hydrology: Science and Practice for the 21st Century. British Hydrological Society, London, pp. 362-371.

Schaefli, B., Hingray, B. and Musy, A., 2005. Climate change and hydropower production in the Swiss Alps: Quantification of potential impacts and related modelling uncertainties. Hydrology and Earth System Sciences. Accepted for publication in a special issue.

Singh, P. and Kumar, N., 1997. Impact assessment of climate change on the hydrological response of a snow and glacier melt runoff dominated Himalayan river. Journal of Hydrology, 193: 316-350.

Singh, P., Kumar, N. and Arora, M., 2000. Degree-day factors for snow and ice for Dakriani Glacier, Garhwal Himalayas. Journal of Hydrology, 235: 1-11.

Spreafico, M., Weingartner, R. and Leibundgut, C., 1992. Atlas hydrologique de la Suisse. Service Hydrologique et Géologique National (SHGN), Bern.

SwissTopo, 1995. Digital height model of Switzerland - DHM25, Waber, Switzerland.

SwissTopo, 1997. Digital National Maps of Switzerland - PM25, Waber, Switzerland.

Torsnes, I., Rye, N. and Nesje, A., 1993. Modern and little ice-age equilibrium-line altitudes on outlet valley glaciers from Jostedalsbreen, Western Norway - an evaluation of different approaches to their calculation. Arctic and Alpine Research, 25(2): 106-116.

Verbunt, M., Gurtz, J., Jasper, K., Lang, H., Warmerdam, P. and Zappa, M., 2003. The hydrological role of snow and glaciers in alpine river basins and their distributed modeling. Journal of Hydrology, 282(1-4): 36-55.

Willis, I. and Bonvin, J.-M., 1995. Climate change in mountain environments: hydrological and water resource implications. Geography, 80(3): 247-261.

WMO, 1986. Intercomparison of models of snowmelt runoff. No. 23, WMO, Geneva.

Chapter 4

Uncertain glacier surface evolution under changing climate[1]

Abstract

This paper presents a glacier surface evolution model for the prediction of the glacier surface in probabilistic climate change impact studies considering a range of potential global-mean warming scenarios. A semi-lumped glacio-hydrological modelling approach is used for the simulation of accumulation and ablation of ice and snow. The outputs of this model enable the estimation of the accumulation area ratio (AAR) of the glacier for a given modelling period. Based on this concept a simple glacier surface evolution model is set up that can be used for the prediction of the glacier surface under future climates. The potential sources of modelling uncertainties, namely the model parameters and the potential global-mean warming, are quantified through a Monte Carlo simulation approach. The developed methodology is illustrated through an application to a glacier in the Swiss Alps, the so-called Rhone glacier. The potential climate-induced reduction of the glacier surface is analysed based on a control period (1961 – 1990) and a future period (2070 – 2099). The predicted distribution of the future glacier surface considering all sources of modelling uncertainty (in particular the

[1] This chapter has been submitted for publication to Journal of Geophysical Research - Atmospheres: Schaefli, B., Hingray, B. and Musy, A.: Uncertain glacier surface evolution under changing climate

uncertainty of potential global-mean warming) shows a complete disappearance of the glacier for 80 % of the simulations. This result is mainly due to the predicted raise of the local mean temperature (median increase of +3.4°C) that is not compensated by additional precipitation.

4.1 Introduction

The prediction of glacier volume or surface evolution under changing climate receives currently an increasing research interest. This interest is motivated by the high climate sensitivity of glacier systems (see, e.g., Oerlemans, 1989; Vincent, 2002) and by the importance of ice-covered areas for the water cycle, for example in connection with sea-level change studies (see, e.g., Raper et al., 2000; Van de Wal and Wild, 2001) or in the context of climate change impact studies on water resources (see, e.g., Willis and Bonvin, 1995; Braun et al., 2000). The present study has been undertaken to predict a potential climate change induced decrease of Alpine glaciers and to assess the related impacts on water resources management, especially on hydropower production (Schaefli et al., 2005a) that provides for example in Switzerland up to 75 % of the consumed electricity (Swiss Federal Office for Energy, 2003).

Numerous studies have addressed the evolution of ice-covered areas in a quantitative way. Part of currently available studies tries to predict the global warming-induced volume loss of entire glacierized regions. These studies are generally based on dynamic flow models of a representative set of well-documented valley glaciers and ice caps and are often related to sea level rise studies (e.g., Oerlemans et al., 1998; Raper et al., 2000; Van de Wal and Wild, 2001). Another group of studies includes mass balance studies of individual glaciers or small glacier systems in order to investigate their climate sensitivity (e.g., Braithwaite and Zhang, 2000; Vincent, 2002).

A review of the available studies shows two major drawbacks: i) Many of these studies analyse the sensitivity of glacier systems to an arbitrary temperature and precipitation change (e.g., Oerlemans et al., 1998; Laumann and Reeh, 1993; Braithwaite and Zhang, 2000). The evolution of glacier systems is the result of the joint action of accumulation and ablation processes and is accordingly strongly influenced by the temporal and spatial distribution of precipitation and temperature. Consequently, a realistic prediction of the glacier surface evolution asks for realistic climate change scenarios. Studies that use currently available climate evolution predictions are however still rare (see, e.g., Van de Wal and Wild, 2001; Schneeberger et al., 2003). Studies using the outputs from more than one climate model or from more than one green house gas emission scenario have not been found (for a further discussion of the necessity of such a multi-model or multi-scenario approach see Section 3). ii) The available models for the simulation of the glacier volume or surface evolution are data intense and applicable only to well-documented glacier systems. The less data demanding glacier mass balance studies do not make the link between the mass balance evolution and the

glacier surface, a variable that is of interest in many climate change impact studies, for example in the area of flood risk analysis (e.g., Loukas et al., 2002), water resources management (e.g., Schaefli et al., 2005a) or ecological studies (e.g., Hall and Fagre, 2003).

The present study faces the challenge to predict the glacier surface evolution given the largest possible range of climate change by using the modelling chain starting with climate model outputs, a method for the production of local scale climate scenarios and a conceptual glacier surface evolution model. For each modelling step, the potential modelling uncertainties are quantified; the glacier surface prediction results therefore in a probability distribution of the future glacier surface instead of a single estimate.

The climate scenarios used for this study are the result of a methodology developed for climate change impact studies taking into account a wide range of potential global-mean warming and related climate changes (see Hingray et al., submitted manuscript)[2]. Instead of a mechanistic approach (e.g., Oerlemans et al., 1998) for the simulation of the glacier surface evolution, we use a conceptual surface evolution model based on the so-called accumulation area ratio (AAR) (Anonymous, 1969) that is classically used to reconstruct former glacier surfaces (e.g., Porter, 1975; Torsnes et al., 1993). The underlying snow and ice accumulation and ablation simulations are carried out through a glacio-hydrological model that uses a degree-day approach for the melt estimation. In the simulation mode, this glacier surface evolution model needs as input the hypsometric curve of the glacier and daily series of temperature and precipitation. For the model calibration, mass balance or discharge data are needed (see Section 2).

Such a parsimonious modelling approach enables the quantification of the modelling uncertainty through Monte Carlo simulations. The uncertainties inherent to the different modelling steps (namely to the climate scenarios production, to the glacio-hydrological and the glacier surface evolution model) are quantified through an appropriate method for each of them. The overall modelling uncertainty is computed by Monte Carlo simulations of the entire system evolution.

In the following, we first present the relevant features of the glacio-hydrological model and the glacier surface evolution model. The model calibration and related modelling uncertainties are discussed. The subsequent section discusses the used climate change scenarios. The developed methodology is applied to a case study in the Swiss Alps, the Rhone glacier, that is presented in some detail in Section 4. Based on this case study, we investigate potential climate change impacts on the glacier surface and quantify corresponding modelling

[2] Hingray, B., Mouhous, N., Mezghani, A., Bogner, K., Schaefli, B. and Musy, A.: Accounting for global warming and scaling uncertainties in climate change impact studies: application to a regulated lakes system. Submitted to Hydrology and Earth System Sciences; hereinafter referred to as Hingray et al., submitted manuscript

uncertainties. The obtained results are presented in Section 5, followed by a short discussion and the main conclusions of this study.

4.2 Model description

The glacier surface evolution is based on the simulation of the accumulation and the ablation of snow and ice. We first present the glacio-hydrological model that is used for this simulation, before presenting the developed glacier surface evolution model. This section is completed by a short discussion of the model calibration technique.

4.2.1 Glacio-hydrological model

The accumulation and ablation of snow and ice is carried out through a glacio-hydrological model developed for discharge simulation at a daily time step, the so-called GSM-SOCONT model (Glacier and SnowMelt – SOil CONTribution model), presented in detail in (Schaefli et al., 2005b). The use of a complete discharge model instead of a simple accumulation and ablation model has the main advantage that the model parameters can be estimated either based on discharge measurements or, if mass balance data are available, through a bi-objective approach based on river discharge and mass balance measurements.

The model uses a semi-lumped approach: The catchment is represented as a set of spatial units, each of which is assumed to have a homogeneous hydrological behaviour. The model has two levels of discretization: The ice-covered part of the catchment is first separated from the not ice-covered part. Next, both parts are subdivided into elevation bands. Each of the resulting spatial units is characterised by its surface and its hypsometric curve. For each unit, the meteorological data series are computed from data observed at neighbouring meteorological stations. Based on these series, snow accumulation and snow- and ice melt are simulated. A reservoir based modelling approach is used to simulate the hydrological response, i.e. the rainfall and melt water – runoff transformation of each unit (Figure 1). The runoff contributions of all units are added to provide the total discharge at the outlet of the entire catchment.

The only modelling steps that are of direct interest for the glacier surface evolution simulation are the interpolation of the meteorological time series and the computation of snow and ice accumulation and melt. They are described in detail hereafter.

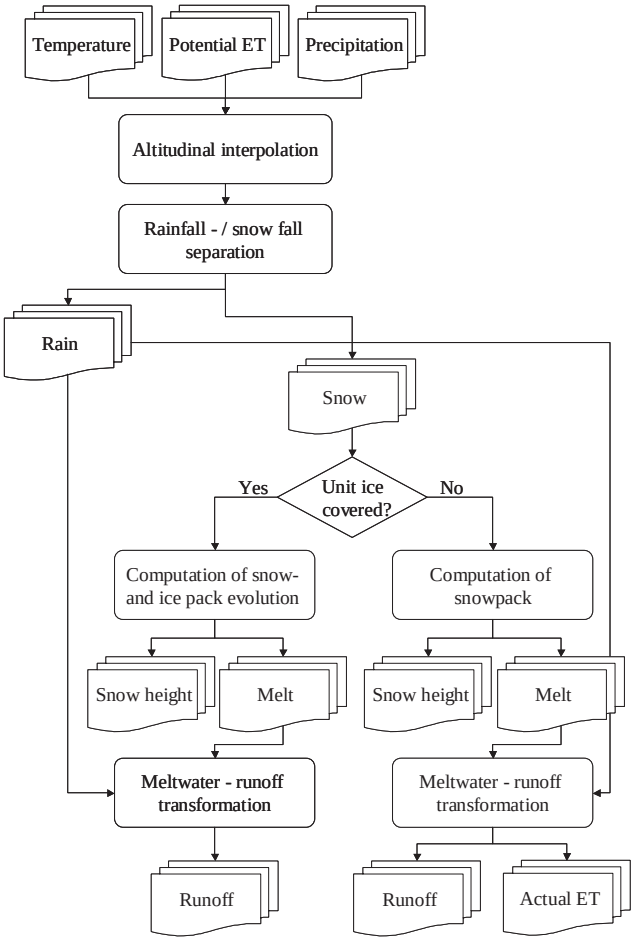

Figure 1: Basic hydrological model structure (for one spatial unit) showing the different submodels and the input and output time series (ET = evapotranspiration)

Spatial interpolation submodel

The temperature and precipitation time series are linearly interpolated according to the mean elevation of the spatial unit. The temperature decrease with altitude is computed through a fixed lapse rate r (°C 100^{-1} m^{-1}) (Equation 1).

$$T_p(t) = T_{ref}(t) + r(H_p - H_{ref}) \quad (1)$$

where $T_p(t)$ (°C) is the mean temperature on day t at a point p and H_p (m a.s.l.) is the altitude of this point, $T_{ref}(t)$ (°C) is the reference temperature and H_{ref} (m a.s.l.) is the corresponding altitude.

The precipitation increase with altitude is taken into account through a precipitation correction factor c_{precip} (% 100^{-1} m^{-1}) (Equation 2).

$$P_p(t) = P_{ref}(t) + c_{precip}(H_p - H_{ref}) \quad (2)$$

where $P_p(t)$ (mm d^{-1}) is the mean precipitation at a point p and P_{ref} (t) (mm d^{-1}) is the reference precipitation.

For a given catchment, both values r and c_{precip} are derived from observed data at different measurement stations. Note that the area-average precipitation is an important source of uncertainty for runoff and water balance simulations. In high mountainous catchments, the glaciers represent the most important water storage reservoir and for water balance simulation, any under- or overestimation of the area-average precipitation can be compensated by simulated ice melt. For a further discussion of this problem refer to (Schaefli et al., 2005b).

Snow and ice pack evolution submodel

For each spatial unit, the temporal evolution of the snowpack is computed through an accumulation and a melt model. The aggregation state of precipitation is determined based on a simple temperature threshold (Equation 3).

$$\begin{aligned} P_{snow} &= P_{tot}\ , \quad P_{liq} = 0 \qquad T \le T_0 \\ P_{snow} &= 0, \qquad P_{liq} = P_{tot} \qquad T > T_0 \end{aligned} \tag{3}$$

where P_{tot} (mm d^{-1}) is the total precipitation on a given day and P_{snow} (mm d^{-1}) respectively P_{liq} (mm d^{-1}) are the solid respectively the liquid precipitation. T (°C) is the mean daily air temperature and T_0 is the threshold temperature that is set to 0 °C.

The potential snowmelt $M_{p,snow}$ (mm d^{-1}) is computed according to a degree-day approach (e.g., Rango and Martinec, 1995):

$$M_{p,snow} = \begin{cases} a_{snow}(T - T_m) & T > T_m \\ 0 & T < T_m \end{cases} \tag{4}$$

where a_{snow} (mm°C^{-1}d^{-1}) is the degree-day factor for snowmelt and T_m is the threshold temperature for melting that is set to 0 °C. The actual snowmelt M_{snow} (mm d^{-1}) is computed depending on the available snow height H_s (mm water equivalent). The same degree-day approach is used for the ice melt computation, replacing all subscripts snow of Equation 4 by the subscript ice. For each elevation band, the actual ice melt M_{ice} (mm d^{-1}) is calculated depending on the snowpack, assuming that there is no ice melt if the glacier surface is covered by snow.

Recent investigations by Ohmura (2001) showed that the use of the degree-day method is justified more on physical grounds than previously has been assumed. The incorporation of radiation data into the basic degree-day equation could potentially give better results for snowmelt estimations (e.g., Kustas and Rango, 1994). For the present probabilistic climate change impact analysis, corresponding input data are not available and the glacio-

hydrological model performance is satisfying with the basic degree-day formulation of Equation 4 (Schaefli et al., 2005b).

In comparable models, most authors use three different aggregation states of water, i.e. snow, ice and firn (a transition state between the two previous) (see, e.g., Baker et al., 1982; Klok et al., 2001). We have shown that for the studied hydro-climatic area, the use of firn does not improve the discharge or mass balance simulation (Schaefli et al., 2005b).

Only for a few glaciers, detailed ice volume measurements exist (Bahr et al., 1997). For the present application, the ice storage of the ice-covered spatial units is supposed to be unlimited. This approach is justified, as the developed glacier surface evolution model is not based on a simulation of the complete mass balance (see Section 2.3). For a given simulation, the glacier surface is supposed to be constant and equal to its average extension over the period. This assumption is a rough approximation; the ice-covered area varies from year to year. In extreme years, glacier snouts can retire or advance considerably. In the Swiss Alps more than 100 m of length change within single years have been observed (e.g., Herren et al., 2001). Such an extreme variation of the snout position concerns however only a small fraction of the total area of a glacier.

Annual mass balance and AAR computation

The presented glacio-hydrological model enables the estimation of the annual mass balance of an entire glacier system: For each spatial unit, the mean annual mass balance is calculated based on the simulated snow accumulation and the simulated snow- and ice melt (Equation 3 and 4). The annual mass balance of the entire glacier is estimated as the area-weighted sum of the mass balance of each spatial unit (Equation 5). For the present application, the measurement year has been fixed to the hydrological year starting on the 1 October.

$$B'_a = \frac{1}{s_g} \sum_{i=1}^{n} (b_{a,i} \cdot s_i) \tag{5}$$

where B'_a (m) is the simulated total annual mass balance of the glacier, $b_{a,i}$ (m) is the annual mass balance of the spatial unit i and s_i (m^2) is the area of the unit i. In close connection to the mass balance are two important descriptors that are classically used to characterise a glacier: the equilibrium line altitude (ELA) and the accumulation area ratio (AAR). The ELA is the line connecting all points with zero balance at the end of a fixed year (Anonymous, 1969) and the AAR is the ratio between the accumulation area and the entire glacier surface.

4.2.2 Simulation of the glacier surface evolution

The simulation of the response of glacier systems to a climate modification can be based on dynamical ice-flow models (e.g., Oerlemans et al., 1998). Such a physical modelling approach is highly data intense and can be applied only to well-investigated glacier systems. The present modelling framework has been developed for climate change impact analysis on water resources systems, i.e. on entire hydrological catchments; this context excludes the use of a physical model.

The evolution of the glacier surface is the result of complex dynamical processes of which the mass balance is one of the major driving forces. A conceptual modelling approach could therefore be based on a continuous simulation of the mass balance evolution coupled to a volume – area scaling relationship (e.g., Bahr et al., 1997). Such an approach requires an estimate of the initial ice volume that exists only for a few glaciers (Bahr et al. (1997) give for example values for 3 Swiss glacier). To avoid this problem, the change of the glacier surface could also be related directly to the change in the mass balance.

The simulated total annual mass balance of a glacier is highly sensitive to the estimation of the glacier surface. Detailed glacier surface evolution data are generally not available on a reasonably small time step (for example on a yearly basis). For the presented model where the ice volume of all ice-covered spatial units is assumed to be infinite, this can lead to considerable mass balance estimation errors in years with high ablation rates. The need of a more robust estimator of the relationship between the climate and the glacier surface lead us to the so-called AAR method. The estimation error of the annual AAR values remains small even for years with high ablation rates as the short-term glacier surface fluctuations in the glacier snout area only concern a small part of the total glacier surface. The annual AAR is strongly correlated to the total annual mass balance of a glacier. The two variables have often a linear relationship that is characteristic for a given glacier (see, e.g., Aellen and Funk, 1990; Kulkarni, 1992; Herren et al., 2002) and the presented glacio-hydrological model has been shown to be able to reproduce this relationship (Schaefli et al., 2005b).

The AAR method assumes that the steady-state accumulation area of the glacier occupies some fixed proportion of the total glacier area (see, e.g., Meier and Post, 1962; Gross et al., 1976). The concept is classically used in the paleoclimatic reconstruction of glacier surfaces (e.g., Porter, 1975; Benn and Lehmkuhl, 2000). These studies assume for a given glacier the existence of a constant steady-state AAR value that can be estimated and used to predict the steady-state glacier area for any period according to Equation 6:

$$A_{ice} = \frac{A_{acc}}{AAR_s} \tag{6}$$

where A_{ice} (km^2) is the total ice-covered area, AAR_s is the steady-state accumulation area ratio and A_{acc} (km^2) is the estimated steady-state accumulation area for the climatic conditions of the considered period.

A glacier is defined as being in a steady state if its dimensions remain constant over the considered period. This is a theoretical concept that is rarely or never encountered in practice (Paterson, 1994). A glacier is a dynamic system that has a certain reaction time to respond to the occurring climate. If the total annual mass balance for a given year is zero, the glacier may still advance or retreat. A steady state could theoretically occur if the total annual mass balance remains zero for many years or when the down slope mass flux of the glacier is in equilibrium with the glacier mass balance (Bahr et al., 1998).

Instead of using the concept of a fixed steady-state AAR value, we use the concept of a mean interannual AAR value, called $AAR_{m.}$ We assume that the AAR_m value, if estimated over a sufficiently long time period, is a good estimator of the relationship between the climate and the glacier area. We further assume that this relationship remains constant for future periods. The estimated AAR_m can be obtained through different glaciological measurement methods (Paterson, 1994) or, as in the present study, through simulation.

4.2.3 Model calibration

The glacio-hydrological model has 7 parameters to calibrate of which only the degree-day factors for snow- and ice melt are relevant for the snow accumulation and snow- and ice melt computation. The calibration of these two parameters is based on the simulated and observed river discharge and the glacier mass balance. The objective functions are the bias between the observed and the simulated signal computed according to Equation 7 for discharge and according to Equation 8 for mass balance.

$$Bias_D = \sum_{j=1}^{n_j} abs(Q_{obs,j} - Q_{sim,j}) \cdot (\sum_{j=1}^{n_j} Q_{obs,j})^{-1} \tag{7}$$

where $Q_{obs,j}$ (mm d^{-1}) is the observed specific discharge on day j, $Q_{sim,j}$ (mm d^{-1}) is the simulated specific discharge on day j and n_j is the number of simulated days.

$$Bias_M = \frac{1}{n_y} \sum_{y=1}^{n_y} [abs(B_{a,y} - B'_{a,y}) \cdot abs(B_{a,y})^{-1}] \tag{8}$$

where $B_{a,y}$ (m) is the observed annual mass balance for year y, $B'_{a,y}$ (m) is the simulated annual mass balance for year y and n_y is the total number of considered years. Note that the modified formulation of the bias function in Equation 8 is necessary because $B_{a,y}$ can be negative whereas $Q_{obs,j}$ is always positive.

For each of these functions, a response surface is generated by varying the two degree-day factors. Schaefli et al. (2005b) showed that for the Rhone catchment both surfaces show a strong correlation between the two parameters, the local optima describing a power function of the type

$$a_{snow} = \alpha \cdot a_{ice}{}^{\beta} + \gamma \tag{9}$$

where α, β and γ are constants. The curves described by the local optima of both response surfaces have one intersection point that can be retained as the global optimum solution. A detailed discussion of the bi-objective calibration procedure is given in (Schaefli et al., 2005b).

4.2.4 Modelling uncertainties

The main uncertainties inherent in the glacier surface evolution model can be split into the different modelling steps, namely the glacio-hydrological simulation of snow and ice accumulation and ablation and the glacier surface update based on the interannual mean AAR value. The uncertainties induced by the glacio-hydrological model refer to the classical hydrological model calibration problem (see, e.g., Beven and Binley, 1992; Gupta et al., 1998). Instead of using a unique "best guess" of the model parameter set, we apply a Bayesian inference method to estimate the posterior distribution of the model parameters (Schaefli et al., submitted manuscript)[3]. The used method is the so-called Metropolis-Hastings algorithm, a Markov Chain Monte Carlo (MCMC) method that becomes increasingly popular in hydrological modelling (see, e.g., Kuczera and Parent, 1998; Bates and Campbell, 2001). Based on the posterior distributions of the glacio-hydrological model parameters, we can obtain a reliable estimate of the uncertainty induced by this modelling step. The parameter inference is based on the observed discharge. The mass balance data are included by restraining the feasible parameter space to a_{ice} – a_{snow} couples that respect the found relationship of minimum bias for the simulated mass balance (Equation 9).

The modelling uncertainties induced by the glacier surface evolution model have three major sources: i) the estimation of AAR_m, ii) the representativeness of the estimated AAR_m for a future climate and iii) the reaction time of the glacier to a given climate. The first refers to the question whether the estimated AAR_m value is really characteristic for the given glacier. In the case of simulated AAR values, part of this uncertainty is directly connected to the glacio-hydrological model parameters already taken into account by the parameter inference method. The chosen reference period can be misleading for the estimation of AAR_m. If this period is a relative warm or cold period in the long-term mean, the corresponding AAR values under- respectively overestimate the characteristic AAR_m value. The uncertainty induced by the AAR_m value estimation can be investigated by drawing randomly this value in a distribution instead of using the simulated mean value. This distribution is estimated based on the simulated

[3] Schaefli, B., Balin Talamba, D. and Musy, A.: Quantifying hydrological modeling errors through finite mixture distributions. Submitted to Journal of Hydrology; hereinafter referred to as Schaefli et al., submitted manuscript.

annual AAR values for the reference period. The minimum and maximum simulated annual values constitute the lower and upper boundaries of the distribution. The entire distribution is modelled by a Log-Weibull distribution. This distribution has been chosen because the distribution has to be limited to the mentioned lower and upper boundaries and because the empiric frequencies of the AAR series for the present case study are right-skewed.

The question whether the assumption of a constant AAR_m value for a future, significantly different climate is reasonable, has a priori to be negated for such a long-term prediction as the one carried out in the present study. A significant retreat of the glacier modifies for example its geometry, the amount of debris cover or the predominant exposition (and accordingly the balance of incoming radiation). In short, the entire dynamic of ablation and accumulation processes could be modified. We assume that this uncertainty is addressed by the random draw of the AAR_m value.

The third source of uncertainty is the reaction time of the glacier, i.e. the time that elapses until a glacier reacts to a modification of the prevailing climate. The analysis of this reaction time would require defining appropriate climate scenarios for a time period preceding the period of interest for which the glacier surface is to be predicted. The used method for climate scenario production (see Section 3) does not enable the production of such preceding climate scenarios. According to Spreafico et al. (1992), the studied Rhone glacier has today a reaction time of between several years and a few decades. We assume that the gradual climate change between the present and the analysed future period (2070-2099) will substantially reduce the ice volume and the glacier surface and as a result its reaction time. We therefore assume that the future modelling period of 30 years is long enough for the glacier to react to the simulated climate and the glacier reaction time will not be investigated (for theoretic considerations referring to the response time of glaciers see, e.g., (Bahr et al., 1998)).

4.3 Climate change scenarios

4.3.1 Generation of local scale climate scenarios

Current available climate changes projections are mainly based on the results of coupled Atmosphere-Ocean General Circulation Models (AOGCMs) or on the results of Regional Climate Models (RCMs) driven by outputs of the former. The spatial resolution of these models (typically around 2.5° of latitude by 3.75° of longitude for AOGCMs and 50 km by 50 km for RCMs) is however too coarse for a direct use of the model outputs, namely precipitation and temperature, as input for glacio-hydrological models (see, e.g., Xu, 1999a). Different methodologies exist for the production of local scale climate change scenarios using for example downscaling models that connect the local meteorological variables directly to synoptic scale variables (see, e.g., Xu, 1999b; Zorita and von Storch, 1999; Bardossy et al., 2002).

In the present study context, we are rather interested in mean values than in the reproduction of extreme events and the development of a sophisticate downscaling model is therefore not justified. We use the pattern scaling methodology developed by Hingray et al. (submitted manuscript) for the generation of the future local scale precipitation and temperature time series. In this method, the local scale meteorological time series for a control period are perturbed based on the corresponding regional scale outputs of a RCM for the same control and future period. The perturbation is carried out according to the method presented by Shabalova et al. (2003). The perturbation equation for the temperature is given hereafter (Equation 10). The procedure for the perturbation of precipitation is given in Appendix 1.

$$T_{scen,s}(t) = [T_{obs,s}(t) - \overline{T}_{obs,s}] * (XSDT_s + 1) + \overline{T}_{obs,s} + XMT_s \quad (10)$$

where the variables are defined as follows: $T_{scen,s}(t)$ (°C) local scale scenario temperature on day t of season s (s = 1: DJF; s = 2: MAM; s = 3: JJA; s = 4: SON); $T_{obs,s}(t)$ (°C) observed temperature on day t of season s; $\overline{T}_{obs,s}$ (°C) observed mean temperature of season s; XMT_s absolute change of the mean temperature of season s; and $XSDT_s$ relative change of the standard deviation of the daily temperature of season s. The absolute change of the mean temperature corresponds to the mean temperature of the RCM output for the future period minus the mean temperature of the RCM output for the control period. The relative change of the standard deviation is defined as the difference between the values obtained from the RCM output for the future period and the control period divided by the RCM output for the control period.

4.3.2 Climate projection uncertainty

Regional climate change projections based on AOGCM / RCM model outputs are highly uncertain, due on one hand to the unknown future greenhouse gas emissions and on the other hand to the highly simplified representation of the true physical processes in these models. For a given greenhouse gas emission scenario, different state-of-the-art AOGCMs and related RCMs simulate different climate evolutions (see, e.g., Räisänen, 2001, 2002). The results of several RCM experiments driven by the same AOGCM can also differ significantly (see, e.g., Frei et al., 2003; Räisänen et al., 2004) but the induced uncertainty is often assumed to be substantially smaller than the one inherited by the driving AOGCM (e.g., Jenkins and Lowe, 2003).

In the context of the present study, the temperature and precipitation outputs of 19 couples of AOGCM-RCM have been analysed (Hingray et al., submitted manuscript). The corresponding data were obtained from the EU project PRUDENCE (Prediction of Regional scenarios and Uncertainties for Defining EuropeaN Climate change risks and Effects, see (Christensen et al., 2002)). This analysis suggested that the RCM inter-model variability cannot be neglected for Europe in general and for case studies in the Swiss Alps in particular.

Even though the outputs of several different AOGCM-RCM are currently available, they cannot be assumed to approximate a large range of potential climate change. The underlying green house gas emission scenarios are generally the so-called SRES-A2 and SRES-B2 scenarios defined by the Special Report on Emission Scenarios (SRES) of the Intergovernmental Panel on Climate Change (IPCC) (Nakicenovic and Swart, 2000). These emission scenarios are respectively a medium-high and a medium-low scenario corresponding to a global-mean warming of respectively around 3.2 °C and 2.4 °C; the exact global warming prediction depends on the used AOGCM (see, e.g., Gordon et al., 2000). These two scenarios cover only a small part of the potential range of global-mean warming.

Wigley and Raper (2001) present an approach based on simple climate models that provides a probability distribution function (PDF) of the global-mean warming between 1990 and different periods in the 21st century. To investigate a large range of potential global-mean warming, we use this PDF to scale the meteorological response from a RCM by different global-mean warming projections. These projections are randomly drawn from the PDF of Wigley and Raper (2001) for the appropriate future period. Such an approach is called pattern scaling technique (Mitchell, 2003). The regional climate response pattern for a RCM is defined as the regional climate change (absolute or relative) per degree of global-mean warming. The regional climate response pattern encodes how the regional climate change is related to the global-mean warming. The used pattern scaling technique is the one presented by Hingray et al. (submitted manuscript). A short description of the methodology is presented in Appendix 2.

The pattern scaling technique is based on the assumption that there is a linear relationship between the scaler (global-mean warming) and the response pattern of regional climate changes obtained from a RCM. Mitchell (2003) has analysed this assumption for spatial changes in mean temperature and precipitation from different AOGCM scenarios. He found that the pattern scaling may be applicable to a wide range of variables. Hingray et al. (submitted manuscript) found that this assumption seems to be reasonable for different case studies in the Swiss Alps. Some studies reported in the literature suggest however that the response pattern may not be linearly correlated with the global warming (e.g., Mitchell, 2003).

In previous work, we used the PDF of Wigley and Raper (2001) to compare the resulting climate change impact uncertainty to the one induced by the inter-RCM variability (Hingray, et al., submitted manuscript; Schaefli et al., 2005a). The results showed that for the considered hydro-climatic region, the inter-RCM variability leads to climate change impact uncertainties that are only slightly smaller than the ones due to the global-mean warming. The impact prediction interval resulting by drawing randomly a global-mean warming under a fixed median RCM response pattern overlaps however completely the prediction interval resulting from inter-RCM variability under a fixed median global-mean warming. This means that the two sources of uncertainty do not induce a relative shift of the impact distribution. Based on this result, we do not consider here the inter-RCM variability. The RCM pattern

used for the generation of local climate scenarios is the one corresponding to the median pattern estimated from the 19 RCM runs available trough the PRUDENCE project (Christensen et al., 2002).

4.4 Case study

In the present study, the glacier surface evolution model has been applied to a glacier situated in the Southern Swiss Alps, the so-called Rhone glacier (Figure 2, longitude 8.39°E, latitude 46.62°N). For the model calibration, we also used data from the river that originates from this glacier, the Rhone river measured at Gletsch. Table 1 gives some important physiographic characteristics of the glacier and of the entire Rhone river catchment. The interpolation of the altitudinal distribution of precipitation is estimated to 3.1 % per 100 m of difference between a given point and the measurement station altitude. This value has been estimated based on several meteorological measurement stations around the catchment and the data given by Funk (1985). The temperature decrease with altitude is fixed to -0.65 °C per 100 m of altitude change. The estimated mean annual precipitation at the mean altitude of the glacier is about 1980 mm and the mean daily temperature –7.3°C (reference period 1961 - 1990).

Table 1: Main physiographic characteristics of the case study glacier and the related hydrological catchment; reference year for glacier surface: 1973 (Müller et al., 1976)

Characteristic	Glacier	Catchment
Area (km^2)	17.38	38.90
Glaciation (%)	100	52.3
Mean slope (°)	16.5	22.9
Min. altitude (m a.s.l.)	2219	1755
Mean altitude (m a.s.l.)	2953	2713
Max. altitude (m a.s.l.)	3630	3612

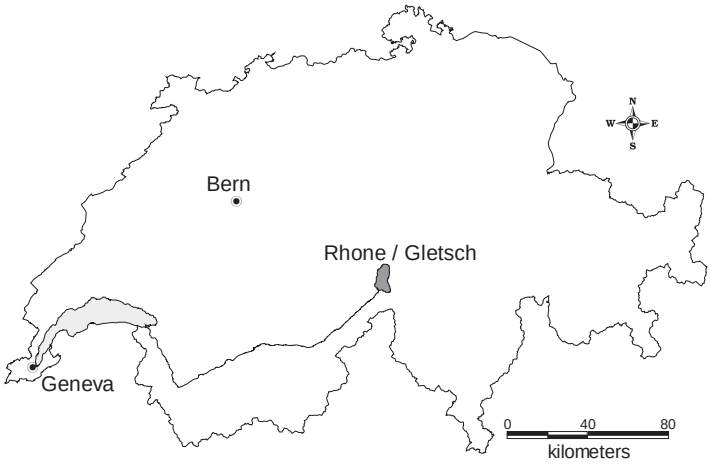

Figure 2: Location of the case study glacier and the related hydrological catchment in the Swiss Alps (SwissTopo, 1997)

4.4.1 Data collection

The spatial discretization of the catchment is carried out based on a digital elevation model with a resolution of 25 m (SwissTopo, 1995) and a digital (vector-based) land cover data set with a digitalisation scale of 1:25,000 (SwissTopo, 1997). The glacio-hydrological model needs daily mean values of temperature, precipitation and potential evapotranspiration as meteorological input. For the model calibration, daily mean discharge measurements and annual mass balance data are needed. The precipitation and temperature time series are obtained from the national weather service MeteoSwiss at a measurement station located within a few kilometres distance of the catchment. The potential evapotranspiration time series are calculated based on the Penman-Monteith version given by Burman and Pochop (1994). The daily discharge data for the Rhone river are provided by the Swiss Federal Office for Water and Geology. The observed annual mass balance data of the Rhone glacier are obtained from the work of Funk (1985) for the hydrological years 1979/80 to 1981/82.

4.4.2 Model set-up

As mentioned in Section 2, the glacio-hydrological model is calibrated through a Bayesian approach yielding a distribution of probable parameter values. The distributions of the degree-day factors for the Rhone catchment are shown in Figure 3. The parameter set with the maximum likelihood has a value of a_{ice} = 8.0 mm°C^{-1}d^{-1} and a_{snow} = 7.8 mm°C^{-1}d^{-1}. This parameter set leads to good estimation results for the observed AAR values (Table 2).

The simulated annual AAR values for the control period are modelled by a Log-Weibull distribution. Figure 4 gives a plot of the empiric frequency versus the fitted theoretic frequency for the annual AAR series simulated with the maximum likelihood parameter set.

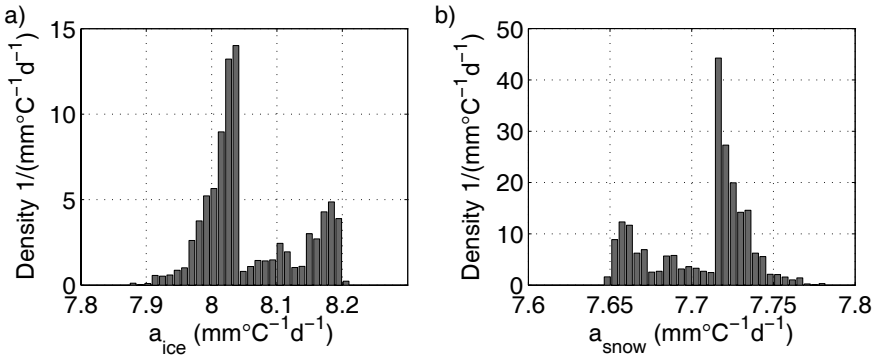

Figure 3: Posterior distribution of the parameters a_{ice} and a_{snow}

Table 2: Observed and simulated annual AAR values for the hydrological parameter set with the maximum likelihood

	AAR (%)	
Year	Obs.	Sim.
1979/80	64	71
1980/81	53	59
1981/82	45	37

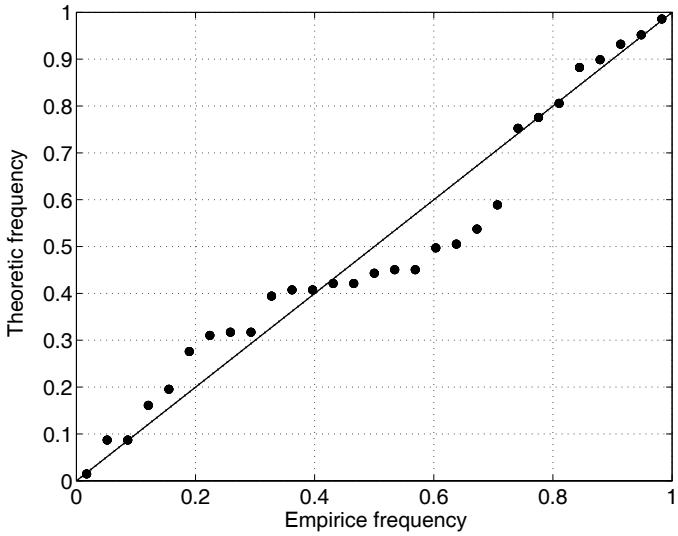

Figure 4: Fit of the Log-Weibull distribution to the annual AAR values; plot of the empiric versus the theoretic frequency (the annual AAR values are simulated with the hydrological parameter set with the maximum likelihood)

4.4.3 Regional climate response pattern

The computation of the local scale meteorological times series corresponding to a given global-mean warming scenario requires the following regional climate change statistics as input (see also Section 3, Appendix 1 and 2):

- XMT_s : the absolute change of the mean temperature (the regional warming)
- XMP_s : the relative change of the mean precipitation
- $XSDT_s$: the relative change of the standard deviation of the daily mean temperature
- $XCVP_s$: the relative change of the coefficient of variation of daily precipitation

These variables are defined for each of the following four seasons: s =1: DJF; s = 2: MAM; s = 3: JJA; s = 4: SON.

These regional climate change statistics are obtained from the output of a RCM driven by an AOGCM for a control period and a future scenario. The absolute change is defined as the value obtained for the scenario run minus the value obtained for the control run. The relative change is defined as the difference between the values obtained for the future run and for the control run divided by the value obtained for the control run.

The regional climate response pattern is obtained by dividing he above regional climate statistics for a given RCM by the corresponding global-mean warming ΔT given by the driving AOGCM. As mentioned in the previous section, we use the mean response pattern for the considered region estimated from the 19 RCM runs available trough the PRUDENCE project (Christensen et al., 2002). The response pattern is given in Table 3.

Table 3: Mean regional response pattern for the Rhone glacier catchment

Season	$XMT_s/\Delta T$	$XSDT_s/\Delta T$	$XMP_s/\Delta T$	$XCVP_s/\Delta T$
DJF	1.082	0.0003	0.0358	-0.0728
MAM	1.137	-0.0068	-0.0038	-0.0012
JJA	1.644	0.1037	-0.0867	0.1864
SON	1.327	-0.0116	-0.0369	0.0824

Note that the regional warming is higher than the global-mean warming (values of $XMT_s/\Delta T$ between 1.08 and 1.6). This tendency is already observed in the Alps, where the observed warming since the early 1980s is of far greater amplitude than the observed global-mean warming. According to Haeberli and Beniston (1998) up to +2°C have been observed for individual sites in the Alps whereas the global average earth surface temperature has increased by about 0.6°C over the 20th century (Folland et al., 2001).

The temperature increase is especially pronounced during the summer season. The precipitation increases slightly during the winter season but the annual mean decreases. For

illustrative purposes, the resulting local scale meteorological time series for a global-mean warming scenario of +1°C are shown in Figure 5.

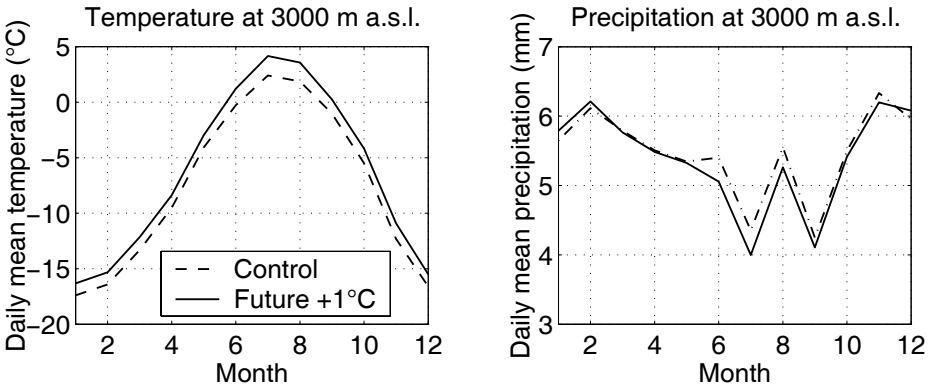

Figure 5: Local climate (reference altitude 3000 m a.s.l.) for the control period and for the future scenario (global-mean warming of +1 °C); a) mean daily temperature (mean warming +1.3°C), b) daily mean precipitation (mean annual reduction = - 1.6 %)

4.5 Results

The glacier surface is simulated for the control period (1961 - 1990) to validate the model concepts and for the future period 2070 to 2099 to analyse the potential climate change impacts. The influence of the different sources of modelling uncertainty on the glacier surface simulation are presented separately and combined through Monte Carlo simulation: The system behaviour is simulated sampling randomly the appropriate parameters for each modelling step. The following three uncertainty levels are considered: i) the parameter estimation of the hydrological model that influences the simulated accumulation area, ii) the AAR_m value of the glacier surface evolution model and iii) the global-mean warming. The three uncertainty levels are successively combined. The corresponding probability density functions are the result of 3000 random samples for simulations considering only one source of uncertainty and of 10,000 random parameter samples if several sources of uncertainty are considered. A random parameter sample contains one randomly drawn parameter value for each parameter that is taken into account at a given level of uncertainty combination.

4.5.1 Control period

The glacier surface evolution model is tested to validate the underlying concept for the observed control period. We simulate the glacier surface evolution for the control period under the AAR_m value uncertainty, under the hydrological model parameter uncertainty and under the combined uncertainty (Table 4 and Figure 6). Note that in the first case, the hydrological parameter set is fixed to the identified maximum likelihood parameter set

whereas in the second case the AAR_m value is fixed to the median simulated value. Under the AAR_m value uncertainty, the resulting median glacier surface slightly underestimates the observed value whereas the glacier surface distribution resulting from the hydrological parameter distribution overestimates the observed surface (Table 4). This result could indicate that the median AAR value overestimates the characteristic AAR_m, which in turn could be due to the snow rich winters in the late 1970ties and early 1980ties, due to which many small glaciers in the Swiss Alps (including the Rhone glacier) experienced an advancing period (Herren et al., 1999). Note that the uncertainty directly induced by the hydrological parameter set is small. The 90 % confidence interval covers only a range of 0.5 km^2.

Considering both sources of uncertainty, the observed glacier surface is well simulated by the median value, the 90 % confidence interval is however quite large (Table 4), ranging from around half to more than twice the observed surface; this result is further discussed hereafter.

We also test whether the model is able to simulate the observed glacier retreat experienced since the control period. In the year 2000, the Rhone glacier had a surface of 16.1 km^2 (Paul, 2003). Using the meteorological times series for the period 1991 - 2000 as an input into the model, the predicted median glacier surface is 16.66 km^2 (Table 4). The model seems to be sensitive enough to react to the climate modification that has been experienced in the Swiss Alps since the control period. The resulting glacier surface distribution is however not significantly different from the one for the control period (see Table 4). We used the statistical test Kolmogorov-Smirnov (Massey, 1956) to test the hypothesis that the simulated glacier surfaces for the two periods have the same continuous distribution. The hypothesis cannot be rejected at a significance level of 5 %. Note that the results for the period 1991 - 2000 are not completely comparable to the ones for the control period as the period is too short to respect the modelling assumptions stated in Section 2.

The unrealistically large intervals for glacier surface prediction are due to the extreme hypothesis underlying the uncertainty analysis: The AAR_m value represents the long-term interannual mean value but we assume that the AAR_m value could take every value between the minimum and the maximum simulated annual value (i.e. for the presented case study between 0.12 and 0.62). The series of annual AAR values corresponds to the finest possible temporal aggregation. A higher aggregation time step could lead to a more realistic result but reduces the sample length for the estimation of the statistical distribution. Further research into the optimal temporal aggregation could help constraining the uncertainty interval. Note that while for the observed periods the annual aggregation leads to unrealistic results, it ensures that the future prediction intervals (that are considerably smaller, see next section) are not underestimated. The obtained distributions for the observed periods have a merely statistical interest to test the model sensitivity.

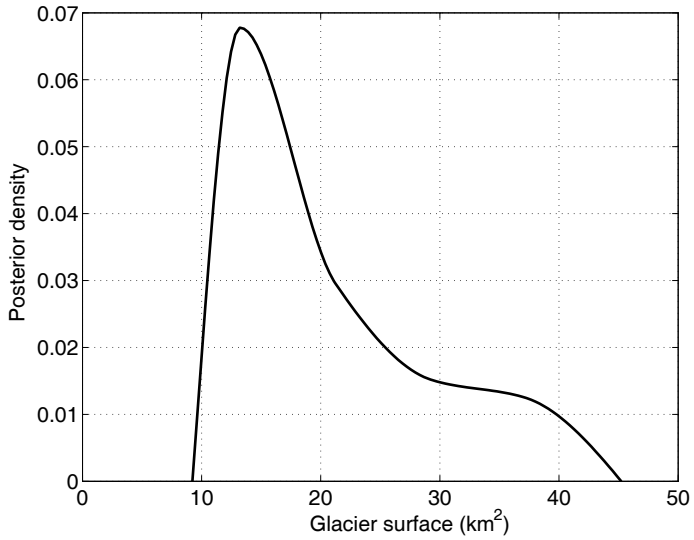

Figure 6: Simulated distribution of the glacier surface for the control period (*AAR_m* and hydrological parameter set drawn randomly)

Table 4: Percentiles of the simulated distributions of the glacier surface (km^2) for the control period and for the period 1991 - 2000 including the uncertainty due to the hydrological parameter set or the *AAR_m* value (*dT*: local temperature increase compared to the control period, *dP* relative precipitation increase compared to the control period)

Time period	*dT* (°C)	*dP* (%)	*AAR_m* value	Hydrological parameter set	Glacier surface (km^2) 5 %	10 %	50 %	90 %	95 %
1961-1990	0	0	Random	Max. likelihood	9.62	10.10	16.96	40.27	44.24
1961-1990	0	0	Median	Random	18.34	18.35	18.60	18.84	18.85
1961-1990	0	0	Random	Random	9.56	10.08	17.34	38.51	43.85
1991-2000	0.77	6.7	Random	Random	9.64	10.10	16.66	39.50	43.64

4.5.2 Future period

Considering the probability distribution of the global-mean warming given by Wigley and Raper (2001) for the period 2070 - 2099, the median warming corresponds to 2.6°C (Figure 7a). At the local scale, the median mean annual warming is 3.4°C with a minimum increase during the winter of 2.9°C and a maximum increase during the summer of 4.6°C (Figure 7b). The median reduction of the mean annual precipitation is -5.3 % with a strong decrease in summer of –20.0 % and a slight increase during the winter of 5.2 %. Note the important simulated variability of mean monthly precipitation during the summer months (Figure 7c).

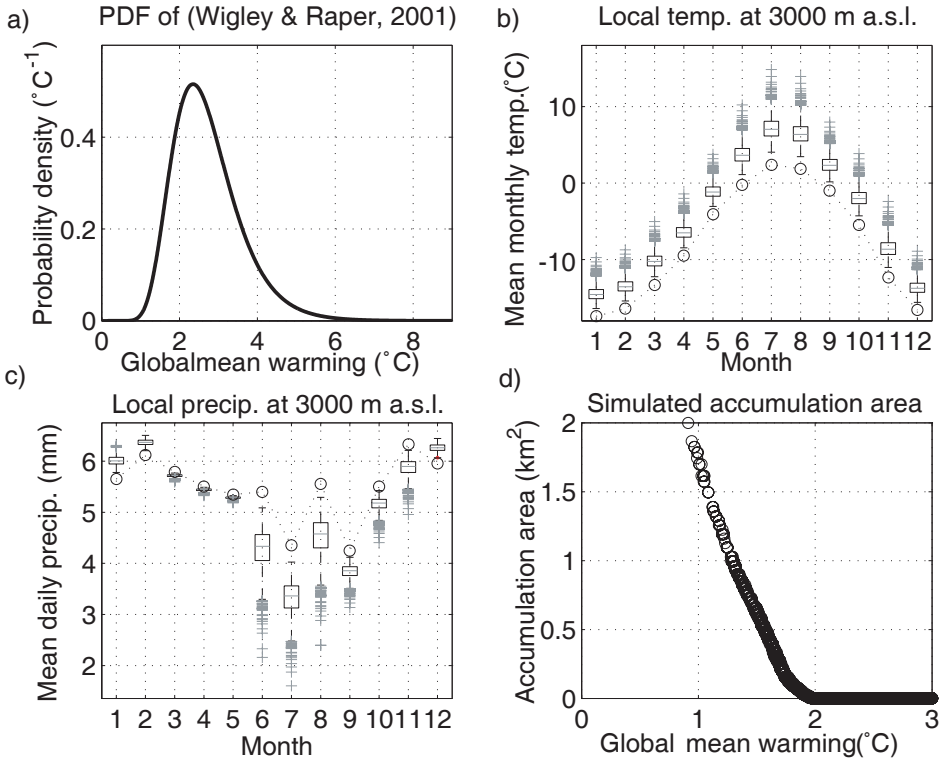

Figure 7: a) Probability distribution of global-mean warming for the period 2070 - 2099 drawn from Wigley and Raper (2001); b) and c) boxplots of future mean monthly temperature respectively precipitation for the case study catchment, the black circles correspond to the mean monthly values for the control period; d) simulated accumulation area as a function of global-mean warming

The predicted median glacier surface for the future period given all considered modelling uncertainties is 0 (Table 5). Only for global-mean warming scenarios smaller than +2.0°C (around 20 % of all scenarios, see Figure 7a), there is some accumulation area left (see Figure 7d; note that the uncertainty induced by the glacio-hydrological parameters on the simulated accumulation leads to a too small spread to be visible in this figure). This result is due to the annual temperature increase and especially to the strong increase during the summer resulting in an enhanced melting of snow and ice that is not compensated by additional precipitation during the accumulation season. For illustrative purposes, Figure 8 shows the simulated mean monthly snow height at a reference altitude (3000 m a.s.l.) for the control period and two global-warming scenarios.

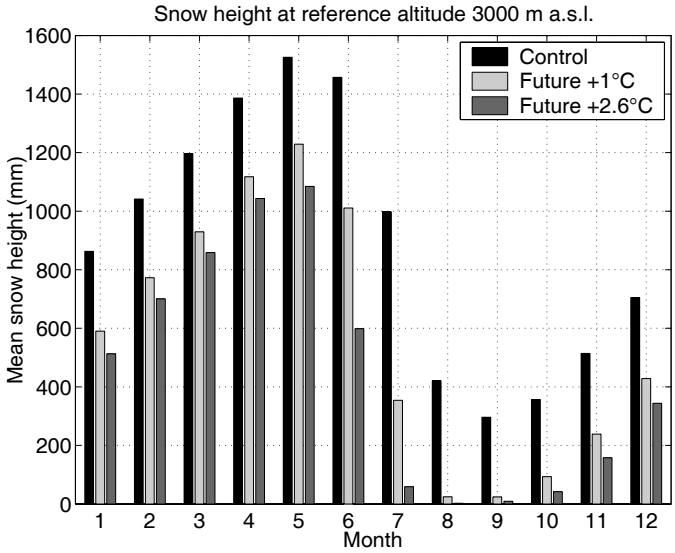

Figure 8: Simulated mean snow height at 3000 m a.s.l. for the control period and two global-mean warming scenarios; the glacio-hydrological parameters are fixed to the parameter set with the maximum likelihood.

Given an altitudinal temperature decrease of –0.65°C per 100 m, a warming of 3.4°C (the median local mean annual warming) corresponds to an upward shift of more than 530 m of the 0°C isotherm. This shift cannot be directly translated into a shift of the ELA as there is no linear relationship between the simulated accumulation area and the 0°C isotherm. Consider nevertheless that the median ELA for the observed period is 3085 m a.s.l. and the highest point of the glacier is 3630 m a.s.l., only about 550 m higher.

The AAR_m value and hydrological parameter uncertainty have also been simulated separately for different global-mean warming scenarios. The simulated glacier surface distributions for a global-mean warming scenario of +1°C are discussed here in some detail. As for the control period, the influence of the hydrological parameter uncertainty on the predicted glacier surface is negligible; for the +1°C scenario, the 90 % confidence interval covers only 0.2 km^2 (Table 5). For the same warming scenario, the 90 % confidence interval due to the combined AAR_m value and hydrological parameter uncertainty covers a range of 10.4 km^2. The shift between the simulated distribution for the control period and for the future period is statistically significant. The 95 % percentile of the future distribution corresponds to the 34 % percentile of the control period and the future median value lies outside the control distribution. Despite the relatively large glacier surface distribution for the control period, the climate change induced shift is statistically significant (Kolmogorov-Smirnov test) for a global-mean warming higher than 0.1 °C.

Table 5: Percentiles of the simulated distributions of the glacier surface (km^2) for the future period including the uncertainty due to the hydrological parameter set, the AAR_m value or the global-mean warming

Time period	Global warming	AAR_m value	Hydrological parameter set	Glacier surface (km^2)				
				5 %	10 %	50 %	90 %	95 %
2070-2099	+ 1.0°C	Median	Random	5.60	5.67	5.67	5.74	5.80
2070-2099	+ 1.0°C	Random	Random	2.94	3.08	5.17	12.14	13.35
2070-2099	Random	Random	Random	0.00	0.00	0.00	0.67	1.73

Figure 9a shows the simulated glacier surface distributions for three global-mean warming scenarios (+0.5°C, +1°C and +1.5°C). Note the interesting effect that the confidence intervals become smaller with higher global-mean warming scenarios (see also Figure 9b): The higher the global-mean warming is, the smaller is the simulated accumulation area and the smaller is the effect of the chosen AAR_m on the total glacier surface. The influence of the AAR_m uncertainty disappears if the glacio-hydrological does not simulate any accumulation (at around +2°C of global-mean warming, Figure 9b). This mathematically induced result is contrary to the classical prediction uncertainty paradigm that states that a prediction for a period more distant in time is more uncertain than one for a closer period.

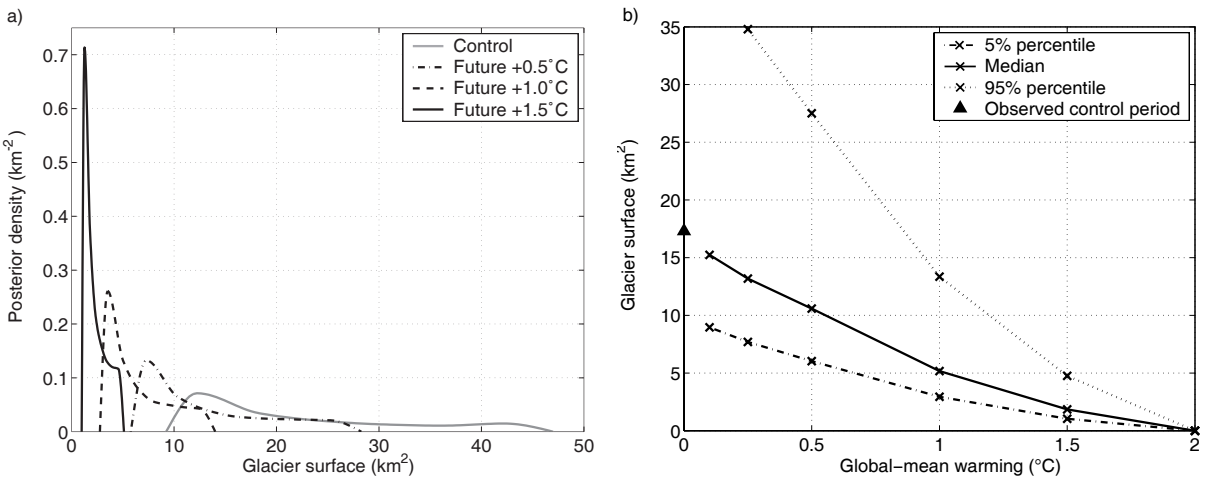

Figure 9: a) Simulated glacier surface distributions for the control period and global-mean scenarios of +0.5°C, +1°C and +1.5°C; b) percentiles of simulated glacier surface distributions as a function of global-mean warming (all distributions account for AAR_m and hydrological parameter uncertainty)

4.6 Conclusions

The present conceptual modelling approach has been developed to investigate climate change impacts on glacier surface evolution in a fully probabilistic framework. The main underlying objective was to include a wide range of potential global-mean warming instead of only one or two climate change scenarios and to develop a method applicable to the glacier systems of entire hydrological catchments. The first objective imposed an important constraint related to the meteorological input times series. With the currently available scientific knowledge and climate change projection data, the presented pattern scaling approach for the computation of regional climate response to a global-mean warming cannot be easily extended to other climate variables that could be relevant for mass balance computation such as solar radiation or wind. Recent research results suggest however that the presented mass balance simulation based on a degree-day approach could be extended to a more complex formulation without needing additional input data (Walter et al., 2005). It should nevertheless be kept in mind that a modelling approach considering only precipitation and temperature as underlying driving forces for the mass balance simulation can only be applied to snowfall-fed glacier systems where the processes of snow- and ice accumulation and ablation are not strongly influenced by other factors such as snow redistribution by wind and avalanches. The AAR concept becomes meaningless for glaciers where the accumulation and ablation areas are separated by steep, unglaciated rock slopes and where the theoretical ELA may be located within a avalanche track where no glacier ice occurs (Benn and Lehmkuhl, 2000).

In the present paper, the developed methodology for glacier surface evolution modelling has been illustrated at the scale of a single glacier. It is applicable to glacier systems at the hydrological catchment scale (see Schaefli et al., 2005a). Instead of simulating the evolution for each single glacier, the AAR values can be estimated for entire glacier systems provided that they are of the same glacier type and that their dynamics can be assumed to be comparable. If no mass balance data are available, the underlying glacio-hydrological model can also be calibrated on river discharge data and regional information on the degree-day factors.

If the mass balance evolution of a glacier is simulated over a long time period, the estimation errors are cumulated, leading to a potentially important total error. In the presented modelling approach, the simulated glacier surface is not directly a function of the mass balance but of the simulated accumulation area. This variable is less sensitive in particular to the melting process in the ablation area where different factors can considerably influence the total annual ablation such as debris cover or the available ice mass.

The predicted distribution of the future glacier surface considering all sources of modelling uncertainty (in particular the uncertainty of potential global-mean warming) shows a complete disappearance of the glacier for 80 % of the simulations. This result is mainly due to the predicted median raise of the local mean temperature (+3.4°C) that is not compensated by

additional precipitation. It has been shown through simulation that even a raise of the global-mean temperature of 0.1°C would lead to a statistically significant retreat of the glacier.

Such a surface reduction is accompanied by a modification of the discharge regime because the prevailing ablation (melt) and accumulation processes are changed. For the studied glacier system, the start of the snow- and ice melt season is considerably shifted. For the global-mean warming scenario of +1°C for example, the snowmelt season starts around two weeks earlier in the interannual mean. In return, ice melt starts around 40 days later as ice-covered areas are left only in high altitudes. The resulting discharge modification can have a considerable impact on different water uses such as hydropower production (see Schaefli et al., 2005a) or irrigation or on flood risk. A reduction of the glacier surface in the Alps may have numerous other repercussions on the related natural environment and on human activities. Even though the presented approach has been developed for an application in climate change impact analysis on water resources management it could be transposed to other types of impact analysis such as land use change studies.

Acknowledgements

We wish to thank the Swiss Federal Office for Water and Geology for providing the discharge data and the national weather service MeteoSwiss for providing the meteorological time series. The model was developed in the context of the European project SWURVE (Sustainable Water: Uncertainty, Risk and Vulnerability in Europe, funded under the EU Environment and Sustainable Development programme, grant number EVK1-2000-00075) that analyses climate change impacts on water resources systems in Europe. The Swiss part of this project was funded by the Federal Office for Education and Science, contract number 00.0117.

References

Aellen, M., and M. Funk (1990), Bilan hydrologique du bassin versant de la Massa et bilan de masse des glaciers d'Aletsch (Alpes Bernoises, Suisse), in *Hydrology in Mountainous Regions I: Hydrological Measurements; the Water Cycle*, edited by H. Lang, and A. Musy, pp. 89-98, IAHS Publ. No. 193, Wallingford, Oxfordshire UK.

Anonymous (1969), Mass-balance terms, *Journal of Glaciology*, *8* (52), 3-7.

Bahr, D.B., M.F. Meier, and S.D. Peckham (1997), The physical basis of glacier volume-area scaling, *Journal of Geophysical Research B - Solid Earth*, *102* (B9), 20355-20362.

Bahr, D.B., W.T. Pfeffer, C. Sassolas, and M.F. Meier (1998), Response time of glaciers as a function of size and mass balance: 1. Theory, *Journal of Geophysical Research B - Solid Earth*, *103* (B5), 9777-9782.

Baker, D., H. Escher-Vetter, H. Moser, H. Oerter, and O. Reinwarth (1982), A glacier discharge model based on results from field studies of energy balance, water storage

and flow, in *Hydrological Aspects of Alpine and High-Mountain Areas,*, edited by J.W. Glen, pp. 103-112, IAHS, Wallingford, Oxfordshire UK.

Bardossy, A., J. Stehlik, and H.J. Caspary (2002), Automated objective classification of daily circulation patterns for precipitation and temperature downscaling based on optimized fuzzy rules, *Climate Research*, *23* (1), 11-22.

Bates, B.C., and E.P. Campbell (2001), A Markov chain Monte Carlo scheme for parameter estimation and inference in conceptual rainfall-runoff modeling, *Water Resources Research*, *37* (4), 937-947.

Benn, D.I., and F. Lehmkuhl (2000), Mass balance and equilibrium-line altitudes of glaciers in high-mountain environments, *Quaternary International*, *65-66*, 15-29.

Beven, K., and A. Binley (1992), The future of distributed models: model calibration and uncertainty prediction, *Hydrological Processes*, *6* (3), 279-298.

Braithwaite, R.J., and Y. Zhang (2000), Sensitivity of mass balance of five Swiss glaciers to temperature changes assessed by tuning a degree-day model, *Journal of Glaciology*, *46* (152), 7-14.

Braun, L.N., M. Weber, and M. Schulz (2000), Consequences of climate change for runoff from Alpine regions, *Annals of Glaciology*, *31*, 19-25.

Burman, R., and L.O. Pochop (1994), *Evaporation, evapotranspiration and climatic data*, 278 pp., Elsevier, Amsterdam.

Christensen, J.H., T.R. Carter, and F. Giorgi (2002), PRUDENCE employs new methods to assess European Climate Change, *EOS Trans, AGU*, *83*, 147.

Folland, C.K., T.R. Karl, J.R. Christy, R.A. Clarke, G.V. Gruza, J. Jouzel, M.E. Mann, J. Oerlemans, M.J. Salinger, and S.-W. Wang (2001), Observed Climate Variability and Change, in *Climate Change 2001: The Scientific Basis. Contribution of Working Group I to the Third Assessment Report of the Intergovernmental Panel on Climate Change*, edited by J.T. Houghton, et al., pp. 99-181, Cambridge University Press, Cambridge, UK.

Frei, C., J.H. Christensen, M. Deque, D. Jacob, R.G. Jones, and P.L. Vidale (2003), Daily precipitation statistics in regional climate models: Evaluation and intercomparison for the European Alps, *Journal of Geophysical Research - Atmospheres*, *108* (D3), doi: 10.1029/2002JD002287.

Funk, M. (1985), Räumliche Verteilung der Massenbilanz auf dem Rhonegletscher und ihre Beziehung zu Klimaelementen, Doctoral thesis, Eidgenössische Technische Hochschule Zürich, Zürich.

Gordon, C., C. Cooper, C.A. Senior, H. Banks, J.M. Gregory, T.C. Johns, J.F.B. Mitchell, and R.A. Wood (2000), The simulation of SST, sea ice extents and ocean heat transports in a version of the Hadley Centre coupled model without flux adjustments, *Climate Dynamics*, *16* (2-3), 147-168.

Gross, G., H. Kerschner, and G. Patzelt (1976), Methodische Untersuchungen über die Schneegrenze in alpinen Gletschergbieten, *Zeitschrift für Gletscherkunde und Glazialgeologie*, *12*, 223-251.

Gupta, H.V., S. Sorooshian, and P.O. Yapo (1998), Toward improved calibration of hydrologic models: Multiple and noncommensurable measures of information, *Water Resources Research*, *34* (4), 751-763.

Haeberli, W., and M. Beniston (1998), Climate change and its impacts on glaciers and permafrost in the Alps, *Ambio*, *27* (4), 258-265.

Hall, M.H.P., and D.B. Fagre (2003), Modeled climate-induced glacier change in Glacier National Park, 1850-2100, *Bioscience*, *53* (2), 131-140.

Herren, E.R., A. Bauder, M. Hoelzle, and M. Maisch (2002), The Swiss Glaciers 1999/2000 and 2001/2002, pp. 73, Glaciological Commission of the Swiss Academy of Sciences, Zürich.

Herren, E.R., M. Hoelzle, and M. Maisch (1999), The Swiss Glaciers 1993/94 and 1994/95, pp. 66, Glaciological Commission of the Swiss Academy of Sciences, Zürich.

Herren, E.R., M. Hoelzle, and M. Maisch (2001), The Swiss Glaciers 1997/98 and 1998/99, pp. 86, Glaciological Commission of the Swiss Academy of Sciences, Zürich.

Jenkins, G., and J. Lowe (2003), Handling uncertainties in the UKCIP02 scenarios of climate change, Hadley Centre, Technical note 44, Exeter, UK.

Klok, E.J., K. Jasper, K.P. Roelofsma, J. Gurtz, and A. Badoux (2001), Distributed hydrological modelling of a heavily glaciated Alpine river basin, *Hydrological Sciences Journal*, *46* (4), 553-570.

Kuczera, G., and E. Parent (1998), Monte Carlo assessment of parameter uncertainty in conceptual catchment models: the Metropolis algorithm, *Journal of Hydrology*, *211* (1-4), 69-85.

Kulkarni, A.V. (1992), Mass balance of Himalayan glaciers using AAR and ELA methods, *Journal of Glaciology*, *38*, 101-104.

Kustas, W.P., and A. Rango (1994), A simple energy budget algorithm for the snowmelt runoff model, *Water Resources Research*, *30* (5), 1515-1527.

Laumann, T., and N. Reeh (1993), Sensitivity to climate-change of the mass-balance of glaciers in southern Norway, *Journal of Glaciology*, *39* (133), 656-665.

Loukas, A., L. Vasiliades, and N.R. Dalezios (2002), Potential climate change impacts on flood producing mechanisms in southern British Columbia, Canada using the CGCMA1 simulation results, *Journal of Hydrology*, *259* (1-4), 163-188.

Massey, F.J. (1956), The Kolmogorov-Smirnov Test for Goodness of Fit, *46*, 68-77.

Meier, M.F., and A.S. Post (1962), Recent variations in mass net budgets of glaciers in western North America, in *Commission of Snow and Ice Symposium of Obergurgl,*, pp. 63-77, IAHS Publ. No. 58, Wallingford, Oxfordshire UK.

Mitchell, T.D. (2003), Pattern scaling - An examination of the accuracy of the technique for describing future climates, *Climate Change*, *60* (3), 217-242.

Müller, F., T. Caflisch, and G. Müller (1976), *Firn und Eis der Schweizer Alpen - Gletscherinventar*, 174 pp., Geographisches Institut, Eidgenössische Technische Hochschule Zürich, Zürich, Switzerland.

Nakicenovic, N., and R. Swart (2000), Special Report on Emissions Scenarios (Intergovernmental Panel on Climate Change), pp. 570, Cambridge University Press, Cambridge, UK.

Oerlemans, J. (1989), Glacier fluctuations and climatic change. Proceedings of the Symposium on Glacier Fluctuations and Climatic Change, held in Amsterdam, 1-5 June 1987, in *Glaciology and quaternary geology*, edited by Bentley C.R., pp. 417, Kluwer Academic Publishers, Dordrecht.

Oerlemans, J., B. Anderson, A. Hubbard, P. Huybrechts, T. Johannesson, W.H. Knap, M. Schmeits, A.P. Stroeven, S.W. Van de Wal, J. Wallinga, and Z. Zuo (1998), Modelling the response of glaciers to climate warming, *Climate Dynamics*, *14* (4), 267-274.

Ohmura, A. (2001), Physical basis for the temperature-based melt-index method, *Journal of applied meteorology*, *40* (4), 753-761.

Paterson, W.S.B. (1994), *The Physics of Glaciers*, 480 pp., Pergamon, Oxford.

Paul, F. (2003), The new Swiss glacier inventory 2000 - Application of remote sensing and GIS, PhD thesis, University of Zurich, Zürich, Switzerland.

Porter, S.C. (1975), Equilibrium-line altitudes of late quaternary glaciers in southern alps, New Zealand, *Quaternary Research*, *5* (1), 27-47.

Räisänen, J. (2001), CO2-induced climate change in CMIP2 experiments: Quantification of agreement and role of internal variability, *Journal of Climate*, *14* (9), 2088-2104.

Räisänen, J. (2002), CO2-induced changes in interannual temperature and precipitation variability in 19 CMIP2 experiments, *Journal of Climate*, *15* (17), 2395-2411.

Räisänen, J., U. Hansson, A. Ullerstig, R. Döscher, L.P. Graham, C. Jones, H.E.M. Meier, P. Samuelsson, and U. Willén (2004), European climate in the late 21st century: regional simulations with two driving global models and two forcing scenarios, *Climate Dynamics*, *22* (1), 13-31.

Rango, A., and J. Martinec (1995), Revisiting the degree-day method for snowmelt computations, *Water Resources Bulletin*, *31* (4), 657-669.

Raper, S.C.B., O. Brown, and R.J. Braithwaite (2000), A geometric glacier model for sea-level change calculations, *Journal of Glaciology*, *46* (154), 357-368.

Schaefli, B., Hingray, B. and Musy, A., 2005a. Climate change and hydropower production in the Swiss Alps: Quantification of potential impacts and related modelling uncertainties. Hydrology and Earth System Sciences, Accepted for publication in a special issue.

Schaefli, B., Hingray, B., Niggli, M. and Musy, A., 2005b. A conceptual glacio-hydrological model for high mountainous catchments. Hydrology and Earth System Sciences Discussions, 2, 73-117.

Schneeberger, C., H. Blatter, A. Abe-Ouchi, and M. Wild (2003), Modelling changes in the mass balance of glaciers of the northern hemisphere for a transient 2 x CO2 scenario, *Journal of Hydrology*, *282* (1-4), 145-163.

Shabalova, M.V., W.P.A. Van Deursen, and T.A. Buishand (2003), Assessing future discharge of the river Rhine using regional climate model integrations and a hydrological model, *Climate Research*, *23*, 223-246.

Spreafico, M., R. Weingartner, and C. Leibundgut (1992), *Atlas hydrologique de la Suisse*, Service Hydrologique et Géologique National (SHGN), Bern.

Swiss Federal Office for Energy (2003), Statistique suisse de l'électricité 2002, pp. 56, Bern.

SwissTopo (1995), Digital height model of Switzerland - DHM25, Wabern, Switzerland.

SwissTopo (1997), Vector25 - The digital landscape model of Switzerland, Wabern, Switzerland.

Torsnes, I., N. Rye, and A. Nesje (1993), Modern and little ice-age equilibrium-line altitudes on outlet valley glaciers from Jostedalsbreen, Western Norway - an evaluation of different approaches to their calculation, *Arctic and Alpine Research*, *25* (2), 106-116.

Van de Wal, R.S.W., and M. Wild (2001), Modelling the response of glaciers to climate change by applying volume-area scaling in combination with a high resolution GCM, *Climate Dynamics*, *18* (3-4), 359-366.

Vincent, C. (2002), Influence of climate change over the 20th Century on four French glacier mass balance, *Journal of Geophysical Research - Atmospheres*, *107*, doi: 10.1029/2001JD000832.

Walter, T.M., E.S. Brooks, D.K. McCool, L.G. King, M. Molnau, and J. Boll (2005), Process-based snowmelt modeling: does it require more input data than temperature-index modeling?, *Journal of Hydrology*, *300* (1-4), 65-75.

Wigley, T.M.L., and S.C.B. Raper (2001), Interpretation of High Projections for Global-Mean Warming, *Science*, *293* (5529), 451-454.

Willis, I., and J.-M. Bonvin (1995), Climate change in mountain environments: hydrological and water resource implications, *Geography*, *80* (3), 247-261.

Xu, C.Y. (1999a), Climate change and hydrologic models: a review of existing gaps and recent research developments, *Water Resources Management*, *13*, 369–382.
Xu, C.Y. (1999b), From GCMs to river flow: a review of downscaling methods and hydrologic modelling approaches, *Progress in Physical Geography*, *23* (2), 229-249.
Zorita, E., and H. von Storch (1999), The analog method as a simple statistical downscaling technique: comparison with more complicated methods, *12* (8), 2474-2489.

Appendix 1: Perturbation of daily rainfall series (after Shabolova et al., 2003)

The Weibull distribution is assumed to give a reasonable fit to the distribution of the daily rainfall amounts. For a random variable U (daily rainfall amount) with the distribution function $F(u)$ where u is a realisation of U, the Weibull distribution is defined as (Equation A1.1):

$$F(u) = \Pr(U \le u) = 1 - \exp\left[-(u/\alpha)^c\right] \tag{A1.1}$$

where $\Pr(U \le u)$ is the probability that U does not exceed u and α and c are respectively the scale and the shape parameter.

For such a distribution, the pth percentile has the following expression:

$$u_p = \alpha\left[-\ln(1-p)\right]^{1/c} \tag{A1.2}$$

For the observed data, both parameters α_{obs} and c_{obs} are estimated by the method of moments such that the distribution preserves the observed mean $E(u)$ and variance $Var(u)$. The theoretical values for the mean (Equation A1.3) respectively the variance (Equation A1.4) are:

$$E(u) = \alpha\,\Gamma\left(\frac{1}{c}+1\right) \tag{A1.3}$$

$$Var(u) = \alpha^2\left[\Gamma\left(\frac{2}{c}+1\right) - \left[\Gamma\left(\frac{1}{c}+1\right)\right]^2\right] \tag{A1.4}$$

For the future time series scenario, the mean (MP_{scen}) and the variation coefficient (CVP_{scen}) of the daily rainfall amounts are estimated based the observed mean (MP_{obs}) and the observed variation coefficient (CVP_{obs}) and their relative changes given by the used regional climate change statistics (see Section 4.3).

The Weibull parameters for the future scenario α_{scen} and c_{scen} are estimated by the method of moments (Equation A1.3 and A1.4). It is assumed that if the daily rainfall amount $u_{obs}(t)$ observed on day t corresponds to the pth percentile in the observed series, the scenario value $u_{scen}(t)$ for the same date corresponds to the same percentile in the scenario series. From these assumptions and Equation A1.2 it follows:

$$u_{scen}(t) = \alpha_{scen} \cdot \left(\frac{u_{obs}(t)}{\alpha_{obs}} \right)^{\frac{c_{obs}}{c_{scen}}} \quad \text{(A1.5)}$$

Note that the Weibull distribution parameters are estimated independently for each season (for both the observed period and the future scenario).

Appendix 2: Meteorological pattern scaling – estimation of scaling ratios (after Hingray et al., 2004, submitted manuscript)

The perturbation methodology for the generation of local scale meteorological time series requires regional climate change statistics as input. These statistics correspond to a 16-values matrix $\mathbf{X} = [XMT_s, XSDT_s, XMP_s, XCVP_s]_{s:1..4}$ where XMT_s is the absolute change of the mean temperature for a given season s (s = 1: DJF; s = 2: MAM; s = 3: JJA; s = 4: SON), XMP_s is the relative change of the mean precipitation, $XSDT_s$ the relative change of the standard deviation of the daily temperature and $XCVP_s$ is the relative change of the coefficient of variation of daily precipitation.

In the following a different notation is used for **X** (Equation A2.1):

$$\mathbf{X} = [X_{v,s}]_{v:1..4,\ s:1..4} \quad \text{(A2.1)}$$

where $X_{v,s}$ is one key statistics v of the daily mean temperature or precipitation series ($X_{1,s} = XMT_s$, $X_{2,s} = XSDT_s$, $X_{3,s} = XMP_s$, $X_{4,s} = XCVP_s$) and where s refers to the season.

Given a RCM called r that has been run for the control period (1961-1990) and for a future period (for example 2070-2099), the response pattern is defined as the following matrix (Equation A2.2):

$$\mathbf{Y}_r = [Y_{v,s,r}]_{v:1..4,\ s:1..4} \quad \text{(A2.2)}$$

where $Y_{v,s,r}$ is the scaling ratio for one of the four key statistics used ($Y_{1,s,r} = YMT_{s,r}$, $Y_{2,s,r} = YSDT_{s,r}$, $Y_{3,s,r} = YMP_{s,r}$, $Y_{4,s,r} = YCVP_{s,r}$) for season s and RCM experiment r. For each variable, the scaling ratio is defined as its regional change (absolute or relative) per degree of global-mean warming. For a given RCM experiment, the scaling ratios are estimated based on Equation A2.3:

$$Y_{v,s,r} = X_{v,s,r} / \Delta T_r \quad \text{(A2.3)}$$

where $X_{v,s,r}$ is the change in variable v for season s predicted by the RCM experiment r between the control and the future period and ΔT_r is the global-mean warming value obtained for the AOGCM used to drive the RCM experiment r.

Chapter 5

Quantifying hydrological modelling errors through finite mixture distributions[1]

Abstract

Bayesian inference of posterior parameter distributions has become widely used in hydrological modelling to estimate the associated modelling uncertainty. The classical underlying statistical model assumes a Gaussian modelling error with zero mean and a given variance. As hydrological modelling residuals rarely respect this basic assumption, data transformations are carried out. The present technical note points out the problems that can arise using such data transformation techniques and proposes instead the use of a finite mixture model. The hydrological and the statistical model parameters are inferred using a Markov chain Monte Carlo method known as the Metropolis-Hastings algorithm. The proposed methodology is illustrated for a rainfall-runoff model applied to a highly glacierized alpine catchment. The associated total modelling error is modelled using a mixture of two normal distributions, the mixture components referring respectively to the low and the high

[1] This chapter has been submitted for publication to Journal of Hydrology: Schaefli, B., Balin Talamba, D. and Musy, A.: Quantifying hydrological modeling errors through finite mixture distributions.

flow discharge regime. The obtained results show that the use of a finite mixture model constitutes a promising solution to model hydrological modelling errors and could give new insights into the model behaviour.

5.1 Introduction

The quantification of hydrological modelling uncertainties is currently one of the key issues of hydrological research. Especially in the area of conceptual modelling, the uncertainty inherent to any types of prediction receives an increasing interest. Conceptual models represent a highly simplified description of the natural phenomena underlying a hydrological response. Some of their model parameters can therefore not be measured directly but have to be calibrated using observed data of the simulated catchment response. In the past, the determination of the best or the most probable parameter set has been subject to intense research (see, e.g., Duan et al., 1992) whereas current research concentrates on the estimation of the posterior parameter distribution (see, e. g., Kuczera and Parent, 1998; Vrugt et al., 2003). Monte Carlo methods have become widely used for the Bayesian inference of posterior parameter distributions, the most known in the area of hydrological modelling being the so-called GLUE method (Generalized Likelihood Uncertainty Estimation) (Beven and Binley, 1992) – an importance sampling technique - and different types of Markov Chain Monte Carlo (MCMC) sampling techniques, the most frequently used in hydrological modelling being the so-called Metropolis algorithm (Metropolis et al., 1953).

The Bayesian inference of posterior parameter distributions requires the definition of an appropriate statistical model and of a model error distribution in order to formulate the corresponding likelihood function. In hydrological modelling, the classical normality assumption is generally not respected, as the modelling residuals are typically not homoscedastic but depend on the system state and the dominating hydrological processes. This problem is classically solved by applying an appropriate data transformation function that normalises the residuals (see, e.g., Bates and Campbell, 2001; Thyer et al., 2002; Vrugt et al., 2003). The use of such data transformations is interesting from a statistical point of view because they represent the simplest way to variance stabilisation. However, if the posterior distribution of the model error is used for uncertainty prediction, an important problem arises: The prediction of the modelling uncertainty of a hydrological response requires the application of the appropriate data retransformation. This brings two problems: i) The data transformation cannot be extrapolated beyond the limits of the observed values used for the parameter estimation. Its application to extreme values could induce a bias. ii) The retransformation leads generally to a skewed posterior distribution. Accordingly, the mean value is biased with respect to the median.

In many applications - where the prediction of the posterior distribution of the hydrological response is the endpoint of the study - this fact is negligible. It represents however a problem

if the predicted individual values composing the resulting posterior distribution are used as an input into further models. A simple example shall illustrate this problem: We predict the distribution of the daily discharge in a river feeding a managed accumulation lake. Applying a logarithmic transformation to the data for the parameter estimation, the posterior distribution is right skewed, i.e. the mean daily discharge is higher than the median daily discharge. This implies that on average, the series of daily discharge overestimate the total amount of water available in the system. The use of these biased series as an input into a management model of the lake outflow is questionable.

The problem of retransformation bias is encountered in various modelling fields using data transformation and especially logarithmic transformation (see, e.g., Newman, 1993; Cohn, 1995). In the area of hydrological modelling, it has first been discussed by Lane (1975). Bias correction methods exist to solve this problem (see, e.g., Thomas, 1985; Ferguson, 1986; Koch and Smillie, 1986). They may be problematic in applications where beside the retransformed output variable other state variables are used as an input into further models. The bias correction should be passed on these state variables; otherwise they are somehow disconnected from the model output. This is could be an interesting problem to study but will not be further discussed here.

Data transformation is just one method among others to variance stabilisation. In this technical note, we illustrate the use of a simple parametric method, the so-called finite mixture distribution that approaches highly complex distributions through a weighted sum of standard distributions such as the normal distribution (see the work of Bardsley (2003) for an application in hydrological modelling). In the presented application, the parameters of these distributions are estimated through a Metropolis-Hastings algorithm (Hastings, 1970). We first present the finite mixture model, followed by a short overview of the used Metropolis-Hastings algorithm and a discussion of some relevant implementation aspects. The statistical model and the inference of its parameters are illustrated for a case study in the Swiss Alps.

5.2 Finite mixture model

The catchment response simulated through a hydrological model can be represented in a general statistical framework (Equation 1).

$$q_t = h(\mathbf{x}_t, \boldsymbol{\beta}) + \tau_t \tag{1}$$

where q_t is the hydrological response on time step t (t = 1,..,n), $h(\mathbf{x}_t, \boldsymbol{\beta})$ is the hydrological transfer function mapping the inputs $\mathbf{x}_t$ (containing input variables such as precipitation, temperature and potential evapotranspiration) into the hydrological response given the model parameter vector $\boldsymbol{\beta}$ and τ_t is the modelling error.

This model can be extended to an AR(1) model in order to account for the autocorrelation occurring classically in hydrological model residuals (Equation 2).

$$q_t = h(\mathbf{x}_t, \boldsymbol{\beta}) + \rho\lambda_{t-1} + \varepsilon_t \tag{2}$$

where ρ is the lag-one autoregressive parameter, $\lambda_{t-1} = q_{t-1} - h(\mathbf{x}_{t-1}, \boldsymbol{\beta})$ is the residual of the time step t-1 and ε_t is the modelling error.

The probabilistic structure of many hydrological phenomena is too complex to be modelled by a classical statistical distribution such as a normal distribution. A parametric solution to account for the complexity in hydrological models is to approach the true residual distribution $g(\varepsilon_t)$ by a so-called finite mixture distribution (see, e.g., Robert, 1996; Gelman et al., 1995):

$$g(\varepsilon_t) \approx \hat{g}(\varepsilon_t) = \sum_{i=1}^{m} w_i f(\varepsilon_t \mid \phi_i) \tag{3}$$

where $w_1 + .. + w_m = 1$. $f(\varepsilon_t \mid \phi_i)$ are called the components of the mixture and m is the number of components. As Robert (1996) points out, the mixture components not necessarily possess a significance for the phenomenon modelled. They rather correspond to local zones of support of the true distribution. In some situations, however, they can be interpretable.

The residuals of hydrological models are known to be heteroscedastic for various reasons including the following: i) The observed data (model input and output) have not a constant measurement error throughout the year. For the discharge measurement, this error can for example depend on the flow regime or on the temperature (freezing). ii) The model does not yield the same simulation quality for all types of occurring processes. Low flow situations are typically better modelled (smaller residuals) than peak events (high residuals).

Different methods exist to estimate the number of mixture components and the corresponding parameters (for a review of mixture estimation methods, see e.g., Titterington et al. (1985), for recent developments see, e.g., James et al. (2001); Wang and Fu (2004)). The number of mixtures can however also be fixed by some prior knowledge about the modelled phenomenon. In the present application to a hydrological rainfall-runoff model, we fix the number of components to two, corresponding respectively to the high and the low flow period. These two periods are separated based on a discharge increase and decrease criterion (Equation 4 and 5). The set of start days of the high flow regime (T_H) respectively of the low flow regime (T_L) are defined as

$$\begin{aligned} T_H &= \{t \mid I(\bar{q}_{t+1}\bar{q}_t^{-1} > k) = 1\} \\ T_L &= \{t \mid I(\bar{q}_t\bar{q}_{t+1}^{-1} < k) = 1\} \end{aligned} \tag{4}$$

where $\bar{q}_t$ is the median value of q_j, $j = t-4,..,t+4$. I(.) is an indicator function taking the value 1 if its argument is true, and 0 otherwise. k is the increase and decrease threshold parameter. We define t_H as a time step lying between a start day of a high flow period and a start day of a low flow period. Accordingly, the sets of high flow discharge Q_H respectively low flow discharge Q_L are defined as

$$\begin{aligned} \mathbf{Q}_H &= \{q_t \mid t = t_H\} \\ \mathbf{Q}_L &= \{q_t \mid q_t \notin \mathbf{Q}_H\} \end{aligned} \tag{5}$$

The two-component mixture model can then be written as

$$q_t = h(\mathbf{x}_t, \boldsymbol{\beta}) + I(q_t \in \mathbf{Q}_H)(\rho_1 \delta_{t-1} + \varepsilon_{1,t}) + I(q_t \in \mathbf{Q}_L)(\rho_2 \delta_{t-1} + \varepsilon_{2,t}) \tag{6}$$

where $\delta_{t-1} = q_{t-1} - h(\mathbf{x}_{t-1}, \boldsymbol{\beta})$ is the residual of the time step t-1 and $\varepsilon_{i,t}$ is the normally distributed modelling error having zero mean and the variance σ_i^2 (i = 1, 2).

The estimation of the model parameters is based on a Bayesian inference method, presented in the following section for the general case of a finite mixture model with m univariate normal components.

5.3 Parameter inference

5.3.1 Metropolis-Hastings algorithm

Lets call $\boldsymbol{\theta}$ the vector containing the parameters $\boldsymbol{\beta}$ of the hydrological transfer function, the threshold k, the autocorrelation vector $\boldsymbol{\rho} = [\rho_1, \rho_2]^T$ and the standard deviation vector $\boldsymbol{\sigma} = [\sigma_1, \sigma_2]^T$ (Equation 7).

$$\boldsymbol{\theta} = \left[\boldsymbol{\beta}^T, k, \boldsymbol{\rho}^T, \boldsymbol{\sigma}^T\right]^T \tag{7}$$

According to Bayes' theorem, the posterior distribution $p(\boldsymbol{\theta}|\mathbf{D})$ of the model parameter vector $\boldsymbol{\theta}$ given the data $\mathbf{D}=\{q_t, \mathbf{x}_t, t = 1,..,n\}$ is proportional to a prior distribution $p(\boldsymbol{\theta})$ multiplied by the likelihood $p(\mathbf{D}|\boldsymbol{\theta})$ (Equation 8).

$$p(\boldsymbol{\theta} \mid \mathbf{D}) \propto p(\boldsymbol{\theta}) \cdot p(\mathbf{D} \mid \boldsymbol{\theta}) \tag{8}$$

In the present approach, the posterior distribution $p(\boldsymbol{\theta}|\mathbf{D})$ is inferred by a Markov chain Monte Carlo (MCMC) sampling method called Metropolis-Hastings algorithm (Hastings, 1970). This algorithm is a generalisation of the Metropolis algorithm (Metropolis et al., 1953). For a detailed discussion of MCMC methods refer for example to Gilks et al. (1996), for the

Metropolis-Hastings algorithm refer to Chib and Greenberg (1995) and for its application in conceptual hydrological modelling for example to Kuczera and Parent (1998), Bates and Campbell (2001) or Marshall et al. (2004). The core of this algorithm is formed by the following steps:

i. Based on the current state $\boldsymbol{\theta} = \boldsymbol{\theta}^{(j)}$, randomly sample a proposal state $\boldsymbol{\theta}^*$ from a multivariate jump probability function $J(\boldsymbol{\theta}^*|\boldsymbol{\theta})$.

ii. Compute the transition probability ψ (Equation 9).

$$\psi = \frac{p(\boldsymbol{\theta}^* \mid \mathbf{D})}{p(\boldsymbol{\theta} \mid \mathbf{D})} \cdot \frac{prob\ (\boldsymbol{\theta}^* \rightarrow \boldsymbol{\theta})}{prob\ (\boldsymbol{\theta} \rightarrow \boldsymbol{\theta}^*)} \tag{9}$$

where $prob\ (\boldsymbol{\theta}^* \rightarrow \boldsymbol{\theta})$ is the probability to draw $\boldsymbol{\theta}$ given $\boldsymbol{\theta}^*$.

iii. Randomly sample a variable u from a uniform distribution over the interval 0 to 1.

iv. If $u \leq \psi$ then retain the proposal state $\boldsymbol{\theta}^*$, i.e. $\boldsymbol{\theta}^{(j+1)} = \boldsymbol{\theta}^*$. Otherwise remain at the current state, i.e. $\boldsymbol{\theta}^{(j+1)} = \boldsymbol{\theta}$.

This formulation is a generalisation of the Metropolis algorithm where, contrary to here, the jump probability function is symmetric, i.e. $J(\boldsymbol{\theta}^*|\boldsymbol{\theta}) = J(\boldsymbol{\theta}|\boldsymbol{\theta}^*)$. The stationary distribution of the Markov chain generated through the Metropolis-Hastings algorithm will be $p(\boldsymbol{\theta} \mid \mathbf{D})$ regardless of the form of the jump probability function (Gilks et al., 1996).

5.3.2 Algorithm implementation

The prior distributions as well as the choice of the jump distribution have an important influence on the convergence rate of the chain to its stationary distribution. Some details referring to the algorithm implementation are thus presented here. We first discuss the estimation of the likelihood of the statistical model of Equation 6, followed by the chosen priors, the jump function, the algorithm initialisation and the convergence monitoring.

Likelihood estimation

Given the finite mixture distribution $\hat{g}(\varepsilon_t)$ (Equation 3), we can write $\varepsilon_t \sim \hat{g}(\varepsilon_t)$ under the hierarchical structure

$$\varepsilon_t \sim f(\varepsilon_t \mid \boldsymbol{\theta}_{z_t}) \tag{10}$$

where $\boldsymbol{\theta}_{z_t} = [\boldsymbol{\beta}^{\mathrm{T}}, k, \rho_{z_t}, \sigma_{z_t}]^{\mathrm{T}}$ and z_t is an index identifying the mixture component that generates the observed value ε_t. z_t takes the value i (i = 1,..,m) with a probability w_i. z_t can be unknown (we would then refer to it as the missing data part of the sample) or known as in the present application where z_t can be written as

$$z_t = \sum_{i=1}^{2} i \cdot I(q_t \in \mathbf{Q}_H) + i \cdot I(q_t \in \mathbf{Q}_L) \tag{11}$$

For known z_t, the likelihood $p(\mathbf{D}|\boldsymbol{\theta})$ can be written as (Robert, 1996):

$$p(\mathbf{D}|\boldsymbol{\theta}) = \prod_{t=1}^{n} g(\varepsilon_t) = \prod_{t:z_t=1} f(\varepsilon_t|\boldsymbol{\theta}_1) \ldots \prod_{t:z_t=m} f(\varepsilon_t|\boldsymbol{\theta}_m) \tag{12}$$

If the modelling errors ε_t are normally distributed, homoscedastic and independent, Equation 12 becomes

$$\begin{aligned} p(\mathbf{D}|\boldsymbol{\theta}) = & \left[\frac{1}{(\sigma_1\sqrt{2\pi})^{n_1}} \ldots \frac{1}{(\sigma_m\sqrt{2\pi})^{n_m}}\right] \\ & \cdot \exp\left[-\frac{1}{2\sigma_1^{\,2}} \sum_{t:z_t=1}^{n_1} \varepsilon_t^{\,2}(\boldsymbol{\theta}_1) - \ldots - \frac{1}{2\sigma_m^{\,2}} \sum_{t:z_t=m}^{n_m} \varepsilon_t^{\,2}(\boldsymbol{\theta}_m)\right] \end{aligned} \tag{13}$$

where n_i is the number of observed values ε_t generated by the component i and $\sum_{i=1}^{m} n_i = n$.

Priors and jump function

For the generation of a proposal state, we use two different types of jump functions. Lets call $\boldsymbol{\varphi}$ the vector containing all parameters except the standard deviations, i.e. $\boldsymbol{\varphi} = [\boldsymbol{\beta}^{\mathrm{T}}, \ k, \boldsymbol{\rho}^{\mathrm{T}}]^{\mathrm{T}}$. The proposal state of $\boldsymbol{\varphi}$ is generated through a multi-normal distribution $N(\boldsymbol{\varphi}, s\,\boldsymbol{\Sigma})$ where $\boldsymbol{\Sigma}$ is the covariance matrix and s an adaptive scaling factor that ensures an acceptable jump rate that is defined as the number of jumps to a proposal state divided by the total length of the chain (for further details, refer for example to Kuczera and Parent (1998)).

For the generation of a proposal state of σ_i, we introduce the following definitions:

$$y_i = \frac{1}{\sigma_i^{\,2}} \tag{14}$$

$$S_i = \frac{1}{2} \sum_{t:z_t=i} \varepsilon_t^{\,2}(\boldsymbol{\theta}_i)\,. \tag{15}$$

The proposal state of σ_i is generated by drawing a proposal state of y_i in the conditional distribution of y_i given $\boldsymbol{\varphi}$ that is a gamma distribution having the mean r_i / S_i and the variance r_i / S_i^2 where $r_i = n_i / 2$. The use of a gamma jump function ensures a better convergence of the algorithm toward its stationary distribution than including the σ_i in the multi-normal jump function.

Using the above notations, the likelihood can be written as:

$$p(\mathbf{D}|\boldsymbol{\theta}) = [\frac{1}{(\sqrt{2\pi})^{2r_1}} y_1^{r_1} ... \frac{1}{(\sqrt{2\pi})^{2r_m}} y_m^{r_m}] \cdot \exp[-y_1 S_1 - ... - y_m S_m] \tag{16}$$

Using the proposed two types of jump functions, the transition probability ψ becomes

$$\psi = \prod_{i=1}^{m} \{(y_i^* y_i)^{(r_i^* - r_i)} \frac{S_i^{*\, r_i^*}}{S_i^{r_i}} \exp[(y_i + y_i^*)(S_i - S_i^*)] \frac{\Gamma(r_i)}{\Gamma(r_i^*)}\} \tag{17}$$

In order to avoid numerical problems, we use the log value of the transition probability. Using Stirling's approximation of $\Gamma(n)$ (see Appendix 1), Equation 17 can be written as

$$\begin{aligned} \log(\psi) = \sum_{i=1}^{m} \{ & (r_i^* - r_i)[\log(y_i) + \log(y_i^*)] + r_i^*[\log(S_i^*) + 1] - r_i[\log(S_i) + 1] \\ & + (y_i + y_i^*)(S_i - S_i^*) + (r_i - 0.5)\log(r_i - 1) - (r_i^* - 0.5)\log(r_i^* - 1)\} \end{aligned} \tag{18}$$

The complete development of Equation 17 and 18 is given in Appendix 2.

The prior distributions of the components of $\boldsymbol{\varphi}$ are uniform distributions, the limits of which are defined by theoretic considerations (e.g. non-negativity condition) and previous modelling experience. For the parameter y_i an non-informative prior distribution of the form $p(y_i) = 1/y_i$ is used.

Initialisation

The initialisation of the covariance matrix and the scaling factor can be crucial for an effective convergence of the chain to its stationary distribution. Several authors use a first-order approximation evaluated at the globally optimal parameter estimates obtained through the use of a global optimisation algorithm (see, e.g., Thyer et al., 2002; Vrugt et al., 2003). For hydrological models, this global optimum, if it exists, can be difficult to determine. For the present application it is unknown and we therefore initialise the covariance matrix as the identity matrix. The initial scaling factor is set to $2.4\sqrt{n}$ where n is the number of elements in the vector $\boldsymbol{\varphi}$ (Gelman et al., 1995).

Convergence

The convergence of this algorithm strongly depends on the choice of the covariance matrix $\mathbf{\Sigma}$ of the multi-normal proposal distribution and the scaling factor s. They are updated every 250 samples as suggested by Kuczera and Parent (1998); the covariance matrix is estimated based on these last 250 samples and the scaling factor s is adjusted based on the recommendations of Gelman et al. (1995) who state that for higher dimensional problems (dimensions > 5) the optimal acceptance rate is around 0.23. For a further discussion of this optimal acceptance rate see, e.g., Chib and Greenberg (1995).

The convergence of the algorithm is monitored using multiple chains with different starting points. After convergence these chains should stem from the same limiting distribution, the posterior distribution. We use the quantitative convergence diagnostic of Gelman and Rubin (1992) to test the convergence of the algorithm. This diagnostic is based on the mean of the within chain variances and on the variance between the means of the chains assuming that convergence is reached if the relationship between these two values is close to 1 (for an application in hydrology, see, e.g., Vrugt et al., (2003)).

5.4 Case study

The case study catchment is a highly glacierized catchment located in the Southern Swiss Alps (7.36°E, 45.96°N) feeding a hydropower accumulation lake called Mauvoisin. The hydrological regime is strongly influenced by glacier and snowmelt. It is of the so-called a-glacier type (Spreafico et al., 1992): The maximum monthly discharge takes place in July and August and the minimum monthly discharge (around 100 times less) in February and March.

The hydrological precipitation – runoff transfer is simulated at a daily time step through a conceptual semi-lumped model called GSM-SOCONT (Schaefli et al., 2005). The hydrological model has the following 8 parameters to calibrate: the altitudinal precipitation correction factor (c_{precip}), two degree-day factors for snow- and ice melt computation (a_{snow} respectively a_{ice}) and 5 reservoir parameters for the transformation of rainfall and melt into discharge. The reference daily discharges are the daily inflows into the accumulation lake of Mauvoisin. The period 1997 to 1999 is used for the calibration and the period 1992 to 1996 for the model validation. This hydrological transfer function leads to highly heteroscedastic, autocorrelated residuals (Figure 1).

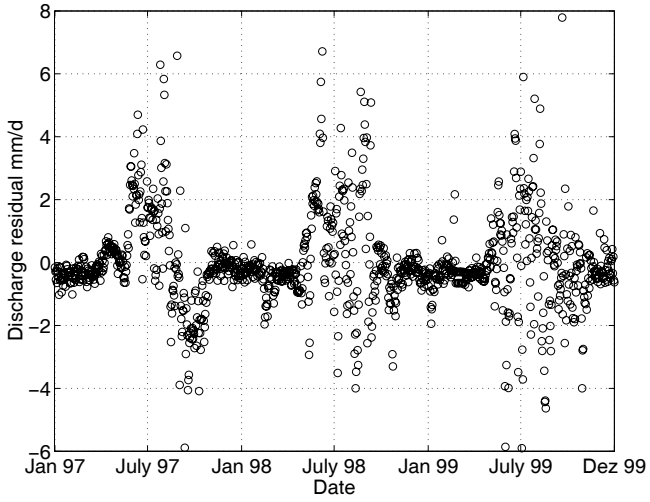

Figure 1: Observed residuals of the discharge simulation for the Mauvoisin catchment (simulated with the maximum likelihood parameter set)

5.5 Results

A synthetic data series was generated with this hydrological model, in order to verify that the applied MCMC method is able to recover the true synthetic parameters and especially the threshold for the flow regime separation and the standard deviations for both types of regimes. For the test of convergence, five parallel chains were initialised with randomly drawn parameters around the true parameter values (in an interval +/- 50%). The true values and the posterior mean values are close (Table 1) indicating that the applied inference method is able to recover the synthetic parameters.

Table 1: True parameter values and posterior mean values for the synthetic data series (for illustrative purposes, two hydrological parameters are indicated)

	a_{ice} (mm/°C/d)	a_{snow} (mm/°C/d)	c_{precip} (%/100m)	k (-)	ρ_1 (-)	ρ_2 (-)	σ_1 (-)	σ_2 (-)
True value	9.20	4.50	3.50	1.30	0.86	0.32	1.70	0.40
Posterior mean	9.14	4.72	3.62	1.32	0.84	0.35	1.64	0.44

Figure 2 shows the marginal posterior distributions of the statistical parameters for the real data set for the presented case study catchment. Note that the posterior distributions of the autocorrelation coefficients are almost identical for the high flow and the low flow regime (see also Table 2). These high autocorrelation coefficients are typical for hydrological

discharge models. Any over- or underestimation of the discharge on a given day is compensated the following days resulting in a strong autocorrelation of the residuals.

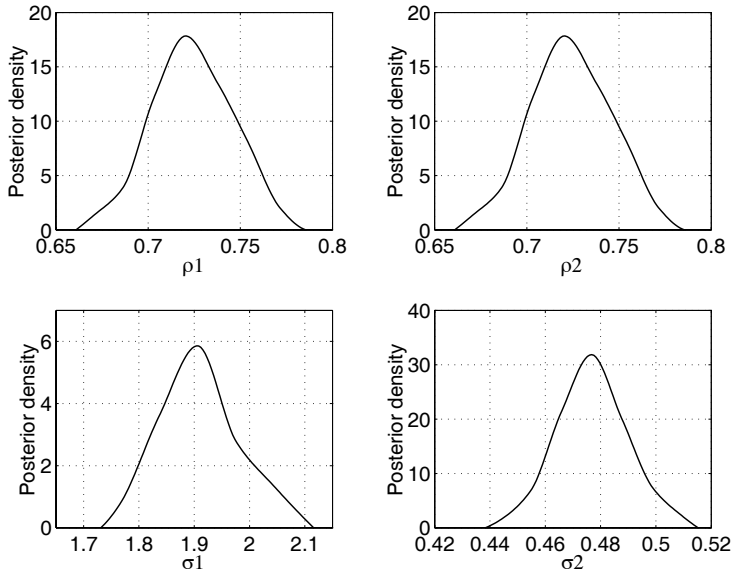

Figure 2: Posterior distribution of the autocorrelation coefficients and the standard deviations

Table 2: The median posterior parameter values and the 5 % and 95 % confidence limits

	a_{ice} (mm/°C/d)	a_{snow} (mm/°C/d)	c_{precip} (%/100m)	k (-)	ρ_1 (-)	ρ_2 (-)	σ_1 (-)	σ_2 (-)
5 % percentile	4.94	4.57	0.91	1.67	0.69	0.69	1.79	0.46
Median	5.38	4.81	1.33	1.69	0.73	0.72	1.90	0.48
95 % percentile	6.04	5.07	1.77	1.72	0.76	0.76	2.03	0.50

The residuals of each of the two flow regimes respect the normality assumption except for some extreme values (Figure 3). They are homoscedastic (Figure 4) and their mean value μ_i (i = 1, 2) is close to zero for both flow regimes and both simulation periods (μ_1 = 0.02, μ_2 = 0.02 for the calibration period and μ_1 = 0.07, μ_2 = -0.04 for the validation period). Figure 4 suggests however, that during the high flow period, some autocorrelation remains. Note the considerably lower standard deviation values during the low flow regime (σ_2) than during the high flow (σ_1) leading to smaller confidence intervals during the low flow period (Figure 5). This result underlines the initial assumption that the chosen hydrological model structure better reproduces the low flow regime than high discharge events. For the present case study, his is partly due to the involved processes but also to the input measurement error: during the

low flow period there is almost no liquid precipitation, the most difficult to estimate input variable.

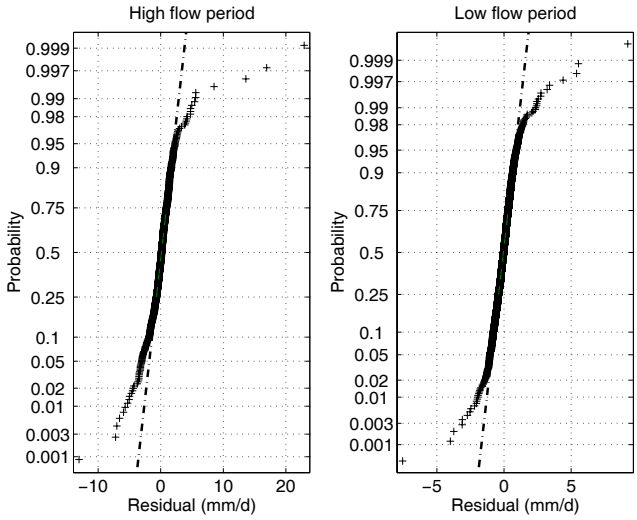

Figure 3: Normal probability plot for residuals during high flow period (left) and the low flow period (right); both plots for the validation period (crosses: observed residuals; dash-dot line: normal distribution)

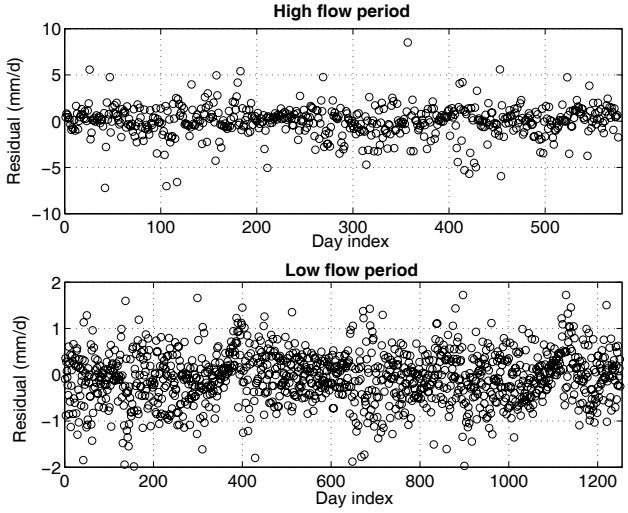

Figure 4: Residuals during the high flow period (top) and the low flow period (bottom) for the maximum likelihood parameter set (both plots for validation period); for enhanced readability, the extreme values (see Figure 3) have been removed

The observed daily discharge is well reproduced by the prediction model, 91 % of the data points of the validation period lie within the 90 % confidence limits (Figure 5). Note the fact, that the observed series contains negative values that are due to the measurement method (the discharge corresponds to the lake inflow estimated as the difference between the lake outflow

and the accumulated volume). This measurement error is included in the estimated overall modelling uncertainty but cannot be quantified separately through the presented approach.

Due to the chosen mixture identification method, there is an abrupt change between the two mixture components (see the sudden increase of the confidence interval at the regime transition in Figure 5 at around day 1600). The use of more than two mixture components could help avoiding this problem.

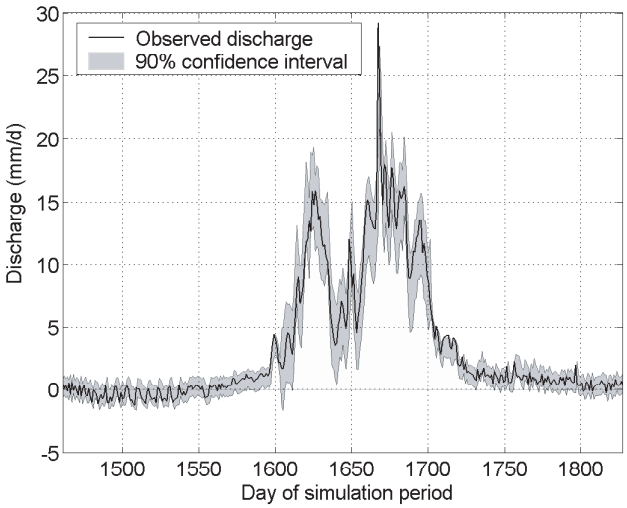

Figure 5: Observed discharge during validation period and 90 % confidence interval induced by parameter uncertainty and modelling error (the negative observed values are due to the measurement error)

5.6 Conclusion

Statistical modelling of hydrological responses has to deal with sometimes highly complex residual distributions. An appropriate transformation of the variable space can help to normalise such residuals but it is important to emphasize that such an approach can be problematic, namely if the predictive distribution of the retransformed variable is to be used as an input into further models. The relative significance of the resulting bias has to be assessed for every individual application (for the presented case study, we have found retransformation biases up to 70 % when using a log-transformation to stabilise the error variance).

The proposed finite mixture model represents a simple parametric method to approach complex residual distributions. The parameter of the finite mixture model can be estimated through a Bayesian inference method such as the proposed MCMC method that has become frequently used in hydrological modelling. In the presented application, the mixture components are assumed to be related to the flow regime and to have an interpretable

meaning for the used model. As outlined for the case study, the inferred distribution parameters can give interesting insights into the performance of the hydrological transfer function during the two different periods.

In hydrological modelling, it could be reasonable to assume the existence of more than two mixture components. They could for example be induced by variable measurement errors of the input and the output or by the variable dominance of several hydrological processes throughout the year. Estimation techniques exist to determine an unknown number of mixture components of a complex distribution (see, e.g., James et al., 2001; Wang and Fu, 2004). The application of such methods in hydrological modelling seems promising as the resulting components could give additional insights into the model behaviour and the measurement errors.

Acknowledgements

We would like to thank Dr. Eric Parent for his help on algorithm implementation issues. This work is part of the SWURVE (Sustainable Water: Uncertainty, Risk and Vulnerability in Europe) project, funded under the EU Environment and Sustainable Development program, grant number EVK1-2000-00075. The Swiss part of this project was funded by the Federal Office for Education and Science, contract number 00.0117. We also wish to thank the Forces Motrices de Mauvoisin for providing the discharge data and the national weather service MeteoSwiss for providing the meteorological time series.

References

Bardsley, W.E., 2003. Temporal moments of a tracer pulse in a perfectly parallel flow system. Advances in Water Resources, 26(6), 599-607.

Bates, B.C. and Campbell, E.P., 2001. A Markov chain Monte Carlo scheme for parameter estimation and inference in conceptual rainfall-runoff modeling. Water Resources Research, 37(4), 937-947.

Beven, K. and Binley, A., 1992. The future of distributed models: model calibration and uncertainty prediction. Hydrological Processes, 6(3), 279-298.

Chib, S. and Greenberg, E., 1995. Understanding the Metropolis-Hastings algorithm. American Statistician, 49(4), 327-335.

Cohn, T.A., 1995. Recent advances in statistical methods for the estimation of sediment and nutrient transport in rivers. U.S. National Report to International Union of Geodesy and Geophysics 1991-1994. Review of Geophysics, 33(Part 2 Suppl. S), 1117-1123.

Duan, Q., Sorooshian, S. and Gupta, V., 1992. Effective and efficient global optimization for conceptual rainfall-runoff models. Water Resources Research, 28(4), 1015-1031.

Ferguson, R.I., 1986. River loads underestimated by rating curves. Water Resources Research, 22(1), 74-76.

Gelman, A., Carlin, J.B., Stren, H.S. and Rubin, D.B., 1995. Bayesian Data Analysis. Chapmann and Hall, New York, 526 pp.

Gelman, A. and Rubin, D.B., 1992. Inference form iterative simulation using multiple sequences. Statistical Science, 2(4), 457-572.

Gilks, W.R., Richardson, S. and Spiegelhalter, D.J., 1996. Markov Chain Monte Carlo in Practice. Chapman & Hall, London, 486 pp.

Hastings, W.K., 1970. Monte Carlo sampling methods using Markov chains and their applications. Biometrika, 57, 97 - 109.

Havil, J., 2003. Gamma: Exploring Euler's Constant. Princeton University Press, Princeton, 266 pp.

James, L.F., Priebe, C.E. and Marchette, D.J., 2001. Consistent estimation of mixture complexity. Annals of Statistics, 29(5), 1281-1296.

Koch, R.W. and Smillie, G.M., 1986. Bias in hydrologic prediction using log-transformed regression models. Water Resources Bulletin, 22(5), 717-723.

Kuczera, G. and Parent, E., 1998. Monte Carlo assessment of parameter uncertainty in conceptual catchment models: the Metropolis algorithm. Journal of Hydrology, 211, 69-85.

Lane, W.L., 1975. Extraction of information on inorganic water quality, Colorade State University, Fort Collins.

Marshall, L., Nott, D. and Sharma, A., 2004. A comparative study of Markov chain Monte Carlo methods for conceptual rainfall-runoff modeling. Water Resources Research, 40(2), doi: 10.1029/2003WR002378.

Metropolis, N., Rosenbluth, A.W., Rosenbluth, M.N., Teller, A.H. and Teller, E., 1953. Equation of state calculations by fast computing machines. Journal of Chemical Physics, 21(6), 1087-1092.

Newman, M.C., 1993. Regression-analysis of log-transformed data - statistical bias and its correction. Environmental Toxicology and Chemistry, 12(6), 1129-1133.

Robert, C.P., 1996. Mixtures of distributions: inference and estimation. In: W.R. Gilks, S. Richardson and D.J. Spiegelhalter (Editors), Markov Chain Monte Carlo in Practice. Chapman & Hall, London, pp. 441-464.

Schaefli, B., Hingray, B., Niggli, M. and Musy, A., 2005. A conceptual glacio-hydrological model for high mountainous catchments. Hydrology and Earth System Sciences Discussions, 2, 73-117.

Spreafico, M., Weingartner, R. and Leibundgut, C., 1992. Atlas hydrologique de la Suisse. Service Hydrologique et Géologique National (SHGN), Bern.

Thomas, R.B., 1985. Estimating total suspended sediment yield with probability sampling. Water Resources Research, 21(9), 1381-1388.

Thyer, M., Kuczera, G. and Wang, Q.J., 2002. Quantifying parameter uncertainty in stochastic models using the Box-Cox transformation. Journal of Hydrology, 265, 246-257.

Titterington, D.M., Smith, A.F.M. and Makov, U.E., 1985. Statistical analysis of finite mixture distributions. Wiley, Chichester, 243 pp.

Vrugt, J.A., Gupta, H.V., Bouten, W. and Sorooshian, S., 2003. A shuffled complexe evolution Metropolis algorithm for optimization and uncertainty assessment of hydrologic models. Water Resources Research, 39(8), doi: 10.1029/2002WR001642.

Wang, L. and Fu, J.C., 2004. A practical sampling approach for Bayesian mixture model with unknown number of components. Technical report. Department of Statistics, University of Manitoba, Manitoba.

Appendix 1: Stirling's approximation

The gamma function is defined to be an extension of the factorial to complex and real number arguments. For a natural number *n*, the gamma function is related to the factorial as follows

$$\Gamma(n+1) = n! \tag{A1.1}$$

Its value can be approximated by the so-called Stirling's approximation (see, e.g., Havil, 2003) that says that for large *n*

$$n! \approx n^n e^{-n} \sqrt{2\pi n} \tag{A1.2}$$

From Equation A1.1 and A1.2 it follows that for $x >> 1$

$$\Gamma(x) \approx (x-1)^{x-0.5} e^{-(x-1)} \sqrt{2\pi} \tag{A1.3}$$

Appendix 2: Transition probability

According to Bayes' theorem (Equation 8) and Equation 9, the transition probability can be written as

$$\psi = \frac{p(\boldsymbol{\theta}^*)}{p(\boldsymbol{\theta})} \frac{p(\mathbf{D}\,|\,\boldsymbol{\theta}^*)}{p(\mathbf{D}\,|\,\boldsymbol{\theta})} \frac{prob\ (\boldsymbol{\theta}^* \rightarrow \boldsymbol{\theta})}{prob\ (\boldsymbol{\theta} \rightarrow \boldsymbol{\theta}^*)} \tag{A2.1}$$

where $p(\boldsymbol{\theta}^*)$ is the prior distribution of parameter vector $\boldsymbol{\theta}^*$, $p(\mathbf{D}\,|\,\boldsymbol{\theta}^*)$ the likelihood and $prob\ (\boldsymbol{\theta}^* \rightarrow \boldsymbol{\theta})$ the probability to draw $\boldsymbol{\theta}$ given $\boldsymbol{\theta}^*$.

Assuming uniform prior distributions for $\boldsymbol{\varphi}$ and non-informative priors for $\mathbf{y} = [y_i, i = 1, .. , m]^T$ and given the likelihood for the mixture model (Equation 13), the first part of Equation A2.1 can be written as

$$\frac{p(\boldsymbol{\theta}^*)}{p(\boldsymbol{\theta})} \frac{p(\mathbf{D}\,|\,\boldsymbol{\theta}^*)}{p(\mathbf{D}\,|\,\boldsymbol{\theta})} = \prod_{i=1}^{m} \frac{y_i}{y_i^*} \frac{(2\pi)^{-2r_i^*} y_i^{*(r_i^*)} \exp(-y_i^* S_i^*)}{(2\pi)^{-2r_i} y_i^{(r_i)} \exp(-y_i S_i)} \tag{A2.2}$$

Note that $r_i \neq r_i^*$ but $\sum_{i=1}^{m} 2r_i = \sum_{i=1}^{m} 2r_i^* = n$. It follows that

$$\prod_{i=1}^{m} \frac{(2\pi)^{-2r_i^*}}{(2\pi)^{-2r_i}} = 1 \tag{A2.3}$$

Two different types of jump functions are used, a multi-normal for **φ** and a gamma distribution for **y**. The multi-normal distribution being symmetric, $prob(\boldsymbol{\theta}^* \rightarrow \boldsymbol{\theta})$ reduces to $prob(\mathbf{y}^* \rightarrow \mathbf{y})$. Under an asymmetric gamma distribution, this probability equals

$$prob\ (\mathbf{y}^* \rightarrow \mathbf{y}) = \prod_{i=1}^{m} \frac{S_i^{*r_i^*} y_i^{r_i^*-1} \exp(-y_i S_i^*)}{\Gamma(r_i^*)} \tag{A2.4}$$

Note that $prob(\mathbf{y}^* \rightarrow \mathbf{y}) \neq prob(\mathbf{y} \rightarrow \mathbf{y}^*)$. From Equation A2.1 to A2.4 it follows that

$$\psi = \prod_{i=1}^{m} \{(y_i^* y_i)^{r_i^*-r_i} \frac{S_i^{*\,r_i^*}}{S_i^{r_i}} \exp[(y_i + y_i^*)(S_i - S_i^*)] \frac{\Gamma(r_i)}{\Gamma(r_i^*)}\} \tag{A2.5}$$

The log-value of Equation A2.5 can be approximated using Stirling's approximation (Equation A1.3) that for the present case becomes:

$$\log \prod_{i=1}^{m} \frac{\Gamma(r_i)}{\Gamma(r_i^*)} = \sum_{i=1}^{m} [(r_i - 0.5)\log(r_i - 1) - (r_i^* - 0.5)\log(r_i^* - 1) - r_i + r_i^*] \tag{A2.6}$$

From Equation A2.1 to A2.6 it follows that

$$\begin{aligned} \log(\psi) = \sum_{i=1}^{m} \{ & (r_i^* - r_i)[\log(y_i) + \log(y_i^*)] + r_i^*[\log(S_i^*) + 1] - r_i[\log(S_i) + 1] \\ & + (y_i + y_i^*)(S_i - S_i^*) + (r_i - 0.5)\log(r_i - 1) - (r_i^* - 0.5)\log(r_i^* - 1)\} \end{aligned} \tag{A2.7}$$

Chapter 6

Climate change and hydropower production in the Swiss Alps: Quantification of potential impacts and related modelling uncertainties[1]

Abstract

This paper addresses two major challenges in the field of climate change impact analysis on water resources systems: i) incorporation of the largest possible range of potential climate change scenarios and ii) quantification of related modelling uncertainties. The developed methodology of climate change impact modelling is presented and illustrated through an application to a hydropower plant in the Swiss Alps that uses the discharge of a highly glacierized catchment. The potential climate change impacts are analysed in terms of system performance for the control period (1961 – 1990) and for the future period (2070 – 2099) under a range of climate change scenarios. The system performance is simulated through a set of 4 model types including the production of regional climate change scenarios based on

[1] This chapter has been accepted for publication in Hydrology and Earth System Sciences (in a special issue presenting the results of the European project SWURVE – Sustainable Water: Uncertainty, Risk and Vulnerability in Europe): Schaefli, B., Hingray, B. and Musy, A.,: Climate change and hydropower production in the Swiss Alps: quantification of potential impacts and related modelling uncertainties.

global warming scenarios, the corresponding discharge model, the model of glacier surface evolution and the hydropower management model. The modelling uncertainties inherent to each model type are characterised and quantified separately. The overall modelling uncertainty is simulated through Monte Carlo simulation of the system behaviour for the control and the future period. The obtained results for both periods lead to the conclusion that potential climate change has as statistically significant negative impact on the system performance.

6.1 Introduction

High mountainous water resource systems are particularly sensitive to climate change impacts. The hydrological regime of such environments is strongly influenced by water accumulation in form of snow and ice and the corresponding melt processes. A modification of the prevalent climate and especially of the temperature can therefore considerably affect the hydrological regime and induce important impacts on the water management. This could have a significant impact on water uses highly dependent on the hydrological regime, such as hydropower production. In Switzerland, hydropower represents about 75 % of consumed electricity, of which around 60 % are produced by accumulation (Swiss Federal Office for Energy, 2003). Beside the evident economic interest of electricity production, accumulation hydropower plants have an important socio-economic role at different scales. In the Swiss Alps - at the very local scale - related infrastructures and employment opportunities can encourage a decentralised rural settlement. This aspect is reinforced if the accumulated water serves some secondary water uses such as irrigation for example. At a more regional scale, dams and accumulation lakes prevent the downstream areas from flooding.

In Switzerland, the different stakeholders are just starting to become concerned about potential climate change impacts. While shareholders expect the temperature raise to induce more ice melt and therefore a raise in electricity production and economic gain, the local population is more concerned about questions referring to the system security.

Despite the importance of hydropower production and its potential sensitivity to climate change, relatively few studies have addressed these issues. Most climate change impact studies just analyse the direct effect of climate change on the water cycle rather than to consider the impacts in terms of water management. Garr and Fitzharris (1994), Robinson (1997) and Westaway (2000) analysed the climate sensitivity of accumulation or mixed power plants in terms of total annual hydroelectricity production and consumption in the eastern United States, in New Zealand and Switzerland respectively. Mimikou and Baltas (1997) assessed the reliability of a hydropower production scheme in Greek under 3 different climate scenarios based on global circulation model (GCM) outputs. Harrison and Whittington (2002) analysed the financial and technical viability of hydropower projects under climate change for the Zambezi river. Bergstrom et al. (2001) studied the potential climate change impact on

hydropower production in Northern countries but for hypothetic, not existing and not planned hydropower plants. They made an attempt to integrate the modelling uncertainty due to the choice of the GCM and to the parameterisation of the evapotranspiration (ET).

The present study aims at quantifying the climate change impacts on the management performance at the scale of a single hydropower plant at a daily time step in order to analyse everyday management situations - including extreme situations - rather than average electricity production. Payne et al (2004) and Christensen et al. (2004) have carried out a comparable climate change impact analysis for hydropower production in large catchments in the western United States. They used three ensembles of a business-as-usual future climate scenario and two different downscaling methodologies for their impact analysis. Their results cover therefore only a small part of potential climate change induced system modifications. Another important limit is pointed out by (Barnett et al., 2004) - a companion paper of the two case studies – who state the need of confidence limits rather than single estimates of climate change impacts.

The methodology used in the present study has been developed in order to answer these two major challenges in the field of climate change impact research: cover the largest possible range of potential climate change impacts and quantify all related modelling uncertainties. The obtained results are therefore not central estimates of the expected system modifications but the entire range of possible changes with associated probabilities. Ultimately, these results should enable the answer to the following question: Given the modelling uncertainties, does climate change cause a statistically significant modification of the system performance?

The presented analysis does not address other potential modifications of the studied system such as modifications of the electricity demand induced by climate change, population growth or technological progress that can be assumed to have a considerable impact on the system management. The potential impact of climate change is analysed considering the water resources system, as it exists today.

6.2 Methodology: overview

The analysis of potential climate change impacts on the management of a water resources system requires setting up an integrated simulation tool in order to simulate the behaviour of the system for different climatic situations. In the context of hydropower production in a highly glacierized catchment, this simulation tool includes four types of models: a water management model, a hydrological model, a glacier surface evolution model and a model for the generation of local scale meteorological times series under a given climate change scenario. The first three model types, the required input data and the model calibration are discussed hereafter (see Section 3). In the present study context, a modelling time step of one day has been chosen – this enables a detailed analysis of the daily hydropower production performance. At the chosen spatial and temporal scale, the water routing through the

hydraulic system can be assumed to be negligible. Consequently, the only part of the hydraulic system that is modelled is the accumulation lake, the filling evolution of which is modelled based on a simple continuity equation.

The future local scale meteorological times series - namely daily mean precipitation and temperature - are generated by perturbing the observed series for a control period according to the method developed by Shabalova et al. (2003). In this method, the perturbation of local scale precipitation and temperature is carried out based on the corresponding regional scale outputs of a Regional Climate Model (RCM) for the same control and future period. As an example, the scaling equation for temperature is given hereafter (Equation 1).

$$T_{scen,s}(t) = [T_{obs,s}(t) - \overline{T}_{obs,s}] * \sigma_{fut,s} / \sigma_{cont,s} + \overline{T}_{obs,s} + (\overline{T}_{fut,s} - \overline{T}_{cont,s}) \quad (1)$$

where $T_{scen,s}(t)$ (°C) is the local scale scenario temperature on day t of the season s (s = 1, 2, 3, 4), $T_{obs,s}(t)$ the corresponding observed temperature, $\overline{T}_{obs,s}$ the observed mean daily temperature of the season s, $\sigma_{fut,s}$ respectively $\sigma_{cont,s}$ the seasonal standard deviations of daily temperatures of the future respectively the control climate experiments and $\overline{T}_{fut,s} - \overline{T}_{obs,s}$ the difference in mean daily temperature between the future and the control climate experiments.

In the present study, the necessary RCM statistics for the times series perturbation are the result of the global warming – regional climate - scaling methodology presented in a companion paper included in this volume (Hingray et al., 2005a, submitted manuscript[2]). Note that the future potential evapotranspiration (PET) has been interpolated as a function of the future temperature based on the observed relationship for the control climate, assuming that this relationship remains constant in the future.

The integrated simulation tool is used to simulate the system behaviour under observed climate for the control period 1961 - 1990 and under future climate scenarios for the period 2070 – 2099. A case study-specific indicator set is elaborated (see Section 3) in order to evaluate the system performance and to compare the control and the future situation. The main objective of the present study is to quantify the associated modelling uncertainties. The potential sources of uncertainty are discussed in Section 4 and the most relevant ones included in an overall uncertainty analysis of climate change impacts based on Monte Carlo simulations (see Section 5).

[2] Hingray, B., Mezghani, A. and Buishand, T.A., 2004. Elaboration of regional climate change pdf's from uncertain global-mean warming and uncertain scaling relationship. Submitted to Hydrology and Earth System Sciences; hereinafter referred to as Hingray et al., 2005a, submitted manuscript.

The application of this general methodology is specific to a given modelling context. The used case study is therefore presented (Section 3) before discussing in further detail the climate change impact analysis and the integration of modelling uncertainties.

6.3 Case study: Dam of Mauvoisin

6.3.1 System description

The dam and accumulation lake of Mauvoisin is part of a hydropower plant located in the southern Swiss Alps (Figure 1). The owner and manager of the hydropower plant is the stock corporation Forces Motrices de Mauvoisin (FMM). The accumulation basin - filled for the first time in 1958 – can store a total volume of 204 million m^3 of water, corresponding to 660 GWh. This water storage corresponds to around 75 % of the mean annual discharge from the connected hydrological catchment. Consequently, the hydropower production is highly flexible in time, the main economic interest for the managers being to shift the electricity production from summer when the hydrological inflow is high to winter when the electricity demand is high. The mean annual electricity production is about 1000 GWh corresponding to 2.5 % of the total Swiss hydropower production.

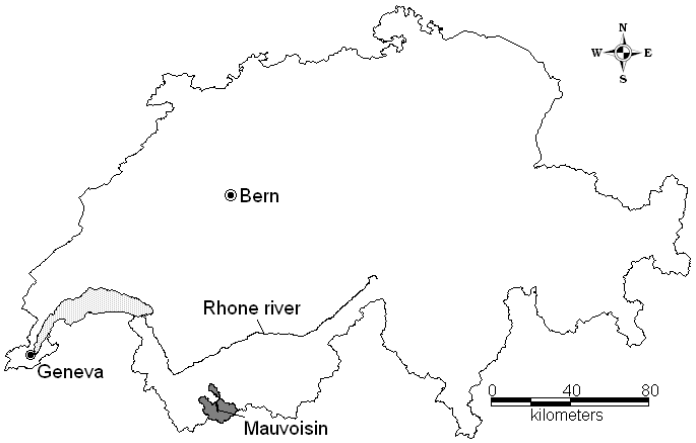

Figure 1: Location of the Mauvoisin catchment in the Swiss Alps © Swiss Federal Office of Topography

Table 1 gives the mean physiographic and meteorological characteristics of the natural and artificially connected catchment feeding the accumulation lake. The maximum daily water inflow into the lake is about 6 millions m^3 and the mean annual inflow 265 millions m^3. The hydrological regime is strongly influenced by glacier and snowmelt. It is of the so-called a-

glacier type (Spreafico et al., 1992): the maximum monthly discharge takes place in July and August and the minimum monthly discharge (around 100 times less!) in February and March.

Table 1 : Main physiographic characteristics of the case study catchment (reference year for glaciation: 1989, for hydro-meteorological data 1961 – 1990)

Characteristic	Value
Area (km^2)	169.3
Glaciation (%)	41.4
Mean slope (°)	26.7
Min. altitude (m a.s.l.)	1961
Mean altitude (m a.s.l.)	2940
Max. altitude (m a.s.l.)	4305
Mean annual precipitation (mm)	1530
Mean daily temperature (°C)	-3.6

6.3.2 Data collection

The hydrological and glacier surface evolution model needs three input time series, namely daily mean values of temperature, precipitation and potential evapotranspiration (PET). For the model calibration and validation and the control simulation of the system, we used precipitation and temperature time series from a meteorological station located within the catchment. The PET time series is calculated based on the Penman-Monteith version given by (Burman and Pochop, 1994). Daily mean inflow into the accumulation lake and electricity production data has been obtained from FMM. Based on this data, the hydrological model has been calibrated for the years 1995 to 1999 and validated for the years 1990 to 1994.

6.3.3 Hydrological and glacier surface evolution model

Model structure

The daily discharge simulation is carried out through a conceptual, semi-lumped model developed by the authors and presented in some detail in (Schaefli et al., 2005b). The model has two levels of discretization, one corresponding to the separation between the ice-covered part of the catchment and the not ice-covered part and the other to a subdivision in elevation bands. Each of the resulting spatial units is assumed to have a homogeneous hydrological behaviour. The discharge simulation for each of them includes the following steps: interpolation of meteorological time series based on an altitudinal variation factor, separation

of rain- and snowfall based on a threshold temperature, computation of snow accumulation and snow- and ice melt through a degree-day approach and transformation of rainfall and meltwater into runoff through a reservoir-based modelling approach. Figure 2 shows the hydrological model structure for a given spatial unit. The runoff transformation submodel differs for ice-covered and not ice-covered units. In the first case, two parallel linear reservoirs are used, one for snowmelt and rainfall and one for ice melt – runoff transformation. For not ice-covered spatial units, snowmelt and rainfall – runoff transformation is carried out through two parallel reservoirs, a linear and a non-linear reservoir in order to simulate the slow and the quick flow component of discharge.

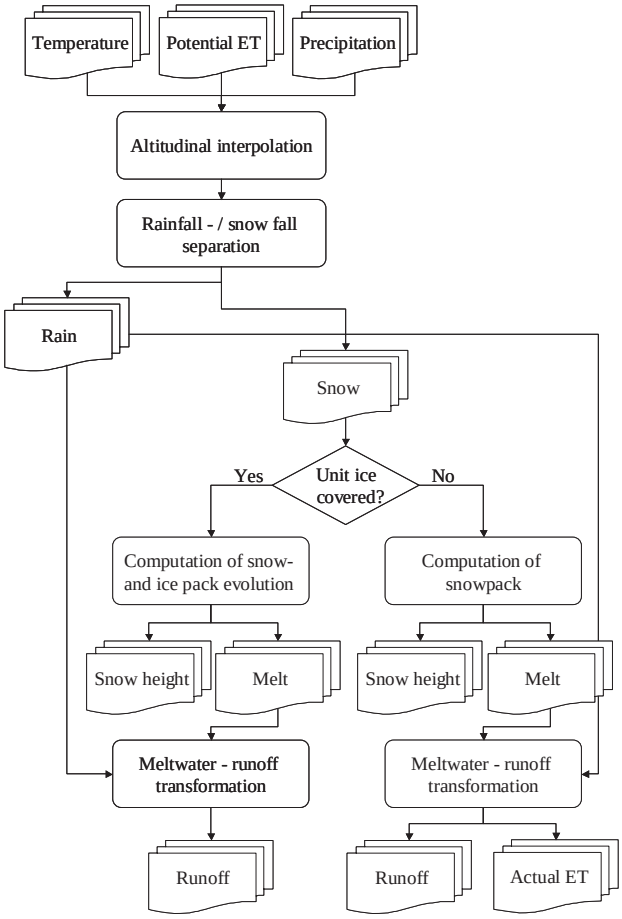

Figure 2: Hydrological model structure for one spatial unit

This hydrological model has the following 8 parameters to calibrate: the altitudinal precipitation correction factor, the degree-day factors for snow- and ice melt, the linear reservoir outflow coefficients for the ice-covered spatial units and for the not ice-covered units, the maximum storage and outflow coefficients for the linear reservoir and the non-linear reservoir coefficient.

The glacier surface is supposed to be constant for a given simulation period. For future scenario simulation, the ice-covered surface has to be updated. In the present study, this update is based on the so-called accumulation area ratio (AAR) (Anonymous, 1969). For a given hydrological year (starting on the 1 October), this ratio can be computed from the sum of spatial units that experience snow accumulation (Schaefli et al., 2005b). Assuming that the mean interannual AAR is characteristic for a given glacier and remains constant for future periods, the glacier surface for future climatic conditions can be estimated according to Equation 2.

$$A_{ice} = \frac{A_{acc}}{AAR_m} \tag{2}$$

where A_{ice} (km^2) is the total ice-covered area and A_{acc} (km^2) the simulated mean interannual accumulation area for the future climatic conditions. AAR_m is the mean interannual accumulation area ratio simulated for the control climatic conditions, for which the total ice-covered area is known. For a further discussion of the glacier surface evolution model, refer to (Schaefli et al., 2005a, submitted manuscript)[3].

Hydrological model calibration

The hydrological model has been calibrated based on a Metropolis-Hastings algorithm according to the methodology presented by Kuczera and Parent (1998). The used algorithm is presented in (Schaefli et al., 2005b, submitted manuscript)[4]. This Markov Chain Monte Carlo (MCMC) methodology gives the posterior distribution of the model parameters and the associated modelling residuals that are supposed to be normally distributed. Consequently, modelling confidence intervals can be simulated for the daily discharge prediction by sampling the joint posterior parameter distribution. Figure 3 illustrates the 20 % confidence interval of the daily discharge for one year of the model validation period. The model parameter set that corresponds to the maximum likelihood yields a Nash-value (Nash and Sutcliffe, 1970) of 0.88 and a bias of 2.5 % for the calibration period. The corresponding values for the validation period are 0.87 respectively 1.0 %.

[3] Schaefli, B., Hingray, B. and Musy, A.: Uncertain glacier surface evolution under changing climate. Submitted to Journal of Geophysical Research - Atmospheres; hereinafter referred to as Schaefli et al, 2005a, submitted manuscript.

[4] Schaefli, B., Balin Talamba, D. and Musy, A., 2004. Quantifying hydrological modeling errors through finite mixture distributions. Submitted to Journal of Hydrology; hereinafter referred to as Schaefli et al, 2005b, submitted manuscript.

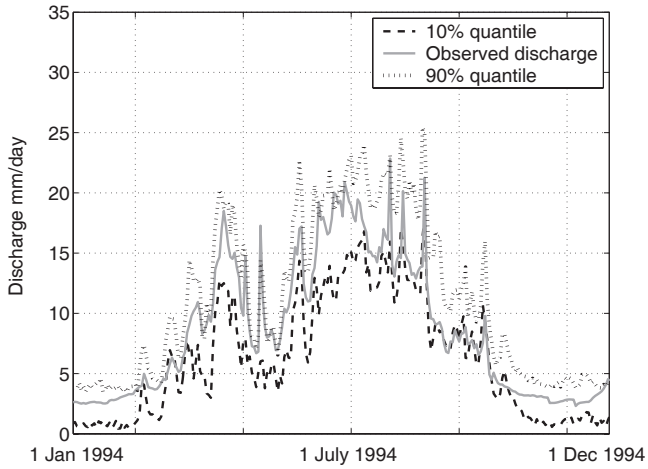

Figure 3: 20 % confidence interval for the daily discharge from the Mauvoisin catchment as simulated by the posterior model parameter distribution obtained through a Metropolis-Hastings algorithm

6.3.4 Management model

The Mauvoisin hydropower plant is composed of several power stations. There is no pump system for water recirculation. For the purpose of the present study, the interest is focused on the release management of the water accumulated by the dam and the corresponding main power station. Three turbines that correspond to a maximum installed power of 127.5 MW and a maximum total discharge of 34.5 m3/s compose it. The hydraulic head varies between 320 m and 490 m and the corresponding electricity production varies between 0.73 and 1.10 kWh per m^3 of water released through the turbines.

The dam belongs to a stock corporation composed of 6 shareholders. Each shareholder exploits its part of the accumulated energy according to its own strategy that is strongly influenced by the electricity demand but also by the annual water inflow into the lake. The dam manager surveys the evolution of the lake level to ensure the safety of the hydropower plant and an optimal lake filling by the end of the snow and glacier melt season (around end of August).

The inflow can be reduced during critic situations by disconnecting some of the 12 water intakes. Such critic situations occur if the water level comes close to 97.7 % of the maximal acceptable level. If the water level reaches the maximal acceptable level, an emergency management plan defines the actions to be undertaken that include water release through the spillway (up to 347 m^3/s). The spillway has never been activated in the past, but in case, its activation could lead to important inundations in the downstream areas. The only other management constraint to be respected refers to the maximal discharge in the river that receives the water released through the turbines: hydropower production has to be stopped if the discharge reaches 930 m^3/s in the Rhone river. There are no minimum discharge

constraints that affect the hydropower management as the minimum discharge in the dammed river is ensured by a diverted spring.

These few considerations show that - except for extreme situations - there are no clearly defined management rules. The evolution of the lake level is dependent on the electricity production strategy of the different shareholders and is therefore strongly influenced by electricity demand and offer (available hydropower). A detailed analysis of historic release and inflow data showed however that the monthly release management is highly dependent on the hydrological regime whereas the release at smaller time steps is conditioned by other factors such as the strong weekly electricity demand cycle (the demand is much lower during weekends). Therefore a mixed deterministic-stochastic model of the water release has been developed: the deterministic part models the mean seasonal release for winter respectively summer months and the stochastic part simulates the daily variations of the release that can be supposed to be conditioned by the electricity market (see Equation 3).

$$r_n = M_s \phi_j + \theta_{n,s,j} \tag{3}$$

where r_n is the release through the turbines on day n of the year, M_s the mean daily release during season s (s = 2 if n between 16 May and 31 August, s = 1 otherwise), Φ_j a weighting factor to distribute electricity production between week- and weekend days (j = 1 if n is a weekday, 2 otherwise) and $\theta_{n,s,j}$ is the residual of day n, given season s and day type j modelled by a Log-Weibull distribution.

The simulated release r_n is called planned release, the actual simulated release on a given day being dependant on the mentioned management constraints, the maximum possible daily release and on the lake level envelope curves. These curves correspond for each day to the highest and lowest lake level observed over the whole exploitation period of the dam. The manager and the shareholders use these curves to guide their daily release decisions and they reflect therefore the management experience gained in the past. They are integrated in the water release simulation tool as follows: whenever the planned release causes the lake level to lie outside these envelope curves, the actual simulated release is adapted in consequence. Spillway activation is simulated according to the emergency plan of the dam.

The management model predicts well the observed daily water release and the lake level evolution. Figure 4 illustrates the simulated and the observed cumulated water release for one year.

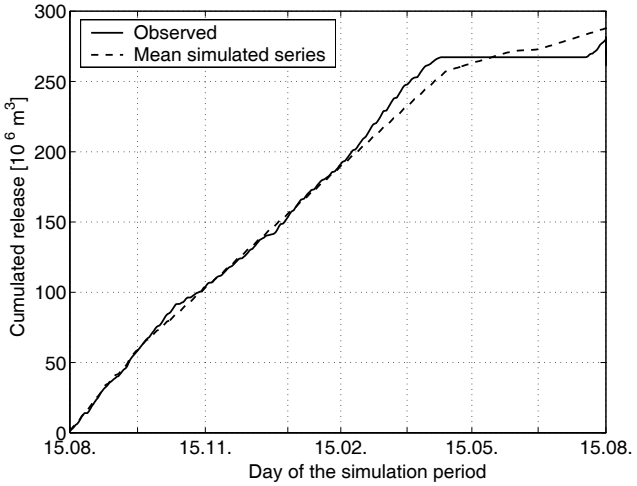

Figure 4: Simulated and observed cumulated daily release for the year 1995 -1996

6.3.5 Impact assessment: performance measurement

In the context of the present study, the climate change impacts on the management system are evaluated in terms of relative changes. A set of relevant indicators is used to compare the future scenarios to the control period. There are two types of indicators used: a set of quantitative criteria evaluating the total annual electricity production and its seasonal distribution. These indicators have been defined based on the management objectives stated by the manager and are system-specific. Additionally more general qualitative indicators are used: the so-called RRV-criteria (Reliability, Resilience, Vulnerability), based on the methodology presented by (Hashimoto et al., 1982). These RRV-criteria measure the number of failure periods, the speed of recovery from the failure states to satisfactory states and the importance of the occurring failure states. In the present application, the main interest is focused on electricity production and the failures states are therefore defined as follows: a failure state occurs when the actual daily release deviates more than 10 % from the daily planned released. A day without failure state that follows a day with failure state is called a restoration state. The vulnerability for a failure state corresponds to the absolute deviation of the actual release from the planned release divided by the maximum possible release through the turbines. See Table 2 for detailed description of all used indicators and the corresponding measurement method. Note that there has never been any spillway activation or dam overtopping situation in the past.

Table 2: List of performance indicator names, signification and measurement method

Indicator name	Signification	Measurement method
Reliability (%)	Frequency of failure states	(1 – sum of failure states) / total number of simulated time periods
Resilience (%)	Speed of recovery	Sum of restoration states / sum of failure states
Vulnerability (%)	Mean extent of failures	Sum of all daily vulnerabilities / number of failure states
Efficiency (%)	Water use efficiency	Sum of water released through the reservoir over entire simulation period
Production (MWh)	Mean annual production	Sum of produced electricity/ number of simulated years
WinterProd (%)	Mean winter production	Sum of electricity produced during winter / total electricity production over the whole simulation period
Spill	Spillway activation index	Sum of days with spillway activation/ length of simulation period
Overtopping	Dam overtopping occurrence	Number of overtopping situations

6.4 Modelling uncertainties

Each of the modelling steps induces its specific modelling uncertainties. The different sources of uncertainty and their quantification are presented separately for each model type and illustrated based on one key output variable for each model type. All simulated probability density functions are the result of 10'000 random samples and corresponding simulations of the system behaviour.

6.4.1 Climate scenario and time series production

The temperature and precipitation time series are produced through the perturbation methodology presented by (Shabalova et al., 2003). This methodology needs as input variables regional climate statistics expressed in terms of absolute or relative seasonal changes between the control and the future scenario climate model run. These statistics are the absolute change of seasonal mean temperature, the ratio of corresponding standard deviations, the ratio of seasonal mean daily precipitation and the ratio of corresponding coefficients of

variation. We use the methodology presented by (Hingray et al., 2005b, submitted manuscript)[5] to sample the entire range of possible regional climate statistics under the global warming probability distribution of (Wigley and Raper, 2001) and the scaling distribution of (Hingray et al., 2005a, submitted manuscript).

Figure 5 illustrates for the case study catchment the resulting distribution of future mean monthly temperature and precipitation together with the mean monthly temperature and precipitation observed for the control period. Two sources of uncertainty are presented: The distribution induced by the scaling relationships under median global warming (+2.62 °C) and the distribution induced by the global warming under median scaling relationships.

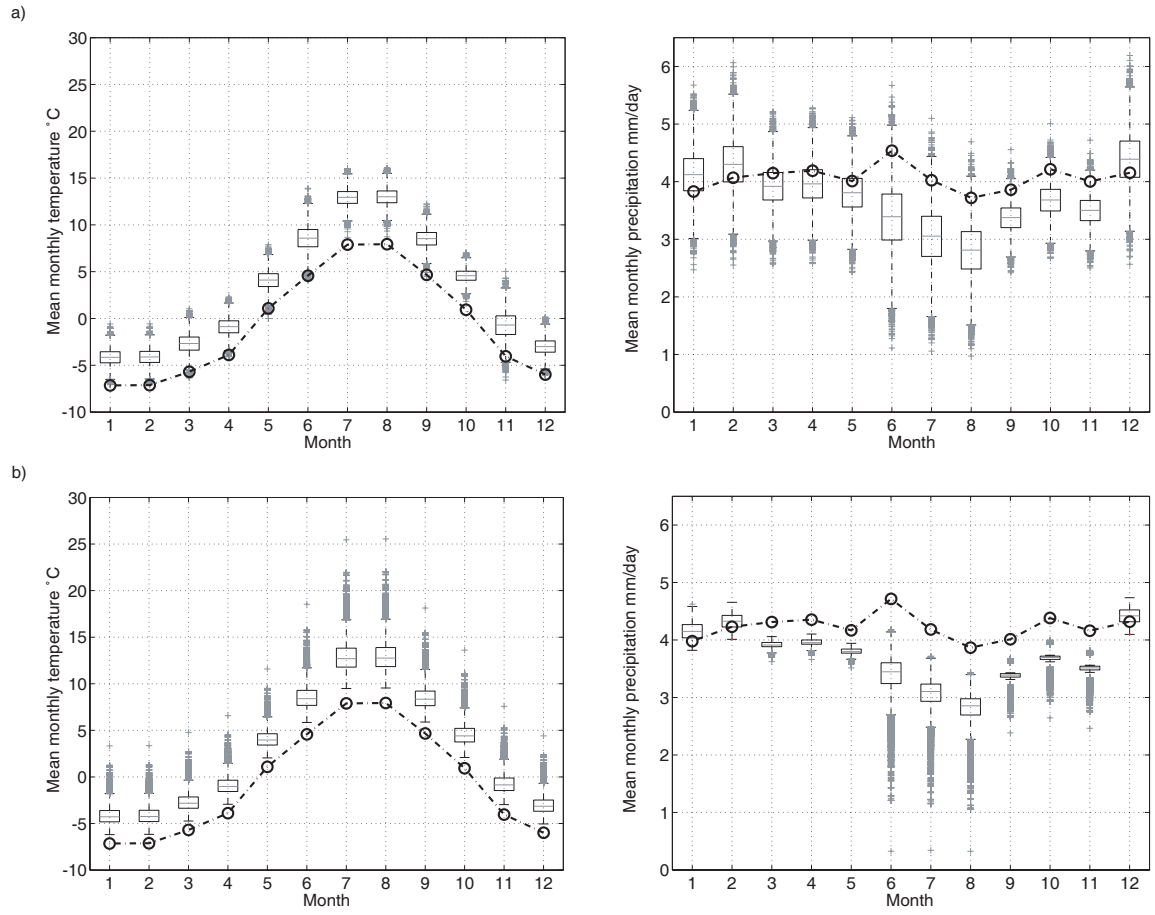

Figure 5: Boxplots of future mean monthly temperature and precipitation for the case study catchment, the black circles correspond to the mean monthly values for the control period; a) induced by the regional scaling distribution given the median global warming (+2.62°C) and b) induced by the global warming distribution given median regional scaling relationships

[5] Hingray, B., Mouhous, N., Mezghani, A., Bogner, K., Schaefli, B. and Musy, A.: Accounting for global warming and scaling uncertainties in climate change impact studies: application to a regulated lakes system. Submitted to Hydrology and Earth System Sciences; hereinafter referred to as Hingray et al., 2005b, submitted manuscript

Under the median global warming and the entire range of regional scaling uncertainty, the mean monthly temperatures of the control period correspond to outliers of the simulated future distributions. This means that even under a median global warming scenario, the predicted temperature increase is significant for all months (Figure 5a). Considering the entire range of global warming, the mean monthly temperatures of the control period are strictly lower than the simulated future distributions (Figure 5b). The simulated distributions of future mean monthly precipitation - both under median global warming and under median regional scaling relationships - show a strong seasonality with less precipitation during summer months, whereas the current climate has only a slight seasonality with maximum precipitation during the month of June. The uncertainty induced by the global warming on the simulated future mean monthly climate leads to 90 % prediction intervals for the temperature of between 2.5 °C (December) and 4.3 °C (August) and to precipitation prediction intervals of between 0.2 mm /day (May) and 1.0 mm/day (June). The uncertainty induced by the scaling relationships on predicted temperature is of the same magnitude (90 % prediction intervals of between 2.4 °C for October and 4.8 °C for November) but considerably higher for precipitation (interval of between 0.8 mm/day for September and 1.9 mm/day for June).

The uncertainty induced by the climate scenario and meteorological time series production has a direct impact on the water inflow into the accumulation lake. Figure 6 presents the uncertainties induced separately by the global warming respectively the scaling distribution on the mean annual inflow into the lake. The 90 % prediction interval is slightly smaller for the uncertainty induced by the scaling relationships than for the uncertainty induced by global warming (interval corresponding to $47*10^6$ m^3/year respectively $54*10^6$ m^3/year).

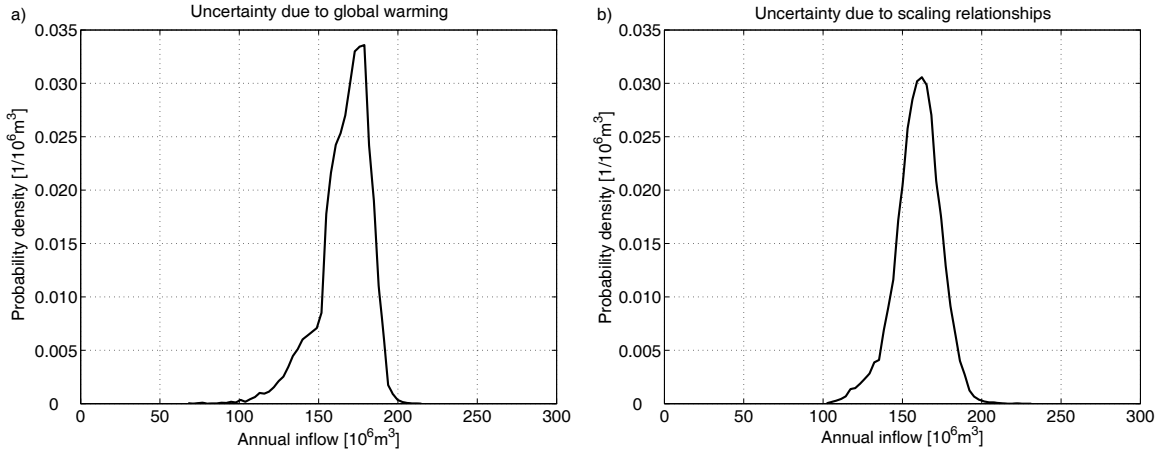

Figure 6: Probability density function of mean annual inflow into the lake: a) induced by the regional scaling distribution given the median global warming, the median AAR-value and the maximum likelihood hydrological parameter set; b) induced by the global warming distribution given the median regional scaling relationships, the median AAR-value and the maximum likelihood hydrological parameter set

6.4.2 Hydrological modelling uncertainty

As mentioned in Section 3, a Metropolis-Hasting algorithm has been used for the calibration of the hydrological model. The resulting joint distribution of the model parameters and the standard deviation of the residuals permits a good estimate of the uncertainty induced by the hydrological model (Schaefli et al., 2005b, submitted manuscript). Figure 7 illustrates the hydrological modelling uncertainty induced on the mean monthly and the mean annual water inflow into the accumulation lake given the observed meteorological time series for the control period and given the median global warming, the median scaling relationships and the median AAR-value for the future period.

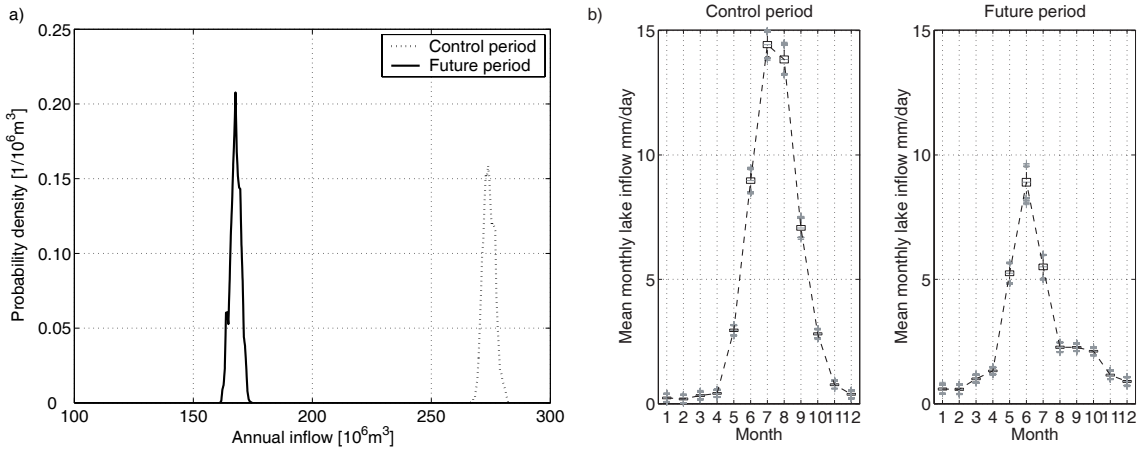

Figure 7: a) probability density function of control and future mean annual inflow into the lake given the observed meteorological times series for the control period and the median global warming, the median scaling relationships and the median AAR-value for the future period, b) boxplots of corresponding mean monthly inflow

The 90 % prediction interval of the mean annual inflow is of the same order of magnitude for the control and the future period ($7.8*10^6$ m^3/year respectively $7.2*10^6$ m^3/year). Figure 7b shows that the increase of winter precipitation and corresponding snow accumulation together with higher temperatures leads to an earlier and stronger snowmelt peak in spring. For the considered median AAR-value, the median future ice-cover of the catchment corresponds to 1.5 % and the glacier melt is therefore small. The evapotranspiration increases due to the higher temperatures and the land cover change (disappearance of the glaciers). The resulting hydrological regime is of the so-called nival type (maximum monthly discharge in June).

6.4.3 Glacier evolution uncertainty

The total ice-covered surface for a given simulation period represents a priori a considerable source of uncertainty. This uncertainty is partly directly due to the hydrological model parameters that condition the cycle of snow and ice accumulation and melt. Another

important part is the link between the mass balance and the glacier surface evolution. Note that the percentage of ice-covered surface is uncertain even for the model calibration period as this surface varies from year to year and as the available data is not frequently updated. Considering the chosen glacier surface evolution model, the last two types of uncertainty are however easily integrated in the present modelling framework. The simulated annual AAR values for the calibration period can be modelled by a Log-Weibull distribution (Schaefli et al., 2005a, submitted manuscript). Therefore - instead of using a fixed mean AAR value in Equation 2 – the mean AAR value is drawn randomly for each simulation. The Log-Weibull distribution has been chosen because the distribution has to be limited to the interval [0, 1] and because the empiric frequencies of the AAR series are right-skewed.

Figure 8 illustrates the so induced uncertainty on the mean annual water inflow given the median global warming, the median scaling relationships and the maximum likelihood hydrological parameter set. The resulting 90 % prediction interval of the mean annual inflow ($5.6*10^6$ m^3/year) is comparable to the one resulting from the hydrological modelling (Figure 8) but considerably smaller than the ones due to the generation of meteorological time series (see Figure 6). This result is due to the fact that under the median future climate scenario, the remaining ice-covered area is small for the entire range of possible AAR-values (between 0 % and 2.9 % of the catchment area).

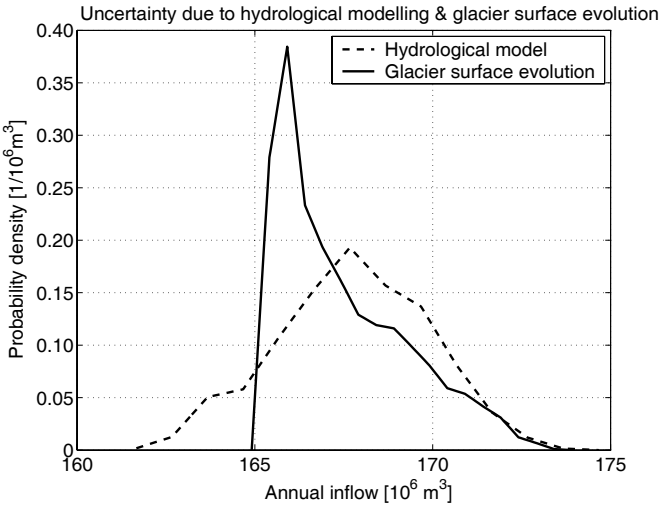

Figure 8: Probability density function of the mean annual water inflow under glacier surface evolution uncertainty (given the median global warming, the median scaling relationships and the maximum likelihood hydrological parameter set) and under hydrological modelling uncertainty (given the median global warming, the median scaling relationships and median AAR-value)

Another potential source of uncertainty is the reaction time of the glaciers, i.e. the time that elapses until a glacier reacts to a modification of the prevalent climate. According to (Spreafico et al., 1992), the glaciers of the case study catchment have current reaction times of between a few years and a few decades. We assume however, that the gradual warming

between the control and the future period will substantially reduce the corresponding ice volumes and surfaces, reducing therefore the reaction times significantly. Accordingly, we assume that the future modelling period of 30 years is long enough for the glaciers to react to the simulated climate.

6.4.4 Management modelling uncertainty

The most important source of uncertainty at this modelling level is the planned daily release through the turbines, the actual daily release being strongly influenced by the water cycle. The presented management simulation tool models the planned daily release by a Log-Weibull distribution. The distribution of all performance indicators is therefore easily obtained by multiple simulation of the system for a given hydrological parameter set, a given AAR-value and a given meteorological scenario. Figure 9 illustrates the distribution of the RRV values given the hydrological parameter set with the maximum of likelihood and given the observed meteorological times series for the control period respectively the median global warming, the median scaling relationships and the median AAR-value for the future period.

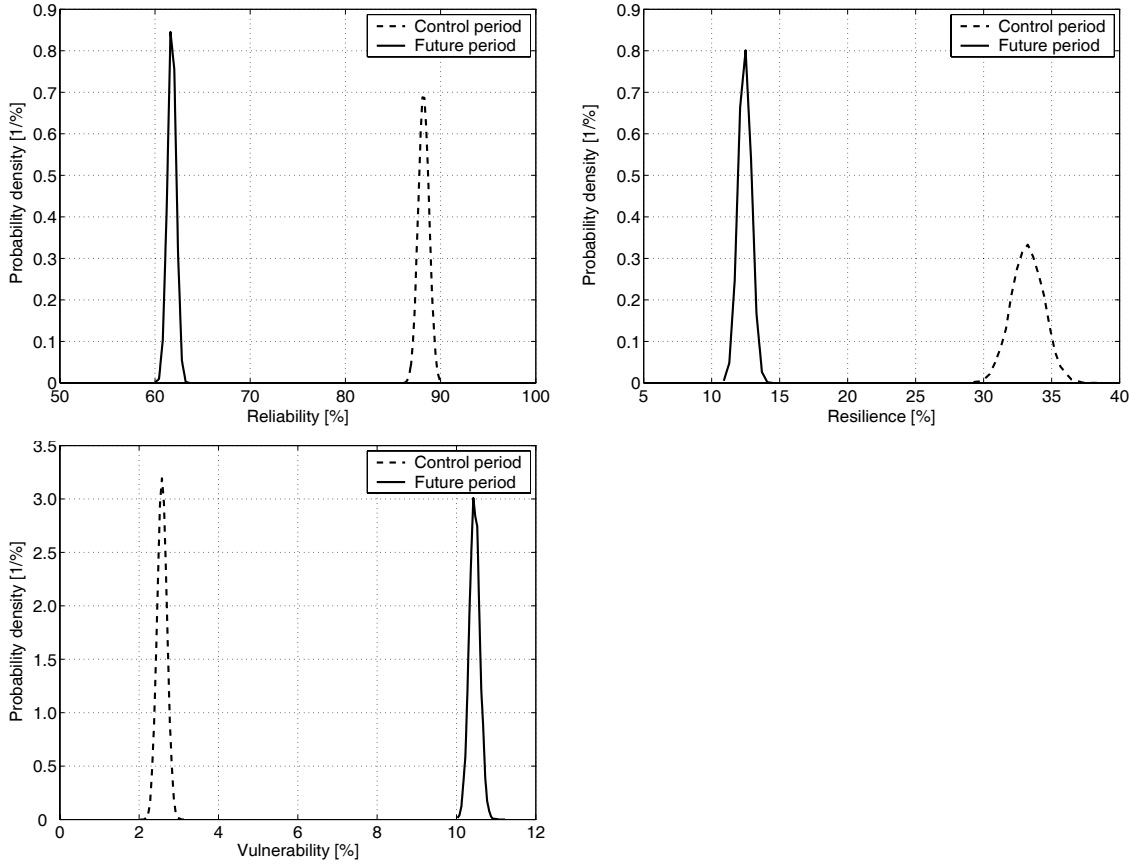

Figure 9: Distribution of the RRV values given the maximum likelihood hydrological parameter set and given the observed meteorological times series for the control period respectively the median global warming, the median scaling relationships and the median AAR-value for the future period

The significant decrease of the reliability and the resilience, respectively increase of the vulnerability for the future period are due to the modification of the water cycle as illustrated in Figure 7b (shift of the peak flow from summer to spring). Note the significant decrease of the 90 % prediction interval for the resilience between the control (3.9 %) and the future period (1.6 %).

6.5 Integrated uncertainty analysis

The uncertainties inherent to each of the presented modelling levels can be combined by Monte Carlo simulation of the system behaviour, sampling randomly the appropriate parameters for each model type. The following 5 uncertainty levels are considered: i) the daily release of the management model, ii) the parameter estimation of the hydrological model, iii) the AAR-value of the glacier surface evolution model, iv) the scaling relationship between global warming and regional statistics and v) the global warming. The previous section has illustrated the modelling uncertainty induced by each of them separately. Hereafter, the 5 uncertainty levels are successively combined in the above order. The corresponding probability density functions are the result of 20'000 random parameter samples and corresponding simulations of the system behaviour. A random parameter sample contains one randomly drawn parameter value for each parameter that is taken into account at a given level of uncertainty combination.

Figure 10 illustrates the shift and/or the flattening of the probability density function of the simulated management reliability when successively combining the first three uncertainty levels. Adding the hydrological parameter uncertainty to the daily release uncertainty shifts the function to the right and flattens it. Adding the uncertainty due to the AAR-value estimation enhances this effect. The influence of the different sources of uncertainty on the overall uncertainty depends on the considered performance criterion (Figure 11). The most important part of the overall uncertainty is however introduced by the generation of the meteorological time series. Adding the scaling uncertainty to the three previous ones flattens the probability distribution function considerably for all performance criteria (Figure 11). The global warming enhances this flattening by lengthening the queues of the distribution. Table 3 illustrates the effect of successive combination of the 5 uncertainty levels based on the 5 %, 50 % and 95 % quantiles of the mean annual electricity production. The global warming covers a large part of the overall uncertainty: the 90 % prediction interval for the overall uncertainty corresponds to 85.5 GWh, of which an interval corresponding to 32.3 GWh are induced by the global warming uncertainty.

Table 3: 5 %, 50 % and 95 % quantiles of the future mean annual electricity production (GWh) for increasing levels of uncertainty

Uncertainty level	5 %	50 %	95 %
Management	146.8	147.0	147.2
Manag & Hydro	148.2	151.8	154.9
Manag, Hydro, Glacier	152.5	157.3	163.2
Manag, Hydro, Glacier, Scaling	128.0	155.1	181.1
All levels of uncertainty	102.7	158.5	188.2

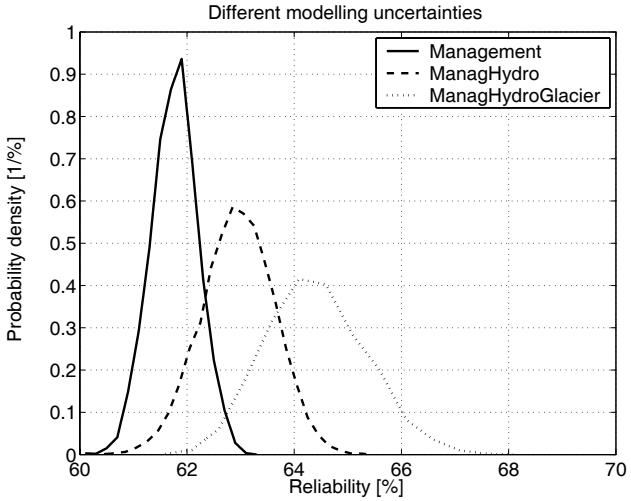

Figure 10: Probability density functions of the management reliability simulated by taking into account the release uncertainty (Management), the release and hydrological parameter uncertainty (ManagHydro), the release, hydrological parameter and AAR-value uncertainty (ManagHydroGlacier)

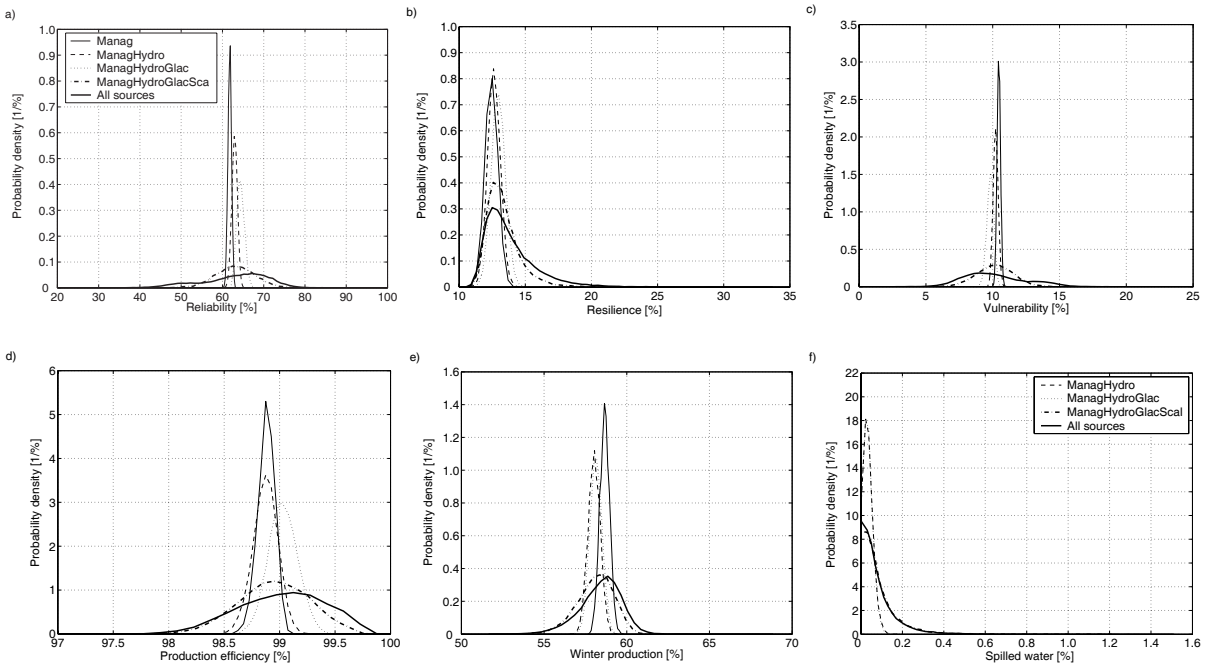

Figure 11: Evolution of the probability density functions of 6 performance criteria due to successive combination of 5 uncertainty levels: daily release (Manag), hydrological parameter estimation (Hydro), AAR-value (Glac), regional scaling relationships (Scal) and global warming; the criterion "spilled water" equals zero for the first level of uncertainty

6.6 Climate change impacts on the hydropower management

Considering all modelling assumptions and all identified sources of modelling uncertainties, we can affirm that climate change will adversely affect the management performance of the system. The probability distributions of the indicator values for the control and the future period are strictly different and the RRV values for the future period are strictly worse than for the control situation. Table 4 and 5 give the 5 % and 95 % confidence limits and the median of the simulated distributions of all the meteorological key variables and the indicators for the control and the future periods. The distributions have been simulated given all related modelling uncertainties. For the future period all mentioned modelling uncertainties are taken into account (i.e. the ones due to global warming, to regional scaling relationships, to hydrological, glacier surface and management modelling), whereas for the control period only the uncertainties due to the hydrological and the management model are included.

The increase of the median value of the mean daily temperature corresponds to +3.4 °C (Table 4). The minimum simulated mean daily temperature is equal to -2.9 °C, the future temperature being therefore strictly higher than for the control period. The mean annual precipitation distributions for the control and the future period are slightly overlapping, the median value of the control period corresponds to the 94.7 % quantile of the future distribution. The increase of simulated actual ET is considerable; the median future value

corresponds to almost the double of the median value for the control period (Table 4). This result is due to the decrease of the glacier surface that augments considerably the catchment area contributing to the actual ET. The hydrological model does not account for evaporation over the ice-covered areas as in the overall water balance it is compensated by the ice melt estimation. Related to the not ice-covered catchment area, the median annual actual ET for the control period corresponds to 358 mm. This shows that the absolute increase between the simulated median value for the control and the future period is small.

Table 4: Median and 5 % and 95 % confidence limits of the distributions of mean daily temperature, mean annual precipitation, mean annual actual ET and glaciation for the control and future period, simulated given all related modelling uncertainties; the temperature corresponds to the mean catchment altitude, precipitation and actual ET are area averaged values; for the control period, there is no uncertainty for the temperature interpolation

	Control period			Future period		
Variable	5%	50%	95%	5%	50%	95%
Temperature (°C)-	-	-3.6	-	-1.8	-0.2	2.5
Precipitation (mm)	1500	1527	1551	1205	1411	1528
Actual ET (mm)	208	210	211	313	394	552
Glaciation (%)	-	41.4	-	0	1.4	6.9

Table 5: Median and 5 % and 95 % confidence limits of the indicator value distributions simulated given all modelling uncertainties for the control and future period

	Control period			Future period		
Indicator name	5%	50%	95%	5%	50%	95%
Reliability (%)	87.3	88.2	89.2	47.3	64.2	74.3
Resilience (%)	31.3	33.2	35.2	11.7	13.3	17.7
Vulnerability (%)	2.4	2.6	2.8	6.8	9.9	14.4
Efficiency (%)	99.5	99.6	99.7	98.3	99.0	99.6
Production (GWh)	246.2	246.5	246.8	102.7	158.5	188.2
WinterProd (%)	62.7	63.0	63.4	56.1	58.6	60.2
Spill (%)	0.00	0.00	0.00	0.00	0.06	0.25
Overtopping	0.00	0.00	0.00	0.00	0.00	0.00

The increase of the temperature over the whole year and the decrease of annual precipitation lead to an important reduction of the simulated ice-covered area and of the available water in the system. Compared to the median hydropower production for the control period, the median future production corresponds to a decrease of 36 % (Table 5). The water use efficiency however remains more or less constant for the future period; the loss of hydropower production is exclusively due to the important decrease of the available water through the decrease of precipitation and ice melt and the increase of evapotranspiration. The hydropower production undergoes a shift of about 7 % from winter to summer production due to a modification of the prevalent hydrological regime. This regime modification explains partly the decrease of the release reliability, as planned release during the winter months cannot be met anymore and production in summer months is sometimes higher than planned. There is a significant increase of the release vulnerability that measures the average difference between planned and actual release through the turbines: the control median value of 2.6 % corresponds to around 70 MWh production difference between planned and actual production whereas the future median value of 9.9 % corresponds to a production difference of around 269 MWh. This considerable worsening of the release vulnerability is accompanied with occasional spillway activation for the future period. The overall water loss through spillway activation is negligible even for extreme climate change scenarios (95 % quantile corresponds to 0.25 % (Table 5) and the highest simulated value to 1.3 %). The corresponding water discharge however could potentially endanger the downstream area. The maximum simulated discharge through the spillway corresponds to 177.4 m^3/s. A detailed risk analysis is beyond the context of the present study. The value can however be compared to the maximum discharge recorded before the dam construction (45 years of data) that corresponds to 59 m^3/s. This shows that the simulated spillway discharge would represent a substantial new hazard. This discharge value has however to be considered with care for the following reasons: i) Contrary to the reality, the management model does not include any meteorological forecast; ii) this value corresponds to an extreme scenario. The maximum spillway activation simulated for the median global temperature increase (+2.65 °C) and taking into account all other modelling uncertainties corresponds to 60 m^3/s and equals the maximum discharge recorded before dam construction. A further analysis of the risk for the downstream inhabited areas is nevertheless recommendable: the risk not only results of the potential hydrological hazard but of its combination with the vulnerability of the system that may have considerably increased since the dam construction.

The above impact analysis on the performance of the studied hydropower system shows that the management system is able to deal with the entire range of predicted climate change. Under the given range of global warming, the overall performance will decrease if the present management system is maintained unchanged, but the overall water use efficiency will remain stable and there will be no lasting damage of the entire hydropower system. The risk for downstream inhabited areas may however increase compared to the control period because of occasionally occurring spillway activations. In the context of climate change impact analysis, special attention should be paid to the sustainability evaluation of the studied systems.

According to (Loucks and Gladwell, 1999), water resource systems can be called sustainable if they are able to satisfy the changing demands placed on them, now and on into the future, without system degradations. The presented analysis cannot draw any conclusions about the system's ability to meet the electricity demand. Its sustainability can therefore not be judged.

6.7 Conclusions

The developed methodology is consistent for the analysis of potential climate change impacts on a real world water resources system and the obtained results answer the main question motivating the present study: Given the modelling uncertainties, climate change *does* cause a statistically significant modification of the system, the performance of which is negatively affected.

All results are conditioned by the underlying modelling assumptions and by the used data on long-term climate projections, namely the global warming probability density function given by (Wigley and Raper, 2001) and the regional scaling relationships derived from 19 regional climate models according to the methodology presented in (Hingray et al., 2005a, submitted manuscript). These two data sources are supposed to incorporate a maximum of currently available scientific knowledge in the area of climate modelling. The different modelling uncertainties that are included in the presented methodology have been chosen based on the following two criteria: i) The authors judged them to be important for the presented case study and ii) necessary data and scientific knowledge exist to include them in the study. Some potential important sources of modelling uncertainties have not been taken into consideration. Especially land cover change induced modifications of the evapotranspiration and its formulation in the hydrological model could be worth of further investigations. Additional research into the generation of at site temporal times series based on regional climate statistics could potentially enlarge the overall modelling uncertainty. We think especially of further work in order to reduce the potential loss of variability and extremes in this interface between the climate models and the hydrological model. The climate change impact analysis could also greatly benefit from an additional evaluation of the natural variability for the control period, for example based on an appropriate weather generator.

Another important modelling uncertainty issue is arising from the conceptual hydrological model. Data scarcity in high mountainous catchment and the need for uncertainty estimation prevented us from using a physically based model. In the area of climate change impact studies, we are however inevitably confronted with the problem of extrapolation of a calibrated model beyond its domain of validation. This general problem could be approached by a model structure uncertainty analysis such as the one presented in (Schaefli et al., 2004). Further research into how to include such structural uncertainties quantitatively in the presented climate change impact analysis has to be done.

The management system performance has been analysed for future climate situations assuming that all other elements of the system remain constant – a quite unrealistic assumption. Climate change induced modifications of the electricity demand could completely modify the system management. Some authors tried to analyse simultaneously the electricity demand and production (see, e.g., Robinson, 1997; Westaway, 2000). The Swiss electricity market is however highly interconnected with the European one and a demand analysis is therefore far beyond the reach of the present study. It could nevertheless be interesting to complete the study by an analysis of different management adaptation strategies such as the one presented by Payne et al. (2004). The used management model does not include any quantitative rainfall forecasts. As they become currently more and more precise, the realism of the management model could be enhanced by including short-term precipitation forecasts.

At the considered temporal prediction horizon (2070 – 2099), the median decrease of hydropower production in the studied system corresponds to 36 % compared to the control period. Given the highly non-linear relationships between the water availability, catchment glaciation, daily precipitation and temperature, it can be assumed that the decrease between the two periods is not linear. Because of the joint action of ice melt increase and precipitation decrease during intermediate periods, the climate change induced modification of water availability is presumably not even monotonous. The analysis of intermediate climate change scenarios would help to determine potentially critical situations due to a possible increase in water inflow into the accumulation lakes and would therefore complete the conclusions on climate change impacts on hydropower production in the Alps. However, further work focusing on in-between periods is conditioned on the availability of multiple climate change predictions, which is currently still problematic.

Acknowledgements

This work is part of the SWURVE (Sustainable Water: Uncertainty, Risk and Vulnerability in Europe) project, funded under the EU Environment and Sustainable Development programme, grant number EVK1-2000-00075. The Swiss part of this project was funded by the Federal Office for Education and Science, contract number 00.0117. We also wish to thank the Forces Motrices de Mauvoisin for providing the discharge data and the national weather service MeteoSwiss for providing the meteorological time series.

References

Anonymous, 1969. Mass-balance terms. Journal of Glaciology, 8(52): 3-7.

Barnett, T., Malone, R., Pennell, W., Stammer, D., Semtner, B. and Washington, W., 2004. The effects of climate change on water resources in the West: introduction and overview. Climatic Change, 62(1-3): 1-11.

Bergstrom, S., Carlsson, B., Gardelin, M., Lindstrom, G., Pettersson, A. and Rummukainen, M., 2001. Climate change impacts on runoff in Sweden - assessments by global climate models, dynamical downscaling and hydrological modelling. Climate Research, 16(2): 101-112.

Burman, R. and Pochop, L.O., 1994. Evaporation, evapotranspiration and climatic data. Elsevier, Amsterdam, 278 pp.

Christensen, N.S., Wood, A.W., Voisin, N., Lettenmaier, D.P. and Palmer, R.N., 2004. The effects of climate change on the hydrology and water resources of the Colorado River basin. Climatic Change, 62(1-3): 337-363.

Garr, C.E. and Fitzharris, B.B., 1994. Sensitivity of Mountain Runoff and Hydro-Electricity to Changing Climate. In: M. Beniston (Editor), Mountain Environments in Changing Climates. Routledge, London, pp. 366-381.

Harrison, G.P. and Whittington, H.B.W., 2002. Susceptibility of the Batoka Gorge hydroelectric scheme to climate change. Journal of Hydrology, 264(1-4): 230-241.

Hashimoto, T., Stedinger, J.R. and Loucks, D.P., 1982. Reliability, Resiliency, and Vulnerability Criteria for Water Resource System Performance Evaluation. Water Resources Research, 18(1): 14-20.

Kuczera, G. and Parent, E., 1998. Monte Carlo assessment of parameter uncertainty in conceptual catchment models: the Metropolis algorithm. Journal of Hydrology, 211(1-4): 69-85.

Loucks, D.P. and Gladwell, J.S. (Editors), 1999. Sustainability Criteria for Water Resource Systems. International Hydrology Series. University Press, Cambridge, Cambridge, 139 pp.

Mimikou, M.A. and Baltas, E.A., 1997. Climate change impacts on the reliability of hydroelectric energy production. Hydrological Sciences Journal, 42(5): 661-678.

Nash, J.E. and Sutcliffe, J.V., 1970. River flow forecasting through conceptual models. Part I, a discussion of principles. Journal of Hydrology, 10(3): 282-290.

Payne, J.T., Wood, A.W., Hamlet, A.F., Palmer, R.N. and Lettenmaier, D.P., 2004. Mitigating the effects of climate change on the water resources of the Columbia river basin. Climatic Change, 62(1-3): 233-256.

Robinson, P.J., 1997. Climate change and hydropower generation. International Journal of Climatology, 17: 983-996.

Schaefli, B., Hingray, B. and Musy, A., 2004. Improved calibration of hydrological models: use of a multi-objective evolutionary algorithm for parameter and model structure uncertainty estimation. In: B. Webb (Editor), Hydrology: Science and Practice for the 21st Century. British Hydrological Society, London, pp. 362-371.

Schaefli, B., Hingray, B., Niggli, M. and Musy, A., 2005. A conceptual glacio-hydrological model for high mountainous catchments. Hydrology and Earth System Sciences Discussions, 2, 73-117.

Shabalova, M.V., Van Deursen, W.P.A. and Buishand, T.A., 2003. Assessing future discharge of the river Rhine using regional climate model integrations and a hydrological model. Climate Research, 23: 223-246.

Spreafico, M., Weingartner, R. and Leibundgut, C., 1992. Atlas hydrologique de la Suisse. Service Hydrologique et Géologique National (SHGN), Bern.
Swiss Federal Office for Energy, 2003. Statistique suisse de l'électricité 2002, Bern.
Westaway, R., 2000. Modelling the potential effects of climate change on the Grande Dixence hydro-electricity scheme, Switzerland. Journal of the Chartered Institution of Water and Environmental Management, 14(3): 179-185.
Wigley, T.M.L. and Raper, S.C.B., 2001. Interpretation of High Projections for Global-Mean Warming. Science, 293(5529): 451-454.

Chapter 7

Use of a multi-objective evolutionary algorithm for parameter and model structure estimation[1]

Abstract

The present paper applies a new clustering evolutionary algorithm to a model structure and parameter estimation problem. Using this multi-objective optimisation algorithm, decision variables referring to the model design can be included in the model optimisation process and several equivalent model structures can be identified. The optimisation algorithm has been designed for energy system design problems and contains a number of features that are new in the area of hydrological model calibration. In particular, this evolutionary algorithm can find multiple local non-dominated parameter sets that enable the joint calibration of different model structures. Its application to hydrological modelling problems is illustrated for a

1 This chapter is published: Schaefli, B., Hingray, B. and Musy, A., 2004. Improved calibration of hydrological models: use of a multi-objective evolutionary algorithm for parameter and model structure uncertainty estimation. In: B. Webb (Editor), Hydrology: Science and Practice for the 21st Century. British Hydrological Society, London, pp. 362-371.

conceptual reservoir-based model for precipitation – runoff transformation. The structure of this model and the related model parameters are estimated jointly. The obtained solutions are equivalent in terms of model performance for the calibration and the validation period. It is however shown that for a future period characterised by a modified climate, the different model structures yield completely different results outlining therefore that the model structure is considerable source of uncertainty in climate change impact studies on water resources.

Using this algorithm, decision variables referring to the model design can be included in the parameter optimisation process and several equivalent model structures can be identified. Based on a case study in the Swiss Alps, the model behaviour under the different optimal design options is illustrated for modified climatic conditions and the implications of model design optimisation are discussed based on these results.

The presented case study in the Swiss Alps shows that for such long-term projections (typically between 50 and 100 years) in non-stationary conditions, the model structure induces uncertainties that are potentially higher than the uncertainty due to the parameter estimation for a given model structure

7.1 Introduction

Powerful optimisation algorithms have become widely used for the automatic calibration of model parameters, and especially evolution-based methods have been found to be efficient in identifying the globally best parameter set. Current research in the area of automatic calibration also addresses the problem of using multiple criteria for the model optimisation, these criteria being calculated on one or different model outputs (see, e.g., Seibert, 2000; Vrugt et al., 2003). An efficient global optimisation algorithm can reliably find the global optimal parameter set but the meaning of such a unique parameter set is questionable especially if its performance in terms of the optimisation objective is not significantly different from other solutions. This parameter uncertainty problem is addressed by recent studies through the application of Markov Chain Monte Carlo methods that become increasingly popular for the estimation of the posterior probability distribution of parameters (see, e.g., Kuczera and Parent, 1998; Vrugt et al., 2003).

These different approaches are all based on a predetermined and fixed hydrological model structure. This structure is usually defined by the parameterisation of the phenomena the modeller judges significant to simulate the system behaviour. The design options have an important impact on the model's ability to reproduce the signal used for calibration and different model structures can lead to virtually the same calibration and validation results. The reproduction of some internal processes can sometimes help to identify the best model structure, the final choice depending essentially on the modeller's experience. If the calibrated model is applied to current climatic and hydrologic conditions, one might not be concerned about this problem. But for future conditions, especially in the context of climate change, the

different model structures can lead to significantly different simulation results and the induced modelling uncertainty is potentially higher than the one due to the model parameter estimation uncertainty. An overall modelling uncertainty assessment should therefore not only be based on one fixed model structure but should include other equivalent model structures.

The present paper addresses the problem of identifying such apparently equivalent model structures by the application of a new clustering evolutionary multi-objective optimisation algorithm that has recently been developed for industrial design problems at the Laboratory of Industrial Energy Systems (Laboratoire d'Energie Industrielle - LENI) of the Swiss Institute of Technology in Lausanne. Using this algorithm, decision variables referring to the model design can be included in the parameter optimisation process and several equivalent model structures can be identified. Its application is illustrated through the joint parameter and model design optimisation for a reservoir based hydrological model that has been developed for climate change impact studies in a glacierized alpine catchment. Based on a case study in the Swiss Alps, the model behaviour under the different optimal design options is illustrated for modified climatic conditions and the implications of model design optimisation are discussed based on these results.

7.2 Hydrological model

The hydrological discharge simulation is carried out at a daily time step through a conceptual, semi-lumped model called GSM-SOCONT (Glacier and SnowMelt – SOil CONTribution model) (Schaefli et al., 2005). The model has two levels of discretization. The ice-covered part of the catchment is first separated from the not ice-covered part. Next, both parts are subdivided into elevation bands. Each of the resulting spatial units is characterised by its surface and its hypsometric curve and is assumed to have a homogeneous hydrological behaviour. The precipitation – runoff transformation is simulated for each spatial unit separately; the runoff contributions of all units are added to provide the total discharge at the outlet of the entire catchment. Figure 1 shows the basic hydrological model structure for a given spatial unit, the different submodels and their interconnections. Hereafter, the basic design of each submodel and the possible variants are presented.

In the model structure presented, the glacier surface is supposed to be constant for a given simulation period. For the future scenario simulation, the ice-covered surface has to be updated. In the present study, this update is based on the assumption that the mean interannual accumulation area ratio (AAR) (Anonymous, 1969) simulated for observed climatic conditions remains constant in the future. For a given hydrological year (starting on the 1 October), the AAR is computed from the sum of spatial units that experience snow accumulation.

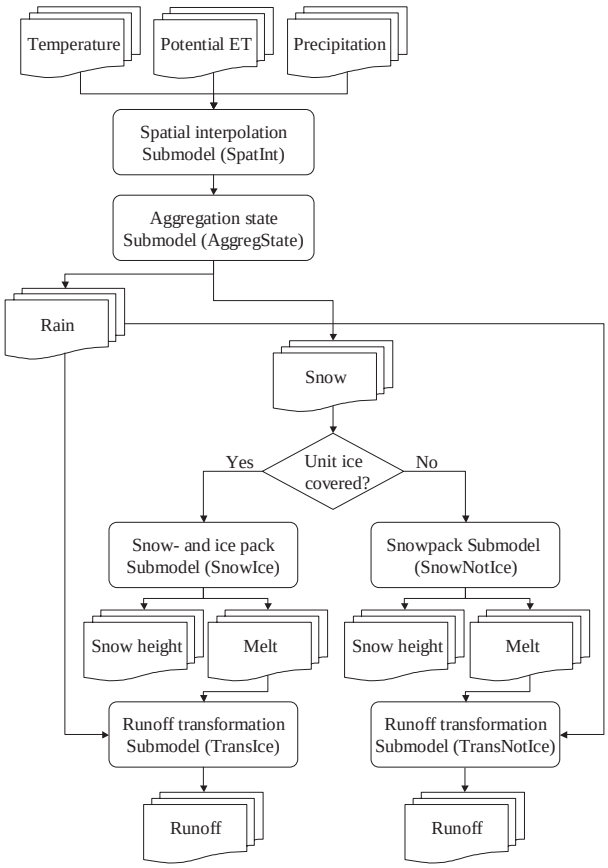

Figure 1: Basic hydrological model structure (for one spatial unit) showing the different submodels and the input and output time series; in brackets: the submodel short names; ET = evapotranspiration

7.2.1 Spatial interpolation submodel

The temperature and precipitation time series are linearly interpolated according to the mean elevation of the spatial unit. The temperature decrease with altitude is fixed to 0.65 °C per 100 m of altitude change (the mean gradient of observed temperature series in the Swiss Alps). The precipitation increase factor, c_{precip} ($\%100^{-1}m^{-1}$) is included in the parameter optimisation procedure as little knowledge about the local altitudinal variation of the precipitation can be derived from observed data.

7.2.2 Aggregation state submodel

The aggregation state submodel computes the nature of precipitation (liquid or solid) and is based on a fuzzy rule (Equation 1):

$$P_{snow} = \max\{0, \min\{P_{tot}, P_{tot}(T_{50} + T_{Trans} - T) \cdot (2T_{Trans})^{-1}\}\}$$
$$P_{liq} = P_{tot} - P_{snow} \quad (1)$$

where P_{snow} (mm d^{-1}) is the snowfall, P_{tot} (mm d^{-1}) the total precipitation, P_{liq} (mm d^{-1}) the rainfall, T (°C) the air temperature, T_{50} (°C) the temperature that corresponds to 50 % of the precipitation falling as snow and $2T_{Trans}$ (°C) the length of the temperature interval over which snowfall and rainfall occurs simultaneously.

7.2.3 Snowpack submodel (not ice-covered spatial units)

The snow height is computed as the difference of incoming snowfall and outgoing snowmelt, M_{snow} (mm d^{-1}) that is computed according to a classical temperature-index approach (Equation 2).

$$M_{snow} = \begin{cases} a_{snow}(T - T_m) & T > T_m \\ 0 & T < T_m \end{cases} \quad (2)$$

where a_{snow} (mm°$C^{-1}d^{-1}$) is the degree-day factor for snowmelt, T (°C) the mean temperature and T_m (°C) the threshold temperature for melting that is set to 0°C. In the basic model configuration, the water flow from the snowpack corresponds to M_{snow}. We also include a more complex approach in the optimisation procedure based on (Kuchment and Gelfan, 1996). This approach assumes that the snowpack has a capacity of retention θ_{snow} and that water flow only occurs if this capacity is reached.

7.2.4 Snow and ice pack submodel (ice-covered spatial units)

On the ice-covered spatial units, the water is stored in three different forms, as snow, ice or firn, the last form being the transition state between snow and ice. The evolution of the snowpack is simulated as in the snowpack submodel. At the end of each hydrological year (30 September), the snow that has fallen during the year but not melted is added to the firn pack. The evolution of this compartment is simulated with the same approach as for snow (Equation 2), using a degree-day factor for firn, a_{firn} (mm°$C^{-1}d^{-1}$), but melt only occurs if the snowpack has disappeared. If at a given day, a spatial unit is covered neither by snow nor by firn, the underlying ice melts according to Equation 2 with a degree-day factor a_{ice} (mm°$C^{-1}d^{-1}$). For the optimisation procedure, we also consider a model variant that uses only snow and ice, i.e. no transition between the two forms occurs.

7.2.5 Runoff transformation submodel for ice-covered units

The rainfall and melt transformation into runoff is based on the model of Baker et al. (1982), who use three parallel linear reservoirs to simulate the water transport to the outlet, one reservoir each for snow, firn and ice. The basic linear reservoir approach is given in Equation 3.

$$Q_j(t) = Q_j(t-1)\ e^{-\frac{1}{k_j}} + I_j(t)\ (1 - e^{-\frac{1}{k_j}}) \tag{3}$$

where $Q_j(t)$ (mm d^{-1}) is the discharge from the reservoir j (j = snow, firn, ice) at time step t and $Q_j(t\text{-}1)$ the discharge at the previous time step. k_j (d) is the storage constant of the reservoir j and $I_j(t)$ (mm d^{-1}) is water inflow into the reservoir j that corresponds to the sum of melt water and rainfall.

7.2.6 Runoff transformation submodel for not ice-covered units

The rainfall – runoff transformation is carried out through a conceptual reservoir-based model named SOCONT developed in our research group and similar to the GR-models (Edijatno and Michel, 1989). It is composed of two reservoirs, a linear reservoir for the slow contribution and a non-linear reservoir for direct or quick runoff. Figure 2 shows the model in detail.

In the basic model form, the snowmelt – runoff transformation is simulated based on Equation 3 with j = snow. The following model variant is used for the optimisation procedure: Rainfall and snowmelt are summed to an equivalent rainfall that is transformed into runoff through the model SOCONT.

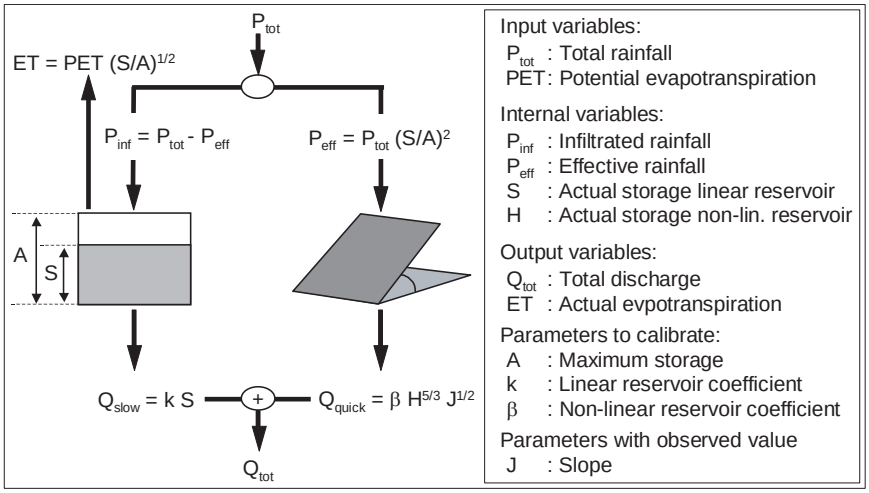

Figure 2: Rainfall-runoff transformation model SOCONT for not ice-covered spatial units

7.3 Optimisation algorithm

The optimisation tool used in the present study is the so-called Queueing Multi-Objective Optimiser (QMOO) that has been developed at LENI and is presented in detail in (Leyland, 2002). This algorithm has been developed in order to improve the optimisation performance on problems of energy system design but is applicable to a wide range of optimisation problems. It has been tested successfully on several theoretical test problems and has been proven to be robust and effective for the resolution of non-linear, non-continuous and mixed real – integer problems in the domain of optimisation of energy systems (Leyland, 2002; Burer et al., 2003) The test problems as well as the real world problems showed that QMOO successfully optimises most of them without requiring any specific tuning to each problem (Leyland, 2002). This means that the algorithm is particularly useful for non-specialist users. In the domain of hydrological model calibration, most recent optimisation tools still require tuning (see, e.g., Reed et al., 2003; Vrugt et al., 2003) and consequently, the user needs to acquire experience in the application of the algorithm or should have a good idea about the behaviour of the problem to optimise.

QMOO is a new generation clustering evolutionary algorithm that handles integer problems (i.e. problems including decision variables of integer type). The algorithm is multi-objective, i.e. it identifies the Pareto-optimal solutions for multiple objective functions. The Pareto-optimality (Pareto, 1896) can be interpreted as follows: A point of the decision variable space is Pareto-optimal if no other point is better in all objectives. The set of all Pareto-optimal points is called Pareto-optimal frontier. Rather than just identifying the global Pareto-optimal frontier, QMOO finds and retains many local Pareto-optimal frontiers - a property that allows the identification of multiple solutions. It is obtained through cluster analysis techniques that ensure local competition between sets of decision variables (so-called individuals) in the decision variable space and that allow the identification of separate local optima simultaneously. This property preserves diversity and helps the algorithm to converge to difficult-to-find optima. In the following, the key features of the algorithm – from the point of view of the application presented in this paper - are briefly reviewed.

Most multi-objective evolutionary algorithms are generation based (in the area of hydrological modelling see, e.g., (Seibert, 2000) and (Reed et al., 2003)), i.e. all individuals are replaced at the same time. QMOO on the other hand is steady-state – creation and removal of an individual are completely separate processes. The current population always contains the – in a Pareto sense - best individuals found so far – or at least as many of them as is practical to store. The algorithm is therefore extremely elitist. The diversity is preserved by dividing the individuals into groups using clustering methods from statistical analysis. The careful choice of the individuals to be removed ensures that convergence continues throughout the optimisation. According to Leyland (2002), another unique property of QMOO is its approach to choosing the combination and mutation operators that are used to assign parameter values to an individual. These operators are chosen according to an

evolutionary process including stochastic operator choice. The user of the algorithm therefore does not have to choose the appropriate operators for a given problem.

When applying QMOO to an optimisation problem the user must define a priori the number of clusters that are expected to be found. Even if certain clustering techniques can theoretically find the correct number of clusters contained in a data set, none of the techniques tested by Leyland (2002) could find the number of clusters in practice. However, this maximum cluster number should not be considered as a tuning parameter of the algorithm: It does not influence the quality of the global optimal solution found by the algorithm but the quantity of additional information provided by a single optimisation run. The number of clusters therefore reflects the diversity of solutions the modeller would like to obtain. In the present optimisation problem, the set-up of the maximum cluster number is straightforward: We would like to optimise all model structures simultaneously and we therefore set the cluster number equal to the number of different model structures. This maximum cluster number is not necessarily achieved as the optimisation algorithm sometimes finds fewer clusters than asked by the modeller.

7.4 Optimisation procedure

7.4.1 Decision variables

The hydrological model to optimise has up to 14 parameters or decision variables to calibrate (the exact number is depending on the model structure). Additionally, we integrate in the optimisation procedure 3 decision variables that refer to the model structure and that are of integer type. Each of the values that can be assigned to them corresponds to a specific submodel set-up. Table 1 presents all the decision variables, their lower and upper boundaries and their meaning. The possible value ranges retained for the model parameters are considerably enlarged compared to values that can be found in literature.

7.4.2 Optimisation objectives

The presented hydrological model has two different outputs that can be used for model calibration: i) the daily discharge at the outlet of the catchment and ii) the variation in space and time of the snow and ice pack for each elevation band. This last output enables the model to simulate the mass balance of the ice-covered units as the difference of incoming snowfall and outgoing melt water over a given period. The overall mass balance of the ice-covered part of the catchment can therefore be estimated for each year according to the method presented by Aellen and Funk (1990). The resulting series of simulated annual mass balances can then be compared to observed values obtained by direct glaciological measurement methods. In

high mountainous catchments, the glaciers represent the most important water storage reservoir. The glacier mass balance estimated over long time periods is thus a good integrator of the overall water balance of the catchment.

For the present case study we use only two different objectives – this facilitates the interpretation of the results - even if at LENI QMOO has been tested successfully with more objectives. The first objective is based on the classical Nash criterion (Nash and Sutcliffe, 1970) calculated on the observed and simulated river discharge series. In order to minimise the objective function, we use the Nash criterion complement to 1. The second objective is the absolute bias between the observed and simulated annual glacier mass balance. In the present context, the bias - even though it is known not to be very discriminative - is a necessary condition for judging the quality of a simulation. The exclusive use of objective functions based on quadratic error could lead to a biased discharge and mass balance estimation.

Table 1: Possible value ranges for the decision variables and the corresponding submodels (for abbreviations see Figure 1)

Variables	Min	Max.	Type	Submodel	Meaning
V_{Ice}	2	3	Integer	SnowIce	Number of snow / ice types
V_{Melt}	0	1	Integer	SnowIce, SnowNotIce	0: Basic model, 1: With retention capacity
V_{Runoff}	0	1	Integer	TransNotIce	0: Basic model, 1: Equivalent rainfall in SOCONT
c_{precip}	-25	25	Real	SpatInt	Precipitation increase factor
T_{50}	-10	10	Real	AggregState	Central value of interval
T_{Trans}	0	10	Real	AggregState	Temperature Interval width
$a_{i,\ i = \{ice,\ snow,\ firn\}}$	0.1	25	Real	SnowIce, SnowNotice	Degree-day factors for ice, snow, firn
$\theta_{i,\ i = \{snow,\ firn\}}$	0	1	Real	TransIce, TransNotIce	Retention capacities for firn, snow
$k_{i,\ i = \{ice,\ snow,\ firn\}}$	0.01	90	Real	TransIce, TransNotIce	Storage coefficients for ice, snow, firn
$log(k)$	-16	-0.1	Real	TransNotIce	Slow reservoir coefficient
A	1	10000	Real	TransNotIce	Max. storage of slow reservoir
β	1	60000	Real	TransNotIce	Quick reservoir coefficient

7.5 Case study

In the present study, the hydrological model has been applied to a catchment situated in the Southern Swiss Alps, the catchment of the Rhone river measured at Gletsch (see Figure 3a).

Table 2 gives some important physiographic characteristics of the catchment. The estimated mean annual precipitation at the mean altitude of the catchment is about 2550 mm and the mean daily temperature -5.0°C (reference period 1981-1999).

Table 2: Main physiographic characteristics of the case study catchment

Characteristic	Value
Area (km^2)	38.9
Glaciation (%)	52.2
Mean slope (°)	22.9
Min. altitude (m a.s.l.)	1755
Mean altitude (m a.s.l.)	2713
Max. altitude (m a.s.l.)	3612

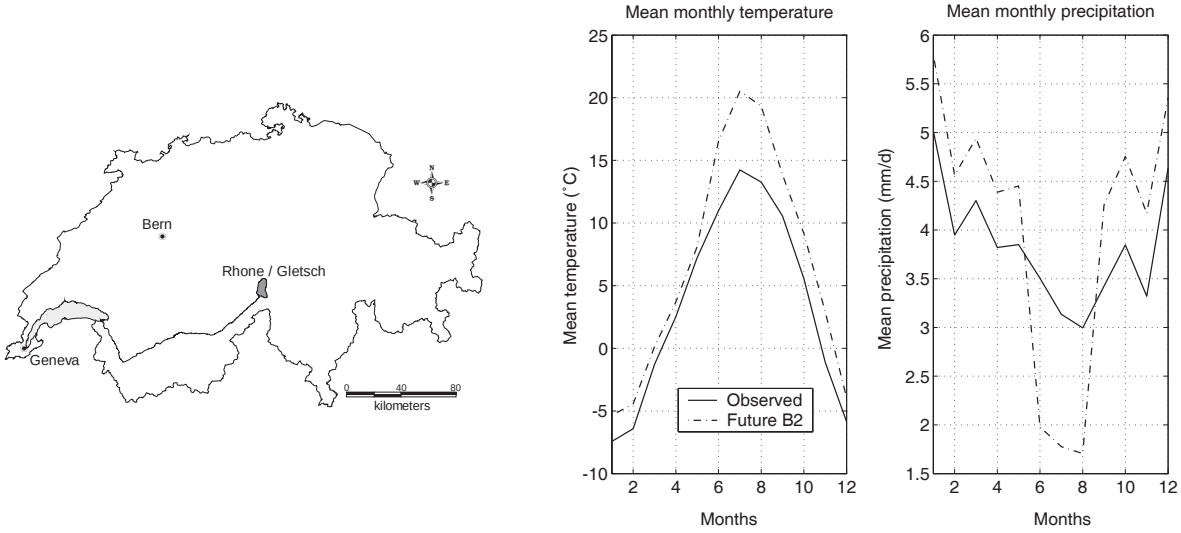

Figure 3: a) Location of the case study catchment in the Swiss Alps © Swiss Federal Office of Topography, b) interannual mean monthly precipitation and temperature for observed period (1983– 1987) and future climate scenario B2 (2093 – 2097)

7.5.1 Data collection

The model needs three input time series, namely daily mean values of temperature, precipitation and potential evapotranspiration. We use precipitation and temperature time series from a meteorological station located within a few kilometres distance of the catchment. The potential evapotranspiration (PET) time series is calculated based on the Penman-Monteith version given by (Burman and Pochop, 1994). The daily mean discharge is measured at the outlet of the catchment. We used the period 1978 to 1982 for calibration and

1983-1987 for validation. For bi-objective optimisation, we used the observed annual mass balance of the Rhone glacier given for the hydrological years 1979/80 to 1981/82 by (Funk, 1985). As an illustration for future climate conditions, we used the method developed by Shabalova et al. (2003) to perturb the observed temperature and precipitation series based on a regional climate model output provided by the Hadley Centre for Climate Prediction and Research. The regional model is the HadRM3H model and the perturbation of observed time series is carried out according to the difference between the control run for the period 1961 – 1990 and the future scenario run for 2070 – 2099 that is based on the IPCC scenario B2 (Houghton, 2001). Figure 3b illustrates the observed time series and the corresponding climate change scenario. The scenario PET is interpolated as a function of the scenario temperature.

7.6 Results

7.6.1 Model optimisation for present climate

The algorithm is applied using an initial population of 500 individuals and setting the number of clusters to 8 that corresponds to the number of possible model set-ups. QMOO identifies only 4 clusters for the given objectives, each of the clusters corresponding to a different model set-up. The algorithm converges quickly, after 9000 model evaluations the local Pareto-optimal frontiers are identified. They are shown in Figure 4a. The algorithm is specially designed to preserve the tail ends of the Pareto-frontiers. This feature explains the "outliers" of cluster 3 and 4 (see Figure 4a). Note that the point density of these frontiers depends on the ability of the algorithm to handle large populations that is essentially limited by computational resources. In the present application, a Matlab® version of QMOO is used on a personal computer, which limits the handled population size to around 80 individuals, about half of them being locally non-dominated when the algorithm stops after a fixed number of objective evaluations.

The found solutions have Nash-values between 0.90 and 0.94 and a bias between 0 and 0.26. This apparently little trade-off has to be interpreted in the presented simulation context. For highly glacierized catchments, high Nash-values are easy to achieve as long as the model reproduces the strong seasonality of the discharge. If we use a very simple model corresponding just to the mean observed discharge for each calendar day, we obtain for the Rhone catchment a Nash value of 0.85 and a bias of 0.02. Consequently there is an important trade-off between solutions having a low bias but Nash-values of 0.9 and solutions having a Nash-value around 0.94 but a bias of 0.26. Table 3 summarises the mean optimal values of the decision variables for each solution cluster.

Table 3: Mean values of the decision variables for each solution cluster

Decision variable	Cluster 1	Cluster 2	Cluster 3	Cluster 4
V_{Ice}	2	3	3	2
V_{Melt}	0	0	1	1
V_{Runoff}	0	1	1	0
c_{precip}	3.1	18.6	7.8	3.4
T_{50}	3.2	3.4	-3.2	1.9
T_{Trans}	2.5	5.5	4.8	2.7
a_{ice}	10.8	16.8	9.7	10.4
a_{firn}	-	12.9	14.6	-
a_{snow}	10.1	3.9	8.7	9.9
θ_{firn}	-	-	0.34	-
θ_{snow}	-	-	0.23	0.55
k_{ice}	2.7	42.9	2.8	3.3
k_{firn}	-	16.3	23.3	-
k_{snow}	28.5	8.3	21.5	27.2
$log(k)$	-8.8	-7.4	-10.1	-9.9
A	1091	7447	7413	2507
β	38178	34717	28777	37589

The 4 retained clusters correspond to the only solution clusters that are able to survive in the overall population. Other clusters – identified by frequent reclustering – do not survive because the individuals composing them are considered having too poor objective values. QMOO fixes this removal criterion as follows: An individual is considered being "too poor" if all its objective function values are worse than the corresponding limit value lim_i defined in Equation 4:

$$lim_i = \max(obj_i) \; + \; 0.5 \; * \; (\max(obj_i) - \min(obj_i)), \quad i = 1, 2, ..., n \tag{4}$$

where obj_i is a vector containing all objective values of the living population for the objective function i and n the total number of objective functions.

Figure 4a suggests that some of the identified locally Pareto-optimal solutions are strictly better than others. It should however be kept in mind that the sub-optimal solution clusters contain nevertheless good solutions and that their sub-optimality for the arbitrarily chosen 5-year calibration period is not necessarily confirmed for another time period. This assumption

is sustained by the simulation results for the validation period. Figure 4b shows a plot of the Nash values for all retained sets of decision variables for the calibration and the validation period. None of the solution clusters has strictly better Nash-values for both time periods.

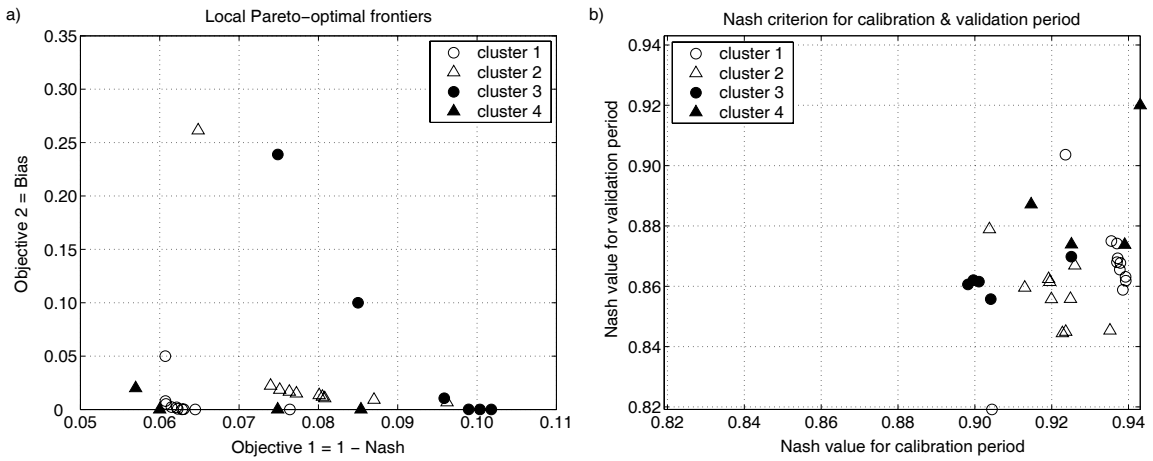

Figure 4:a) Local Pareto-optimal frontiers b) plot of the Nash criterion values for the locally Pareto-optimal sets of decision variables, for calibration and validation period

Figure 4b shows that there is a much wider spread of simulation results for the validation period than for the calibration period. This overall spread is induced by the joint action of all clusters. In a global optimisation approach identifying the global Pareto-optimal frontier, part of the solutions contributing to the spread would not have been retained, as the corresponding individuals would have had to compete with the globally best solutions for the two given objectives.

7.6.2 Model application to future climate scenario

The difference in model performance for distinct time periods is essentially due to the different climatic conditions prevailing during these periods. In the context of the present study, we are particularly interested in the model behaviour under future climate scenarios. We have simulated the future scenario discharge for all retained sets of decision variables and averaged the corresponding simulation results for each cluster. Figure 5 shows the mean monthly results for the discharge, spatially averaged precipitation, liquid precipitation and snowmelt. There is an important difference, not only in the total annual discharge volume but also in the distribution over the year. The differences in the distribution are due to the model structures and the corresponding model parameters, whereas the differences in the discharge volume are due to the altitudinal interpolation of precipitation. For the current situation, this interpolation is balanced by ice melt. For the future scenario, the glacier surface area has drastically reduced. The total runoff volume and the distribution between the different types

of runoff contributions are therefore modified. Consequently, the different model structures lead to quite distinct discharge distributions throughout the year.

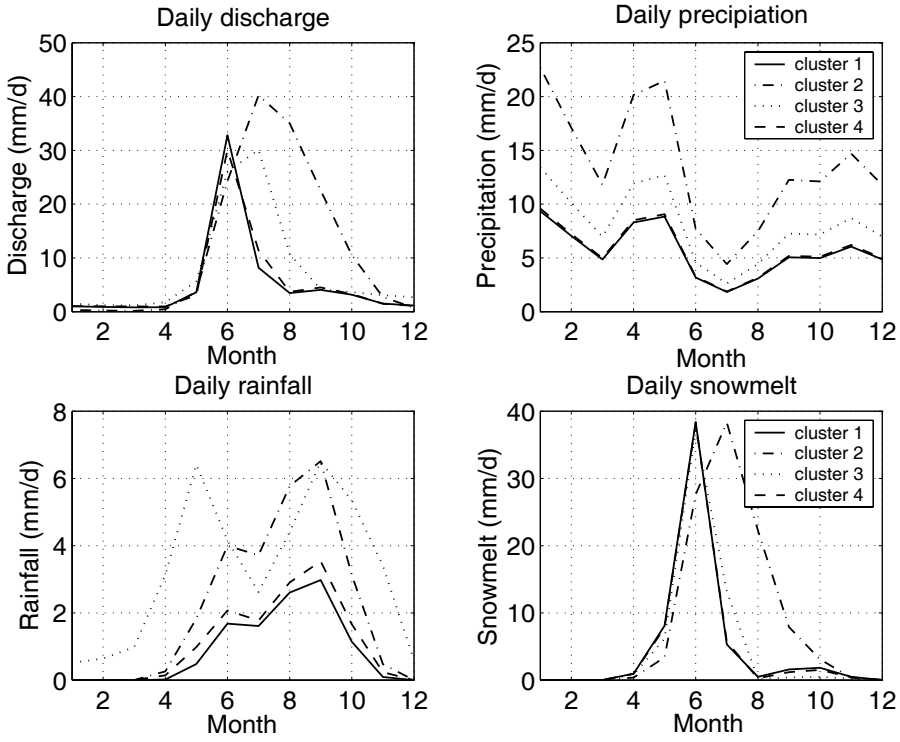

Figure 5: Interannual monthly mean discharge, precipitation, rainfall and snowmelt simulated for the future scenario, average values of the decision variables of each cluster

7.7 Discussion

The application of QMOO to the presented hydrological model led to the identification of 4 different model structures with equivalent results for the given objective functions and over the given calibration and validation time period. For the future time period however, the retained locally Pareto-optimal solutions sets give considerably different discharge simulations. In a classical hydrological modelling approach, the calibration period should be chosen carefully in order to be representative of the current climate and the robustness of the optimisation results in regard to the time period should be assessed. In the context of climate change impact studies, we are inevitably confronted with the extrapolation of modelling results beyond the domain of validity of the model development and we are thus not able to choose a calibration period representative for the future unknown climate and hydrological conditions. The present study showed that the uncertainty due to the model structure could contribute substantially to the overall modelling uncertainty. Even if its relative importance

compared to the parameter estimation uncertainty for a given model set-up cannot be judged here, the uncertainty inherent to the model structure should not be omitted in studies dealing with quantification of modelling uncertainty and climate change impact. Introducing more objective functions could potentially reduce the overall modelling uncertainty. One could especially think of using observed values for some internal model processes to constrain the optimisation solutions. In the context of conceptual modelling, most of the internal variables have however no physical meaning.

We could have chosen to include many other model design options into the optimisation procedure. The presented options correspond to the basic features that could easily be implemented under the given modelling constraints and considering the data availability for future climate scenarios. We therefore do not pretend to cover the whole possible range of model structure uncertainty. The presented case study should rather be considered as an illustration of how to include the model structure efficiently in a model optimisation procedure. For the presented 8 different model set-ups, the joint optimisation of model parameters and structure is around 6 times faster than separate optimisation of each of the model structures (for each model structure, convergence is reached after 6000 to 8000 model evaluations). This computational gain can become quite important if the number of design decision variables and the corresponding possible values increases. Especially if the total number of possible model structures only includes a few competitive structures, a classic approach optimising each model structure represents an important waste of computational resources. Furthermore the QMOO algorithm yields ready-to-use solutions and there is no need for the user to proceed to additional analyses of the solutions.

7.8 Conclusions

The present paper illustrates two important aspects for future hydrological research. First, it shows the benefits that hydrological modelling can experience from collaboration with other disciplines dealing with modelling problems such as - for the present study - industrial energy system design. The presented new generation evolutionary algorithm includes some features that are new in the context of hydrological modelling and that are particularly interesting for the presented problem of model design optimisation. Second, the presented application points out that further research into model structure uncertainty estimation is essential for climate change impact studies. Scientists just started addressing the challenge of estimating the overall modelling uncertainty in the modelling chain beginning with global emission scenarios, global and regional climate models and ending in local or regional hydrological models and corresponding impact models. The presented case study in the Swiss Alps shows that for such long-term projections (typically between 50 and 100 years) in non-stationary conditions, the model structure induces uncertainties that are potentially higher than the uncertainty due to the parameter estimation for a given model structure. The combination of

our current results with an appropriate methodology for quantitative parameter uncertainty estimation – such as the one applied by Kuczera and Parent (1998) - could lead to a good estimate of the overall hydrological modelling uncertainty.

Acknowledgements

We wish to thank Dr. François Maréchal from LENI for having made available the source code of the algorithm QMOO and Dr. Geoff Leyland for its help on the algorithm application and on some theoretical optimisation aspects. The hydrological model has been developed in the context of the European research project SWURVE (Sustainable Water: Uncertainty, Risk and Vulnerability in Europe) that provided the climate change scenario for our case study. The discharge data was provided by the Swiss Federal Office of Hydrology and Geology and the meteorological time series were made available by the national weather service MeteoSwiss. We also wish to thank the anonymous reviewers for their helpful comments.

References

Aellen, M. and Funk, M., 1990. Bilan hydrologique du bassin versant de la Massa et bilan de masse des glaciers d'Aletsch (Alpes Bernoises, Suisse). In: Musy A. (Editor), Hydrology in Mountainous Regions I: Hydrological Measurements; the Water Cycle,. IAHS Publ. No. 193, Wallingford, Oxfordshire UK, pp. 89-98.

Anonymous, 1969. Mass-balance terms. Journal of Glaciology, 8(52): 3-7.

Baker, D., Escher-Vetter, H., Moser, H., Oerter, H. and Reinwarth, O., 1982. A glacier discharge model based on results from field studies of energy balance, water storage and flow. In: J.W. Glen (Editor), Hydrological Aspects of Alpine and High-Mountain Areas. IAHS Publ. no. 138, Wallingford, Oxfordshire UK, pp. 103-112.

Burer, M., Tanaka, K., Favrat, D. and Yamady, K., 2003. Multi-criteria optimization of a district cogeneration plant integrating a solid oxide fuel cell-gas turbine combined cycle, heat pumps and chillers. Energy, 28: 497-518.

Burman, R. and Pochop, L.O., 1994. Evaporation, evapotranspiration and climatic data. Elsevier, Amsterdam, 278 pp.

Edijatno and Michel, C., 1989. Un modèle pluie-débit journalier à trois paramètres. La Houille Blanche, 2: 113-121.

Funk, M., 1985. Räumliche Verteilung der Massenbilanz auf dem Rhonegletscher und ihre Beziehung zu Klimaelementen. Doctoral Thesis, Eidgenössische Technische Hochschule Zürich, Zürich, 183 pp.

Houghton, J.T. (Editor), 2001. Climate change 2001: the scientific basis. Contribution of Working Group I to the Third Assessment Report of the Intergovernmental Panel on Climate Change. Cambrige University Presse, Cambrige, 881 pp.

Kuchment, L.S. and Gelfan, A.N., 1996. The determination of the snowmelt rate and the meltwater outflow from a snowpack for modelling river runoff generation. Journal of Hydrology, 179(1-4): 23-36.

Kuczera, G. and Parent, E., 1998. Monte Carlo assessment of parameter uncertainty in conceptual catchment models: the Metropolis algorithm. Journal of Hydrology, 211(1-4): 69-85.

Leyland, G.B., 2002. Multi-Objective Optimisation Applied to Industrial Energy Problems. Doctoral Thesis, Swiss Institute of Technology, Lausanne, Lausanne, 188 pp.

Nash, J.E. and Sutcliffe, J.V., 1970. River flow forecasting through conceptual models. Part I, a discussion of principles. Journal of Hydrology, 10(3): 282-290.

Pareto, V., 1896. Cours d'économie politique. F. Rouge, Lausanne.

Reed, P., Minsker, B.S. and Goldberg, D.E., 2003. Simplifying multiobjective optimization: An automated desing methodology for the nondominated sorted genetic algorithm-II. Water Resources Research, 39(7): in Press.

Schaefli, B., Hingray, B., Niggli, M. and Musy, A., 2005. A conceptual glacio-hydrological model for high mountainous catchments. Hydrology and Earth System Sciences Discussions, 2, 73-117.

Seibert, J., 2000. Multi-criteria calibration of a conceptual runoff model using a genetic algorithm. Hydrology and Earth System Sciences, 4(2): 215-224.

Shabalova, M.V., Van Deursen, W.P.A. and Buishand, T.A., 2003. Assessing future discharge of the river Rhine using regional climate model integrations and a hydrological model. Climate Research, 23: 223-246.

Vrugt, J.A., Gupta, H.V., Bastidas, L.A., Bouten, W. and Sorooshian, S., 2003. Effective and efficient algorithm for multiobjective optimization of hydrological models. Water Resources Research, 39(8).

Chapter 8

Hydrological modelling uncertainties in a multi-model framework: Multi-objective versus statistical uncertainty[1]

Abstract

Two different concepts of modelling uncertainty coexist in hydrological modelling, the so-called multi-objective and the statistical concept. This paper presents a methodology to quantify the uncertainty induced by the multi-objective equivalence of different models and compares the resulting modelling uncertainty to the one induced by the statistical concept. The multi-objective equivalent models are identified through a clustering evolutionary algorithm that optimises decision variables referring to the model design in parallel with the model parameters. This evolutionary algorithm finds multiple local Pareto-optimal frontiers, which enables the joint calibration of different model structures. A method is presented to assign probabilities to all identified solutions. The resulting modelling uncertainty is compared to the one induced by the statistical concept of posterior model output distribution quantified by a Markov Chain Monte Carlo method (the Metropolis-Hastings algorithm). The relative importance of each of the two sources of prediction uncertainty is assessed for

[1] This chapter has to be submitted: Schaefli, B. and Musy, A.: Hydrological modelling uncertainties in a multi-model framework: Multi-objective versus statistical uncertainty

different time periods for a highly glacierized catchment in the Swiss Alps, the discharge of which is simulated through a conceptual reservoir-based model. The multi-objective uncertainty concept enables a consistent estimate of the output distribution for different time periods whereas the statistical uncertainty suffers from a lack of temporal transferability.

8.1 Introduction

The quantification of modelling uncertainties is currently one of the key issues in hydrological research (see, e.g., Kuczera and Parent, 1998; Beven and Freer, 2001; Vrugt et al., 2005)). This interest is motivated by different practical and scientific considerations: If hydrological simulations are used in management or planning decisions, the estimation of the precision and the exactitude of the obtained results is fundamental to judge the confidence in the results. From a model development point of view, the estimation of modelling uncertainties gives further insights into the behaviour of the used models and contributes to improve them. The present study has been undertaken to quantify the uncertainty associated with hydrological modelling in the context of climate change impact studies. In this context, the quantification of the modelling uncertainties is essential to assess whether a predicted system modification is statistically significant.

Hydrological modelling uncertainties are caused by four different sources (Refsgaard and Storm, 1996): i) errors in the input data, especially in the meteorological data, ii) errors in the recorded observations of the phenomenon to be modelled, iii) uncertainty due to the values of the model parameters and iv) errors and simplifications inherent in the model structure. The parameter estimation uncertainty is probably the most extensively studied in recent hydrological literature. In the past, the determination of the best or the most probable parameter set has been subject to intense research (see, e. g., Wang, 1991; Duan et al., 1992). Current research concentrates on the estimation of the posterior distribution of the parameters (see, e. g., Beven and Binley, 1992; Kuczera and Parent, 1998; Bates and Campbell, 2001) and on multi-objective model optimisation (see e.g., Gupta et al., 1998; Yapo et al., 1998; Vrugt et al., 2003a; Khu and Madsen, 2005). The two corresponding concepts of modelling uncertainty, i.e. the statistical uncertainty and the uncertainty induced by the multi-objective equivalence of different models coexist in hydrological modelling and according to Gupta et al. (1998), a new model calibration paradigm should emerge that incorporates the treatment of both sources of uncertainty.

The statistical uncertainty concept is based on the assumption that for a given data set there is a most probable parameter set and an associated parameter probability distribution. In hydrological modelling, Bayesian inference methods have become classically used to determine such distributions (see, e.g., Beven and Binley, 1992; Kuczera and Parent, 1998). This concept suffers from certain drawbacks: There may not exist an objectively correct choice for the objective function (see, e.g., Gupta et al., 1998; Beven and Freer, 2001).

Several reasons can be invoked: Different model outputs or different aspects of a model output can be used for model calibration. In addition, the model errors do not necessarily have any intrinsic probabilistic properties that can be used to construct a statistical model and the corresponding objective function (e.g. Gupta et al., 1998) but different types of error models can be assumed (see, e.g., Thyer et al., 2002; Schaefli et al., 2005a, submitted manuscript[2]). This problem could be approached through the use of a generalised likelihood function possibly aggregating several objective functions (see Beven and Freer, 2001).

Hydrological model calibration is a profoundly multi-objective problem where the multi-objectivity can either be understood as multi-criteria (several aspects of one model output have to be calibrated) or multi-signal (several outputs have to be calibrated in parallel). An aggregated single objective function is often inadequate to measure whether a simulation reproduces the relevant characteristics of the observed data; especially if several antagonist aspects have to be reproduced, the explicit optimisation of several objective functions may be required.

From this multi-objective point of view, there exists no "correct" optimal model because different objective functions have different optimal solutions. The models are equivalent because in the given objective function space it is not possible to judge the quality of one with respect to the others: They are incomparable. We refer to the so-called Pareto-optimality (Pareto, 1896) that can be interpreted as follows: A point of the objective function space is Pareto-optimal if no other point is better in all objectives. The set of all Pareto-optimal points is called Pareto-optimal frontier (POF).

Gupta et al. (1998) point out that it is important to note that this multi-objective equivalence differs from the equifinality concept introduced by Beven and Binley (1992). Equifinality is defined based on a probabilistic view of the parameter uncertainty. Several models are equifinal because they lead to the same result, to an equally good calibration. From a multi-objective point of view, the equivalence is due to the fact that none of the objective functions is considered having a better ability to judge the quality of the model.

Neither the multi-objective nor the statistical concept can be deemed to better capture the uncertainty induced by the hydrological model on the simulation results. Even though they have been recognised as being complementary (see. e.g., Gupta et al., 1998; Madsen, 2000) we have not found any study assessing them in parallel for a given modelling context.

In the present study we quantify the modelling uncertainty associated with both concepts for a conceptual precipitation – runoff transformation model. While the assessment of the

[2] Schaefli, B., Balin Talamba, D. and Musy, A., 2004. Quantifying hydrological modeling errors through finite mixture distributions. Submitted to Journal of Hydrology; hereinafter referred to as Schaefli et al, 2005a, submitted manuscript.

modelling uncertainty induced by the statistical parameter distribution has become a common task, the question how to determine the output distribution corresponding to the multi-objective equivalent models still remains essentially unanswered. We will discuss why a uniform probability assignment to all identified solutions can be misleading and present a methodology to estimate a probability-weighted multi-equivalent output distribution (see Section 3) based on a probability assignment to each identified point of a POF. For the calibration period, these points are all equivalent and therefore equiprobable but we assume that their relative probability can be judged using additional information such as additional output data for a validation period.

The multi-objective model optimisation is completed through a clustering evolutionary algorithm that identifies not only the global optimum POF but retains also local POFs that correspond to different areas in the decision variable space. The used algorithm has the major advantage that it handles decision variables of integer type that enables the joint optimisation of decision variables referring to the model design and of the corresponding model parameters. Recent studies point out the need to include the model structural uncertainties in modelling uncertainty analysis (see, e.g., Beven and Freer, 2001; Butts et al., 2004) and their quantification is subject to intense research. The use of several different models – a so-called multi-model approach - has been recognised as being a potential solution but very few studies have completed a multi-model uncertainty analysis (e.g., Georgakakos et al., 2004; Butts et al., 2004).

The presented method for the estimation of a multi-objective and multi-model output distribution is illustrated for a highly glacierized catchment located in the Swiss Alps. In the following, we first present the conceptual hydrological model and the multi-objective algorithm for model optimisation before discussing the method developed to quantify the multi-objective modelling uncertainty (Section 3). Some details about the case study are given in Section 4. The obtained results are compared to the uncertainty induced by a statistical uncertainty concept (Section 5). This uncertainty has been estimated through a Markov Chain Monte Carlo method - the so-called Metropolis-Hastings algorithm. This method has become widely used in hydrological modelling (Kuczera and Parent, 1998; Bates and Campbell, 2001; Vrugt et al., 2003b; Marshall et al., 2004). It will therefore only be briefly discussed. The output prediction distributions induced by each of the two uncertainty concepts and the relevance of the two sources of uncertainty is assessed for different observed time periods and a future time period characterised by a climate change. This intercomparison gives valuable insights into the temporal transferability of the models and the uncertainty concepts. The paper is closed by the overall conclusions of this study.

8.2 Hydrological model: structure and optimisation

8.2.1 Model structure

The hydrological discharge simulation is carried out at a daily time step through a conceptual, semi-lumped model called GSM-SOCONT (Schaefli et al., 2005). The model has two levels of discretization referring respectively to the separation of the two main land covers (ice-covered and not ice-covered) and to an altitudinal discretization – each land cover type is divided into elevation bands. Each of the resulting spatial units is characterised by its surface and its hypsometric curve and is assumed to have a homogeneous hydrological behaviour. The discharge contributions of all units are summed to provide the total discharge at the outlet of the entire catchment. The model does not contain any routing routine as the studied catchment is relatively small and has rather steep slopes.

Figure 1 shows the hydrological model structure for a given spatial unit, the different submodels and their interconnections. The basic design of each submodel and the possible variants are presented hereafter. For a detailed description of the model refer to (Schaefli et al., 2005).

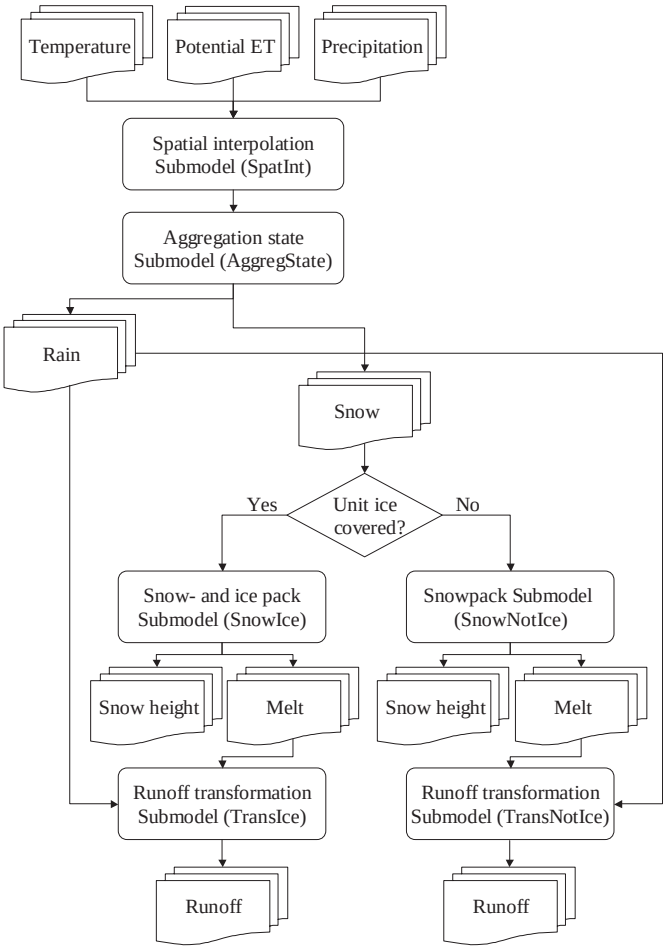

Figure 1: Basic hydrological model structure (for one spatial unit) showing the different submodels and the input and output time series; in brackets: the submodel short names; ET = evapotranspiration

Submodels

The temperature and precipitation time series observed at a reference meteorological station are linearly interpolated according to the mean elevation of the spatial unit (submodel SpatInt). The temperature decrease is fixed to 0.65 °C per 100 m of altitude change. The altitudinal precipitation increase is included as a parameter in the model optimisation process as little knowledge about the local altitudinal variation of the precipitation can be derived from the observed data. The precipitation increase factor c_{precip} fixes the increase in precipitation per 100 m of altitudinal difference between the reference altitude and a point of the catchment. The nature of precipitation (liquid or solid) is computed based on a fuzzy rule with two parameters (submodel AggregState): T_{50} the temperature that corresponds to 50 % of the precipitation falling as snow and T_{Trans} the length of the temperature interval over which snowfall and rainfall occur simultaneously.

The snowmelt on not ice-covered spatial units (submodel SnowNotIce) is computed according to a classical temperature-index approach (Rango and Martinec, 1995). This submodel has one parameter, the degree-day factor for snowmelt, a_{snow}. In the basic model configuration, the water flow from the snowpack corresponds to the computed snowmelt. We include a model variant assuming that the snowpack has a capacity of retention θ_{snow} and that water flow only occurs if this capacity is reached (see, e.g., Kuchment and Gelfan, 1996).

On the ice-covered spatial units (submodel SnowIce), the water is stored in three different forms, as snow, ice or firn, the last form being the transition state between snow and ice. This submodel has three parameters, the degree-day factors for snow, firn and ice (a_{snow}, a_{firn} and a_{ice}). At the end of each hydrological year (30 September), the snow that has fallen during the year but not melted is added to the firn pack. Firn melt only occurs if the snowpack has disappeared and ice melt if the snow and firn packs have disappeared. We also consider a model variant that uses only two solid forms of water, namely snow and ice. The transformation of melt water and rainfall into runoff (submodel TransIce) is completed through three parallel reservoirs, one each for snow, firn and ice. This submodel has the parameters k_j, $_{j = \{snow, firn, ice\}}$ that are the time constants.

For not ice-covered spatial units (submodel TransNotIce) the rainfall – runoff transformation is carried out through a conceptual submodel named SOCONT. It is composed of a linear reservoir for the slow contribution and a non-linear reservoir for direct or quick runoff. It has 3 parameters to calibrate: A the maximum storage of the linear reservoir, k the linear and β the non-linear reservoir coefficient. In the basic model form, the snowmelt – runoff transformation is simulated through a linear reservoir having the time constant k_{snow}. In a model variant, the rainfall and snowmelt are summed to an equivalent rainfall that is transformed into runoff through the model SOCONT.

8.2.2 Optimisation

Optimisation algorithm

The optimisation tool used in the present study is the so-called Queueing Multi-Objective Optimiser (QMOO) developed by Leyland (2002). Its application to hydrological model structure and parameter optimisation has been illustrated in (Schaefli et al., 2004). This algorithm has been developed in order to improve the optimisation performance on problems of energy system design but is applicable to a wide range of optimisation problems without specific algorithm tuning. It has been tested successfully on several theoretical test problems and has been proven to be robust and effective for the resolution of non-linear, non-continuous and mixed real – integer problems (Leyland, 2002; Burer et al., 2003). QMOO is a clustering evolutionary algorithm that handles integer problems, i.e. problems including decision variables of integer type. The algorithm is multi-objective, i.e. it identifies the Pareto-optimal solutions for multiple objective functions. Rather than just identifying the global POF, QMOO finds and retains many local POFs. This property is obtained through cluster analysis techniques that ensure local competition between sets of decision variables (so-called individuals) in the decision variable space and that allow the identification of separate local optima simultaneously (see an illustration in Figure 2). This property preserves diversity and helps the algorithm to converge to difficult-to-find optima. In the present application this feature is particularly interesting as it enables the algorithm to retain several equivalent model structures. For a review of how this property is obtained refer to (Leyland, 2002).

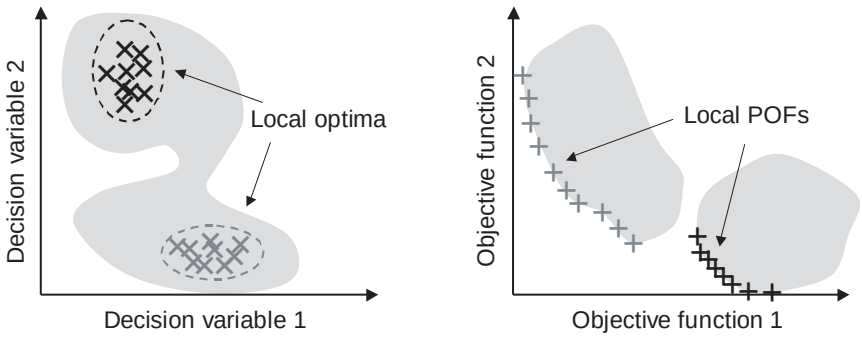

Figure 2: Illustration of the concept of local POFs in the decision variable space (left) and in the objective function space (right); the grey shaded area is the feasible space

Decision variables

The hydrological model has up to 14 parameters or decision variables to calibrate (the exact number depends on the model structure). Additionally, we integrate in the optimisation process 3 decision variables that refer to the model structure and that are of integer type. Each of the values that can be assigned to them corresponds to a specific submodel set-up. Table 1

presents all the decision variables, their lower and upper boundaries and their meaning. In order to avoid physically meaningless results, we imposed a constraint on the degree-factors, namely $a_{ice} > a_{firn} > a_{snow}$, and on the storage coefficients of the melt reservoirs, $k_{ice} < k_{snow}$ (see Schaefli et al., 2005).

Table 1: Possible value ranges of the decision variables, their type and meaning

Variable	Unit	Min	Max.	Type	Meaning
V_{Ice}	-	2	3	Integer	Snow/ ice types; 2: snow, ice; 3: snow, firn, ice
V_{Melt}	-	0	1	Integer	0: Basic model, 1: With retention capacity
V_{Runoff}	-	0	1	Integer	0: Basic model, 1: Equivalent rainfall
c_{precip}	$\%100^{-1}$ m^{-1}	0	10	Real	Precipitation increase factor
T_{50}	°C	-10	10	Real	Central value of interval
T_{Trans}	°C	0	10	Real	Temperature interval width
$a_{i,\ i = \{ice, snow, firn\}}$	$mm°C^{-1}d^{-1}$	0.1	20	Real	Degree-day factors for ice, snow, firn
$\theta_{i,\ i = \{snow, firn\}}$	-	0	1	Real	Retention capacities for snow, firn
$k_{i,\ i = \{ice, snow, firn\}}$	d	0.01	60	Real	Storage coefficients for ice, snow, firn
$log(k)$	$log(h^{-1})$	-16	-0.1	Real	Slow reservoir coefficient
A	mm	1	10000	Real	Max. storage of slow reservoir
β	$m^{4/3}s^{-1}$	1	60000	Real	Quick reservoir coefficient

Objective functions

The objective functions should measure different aspects of the simulated model outputs and be relatively unrelated (see, e.g., Gupta et al., 1998). If the objective functions are strongly correlated, the multi-objective approach does not provide any additional information compared to a single-objective approach.

The hydrological model is calibrated on the observed discharge. For the presented modelling context – climate change impact analysis – the model has to reproduce two main characteristics: the hydrological regime (i.e. the distribution of the daily discharges) and the overall water balance. We therefore use two different objective functions. The one referring to the water balance is the relative bias between the mean observed and simulated discharge (Equation 1). We use the absolute value of the bias to minimise the objective function.

$$Bias = \sum_{t=1}^{n} (q_{obs,t} - q_{sim,t}) \cdot (\sum_{t=1}^{n} q_{obs,t})^{-1} \quad (1)$$

where $q_{obs,t}$ is the observed discharge and $q_{sim,t}$ the simulated discharge on day t.

The bias is known not to be a very discriminative objective function but in the present context it is a necessary condition for judging the quality of a simulation. For the objective function referring to the daily discharge we define a statistical error model. We assume two different error distributions, one for low flow and one for high flow. The resulting error model is a mixture of two normal components (Schaefli et al., 2005a, submitted manuscript) and is written as (Equation 2):

$$\begin{aligned} & q_{obs,t} = h(\mathbf{x}_t, \boldsymbol{\beta}) + I(q_{obs,t} \in \mathbf{Q}_H)(\rho_H \delta_{t-1} + \varepsilon_{H,t}) + I(q_{obs,t} \in \mathbf{Q}_L)(\rho_L \delta_{t-1} + \varepsilon_{L,t}) \\ & \rightarrow \varepsilon_{i,t} \sim N(0, \sigma_i^2) \qquad i \in \{H, L\} \end{aligned} \tag{2}$$

where $h(\mathbf{x}_t, \boldsymbol{\beta})$ is the hydrological transfer function mapping the inputs $\mathbf{x}_t$ (containing input variables such as precipitation, temperature and potential evapotranspiration) into the discharge given the model parameter vector $\boldsymbol{\beta}$. $I(.)$ is an indicator function taking the value 1 if its argument is true, and 0 otherwise. $\mathbf{Q}_H$ is the set of observed high flow discharges and $\mathbf{Q}_L$ the set of low flow discharges. ρ_i is the lag-one autoregressive parameter for the flow regime i ($i \in \{H, L\}$). $\delta_{t-1} = q_{t-1} - h(\mathbf{x}_{t-1}, \boldsymbol{\beta})$ is the residual of the time step *t-1* and $\varepsilon_{i,t}$ is the residual of time step t having zero mean and variance σ_i. For this error model the likelihood function $p(\mathbf{D}|\boldsymbol{\theta})$ can be written as (Schaefli et al., 2005a, submitted manuscript):

$$\begin{aligned} p(\mathbf{D}|\boldsymbol{\theta}) = & \left[\frac{1}{(\sigma_H\sqrt{2\pi})^{n_H}} \cdot \frac{1}{(\sigma_L\sqrt{2\pi})^{n_L}}\right] \\ & \cdot \exp\left[-\frac{1}{2\sigma_1^2}\sum_{t=1}^{n_H} \varepsilon_{H,t}^2(\boldsymbol{\theta}_H) - \frac{1}{2\sigma_L^2}\sum_{t=m}^{n_L} \varepsilon_{L,t}^2(\boldsymbol{\theta}_L)\right] \end{aligned} \tag{3}$$

where $\boldsymbol{\theta} = [\boldsymbol{\beta}, \rho_H, \rho_L, \sigma_L, \sigma_H]$ is the vector containing all model parameters and $\mathbf{D}$ the matrix containing all used input and output data. n_i is the number of values $\varepsilon_{i,t}$ observed during flow regime i. For further details and namely a discussion of the flow regime separation refer to (Schaefli et al., 2005a, submitted manuscript).

The second objective function to minimise is defined as $-\log(p(\mathbf{D}|\boldsymbol{\theta}))$. The use of only two different objective functions facilitates the interpretation of the results. The optimisation algorithm could however handle more objectives (Leyland, 2002).

8.3 Estimation of multi-objective output distributions

Each of the identified points of a POF corresponds to a set of decision variables (referring to the model structure and parameters) and to a related output simulation. The estimation of the associated output distribution implies assigning a probability to each of these points. This

probability is based on a subjective probability concept: The probability assigned to a set of decision variables expresses the degree of belief. In that sense, we adopt a Bayesian point of view.

A Pareto-optimal solution cannot be distinguished as being objectively better than any other solution of the POF. In the absence of any additional information, the same probability has to be assigned to all solutions. This approach raises a main problem: The found Pareto-optimal solutions constitute an approximation of the true POF. If the optimisation problem has decision variables of real type, the POF probably has an infinite number of members. And the POF is not necessarily continuous and can be disjoint (for example if the possible decision variable space is disjoint). This means that whatever the quality of the used algorithm for the POF identification is, the modeller never knows how good the found solutions cover the real POFs. Indicators for the assessment of the algorithm convergence to the true POF and of its coverage exist (for a review see Zitzler et al., 2003). Such indicators are useful to follow the rate of convergence and POF coverage throughout an optimisation run and to assess the optimisation performance for different problems. As the true POF is generally unknown (except for test problems), an absolute quality judgement of the identified POF is however difficult.

A uniform probability assignment to the found solutions bears the risk of overweighing some solutions. This can be illustrated with a simple example: If the algorithm finds a lot of solutions in a certain area of the POF but only a few in an other, the easy to find solutions are overweighed. It is important to point out that the density of the found solutions in a certain area of the POF is not a good indicator of how probable these solutions are but of how the optimisation algorithm has been designed. The QMOO algorithm has been designed to preserve a maximum of diversity while searching for approximations of the POFs. The mentioned clustering technique contributes to this diversity preservation. For computational reasons, a search algorithm cannot handle a too important number of individuals (decision variable sets) while searching for new better approximations. In order to control the size of the handled population (set of retained individuals at a certain stage of search progress), some individuals are sort out during the search for other better approximations of the POFs. For this thinning operation, the QMOO algorithm has been designed to sort out individuals in areas of high density (in the decision variable space). This characteristic helps the algorithm to find new approximations of the POFs in areas where good approximations are difficult to find. The thinning operations keep the population size under control and encourage a good coverage of the POFs.

In order to avoid a too optimistic estimation of the overall uncertainty induced by the multi-objective equivalence, the search algorithm should be designed to ensure a good coverage of the POFs and especially to explore their tail ends. Ideally, the identified POFs should include the single-objective solutions. In the used QMOO algorithm, a tail preservation feature is implemented.

Even though Pareto-optimal solutions are incomparable, one might intuitively expect that some of the Pareto-optimal solutions are better than others with respect to transferability in time (or space). In hydrological modelling, it is well known that the chosen portion of observational data influences the calibration results (see, e.g., Sorooshian et al., 1983; Yapo et al., 1996). The solutions of the POF are Pareto-optimal for the chosen data for calibration. Simulating the same solutions for another time period will not reproduce the POF except if the solutions are very robust to the chosen data, i.e. if the information content of the data used for calibration enables a robust estimate of the model structures or parameters. For most case studies, the Pareto-optimal solutions simulated for a different time period will lead to a cloud of points in the objective space showing a certain correlation.

Using additional data can help assigning probabilities to the Pareto-optimal solutions. The robust solutions and the ones with better objective function values for another period should receive a higher probability. The use of additional information for the quality judgement of the found approximations is not unfamiliar to multi-objective optimisation. The assessment of the (relative) quality of a POF approximation can for example make use of user (decision maker) preferences (e.g., Hansen and Jaszkiewicz, 1998).

We have chosen a two-step approach for probability assignment: We first assign a probability to a given point within an identified POF. Each POF then receives a certain probability with respect to the other POFs. Note that in the following, POF designates the approximation of a true POF identified through optimisation.

8.3.1 Probability assignment to a point of a POF

The basic idea is to use the simulation results for another time period (validation period) to judge the quality and hence the probability of the points of the approximated POFs. Accordingly, the probability of a point is calculated as a function of some quality criteria calculated over the validation period. These quality criteria are not necessarily the same as the objective functions used for the optimisation but should reflect the trade-off between them. A further discussion of the choice of the criteria is given hereafter and in the section presenting the results.

Considering only one criterion, a subjective probability can be assigned as follows: We assume that the simulated criterion values c_{i1} (i = 1, 2, .., n) correspond to a sample of the distribution of criterion C_1. The form and the mean of this distribution are assumed to be known: The mean equals the optimum criterion value c_{1opt} and the distribution is assumed to be normal. The value c_{1opt} is known a priori and corresponds to the - presumably utopian - best value that the criterion C_1 could take. The variance σ_1^2 is estimated through the standard deviation of the sample calculated according to Equation 4.

$$\hat{\sigma}_1^{\,2} = \frac{1}{n-1}\sum_{i=1}^{n}(c_{1opt} - c_{i1})^2 \tag{4}$$

where $\hat{\sigma}_1^{\,2}$ is the estimated variance and n the total number of points of the POF. Each point is then assigned a normalised weight $\overline{w}_{i1}$ that is interpreted as the subjective probability of this point. The weight $\overline{w}_{i1}$ is calculated as a function of the assumed normal density $f_{C_1}(c_{i1} \mid c_{opt1}, \hat{\sigma}_1^{\,2})$ of the point i divided by the sum of the densities of all points (Equation 5).

$$\overline{w}_{i1} = \frac{f_{C_1}\left(c_{i1} \mid c_{opt1}, \hat{\sigma}_1^{\,2}\right)}{\sum_{l=1}^{n} f_{C_1}\left(c_{l1} \mid c_{opt1}, \hat{\sigma}_1^{\,2}\right)} = \frac{\exp[-\frac{1}{2\sigma_1^{\,2}}(c_{opt1} - c_{i1})^2]}{\sum_{l=1}^{n}\exp[-\frac{1}{2\sigma_1^{\,2}}(c_{opt1} - c_{l1})^2]} \tag{5}$$

This approach can be extended to a multi-criteria framework. Lets define **C** as the matrix containing the sample values c_{ij} (i = 1, 2, .., n; j = 1, 2, .., m) where m is the number of objective functions and n the number of points. Lets call $\mathbf{c_i}^{\mathrm{T}}$ (i = 1, 2, .., n) the rows of **C**, i.e. $\mathbf{C} = [\mathbf{c_1}, \mathbf{c_2}, .., \mathbf{c_n}]^{\mathrm{T}}$ and $\mathbf{c_{opt}}^{\mathrm{T}}$ the optimum value vector containing the optimum values for each objective function. Lets further call **w** the vector containing the not normalised weights w_i (i = 1, 2, .., n) calculated considering all m objective functions. The weights w_i are calculated as the multi-normal density of the point i (Equation 6).

$$w_i = \mid 2\pi\hat{\mathbf{\Sigma}} \mid^{-1/2} \exp(-\frac{1}{2}[\mathbf{c_{opt}} - \mathbf{c}_i] \cdot \hat{\mathbf{\Sigma}}^{-1} \cdot [\mathbf{c_{opt}} - \mathbf{c}_i]^T) \tag{6}$$

where $\hat{\mathbf{\Sigma}}$ is the estimated covariance matrix, estimated based on the sample values c_{ij}.

The normalised weights $\overline{w}_i$ are calculated according to Equation 7.

$$\overline{w}_i = \frac{w_i}{\sum_{l=1}^{n} w_i} \tag{7}$$

The proposed weights for the multi-criteria approach have the main advantage that they include information concerning the correlation among the criteria. The properties of these weights shall be discussed for the case of two criteria. Lets consider the weights w_i as a function of z (Equation 8):

$$w_i \sim \exp(-z) = \exp(-\frac{1}{2}\boldsymbol{\varepsilon}_\mathbf{i}\hat{\mathbf{\Sigma}}^{-1}\boldsymbol{\varepsilon}_\mathbf{i}^{\,T}) \tag{8}$$

where $\boldsymbol{\varepsilon}_\mathbf{i} = [\mathbf{c}_\mathbf{opt} - \mathbf{c}_\mathbf{i}] = [\varepsilon_{i1}, \varepsilon_{i2}]$ is the error vector. The elements of the covariance matrix are written as $[\hat{\boldsymbol{\Sigma}}]_{ij} = \hat{\sigma}_i^2$ for $i = j$ and $[\hat{\boldsymbol{\Sigma}}]_{ij} = \hat{\rho}\hat{\sigma}_i\hat{\sigma}_j$ for $i \neq j$.

The values of w_i are high for negative z values and low for positive z values. Lets consider the analytic expression of z (Equation 9):

$$z = \frac{1}{\hat{\sigma}_1^2\hat{\sigma}_2^2(1-\hat{\rho})}(\varepsilon_{i1}^2\hat{\sigma}_2^2 + \varepsilon_{i2}^2\hat{\sigma}_1^2 - 2\hat{\rho}\varepsilon_{i1}\varepsilon_{i2}\hat{\sigma}_1\hat{\sigma}_2) \tag{9}$$

where $\hat{\rho}$ is the estimated linear correlation between the two criteria.

If there is a perfect positive correlation ($\hat{\rho} = 1$) of both criteria, no weights can be assigned; this property is essential as in such a situation the use of both criteria does not provide any additional information. The sign of z depends only on the second part of the right hand side of Equation 9. The following property can be deducted: For given variances and given errors of the same sign the weight is higher for high correlations and particularly low for negative correlations. If the criteria are contradictory but we have the same error sign the point is considered as being improbable. On the other hand, if the errors of a given point are of opposite sign the probability is smaller if the two criteria are positively correlated (they could be respected simultaneously) than if they are negatively correlated.

This output weighting can only be carried out if appropriate criteria can be defined for the weighting approach. They would ideally correspond to the objective functions used for optimisation. This is however not possible if the objective functions cannot be reasonably assumed to be normally distributed having the optimal value as mean value (the classical least-square error for example is not normally distributed around the optimal value 0).

It is noteworthy that the proposed weighting method overcomes a classical problem in the aggregation of the criteria values. The different criteria do not measure the same characteristic, their magnitude and their sensitivity is not the same and accordingly they cannot be simply aggregated into one measure. This problem has been discussed by several authors who used criteria weighting for the investigation of the POF in multi-objective optimisation (see, e.g., Madsen, 2003; van Griensven et al., 2002; Butts et al., 2004).

8.3.2 Probability assignment to a POF

The simplest approach would consist of assigning all local POFs the same probability. As they correspond to distinct areas of the decision variable space, such a uniform approach is justifiable. Some of the local POFs can however be strictly dominated by other POFs (i.e. all points of one POF are strictly better for all objectives than all points of another POF). In such a situation, we would intuitively prefer the dominating POFs rather than the dominated ones. The probability assignment can be based on performance indicators classically used in multi-

objective optimisation to judge different approximations to a POF. We use the concept of non-dominated volume introduced by Zitzler (1999). It measures the volume of the objective space that is not dominated by a point of the approximated POF (see Figure 3). The larger the dominated volume of a local POF is, the better solutions to the optimisation problem it contains and the higher probability it is given. For a bi-objective space, the calculation of the dominated volume of a given point of the objective space is trivial, for higher dimensions it is more difficult but still possible.

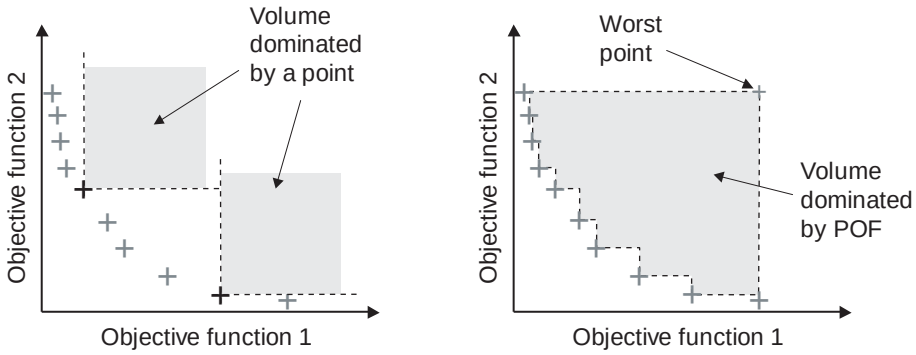

Figure 3: Dominated volume concept

The proposed probability assignment based on this concept measures how large the dominated volume between a POF and a reference point - the so-called worst point – is (Figure 3). We define this point as the point in the objective function space having as coordinates for each objective function the worst objective function value of all identified points of all POFs. The normalised probability of a given POF corresponds to its dominated volume divided by the sum of the dominated volumes of all POFs (Equation 10).

$$p(POF_k) = DV_k \cdot (\sum_{k=1}^{K} DV_k)^{-1} \tag{10}$$

where DV_k is the dominated volume between POF_k (k = 1, 2, .., K) and the worst point and K the total number of identified POFs.

The proposed probability assignment to the points within a POF is based on information provided by the validation period whereas the probability assignment to the POF takes into account the information from the calibration period. The sub-optimality of some local POFs is intimately related to the chosen calibration period and would presumably not be confirmed for another time period. The POF weighting can however not be carried out for a different time period: As mentioned before, the points of the POF would not map into another POF for a different time period and accordingly the concept of non-dominated volume loses its significance.

8.4 Case study

The case study is the catchment of Mauvoisin that is located in the southern Swiss Alps. The discharge from this catchment flows into an accumulation lake that is used for hydropower production. Table 2 gives the mean physiographic and meteorological characteristics of the catchment. The hydrological regime is strongly influenced by glacier and snowmelt. It is of the so-called a-glacier type (Spreafico et al., 1992): The maximum monthly discharge takes place in July and August and the minimum monthly discharge (around 100 times less!) in February and March.

The hydrological model needs three input time series, namely daily mean values of temperature, precipitation and potential evapotranspiration (PET). For the model calibration and validation we used precipitation and temperature time series from a meteorological station located downstream of the considered catchment. The PET time series is calculated based on the Penman-Monteith version given by (Burman and Pochop, 1994). Observed daily mean inflow into the accumulation lake has been obtained from the hydropower company. Based on this data the hydrological model has been calibrated for the years 1995 to 1999 and validated for the years 1989 to 1994.

The daily inflows are recalculated based on the observed accumulation lake level and the daily electricity production, from which the daily water flow through the turbines is estimated. The measurement uncertainty inherent in the lake level measurement corresponds to around 0.3 mm of the specific daily discharge. The uncertainty induced by the water flow through the turbines cannot be quantified as the conversion between produced electricity and discharge depends on the unknown operating point of the turbines. The observed series of daily lake inflow contains negative values during low flow periods. Assuming that these values constitute a sample of the measurement error having zero mean, the minimum daily measurement error has an estimated standard deviation of 0.53.

As an illustration for future climate conditions, we use the outputs of a regional climate model (RCM) run obtained from the Hadley Centre for Climate Prediction and Research in the context of the EU project SWURVE (Sustainable Water, Uncertainty, Risk and Vulnerability in Europe, see Ekström et al., submitted manuscript[3]). The regional model is the HadRM3H model driven by the general circulation model HadCM3 with the greenhouse gas emission scenario B2 as defined by the Intergovernmental Panel on Climate Change (Houghton, 2001). The local scale time series are generated through the methodology presented by Shabalova et al., (2003) that perturbs the observed temperature and precipitation series based on the

[3] Ekström, M., Hingray, B., Mezghani, A. and Jones, P.D.: Regional climate model data used within the SWURVE project. 2: Addressing uncertainty in regional climate model data for five European case study areas. Submitted to Hydrology and Earth System Sciences;

differences between the outputs of a RCM run for a control period (1961 – 1990) and a future period (2070 – 2099). The scenario PET is interpolated as a function of the scenario temperature assuming that the observed relationship for the control period remains the same in the future. The glacier surface is updated based on a conceptual glacier surface evolution model (Schaefli et al., 2005b, submitted manuscript)[4]. The input to this model is the mean area of snow accumulation as simulated by the hydrological model (see also Schaefli et al., 2005).

Table 2: Main physiographic characteristics of the case study catchment; (reference period 1987 - 1999)

Characteristic	Value	
Area (km^2)	169.3	
Glaciation (%)	41.4	for 1989
Mean slope (°)	26.7	
Min. altitude (m a.s.l.)	1961	
Mean altitude (m a.s.l.)	2940	
Max. altitude (m a.s.l.)	4305	
Mean annual precipitation (mm)	1212	at 1841 m a.s.l.
Mean daily temperature (°C)	3.7	at 1841 m a.s.l
Mean annual specific discharge (mm)	1500	

8.5 Results

8.5.1 Multi-objective output distribution

Model optimisation

The application of the QMOO algorithm requires setting up the initial population size and the number of clusters that are expected to be found. The number of clusters reflects the diversity of solutions the modeller would like to obtain in a single optimisation run and does not influence the quality of the global optimum solution. For a further discussion see (Schaefli et al., 2004) and (Leyland, 2002).

[4] Schaefli, B., Hingray, B. and Musy, A.: Uncertain glacier surface evolution under changing climate. Submitted to Journal of Geophysical Research – Atmospheres.

The initial population is set to 500 individuals and the number of clusters to 8 that corresponds to the number of possible model set-ups. The algorithm converges after around 14000 model evaluations to the local POFs. In the present application, a Matlab® version of QMOO is used on a personal computer and the handled population size is around 100 individuals throughout the optimisation.

Note that only four POFs are identified (Table 3 and Figure 4), among which figures the simplest model structure (POF4). Each of the identified POFs corresponds to a different model set-up (Table 3). Accordingly, the local POFs correspond to distinct solutions in the decision variable space and in particular to another area of the hydrological model parameter space (Table 3 and Figure 4). In particular, the meteorological parameters (T_{50}, T_{Trans}, c_{precip}) have rather different values for the four POFs. The optimisation algorithm has been designed to preserve the tail ends of the POFs. This feature explains the "outliers" of POF 2 (Figure 4).

Table 3: Minimum and maximum values of the decision variables for each POF (for units see Table 1)

	POF1		POF2		POF3		POF4	
Variable	Min	Max	Min	Max	Min	Max	Min	Max
V_{Ice}	3	3	2	2	3	3	2	2
V_{Melt}	1	1	1	1	0	0	0	0
V_{Runoff}	0	0	0	0	0	0	0	0
a_{ice}	13.2	13.6	13.6	17.9	5.0	6.5	3.9	6.2
a_{firn}	8.4	8.4	-	-	3.2	3.2	-	-
a_{snow}	2.5	2.5	2.5	2.7	3.0	3.0	2.7	2.7
θ_{firn}	0.90	0.96	-	0.97	-	-	-	-
θ_{snow}	0.00	0.01	0.01	0.02	-	-	-	-
k_{ice}	7.4	10.4	7.7	34.7	4.2	5.0	2.3	5.6
k_{firn}	57.7	58.1	-	-	47.7	49.0	-	-
k_{snow}	27.7	35.1	23.8	33.0	12.0	14.9	8.8	12.3
$log(k)$	-13.7	-13.7	-13.9	-10.5	-4.7	-4.7	-5.2	-4.6
A	65	82	72	945	172	210	766	818
β	1451	1453	1315	1753	39091	39357	45323	47630
T_{50}	-0.6	-0.6	-1.4	-0.4	7.9	8.0	0.3	0.7
T_{Trans}	1.8	1.8	1.6	1.8	15.3	15.6	4.1	4.2
c_{precip}	4.7	4.9	4.7	7.5	8.3	8.5	6.8	9.0
σ_H	1.99	2.04	1.91	2.33	2.11	2.12	1.89	2.00
σ_L	0.48	0.48	0.47	0.49	0.48	0.48	0.49	0.49
ρ_H	0.91	0.93	0.90	0.92	0.68	0.73	0.68	0.83
ρ_L	0.87	0.91	0.86	0.90	0.82	0.83	0.80	0.85

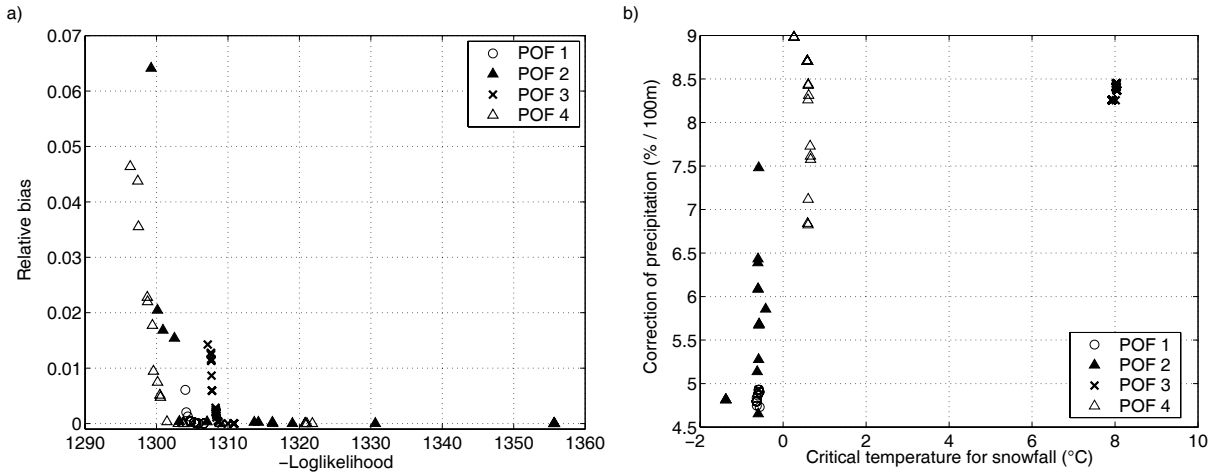

Figure 4: Identified local POFs a) in the objective function space; b) in the parameter space formed by the critical temperature of snow- and rainfall separation T_{50} (°C) and the altitudinal precipitation correction factor c_{precip} (% 100^{-1} m^{-1})

The retained solutions correspond to Nash-values (Nash and Sutcliffe, 1970) between 0.67 and 0.92 and the absolute bias between 0.05 % and 6.5 %. This shows that there is a considerable trade-off between the Pareto-optimal solutions. For the validation period the Nash values are between 0.60 and 0.87 and the absolute bias between 0.2 % and 8.7 %.

The estimated autocorrelation is consistently high for all POFs and there is no significant difference between the high and the low flow regime (Table 3). Note the important result that the estimated standard deviation is nearly the same for all model structures for both flow regimes. This overall modelling error aggregates the model structural error as well as the error contained in the used input and output data. The identified model structures are presumably not different enough to lead to structural errors of significantly different orders of magnitude over the calibration period. The input and output data error on the other hand is the same for all models. The high standard deviation during the high flow period is presumably induced by the highly error prone estimation of area average precipitation and of the representativeness of the measured precipitation events for the entire catchment (Schaefli et al., 2005). The estimated standard deviation of the modelling error during the low flow period nearly coincides with the minimum estimate of the measurement error (standard deviation of 0.53, see Section 4). This result suggests that the total modelling error during this flow regime is essentially due to the discharge measurement error. During the low flow period there is virtually no liquid precipitation; the input measurement error can be supposed to be very small. The hydrological model is known to reproduce well the low discharge (Schaefli et al., 2005) and it seems plausible to assume that structural model errors are small during the flow regime. An analysis of the simulated distribution of the flow-duration curves shows however that this assumption is not entirely defendable (see hereafter).

Probability assignment

The criteria used for the probability assignment should reflect the trade-off between the identified Pareto-optimal solutions. The simplest choice would be to consider the same criteria as for the optimisation procedure. The weighting methodology is however based on the assumption that the criteria are normally distributed with a known mean value; for the optimisation, the used criteria have to be minimised. The bias objective function can be easily transformed in a weighting criterion if we do not take the absolute value. This criterion – the bias between the mean observed and simulated discharge - is called $bias_{m.}$

The second criterion is a bias statistic of the residuals calculated by flow group (see, e.g. Sorooshian et al., 1983). For each flow group *i*, the bias between the mean observed and simulated discharge is calculated according to Equation 1. The used criterion is the mean values of these biases ($bias_g$). The retained flow groups have the following ranges: <1, 1-5, 5-7, 7-10, 10-13, 13–16, 16–22 and >22 mm/d. These flow groups have been chosen in order to maximise the correlation between this criterion and the likelihood function. For the calibration period, the criterion $bias_g$ is strongly correlated to the maximum likelihood objective function used for optimisation (correlation higher than 0.95 for all POFs). The optimum value for both criteria $bias_m$ and $bias_g$ is 0.

The probabilities assigned to the different POFs based on the dominated-volume concept are almost uniform (Table 4), i.e. all identified model structures are almost equally probable. The simplest model structure (POF4) has however a slightly higher probability than the others. This almost uniform POF probability is not induced by a characteristic of the optimisation algorithm but conditioned by the optimisation problem. In other applications of the algorithm to hydrological model optimisation, we have found not uniform POF weighting. Note also that there is no linear relationship between the probability assigned to a POF and the number of points composing it (Table 4).

Table 4: Probabilities assigned to the POFs, numbers of points composing them and median values of the associated distribution of the mean annual discharge for the calibration and the validation period (in brackets, the difference to the observed value)

			Mean annual discharge (mm)	
POF number	Probability	# points	Calibration	Validation
POF 1	0.24	19	1805 (+74)	1460 (-35)
POF 2	0.26	20	1790 (+59)	1512 (+17)
POF 3	0.23	34	1720 (-11)	1570 (+75)
POF 4	0.27	20	1690 (-41)	1560 (+65)
Multi-model	1.00	94	1721 (-10)	1560 (+65)

The points composing the POFs show an important spread in the two-dimensional space formed by the two criteria $bias_m$ and $bias_g$ (Figure 5). As a consequence their probabilities calculated according to Equation 7 and 10 vary strongly (Figure 6).

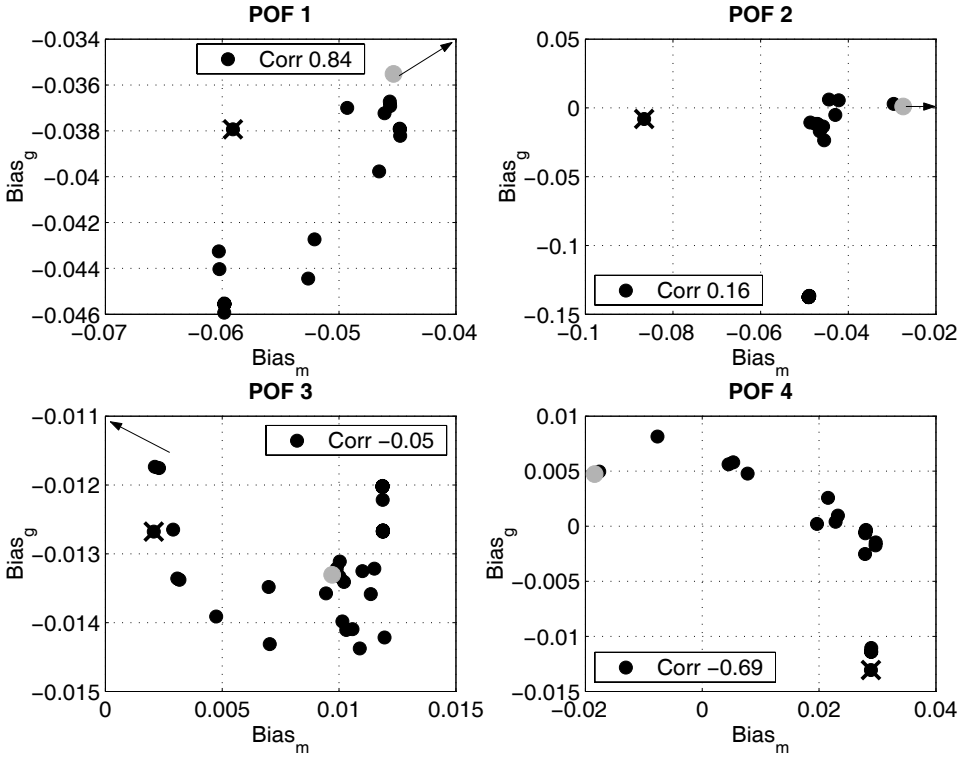

Figure 5: Points of the POFs in the criteria space for the validation period (the brighter dot corresponds to the point with maximum probability, the cross to the point with minimum probability; the arrow indicates the location of the theoretic optimum that can be outside the range of the plot)

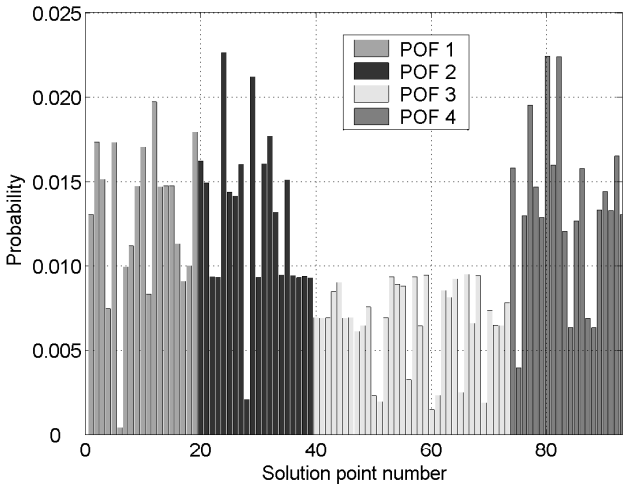

Figure 6: Probabilities assigned to the points composing the different POFs (including POF weighting)

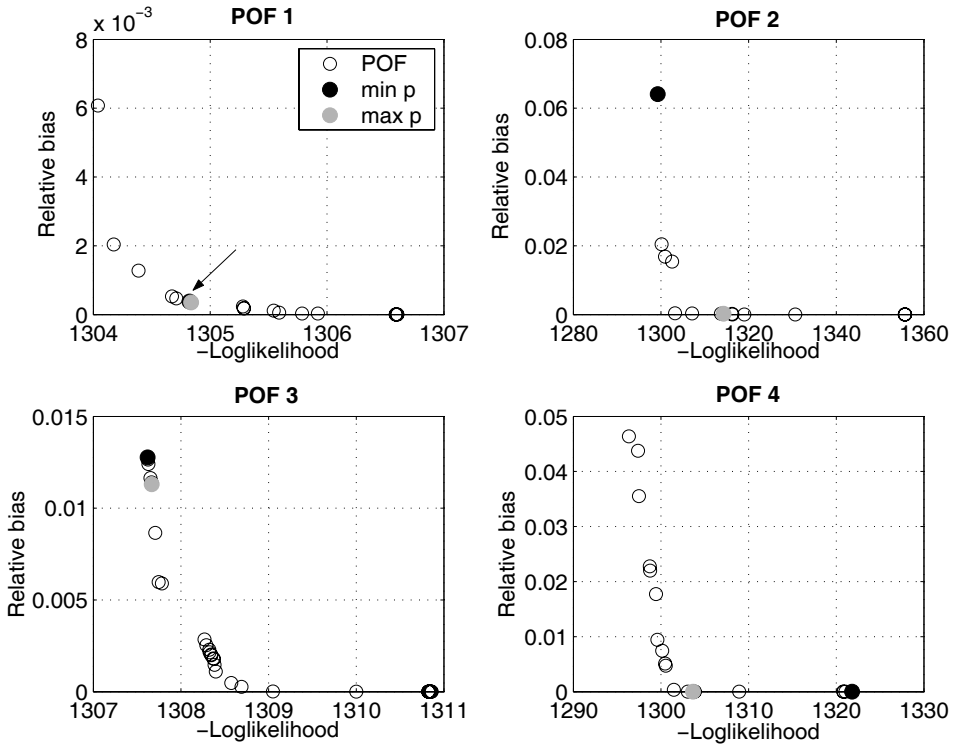

Figure 7: Location of the points with minimum and maximum probability within the approximated POFs (in the plot for POF 1, the arrow indicates the location of the point with minimum probability)

The minimum probability corresponds to one of the tail ends for three POFs (Figure 7) whereas for POF1 the point with minimum probability neighbours the point with the maximum probability on the POF (Figure 7). The two criteria $bias_m$ and $bias_g$ show a strong positive correlation for POF1 (both criteria can be fulfilled simultaneously) but this worst point is among the best for one criterion and among the worst for the other; the highest probability is assigned to the best point for both criteria. For POF1, POF2 and POF4, the point with the highest probability corresponds to the area of the POFs with the highest trade-off for the calibration period (Figure 7). For POF3, this point is close to one of the tail ends because for the validation period this point corresponds to the maximum trade-off area. Note that for this POF the difference of the assigned probabilities is much less important than for the other POFs due to the fact the for the validation period there is much less spread than for the other POFs and no detectable pattern in the performance of the points in the validation criteria space. The worst point corresponds to a tail end that is reproduced in the validation criteria space (this point has the best value for $bias_m$ but not for $bias_g$).

Multi-objective output distribution

In the following - if nothing else is stated - all simulated model output distributions include the randomly generated modelling error. The model is used in a prediction mode, i.e. the autoregressive component of the modelling error is unknown and drawn randomly.

The mean annual discharge has been chosen as a reference model output to analyse the effect of the probability assignment. We simulated the mean annual discharge for all solution points and compared the cumulative density function (cdf) obtained under an equiprobability assumption and under the proposed probability assignment (including point and POF weighting). The probability assignment only slightly modifies the cdf resulting from the multi-model approach (Figure 8). Considering the POFs individually, the result is different: The probability assignment modifies considerably their cdfs (Figure 8c and d). The probability assignment reduces the 90 % prediction intervals for all individual POFs. For POF2 this reduction reaches 100 mm for the calibration period. This effect is however smoothed out if all POFs are joined to one global cdf.

For a given POF, the effect of the solution weighting on the output cdf depends on the spread of the criteria values; the higher their variability is, the higher is the influence of the weighting on the output distribution. The cdf of the POF with the smallest variability (POF1) is almost not influenced by the probability assignment. In the present application, the POFs with the smallest trade-off for the calibration period have also the smallest spread in the criteria space for the validation period; this result is not necessarily confirmed for other case studies.

The probability assignment shifts the median values of the individual POFs. This shift can increase the bias of the median value (see for example Figure 8d) but the multi-model output distribution is not affected. For the calibration period the median value of the predicted mean annual discharge distribution has a bias of 0.5 % with respect to the observed value. For the validation period this bias corresponds to 4 %. The increase of the bias for the validation period could indicate a lack of temporal transferability of the identified models.

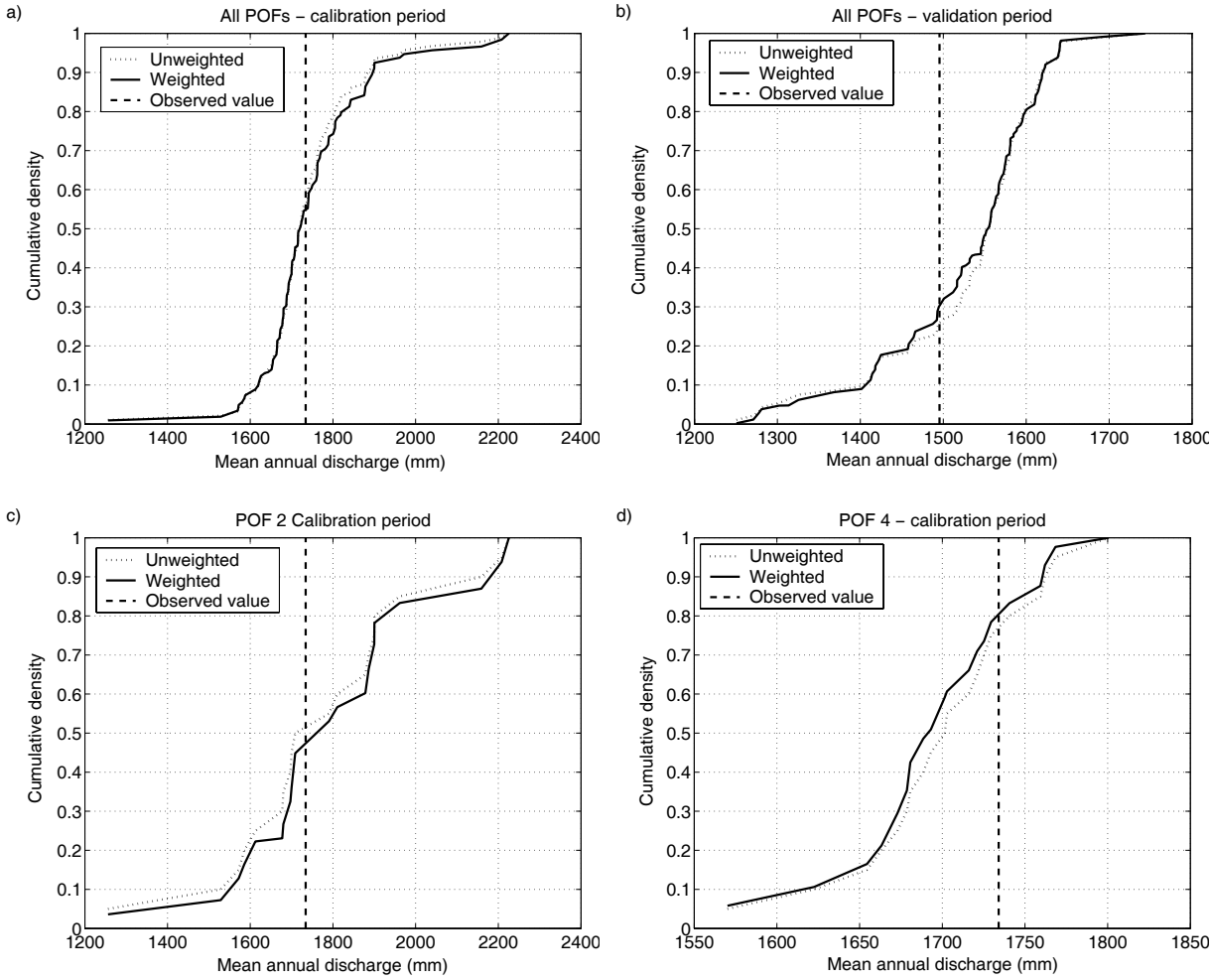

Figure 8: Cdfs of the mean annual discharge considering either that alls solutions are equiprobable (*unweighted*) or the proposed probability assignment (*weighted*); a) multi-model calibration period, b) multi-model validation period, c) only POF2 calibration period, d) only POF4 calibration period

For the calibration period, the multi-model distribution predicts the observed mean annual discharge better or evenly well as the individual POFs. For the validation period, the solutions composing POF1 and POF2 give better results for the validation period than the multi-model distribution (Table 4). Note however that these two models give the worst estimation of the mean annual discharge for the calibration period.

For the assessment of the overall discharge prediction quality, we also consider the predicted daily discharge that corresponds to the second optimisation objective. If we consider the estimated minimum error distribution of the observed discharge, the 90 % prediction interval includes the 90 % observational interval on 85 % of the days for the calibration period and the validation period (see Figure 9a). This apparently good result is due to a large prediction interval induced by the total modelling error. For the 90 % prediction interval induced exclusively by the parameter uncertainty these values drop to 42 % for the calibration period and to 33 % for the validation period. These poor results for the daily discharge are presumably due to the high trade-off between models that reproduce well the daily discharge

and the ones that simulate well the mean annual discharge. The question whether this problem could be due to a deficiency in the model structure will be further discussed hereafter.

8.5.2 Statistical output distribution

We have inferred the posterior parameter distribution for all retained model structures with a Markov Chain Monte Carlo method, the so-called Metropolis-Hastings algorithm (see, e.g. (Kuczera and Parent, 1998); (Bates and Campbell, 2001). The statistical error model is the same as the one used for the multi-objective optimisation (for details see Schaefli et al., 2005a, submitted manuscript). In the following, we refer to the model structures corresponding to the four identified POFs as M1 to M4. The multi-model output distribution is estimated by weighting the outputs of the four model structures based on the probabilities assigned to the corresponding POFs.

The inference of the posterior parameter distribution corresponds to a single-objective optimisation. The resulting parameter distributions overlap partially the multi-objective solution space (see an example for M4 in Table 5). The 90 % intervals of the posterior parameter distributions contain between 26 % (M2) and 89 % (M3) of the multi-objective parameter values. For a given model structure the solution spaces of the statistical and the multi-objective optimisation overlap more if the corresponding POF has only a small trade-off between the tail ends.

Table 5: Parameter values for model M4 identified through multi-objective optimisation (parameter set with maximum likelihood, minimum value and maximum value of all solution points) and percentiles of the posterior parameter distribution (for units refer to Table 1)

	Multi-objective optimisation			Statistical calibration		
Parameter	Max likelihood	Min value	Max value	5 % percentile	Posterior median	95 % percentile
a_{ice}	5.8	3.9	6.2	5.3	5.7	6.3
a_{snow}	2.7	2.7	2.7	2.6	2.8	2.9
$log(k)$	-4.7	-5.2	-4.6	-4.7	-4.6	-4.5
A	787	766	818	762	782	851
β	47320	45323	47630	27054	48849	56327
k_{ice}	3.7	2.3	5.6	3.5	3.7	3.8
k_{snow}	10.6	8.8	12.3	9.3	10.3	12.4
c_{precip}	6.8	6.8	9.0	6.0	6.8	7.3
ρ_H	0.71	0.68	0.83	0.67	0.71	0.77
ρ_L	0.81	0.80	0.85	0.75	0.79	0.81
σ_H	1.91	1.89	2.00	1.82	1.90	1.98
σ_L	0.49	0.49	0.49	0.46	0.49	0.51

The 90 % prediction intervals of the simulated daily discharge brackets the 90 % observational interval on 92 % of the days during the calibration period and on 88 % during the validation period. As for the multi-objective modelling uncertainty, this good results come with a large prediction interval (Figure 9b). The parameter uncertainty alone includes only 41 % (calibration period) respectively 31 % (validation period) of the observed values. This result could be due to important structural deficiencies of the models. The too optimistic estimation of the posterior parameter distribution is however typical for the chosen parameter inference method (see, e.g. Vrugt et al., 2003b) and could also be due to the underlying likelihood function. The error term is raised to a large power and therefore only the direct vicinity of the optimum solution can survive to the model optimisation process (for a further discussion see Beven and Freer, 2001).

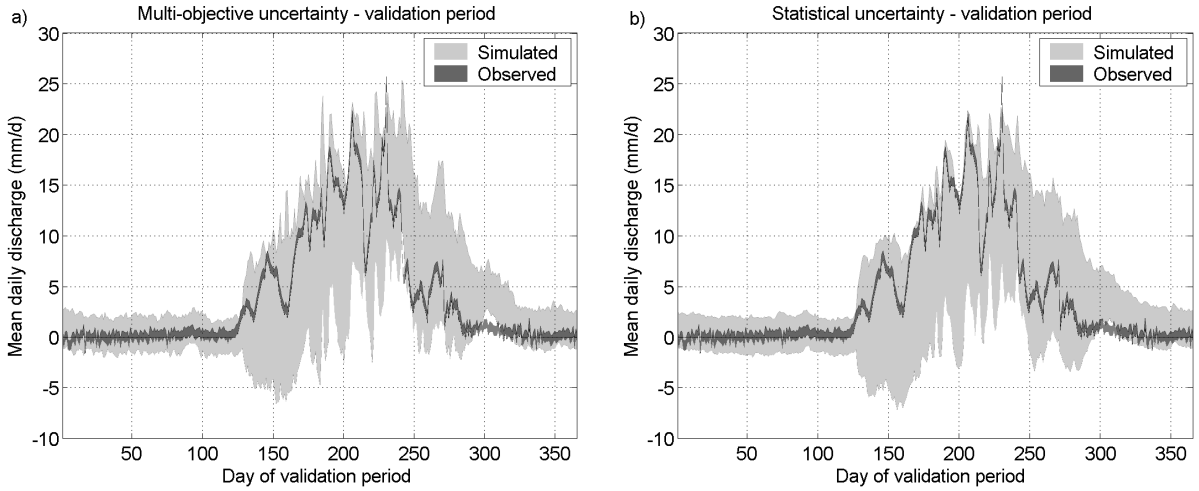

Figure 9: 90 % interval of the observed and the simulated daily discharge for the validation period; the observed interval includes the estimated minimum error, the simulated is the one induced a) by the multi-objective output distribution and b) by the posterior parameter distribution (modelling error included)

For the mean annual discharge, the statistical output distribution shows a bias of 4 % during the calibration period (Figure 10a). The likelihood function used for the inference of the posterior parameter distribution does not explicitly penalise solutions that lead to a bias (see Equation 3). Such solutions are however contrary to the modelling assumption of an unbiased error term and should be sorted out during a postcalibration assessment of the modelling assumptions (this remark of course also holds for the multi-objective optimisation). We have shown in previous work that the modelling assumptions hold well for the maximum likelihood parameter set but this is not necessary the case for all other parameter sets that compose the posterior parameter distribution. This problem is not easily solved in a thorough statistical approach. For multi-objective optimisation, we could use a generalised likelihood measure (Beven and Freer, 2001) to circumvent this problem but we would loose the possibility to estimate the modelling error in parallel to the parameter optimisation.

8.5.3 Multi-objective versus statistical output distribution

The relative importance of the two concepts of modelling uncertainty depends on the chosen portion of data for the parameter and modelling error estimation. The four model structures underlying the multi-model output distribution and their parameters identified according to the two uncertainty concepts encode differently the main processes governing the catchment response. The importance of the individual processes is influenced by the hydro-climatic conditions. The observed data shows that the calibration and the validation period do not have the same characteristics: The mean annual discharge during the calibration period is around 14 % higher. The validation period was a warm period compared to the calibration period. The former therefore experienced less snow accumulation and more ice melt.

In addition to the time periods used for modelling uncertainty estimation, we assess the multi-model output distribution related to the two uncertainty concepts for two other time periods, the so-called control time period (1961 - 1990), for which the input time series are observed, and a future time period (2070 – 2099) characterised by a climate change. The corresponding meteorological input time series are based on RCM outputs for the climate change scenario B2 (see Section 4).

Calibration and validation period

A comparison of the mean annual discharge distributions predicted by the statistical and the multi-objective uncertainty concepts shows that the 90 % uncertainty intervals of the individual models are consistently higher for the statistical concept than for the multi-objective concept (Figure 10c and d). The variability induced by the modelling error is of the same order of magnitude for both concepts but the variability of the mean annual discharge exclusively induced by the parameter uncertainty is higher for the statistical concept than for the multi-objective concept. This result is due to the fact that the use of more than one objective function constrains the feasible parameter space more than in a single-objective optimisation.

For the individual model structures the two distributions can be relatively close (Figure 10d) or considerably shifted one with respect to the other (Figure 10c). The higher the trade-off between the tail ends of a given POF, the more distant are the two distributions. This is due to the fact that the statistical distribution is centred on the maximum of likelihood. If the trade-off is high, this leads to an important bias. As a result the multi-model distribution predicted by the multi-objective uncertainty concept has a significantly smaller 90 % interval for both periods (Figure 10a and b).

For the validation period the median value of the statistical distribution perfectly matches the observed value whereas this is not the case for the calibration period. We therefore believe that this is due to pure chance.

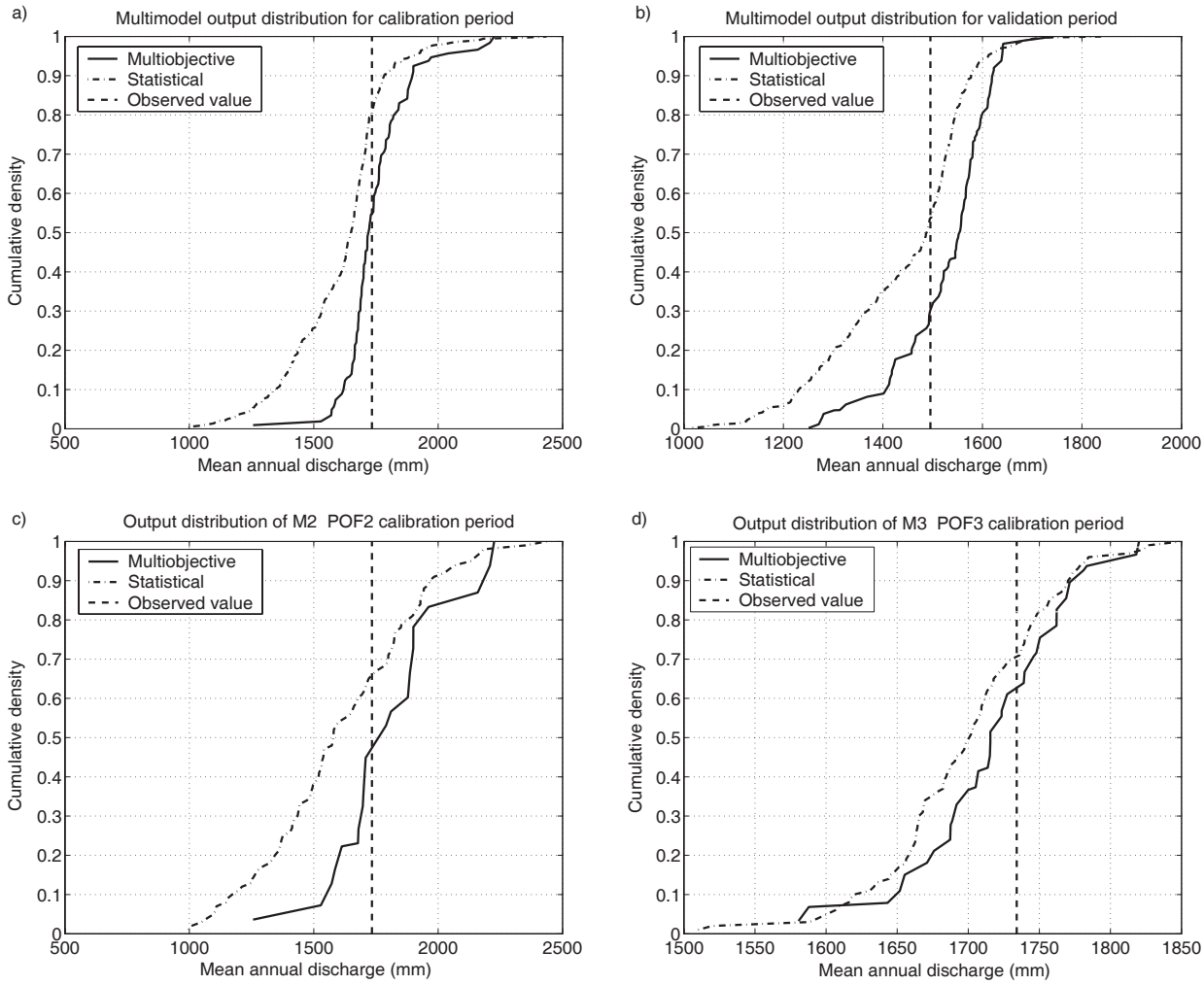

Figure 10: Cdfs of the mean annual discharge considering the statistical and the multi-objective uncertainty; a) multi-model calibration period), b) multi-model validation period, c) M2-POF2 calibration period, d) M3-POF3 calibration period

For the calibration period, the statistical concept seems to better predict the flow-duration curves. The 90 % interval brackets 88 % of the observed flow-duration curve whereas for the multi-objective distribution only 75 % are included. This result is however due to a lack of precision of the statistical distribution. For both periods, the 90 % intervals of the simulated flow-duration curves are much larger than for the multi-objective distribution (Figure 11). This result is closely related to the problem that each of the four models composing the multi-model distribution gives a biased estimate of the discharge and that the predictions of the models are shifted one with respect to the others.

The distributions associated with both concepts have difficulties to predict the low flow discharges (Figure 11). The phenomenon is more pronounced during the validation period and as a result both simulated distributions only include 65 % of the observed flow-duration curve for the validation period. This result is presumably due to an erroneous simulation of the

discharge recession in autumn (see an example in Figure 9). The inability of both uncertainty concepts to predict these discharges could indicate a structural model deficiency.

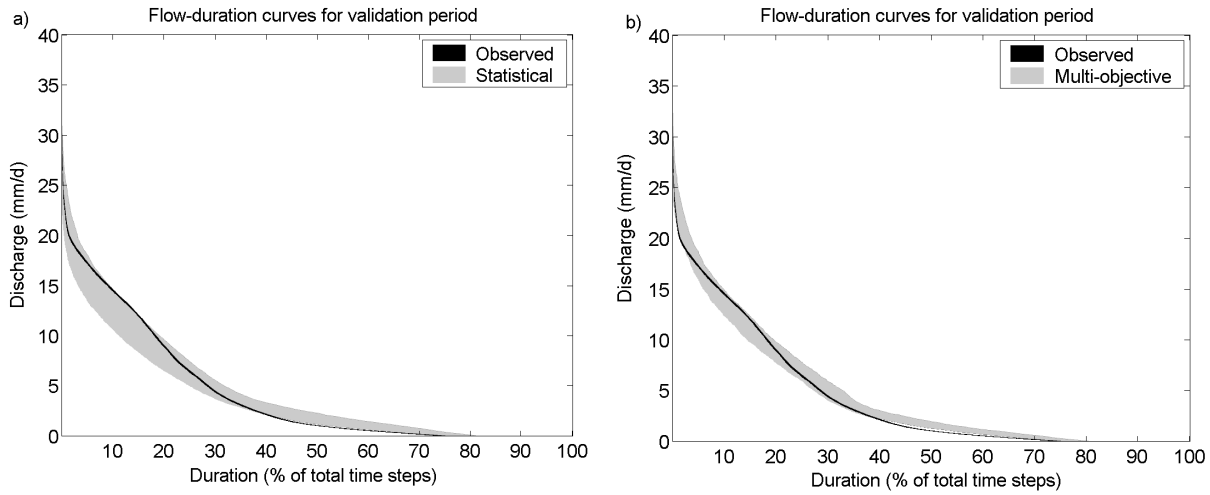

Figure 11: 90 % intervals of the observed and simulated flow-duration curves for the calibration period; the observed interval includes the estimated minimum error, the simulated is the one induced a) by the statistical uncertainty concept and b) by the multi-objective uncertainty concept

This assumption is supported by an analysis of the flow-duration curve distributions induced exclusively by the parameter uncertainty, i.e. without the modelling error. The 90 % interval simulated through the statistical parameter uncertainty brackets 76 % of the observed flow-duration curve during the calibration period but only 35 % during the validation period. The corresponding results for the multi-objective parameter uncertainty are respectively 68 % and 25 %. There is a lack of temporal transferability of the identified models that would be worth of further investigation.

Control period

The mean annual hydro-climatic conditions are comparable to the calibration period. The control period was 0.1 °C warmer and had 2% less precipitation. The distributions of the flow-duration curves predicted by the two uncertainty concepts differ strongly (Figure 12a). As for the calibration and the validation period, the statistical concept leads to a much larger interval. Considering the associated distribution of the mean annual discharge (Figure 12b), the statistical concept induces a much larger 90 % prediction interval. The resulting distribution is multi-modal: As discussed before, the statistical model optimisation leads to a more or less pronounced bias that varies with the hydro-climatic conditions. For the control period the relative shift of the predictions of the different models is more pronounced than for calibration and the validation period. The multi-objective uncertainty concept gives a

consistent estimate of the mean annual discharge. This shows that the multi-objective optimisation is much more robust to a temporal transfer.

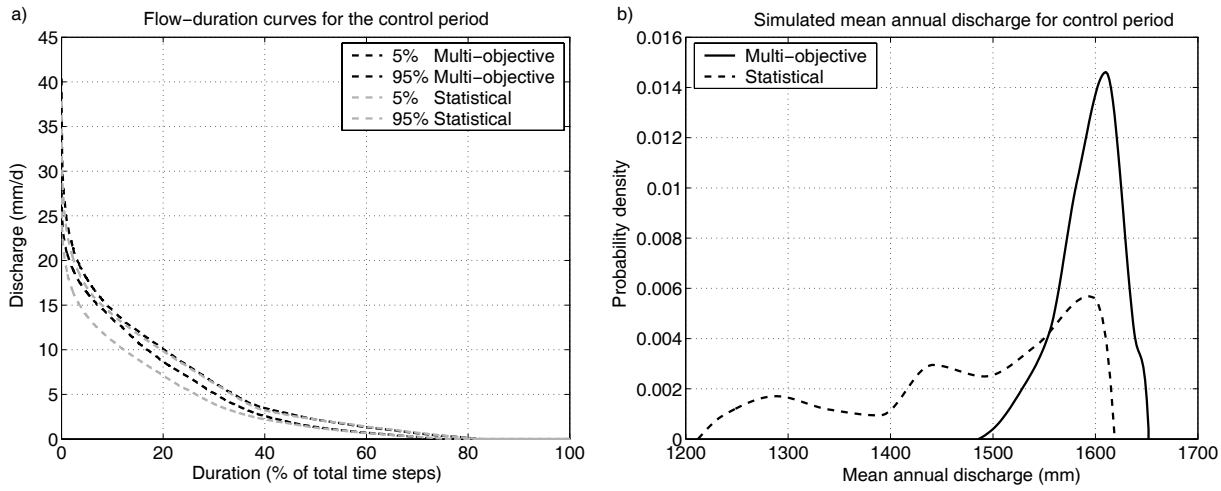

Figure 12: a) 90 % interval of the simulated flow-duration curves for the multi-objective and the statistical optimisation; b) associated distributions of mean annual discharge

Future period

The climate change scenario corresponds to a global-mean warming of around 2.4°C. The corresponding regional climate shows a temperature increase of 3.1°C and a precipitation decrease of 8 %. This considerable climate change induces an important modification of the hydrological regime accompanied by a reduction of the glacier surface. The future glacier surface is updated according to the method presented by Schaefli (2005). The simulated future glacier surface corresponds to around 4 % of the catchment surface. The exact value depends on the hydrological model design and on the corresponding parameter set, namely on the degree-day factors and the meteorological parameters.

The four identified model structures lead to a multi-modal prediction of the future glacier surface (Figure 13a). The associated prediction of the mean annual discharge is strongly bi-modal for both uncertainty concepts (Figure 13b). The two concepts lead to nearly the same prediction of the mode centred on 1350 mm but to a shifted prediction for the second mode.

Note that the hydrological parameters condition on one hand the simulated glacier surface and on the other hand the associated glacio-hydrological response. The rather consistent prediction of the future mean annual discharge for both uncertainty concepts is the consequence of this joint action on two different modelling aspects. The perhaps most interesting result is that for both uncertainty concepts, the predicted climate change is significant (the control mean annual discharge lies in between the two modes for each concept) but we cannot predict whether it increases or decreases. This result is exclusively due to the chosen multi-model approach. A single model approach would have lead to the

conclusion either that the discharge decreases or that it increases depending on the retained model structure.

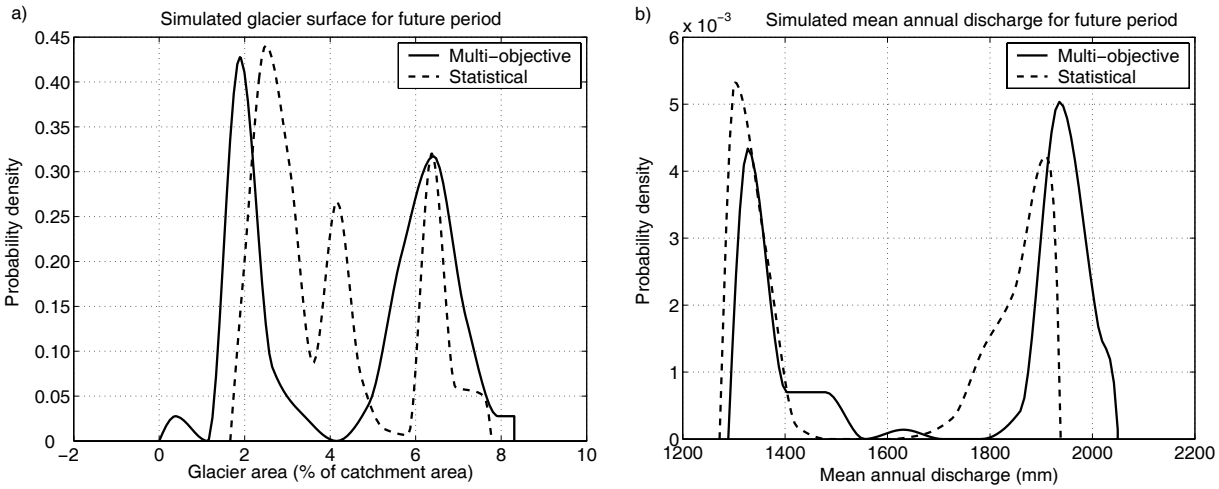

Figure 13: a) Simulated distribution of future glacier surface under the two uncertainty concepts, b) simulated distribution of mean annual discharge under the two uncertainty concepts

8.6 Conclusions

We have presented a method to estimate the model output distribution induced by the multi-objective modelling uncertainty in a multi-model framework. Each of the models corresponds to a POF composed of a number of decision variable sets. The associated modelling uncertainty is estimated by assigning a probability to each POF according to the volume it dominates in the objective space. Additionally each point within a POF receives a probability that depends on its performance for a validation time period.

The retained POFs are identified through an evolutionary clustering algorithm that finds local POFs. The proposed POF weighting is however applicable to multi-model frameworks where every model is optimised separately and could give interesting results in applications where the used models perform significantly differently (see, e.g., the POFs presented by (Butts et al., 2004)). The proposed probability assignment to a point within a POF aggregates the values of different criteria calculated over the validation period assuming that they are normally distributed and covariant. This method overcomes a classical problem of criteria aggregation that is that the individual criteria do not have the same order of magnitude. Additionally, it accounts for the interactions between the criteria. It is important to emphasize that the presented probability assignment does not rely on a subjective preference for any of the objective functions, the classical solution to assign preferences to any of the Pareto-optimal solutions (see, e.g., Gupta et al., 1998).

The obtained multi-objective output distribution is nevertheless subjective because the choice of the objective functions for the optimisation and of the criteria for probability assignment is subjective. This subjectivity however arises in any modelling problem as a conjunction of the modelling context and the modeller's expertise to judge what observed aspects the model should reproduce. The method has been developed to quantify hydrological modelling uncertainties in climate change impact studies. This context imposed the choice of an objective function related to the bias of the mean annual discharge and a likelihood function of the daily discharge.

In a classical multi-objective optimisation approach, the Pareto-optimal solutions correspond to a minimal estimate of the modelling error (see, e.g., Gupta et al., 1998). The trade-off represented by the Pareto-optimal solutions expresses the model inability to match all the observed model output characteristics it has been designed to simulate. In the presented approach, the daily residual distribution is estimated during the model optimisation process. We therefore obtain an estimate of the overall modelling uncertainty induced by each model structure and by all model structures jointly. This modelling error aggregates the model structural error and the uncertainty inherent in the observed model input and output. In the present study no attempt has been made to account explicitly for the model input uncertainties. Their quantification could be greatly beneficial to the apprehension of the overall modelling uncertainty.

The multi-objective equivalence concept cannot be considered as being complete in itself. We have compared the estimated modelling uncertainty induced by the multi-objective concept to the one inherent in the statistical concept. The multi-objective optimisation shows that the likelihood function is strongly antagonist to the bias function and hence the maximum of likelihood cannot be achieved in parallel with a minimum bias. This indicates that for the presented case study, the statistical uncertainty concept will always lead to a biased estimate of the model output distribution. This problem is enhanced by the fact that in a single-objective optimisation based on the likelihood function, solutions inducing a bias are not penalised by this objective function. This biased estimate becomes particularly striking if the associated modelling uncertainty is simulated for another time period than the one used for model optimisation. We showed that the different model structures underlying the multi-model distribution lead to an inconsistent prediction of the mean annual discharge for a control period when considering the statistical uncertainty concept whereas the multi-objective output distribution is robust to this temporal transfer. Similar results can be expected for other case studies if there is a high trade-off between the error and the bias function. The joint analysis of both uncertainty concepts is nevertheless essential as it can give valuable insights in the behaviour of the models. For the presented case study, neither of the model is able to well predict the discharge recession in late autumn revealing therefore a not negligible model structural deficiency.

The use of the proposed likelihood function in either model calibration approach is based on the assumption that during each flow regime the hydrological modelling errors are normally

distributed, have zero mean and are homoscedastic. This assumption should be verified in a postcalibration evaluation. Even though the errors are always slightly biased, the assumption holds well for the maximum likelihood point identified through statistical calibration (Schaefli et al., 2005a, submitted manuscript). The residuals will however not necessarily have the same assumed structure in other areas of the parameter space or for other time periods.

Some of the identified POFs are presumably more robust for a temporal transfer than others. This aspect has not been considered in the proposed probability assignment. Further research is necessary to develop appropriate methods to judge the robustness of the POFs. We think in particular to make use of the dependence structure of the Pareto-optimal solutions in the objective space if simulated for a validation time period. The way in which the Pareto-optimal solutions map into the objective space for other time periods should give exploitable indications about the transferability of the model structure. Such an analysis could in particular evaluate the behaviour of the points composing the POFs if time periods having specific properties (wet or dry periods, warm or cold periods) are used for the calibration and the validation period.

The proposed probability assignment does not consider another potentially exploitable property of the Pareto-optimal solutions: The parameter sets composing a given POF do exhibit correlations among each other and with the objective functions. In some optimisation problems, strong correlations between the decision variables or with the objective functions can be an indication that the algorithm has converged to the true POF, for example if theoretic considerations enable a prediction of the relationship between the decision variables or between the decision variables and the objective functions (see, e.g., Marechal et al., 2004). For hydrological modelling, the found correlations are difficult to interpret but would be worth of further investigation, especially with a view to identify structural deficiencies of the model.

The presented methodology associates the uncertainty induced by optimising not only the model parameters but also the parameter structure itself. We do not pretend that the proposed model designs cover the whole range of possible model structures. The obtained results emphasize however how important model intercomparison is. The used optimisation algorithm would theoretically enable the identification of the optimal model structures starting with minimal assumptions about the number of used storage reservoirs, the driving fluxes (precipitation, potential evapotranspiration) and the fluxes connecting the different reservoirs (see the basic antanomy of a hydrological model presented by Kuczera (1982)).

Associating different model structures into one model output prediction raises a not negligible problem: The predicted model output distribution does not correspond to any of the model structures. Accordingly, a percentile of the resulting predictive output distribution cannot be interpreted as an estimate of the probability of simulating a particular output; it corresponds just to a percentile of the model prediction. The concept of multi-model prediction is accepted in flood forecasting (see, e.g., Shamseldin et al., 1997; Xiong et al., 2001; Butts et al., 2004;

Georgakakos et al., 2004) but it is undesirable in modelling contexts analysing the hydrological behaviour and the driving processes. Our method has been developed to investigate the predictability of the hydrological response to a climate modification. From this point of view, the association of different model structures to a multi-model prediction is necessary unless the available data and the process understanding enable a confident choice of the best model structure. We believe that these conditions are currently not fulfilled for many hydrological systems and especially not for high mountainous catchments.

For the presented case study, the multi-model approach results in a strongly bi-modal catchment response for the future period making therefore a prediction of the climate change impact impossible. This result emphasizes that climate change impact studies that do not consider explicitly the structural uncertainties inherent in hydrological models could be strongly misleading.

Finally we would like to remember that all the obtained results are conditional on the used hydrological transfer functions, the statistical error model, the series of input and output data and the criteria for multi-objective output distribution. The different choices are the best we expect to be able to make for the given modelling context but as Beven and Freer (2001) emphasize, it is difficult to justify a unique set of prediction limits just as it is difficult to justify a unique optimal model of the system.

Acknowledgements

We wish to thank Dr. François Maréchal from LENI for having made available the source code of the algorithm QMOO and Dr. Geoff Leyland for its help on the algorithm application and on some theoretical optimisation aspects. We also wish to thank the Forces Motrices de Mauvoisin for providing the discharge series and the national weather service MeteoSwiss for providing the meteorological time series.

References

Bates, B.C. and Campbell, E.P., 2001. A Markov chain Monte Carlo scheme for parameter estimation and inference in conceptual rainfall-runoff modeling. Water Resources Research, 37(4): 937-947.

Beven, K. and Binley, A., 1992. The future of distributed models: model calibration and uncertainty prediction. Hydrological Processes, 6(3): 279-298.

Beven, K. and Freer, J., 2001. Equifinality, data assimilation, and uncertainty estimation in mechanistic modelling of complex environmental systems using the GLUE methodology. Journal of Hydrology, 249(1-4): 11-29.

Burer, M., Tanaka, K., Favrat, D. and Yamady, K., 2003. Multi-criteria optimization of a district cogeneration plant integrating a solid oxide fuel cell-gas turbine combined cycle, heat pumps and chillers. Energy, 28: 497-518.

Burman, R. and Pochop, L.O., 1994. Evaporation, evapotranspiration and climatic data. Elsevier, Amsterdam, 278 pp.

Butts, M.B., Payne, J.T., Kristensen, M. and Madsen, H., 2004. An evaluation of the impact of model structure on hydrological modelling uncertainty for streamflow simulation. Journal of Hydrology, 298(1-4): 242-266.

Duan, Q., Sorooshian, S. and Gupta, V., 1992. Effective and efficient global optimization for conceptual rainfall-runoff models. Water Resources Research, 28(4): 1015-1031.

Georgakakos, K.P., Seo, D.-J., Gupta, H., Schaake, J. and Butts, M.B., 2004. Towards the characterization of streamflow simulation uncertainty through multimodel ensembles. Journal of Hydrology, 298(1-4): 222-241.

Gupta, H.V., Sorooshian, S. and Yapo, P.O., 1998. Toward improved calibration of hydrologic models: Multiple and noncommensurable measures of information. Water Resources Research, 34(4): 751-763.

Hansen, M.P. and Jaszkiewicz, A., 1998. Evaluating the quality of approximations of the nondominated set. IMM-REP-1998-7, Institute of Mathematical Modelling, Technical University of Denmark.

Houghton, J.T. (Editor), 2001. Climate change 2001: the scientific basis. Contribution of Working Group I to the Third Assessment Report of the Intergovernmental Panel on Climate Change. Cambrige University Presse, Cambrige, 881 pp.

Khu, S.T. and Madsen, H., 2005. Multiobjective calibration with Pareto preference ordering: An application to rainfall-runoff model calibration. Water Resources Research, 41, W03004, doi: 10.1029/2004WR003041.

Kuchment, L.S. and Gelfan, A.N., 1996. The determination of the snowmelt rate and the meltwater outflow from a snowpack for modelling river runoff generation. Journal of Hydrology, 179(1-4): 23-36.

Kuczera, G., 1982. On the relationship between the reliability of parameter estimates and hydrologic time-series data used in calibration. Water Resources Research, 18(1): 146-154.

Kuczera, G. and Parent, E., 1998. Monte Carlo assessment of parameter uncertainty in conceptual catchment models: the Metropolis algorithm. Journal of Hydrology, 211(1-4): 69-85.

Leyland, G.B., 2002. Multi-Objective Optimisation Applied to Industrial Energy Problems. Doctoral Thesis, Swiss Institute of Technology, Lausanne, Lausanne, 188 pp.

Madsen, H., 2000. Automatic calibration of a conceptual rainfall-runoff model using multiple objectives. Journal of Hydrology, 235(3-4): 276-288.

Madsen, H., 2003. Parameter estimation in distributed hydrological catchment modelling using automatic calibration with multiple objectives. Advances in Water Resources, 26(2): 205-216.

Marechal, F., Palazzi, F., Godat, J. and Favrat, D., 2004. Thermo-economic modelling and optimisation of fuel cell systems. Fuel Cells: From Fundamentals to Systems, in press.

Marshall, L., Nott, D. and Sharma, A., 2004. A comparative study of Markov chain Monte Carlo methods for conceptual rainfall-runoff modeling. Water Resources Research, 40(2): W02501.

Nash, J.E. and Sutcliffe, J.V., 1970. River flow forecasting through conceptual models. Part I, a discussion of principles. Journal of Hydrology, 10(3): 282-290.

Pareto, V., 1896. Cours d'économie politique. F. Rouge, Lausanne.

Rango, A. and Martinec, J., 1995. Revisiting the degree-day method for snowmelt computations. Water Resources Bulletin, 31(4): 657-669.

Refsgaard, J.C. and Storm, B., 1996. Construction, calibration and validation of hydrological models. In: M.B. Abbott and J.C. Refsgaard (Editors), Distributed hydrological modelling. Kluwer Academic Press, Dordrecht, Netherlands, pp. 41-54.

Schaefli, B., 2005. Uncertain glacier surface evolution under changing climate. In: Quantification of modelling uncertainties in climate change impact studies on water resources: Application to a glacier-fed hydropower production system in the Swiss Alps. Doctoral thesis. Swiss Institute of Technology, Lausanne.

Schaefli, B., Hingray, B. and Musy, A., 2004. Improved calibration of hydrological models: use of a multi-objective evolutionary algorithm for parameter and model structure uncertainty estimation. In: B. Webb (Editor), Hydrology: Science and Practice for the 21st Century. British Hydrological Society, London, pp. 362-371.

Schaefli, B., Hingray, B., Niggli, M. and Musy, A., 2005. A conceptual glacio-hydrological model for high mountainous catchments. Hydrology and Earth System Sciences Discussions, 2, 73-117.

Shabalova, M.V., Van Deursen, W.P.A. and Buishand, T.A., 2003. Assessing future discharge of the river Rhine using regional climate model integrations and a hydrological model. Climate Research, 23: 223-246.

Shamseldin, A.Y., O'Connor, K.M. and Liang, G.C., 1997. Methods for combining the outputs of different rainfall-runoff models. Journal of Hydrology, 197(1-4): 203-229.

Sorooshian, S., Gupta, V.K. and Fulton, J.L., 1983. Evaluation of maximum-likelihood parameter-estimation techniques for conceptual rainfall-runoff models - influence of calibration variability and length on model credibility. Water Resources Research, 19(1): 251-259.

Spreafico, M., Weingartner, R. and Leibundgut, C., 1992. Atlas hydrologique de la Suisse. Service Hydrologique et Géologique National (SHGN), Bern.

Thyer, M., Kuczera, G. and Wang, Q.J., 2002. Quantifying parameter uncertainty in stochastic models using the Box-Cox transformation. Journal of Hydrology, 265(1-4): 246-257.

van Griensven, A., Francos, A. and Bauwens, W., 2002. Sensitivity analysis and auto-calibration of an integral dynamic model for river water quality. Water Science and Technology, 45(9): 325-332.

Vrugt, J.A., Diks, C.G.H., Gupta, H.V., Bouten, W. and Verstraten, J.M., 2005. Improved treatment of uncertainty in hydrologic modeling: Combining the strengths of global optimization and data assimilation. Water Resources Research, 41.

Vrugt, J.A., Gupta, H.V., Bastidas, L.A., Bouten, W. and Sorooshian, S., 2003a. Effective and efficient algorithm for multiobjective optimization of hydrological models. Water Resources Research, 39(8).

Vrugt, J.A., Gupta, H.V., Bouten, W. and Sorooshian, S., 2003b. A shuffled complexe evolution Metropolis algorithm for optimization and uncertainty assessment of hydrologic models. Water Resources Research, 39(8): 1201.

Wang, Q.J., 1991. The genetic algorithm and its application to calibrating conceptual rainfall-runoff models. Water Resources Research, 27(9): 2467-2471.

Xiong, L.H., Shamseldin, A.Y. and O'Connor, K.M., 2001. A non-linear combination of the forecasts of rainfall-runoff models by the first-order Takagi-Sugeno fuzzy systems. JOurnal of Hydrology, 245: 196-217.

Yapo, P.O., Gupta, H.V. and Sorooshian, S., 1996. Automatic calibration of conceptual rainfall-runoff models: Sensitivity to calibration data. Journal of Hydrology, 181(1-4): 23-48.

Yapo, P.O., Gupta, H.V. and Sorooshian, S., 1998. Multi-objective global optimization for hydrologic models. Journal of Hydrology, 204(1-4): 83-97.

Zitzler, E., 1999. Evolutionary algorithms for multiobjective optimisation: methods and applications. PhD Thesis, Eigenössische Technische Hochschule, Zürich, 122 pp.

Zitzler, E., Thiele, L., Laumanns, M., Fonseca, C.M. and da Fonseca, V.G., 2003. Performance assessment of multiobjective optimizers: An analysis and review. IEE Transactions on Evolutionary Computation, 7(2): 117-132.

Chapter 9

Conclusion: Prediction of climate change impacts – an illusion ?

9.1 Introduction

If we had perfect climate change evolution predictions, we could predict their impact on our environment. This paradigm currently motivates most climate change impact studies not only in the field of hydrological research but in all areas directly influenced by the climate, for example ecology, agricultural production, energy consumption etc. This implies that the limiting factor in climate change impact studies is considered to be our ability to predict future climate. Even if climate models experience fast progress by incorporating more detailed mathematical descriptions of the climate system and its driving forces, the prediction of its evolution will always be hindered by the prediction of the evolution of the greenhouse gas emissions.

Our first results enforced the stated paradigm. Applying a probabilistic climate change impact evaluation methodology we came in fact to the conclusion that the uncertainty induced by the global mean-warming is much higher than the one induced by the system response to this warming. This enhanced the hypothesis that we could predict the system evolution if the climate models would do a better job in terms of modelling uncertainty and if we could predict the evolution of the greenhouse gas emissions. This somehow simplistic vision of the problem could however not be maintained: An investigation of the effect of the hydrological model structure on the resulting predicted climate change impact showed that we can predict

that the hydrological response will change but not the direction of this change. This is perhaps the most striking result of the present research study because it calls into question the predominating paradigm. In the following we will give a short overview over the main results and how they integrate to the overall conclusions.

We will end with a short discussion of the future research questions raised by the present research or left open including namely the questions how the hydrological uncertainty could be restrained, which sources of hydrological modelling uncertainty should be studied in further detail and which new methods referring to the quantification of modelling uncertainties could be considered.

9.2 Main results

The developed simulation framework for climate change impact studies enables a fully probabilistic prediction of climate-induced modifications of a managed high mountainous water resources system. Based on this modelling tool, the probability distributions of relevant system outputs can be simulated for different climate conditions to assess climate induced system modifications. The probability distributions are the result of Monte Carlo simulations of the system behaviour considering the probabilistic component of the different models composing the simulation tool. These models are of two types, related respectively to the climate change scenario production and to the simulation of the behaviour of the water resources system. The former have been developed within our research group in parallel of the work on this PhD thesis (Hingray et al., 2005a, submitted manuscript[1]) whereas the latter have been specifically developed to analyse the case study of this thesis. For each model type different modelling constraints referring essentially to the available input data had to be considered. An important characteristic of all models is that their contribution to the overall modelling uncertainty can be quantified.

The developed water management model enables the simulation of the daily water release and hydropower production without knowing the underlying management rules or driving forces that are difficult to determine. The resulting mixed deterministic-stochastic model enables a good reproduction of the observed water management. The input into this management model is the daily discharge from the connected hydrological catchment. The precipitation-runoff transformation model developed for this purpose simulates well the hydrological regime and

[1] Hingray, B., Mouhous, N., Mezghani, A., Bogner, K., Schaefli, B. and Musy, A.: Accounting for global warming and scaling uncertainties in climate change impact studies: Application to a regulated lakes system. Submitted to Hydrology and Earth System Sciences; hereinafter referred to as Hingray et al., 2005a, submitted manuscript.

reproduces some basic glaciological characteristics such as the accumulation area of the total ice covered area. This feature is essential for the simulation of the ice cover evolution induced by a potential climate change. The glacier retreat is supposed to be the dominating land cover change process. Its evolution is simulated through a conceptual glacier surface model relating the glacier surface for a given time period to the mean simulated snow accumulation area. The developed conceptual model corresponds to an extremely simplified representation of the complex processes that govern the dynamics of a glacier system. The accompanying method for a stochastic generation of the predicted glacier surfaces has been shown to ensure a good coverage of the related modelling uncertainty.

The hydrological model is conceptual and has to be calibrated. All input data – namely daily temperature, precipitation and potential evapotranspiration – can be obtained from current available climate model outputs – a necessary condition for its application in the present context. This constraint largely contributed to the choice of a highly parsimonious model structure. In a first step we used a predetermined fixed model structure to simulate the hydrological response. We assessed the overall statistical uncertainty inherent in the model parameters and the total modelling error through a Bayesian inference of their posterior distribution. The inference was completed through a Metropolis-Hastings algorithm - a Markov Chain Monte Carlo method. The application of such a method requires the definition of an appropriate statistical error model. Hydrological models are known to have complex residual distributions. We therefore developed a parametric method to approach such distributions based on a finite mixture model. The inferred posterior distribution of the model parameters and the modelling error enables a good estimation of the statistical modelling uncertainty induced by the hydrological model.

The application of the modelling tool (including the basic design of the hydrological model) to the Mauvoisin hydropower plant showed that climate change would have a statistically significant negative impact on the hydropower production. This conclusion is based on the comparison of the simulated distributions of the hydropower production and several other performance indicators for a control period (1961 to 1990) to the corresponding distributions for a future period (2070 – 2099). At this time horizon, the median simulated decrease of hydropower production would correspond to 36 % compared to the simulated median production for the control period. This important reduction of the hydropower production is due to a significant decrease of the hydrological discharge and a modification of the hydrological regime. The control period is characterized by a glacier regime (maximum monthly discharge in July and August) whereas the future discharge corresponds to nival type (maximum monthly discharge in June).

The climate scenarios that induce this regime modification are characterized by a median increase of the daily mean temperature of 3.4 °C, about 0.8 °C more than the predicted median global-mean warming given by Wigley and Raper (2001). The 5 % respectively 95 % percentiles of the future temperature distribution correspond to an increase of 1.8 °C respectively 6.1 °C. The simulated median future annual precipitation corresponds to a decrease of 8 % compared to the simulated median value for the control period, the 5 %

percentile to a decrease of 21 % and the 95 % percentile of the future annual precipitation distribution corresponds to the median value for the control period. As a result, the median simulated glacier surface for the future period corresponds to 1.4 % of the total catchment area compared to 41 % for the control period.

The relative contribution of the different sources of modelling uncertainty on the overall discharge prediction uncertainty has been assessed. The prediction uncertainties induced respectively by the used hydrological model and the glacier surface evolution model on the mean annual discharge have been shown to be of the same order of magnitude. Both sources of modelling uncertainty contribute much less to the total prediction uncertainty than the uncertainties inherent in the climate evolution simulation. These uncertainties are due to the uncertain global-mean warming on one hand, to the regional climate response on the other. For the considered hydro-climatic area, the regional climate response has been shown to induce almost as much uncertainty on the future discharge prediction as the global-mean warming itself.

These results are conditional on the applied models and on the data used to develop and to drive them. The hydrological model plays a key role as it translates the meteorological input into water inflow into the hydropower production system. It intervenes at two levels in the system behaviour, namely in the simulation of the hydrological discharge and of the land cover evolution. The developed conceptual model for discharge simulation corresponds to a highly simplified representation of the natural processes. The related discharge prediction uncertainties have different origins, namely the used input and output data, the model parameter values and the model structure itself. This last source of uncertainty has not been assessed in the results presented so far.

The structure of a conceptual model is generally arbitrarily fixed based on some a priori knowledge. In rainfall-runoff modelling, the reservoirs and their connections are chosen according to previous modelling experience and their ability to reproduce the observed catchment response. We optimised several slightly different model structures in parallel and showed that they reproduce equally well the observed discharge for the calibration and the validation period. They lead however to quite different predictions of the system output for a future climate. This suggests that the inter-model variability of the discharge predictions is potentially higher than the modelling uncertainty inherent in each of them – even if the different model structures correspond to only slight variations of the basic model structure.

The different model structures have been optimised considering two objective functions. The used optimisation algorithm is a clustering evolutionary algorithm developed for energy system design (Leyland, 2002). It includes some features that are new in the context of hydrological modelling; in particular it can handle decision variables referring to the model structure and find and retain local optima. The identified model structures are equivalent for the calibration period in terms of the concept of multi-objective equivalence.

This points out that beside the model structural uncertainties, another important aspect should be included in the uncertainty analysis: The statistical uncertainty concept cannot be

considered as being complete in itself; it has to be assessed in parallel with the multi-objective equivalence concept. The statistical uncertainty concept is based on the paradigm that for a given model structure, a given data set and a given objective function there is a most probable parameter set and an associated parameter probability distribution. Hydrological model calibration is however a profoundly multi-objective problem where either several aspects of one model output or several model outputs have to be calibrated jointly. From a multi-objective point of view, there is no optimal parameter set because different objective functions have different optimal solutions. This uncertainty concept is particularly important in the presented hydrological modelling context where the hydrological model has to respect two generally antagonist calibration criteria: For the purposes of long term prediction it has to be unbiased and to be useful as an input into the management model it has to reproduce the hydrological regime.

Based on these considerations, the modelling uncertainty associated with the hydrological simulation of the system behaviour has - in a second step - been quantified considering the model structural uncertainties under the statistical and multi-objective uncertainty concepts. The question how to predict the model output distribution under the multi-objective equivalence concept has only been partially answered in hydrological modelling. We propose a method based on additional information coming either from additional data periods or from additional data types. The method is applied to the multi-model optimisation framework.

The estimated multi-objective model output distribution enables a consistent prediction of the multi-model uncertainty for different observed time periods whereas the statistical modelling uncertainty shows an important bias. For the future period, both approaches lead to a strongly bi-modal distribution of the mean annual discharge and the distribution for the control period lies in between the two modes. This results implies that we can predict that the system will be substantially modified but we cannot predict whether the mean annual discharge will increase or decrease. Note that it is of course possible that the true reaction of the system to the projected climate change is not contained in the prediction interval because neither of the models is able to give an unbiased estimate of the future solution.

9.3 Case study specificity of the methods and the results

The question how climate change affects the water resources and how uncertain the predictions are cannot be answered based on some general considerations but has to be investigated for a given case study. In the following we will shortly discuss how case study specific our methods and findings are and which general conclusions can be drawn.

Considering the model chain starting with the management model and ending with the generation of climate change scenarios, the model specificity decreases rapidly. The management model has been developed for the Mauvoisin case study. Its transferability to other case studies has not been considered during the model development. As the underlying

management strategies can be supposed to be comparable for most accumulation hydropower plants in the Alps, it could potentially be transferred.

The glacio-hydrological model can be applied to any other catchment governed by the same runoff formation processes. Its ability to reproduce the major runoff regime characteristics has been demonstrated for three different catchments in the Swiss Alps having different sizes, glaciation ratios and climatic conditions. The glacier evolution model is transferable to any valley glacier for which the necessary input data can be obtained. The used method for climate change scenario production is applicable to any region of the world provided that the necessary global circulation model and regional climate model outputs exist (see Hingray et al., 2005b, submitted manuscript[2] for an application to different case studies in Europe).

The methods for uncertainty quantification are specific to the different models. The ones developed for the estimation of the hydrological modelling uncertainty in a single model or multi-model framework are transferable to any calibrated hydrological model. Computational resources however still limit the use of Monte Carlo approaches highly demanding in terms of simulation time. The uncertainty assessment method has been developed specifically for the context of climate change impact studies. It can be transferred to any other hydrological modelling context asking for the quantification of the output prediction uncertainty (except for real time applications).

The specificity of the obtained results is also depending on the different modelling scales. The climate change impacts on the hydrological regime are highly case study specific. The system solicitation - the climate modification - can be supposed to be comparable at a larger scale covering a few grid cells of a regional climate simulation. The resulting impacts depend however on the system sensitivity that in return is conditioned by the present state, for example the hypsometry and ice cover of the catchment and the current temperature distribution and pluviometry. It is not possible to generalize the obtained results without simulation.

While the impact predictions cannot be extrapolated without any specific simulations, the obtained results referring to the modelling uncertainty are more general. We have shown that the regional response to a given global-mean warming induces almost as much uncertainty on the predicted system evolution as the global-mean warming itself. An analysis of the available regional climate model outputs for this study suggests that this result can be generalized to a larger Alpine area (see also Jasper et al., 2004). The glacio-hydrological prediction uncertainty is in return highly case study specific. Especially the relative importance of land cover evolution uncertainty and hydrological modelling uncertainty depends on the

[2] Hingray, B., Mezghani, A., Buishand, A.: Elaboration of regional climate change pdf's from uncertain global-mean warming and uncertain scaling relationship. Submitted to Hydrology and Earth System Sciences; hereinafter referred to as Hingray et al, 2005b, submitted manuscript.

hydrological context. The glacier surface evolution uncertainty decreases as a function of the global-mean warming. The hydrological modelling uncertainty depends on the catchment and on the quantity and quality of the observed data. For the present case study, the meteorological input data is highly uncertain inducing therefore an important total modelling uncertainty. This problem is well known in high mountainous areas and contributes partly to our inability to chose a unique best model structure.

9.4 Overall conclusions

The methods developed for the quantification of the different sources of modelling uncertainty enable a consistent estimation of the contribution of each modelling step to the overall prediction uncertainty. We have shown that the uncertainties induced by the prediction of the climate evolution are much higher than the ones induced by the management model, the glacio-hydrological and the land cover evolution model. It is however important to emphasize that this result is conditioned by the underlying modelling assumptions and especially by the used data on long-term climate projections, namely the global warming probability density function given by Wigley and Raper (2001) and the regional scaling relationships derived from the regional climate models according to the methodology presented by Hingray et al. (2005a, submitted manuscript).

This main conclusion corresponds to what could have been expected a priori (without any system modelling). The really interesting results are the following two:

1) The different regional climate responses related to predicted global climate changes induce nearly as much uncertainty on the future hydrological regime as the global-mean warming itself.

According to the results of Wigley and Raper (2001), the global-mean warming for the studied period 2070 to 2099 could range from +0°C to more than +9°C. This wide range translates how uncertain the evolution of the anthropogenic climate forcing and the corresponding climate simulations are. We showed however that the resulting uncertainty is only slightly higher than the one inherent in the regional climate responses simulated by different climate models. This result has the important implication that climate change impact studies should not only consider different greenhouse gas emission scenarios but especially the results for different regional and local scale climate models. Note that we have not considered two important sources of uncertainty associated with the prediction of a modification of the local scale climate: The production of the local scale time series and the natural variability of the system. For both problems, appropriate modelling techniques exist. The uncertainty induced by moving from the regional scale to the local scale could be investigated by different downscaling techniques (for a review, see Xu, 1999) and the natural variability by the application of a stochastic weather generator and analysis of the

corresponding results (for a review see Wilks and Wilby, 1999). The investigation of these two additional sources of uncertainty would in particular enable to consider extreme events that have not been tackled in the present research. Hydropower production has to deal with different problems related to extreme weather events such as extreme inflow conditions, catchment erosion and lake sedimentation.

2) Even though the climate projection induces much more uncertainty on the discharge prediction than the system behaviour itself, we cannot predict the direction of the associated system response.

The available data, the current discharge modelling techniques and the knowledge about the underlying processes are not sufficient to predict the response of the studied hydrological system to a potential long-term climate change. Even if we had perfect climate evolution predictions we would not be able to predict the direction of their impact (discharge increase or decrease) on the considered water resources system at the chosen time horizon. It is important to point out that this conclusion is to a large extend conditioned by the data availability for the model development but also for the input for future climate situations.

The historic data availability can only grow slowly and only for a small area of the entire Earth. There are a few high mountainous catchments that are studied intensively and for which more detailed data is available for model optimisation. For these catchments more complex models incorporating a maximum of currently available process knowledge can be set up. A detailed analysis of such experimental catchments could be beneficial for other less well-studied catchments but the spatial transfer of the corresponding models and results is still difficult especially in heterogeneous high mountainous catchments. Additionally, more complex models may require types of input data that are not easy to obtain for the future period even if climate models and their spatial resolution can be supposed to experience a fast progress in the next years.

There is an urgent need to develop methods that can be applied to real-world water resources management questions and hence to data scarce catchments. The turn to better investigated catchments as case studies should not be the only answer to the highlighted problem of unpredictability of the system evolution. This unpredictability is the conjunctional result of data availability, modelling techniques, process knowledge *and* the chosen temporal horizon. The period 2070 to 2099 has been chosen because for this period many climate model outputs are available. Additionally, such a long-term analysis is interesting because the analysed case study represents typically an area of long-term economic investments[3]. We believe however

[3] The investment horizon for large hydropower production systems in the Alps is around 20 to 50 years and the planned life cycle of a dam around 100 years. In Switzerland the hydropower concessions are delivered for 80 years. Most of Swiss dams have been constructed in the 1950ties and the concessions are to be renewed soon.

that the analysis of a less distant time period could enhance the predictability of the system reaction.

We finally would like to draw the attention to an important point referring to the case study. Hydropower production has been chosen as a case study because in the Alps, it represents an area of water resources management highly vulnerable to climate change. Our study has shown how important the impacts of the predicted modification of the hydrological regime on hydropower production could be for a glacier-fed accumulation hydropower plant. As pointed out at several times, the presented climate change impact analysis studies the modification of the glacio-hydrological system and does not assess other potential modifications of the water resources system. Over the considered time horizon, other system modifications are presumably much stronger than potential climate change; especially the annual distribution of the electricity demand could be considerably modified by the evolution of the population and of the economic and the politic context governing the electricity market, by technological progress and also by climate change. However, further investigation into the future hydropower offer (i.e. the water availability) is essential to compare the different sources of a potential management system modification.

9.5 Future research questions

We would first like to underline that climate change impact studies should be continued in any field of application and especially in hydrology. Impact analysis should not only be apprehended from the conventional viewpoint of anticipation of potential desirable or undesirable future system states to save costs in a wider sense. Instead, an important result of any impact analysis should be a better understanding of the system behaviour not only for the hypothetic future state but also for the current situation.

The prediction of a hypothetical future state based on conceptual hydrological models will always remain problematic. In the words of Kuczera (1982, p. 146) a “calibrated model can mimic observed runoff with almost embarrassing precision”. This statement expresses the fundamental problem of conceptual modelling: The models work well but it is difficult to show exactly why. In the present research different methods have been developed to determine how good the model output really is in mimicking the observations. But the quantification of the modelling uncertainty is never an aim in itself: In the present research context, the main underlying objective was to determine whether the predicted system modifications are statistically significant. The next step should be to use the gained insight into the model behaviour to analyse in detail the factors that influence the modelling uncertainty and how it could be reduced.

A better understanding of the model functioning and of the origin of the modelling errors should be a prerequisite to transposing the model in time. In fact, currently no modeller would be naïve enough to believe that a calibrated model is transposable in space without any

adaptation, why should it be in time? At best, we can hope that the estimated uncertainty intervals induced by the model structures and parameters contain the "true" solution. A rigorous evaluation would require proving the transposability. In the present research, the available historic data covers too short time periods to test the model for conditions comparable to the modifications expected by the human induced climate change. Further investigation into methods to test this temporal transposability is indispensable.

The large prediction intervals that result from the presented uncertainty analysis somehow augment our belief that the true system reaction is contained but this comes with the cost of producing "useless" results. The uncertainty inherent in the hydrological discharge predictions could be reduced by different means. Additional data could help to better constrain the hydrological model and therefore to decrease the number of potentially good models. We especially think of data referring to different internal variables of the model. A promising but costly approach is the use of aerial photographs to follow the depletion of the snow cover (see, e.g., Blöschl et al., 1991). The use of additional historic data could also help to improve the model structure allowing for example the model parameters to undergo a seasonal variation or to be connected to some observable state variables (for example the albedo of the snow cover).

If more detailed data becomes available, an interesting research question arises: How can the total model output uncertainty estimated by the presented methods be passed on the state variables (for example on the snow height)? This problem is rarely considered in uncertainty quantification approaches. It is however particularly important in applications where the state variables are used as an input into further models (as in the presented simulation tool where the accumulation area is used for land cover prediction).

The presented methods for uncertainty quantification open several interesting fields of research referring to model optimisation and uncertainty quantification. A first important issue is related to the Monte Carlo simulations. This approach is still highly if not too demanding in computational resources. Our hydrological model (implemented in Matlab) is semi-lumped and an entire model run including climate change scenario computation takes around 10 seconds for 30 years on a daily time step (on a personal computer with an Intel Pentium M processor 1500 MHz). Currently used distributed models can ask for much more computational resources. A possible solution to circumvent this problem would consist of so-called Quasi-Monte Carlo simulations. As far as we are aware, they are not yet applied in hydrological modelling but in many other computational problems (see, e.g., Fox, 1999; Niederreiter, 2004).

Quasi-Monte Carlo methods are based on the idea that - compared to a classical Monte Carlo approach - integral estimation convergence can be considerably fastened by the use of optimally placed integration points: The random numbers of a classical Monte Carlo simulation approach are replaced by quasirandom numbers. These are numbers selected from quasirandom sequences of n-tuples having the important property of being deterministically chosen to fill the n-space more uniformly than uncorrelated random points. The use of

quasirandom integration points will result in an error bound of the order of $(\ln N)^s/N$ (where s is the number of integral dimensions and N the sample size) rather than the usual $1/N^{0.5}$ of the standard Monte Carlo method. In sufficiently hard problems where N must be very large to obtain reasonable error bounds, quasi-Monte Carlo methods are thus to be preferred (e.g., Spanier, 1994). The inference of the posterior parameter distribution of hydrological models can be considered as being such a problem.

Another interesting research field refers to the multi-modality of posterior parameter distributions. For models with a highly complex response surface, the presented MCMC method only converges if the modeller has a good a priori knowledge of the optimal parameter space. The use of efficient optimisation algorithms helps reducing the simulation time by providing a rapid overview over good parameter sets that can be used as a starting point for the inference of the posterior parameter distributions. Another interesting approach for efficient inference of multi-modal parameter distributions is the use of so-called population Monte Carlo algorithms (for a rapid survey, see Iba, 2001) also known as particle filtering methods and including namely sequential Monte Carlo methods (see Doucet et al., 2001). These methods are based on the use of several "walkers" or "particles" representing a high-dimensional vector (in our case the model parameter vector) that evolve independently in the state space. Their weights are regularly updated and walkers with small weights are removed whereas walkers with heavy weights are split into multiple walkers. The method is somehow analogue to the principle of evolutionary algorithms; they are however designed for optimisation whereas the population Monte Carlo algorithms are intended to compute the product of matrices, integrals or marginal distributions (Iba, 2001). We especially think of further investigation of the annealed importance sampling technique presented by Neal (2001) that combines the strength of importance sampling and MCMC methods and that is closely related to population Monte Carlo algorithms.

The inference of posterior parameter distribution requires the definition of an appropriate residual modal. We proposed a method to approach complex hydrological residual distributions by a mixture of several normal distributions. The number of mixture components is determined a priori and the separation between the mixtures is based on a flow increase respectively decrease criterion. This raises two interesting areas of further investigation. First, it would be important to test whether such a separation method can be reasonably expected to be transposed to different time periods or whether the flow regime separation should be related to some other observable system states. We could for example use the temperature evolution as an indicator. Another interesting aspect is the identification of the a priori unknown number of mixture components (e.g., Wang and Fu, 2004). Such an approach seems promising for hydrological models as the resulting components could give additional insights into the model behaviour and the observational errors.

Another important issue related to the modelling uncertainty quantification is the explicit accounting for the various sources of model input uncertainties, especially the ones inherent in the elaboration of the model input series of precipitation and potential evapotranspiration. The uncertainty induced by the representativeness of the area average precipitation and the

rainfall patterns are subject to intense research (e.g., Obled et al., 1994; Chaubey et al., 1999; Brath et al., 2004). The question how the uncertainty inherent in the precipitation estimations could be explicitly quantified in a framework for the estimation of the output prediction uncertainty remains however essentially unanswered.

Many climate change impact studies unjustifiably neglect the uncertainty inherent in the estimation of potential and actual evapotranspiration (for an attempt to quantify it, see (Andreassian et al., 2004)). Evaporative processes represent an important water and energy flux between the Earth's surface and the atmosphere and their understanding and description should be part of the analyse of a hydrologic system as a whole (e.g., Parlange et al., 1995). For the studied hydrological system, evapotranspiration only represents a small component of the hydrological cycle for the observed periods but it can be supposed to become much more important for future periods. Its contribution to the total water balance is highly difficult to estimate as it is either considerably smaller or of the same order of magnitude as the error to be expected on the estimation of the area average precipitation. Additionally, the error committed on both components can be compensated by ice melt.

The prediction of future evapotranspiration is also closely related to the prediction of a potential land use change induced by climate change or other natural and anthropogenic processes. The presented hydrological model considers only two major land cover types for the present situation. As for example the tree line could be expected to undergo an altitudinal shift, additional land cover types should be included in the model. This however brings an important problem: How to include land use types that currently do not exist in the considered system? This problem could for example be approached by the use of regionalisation techniques (see, e.g., Hundecha and Bardossy, 2004).

The above considerations only cover a few aspects of emerging questions for future research into the prediction of the long-term evolution of hydrological systems. We believe that research into prediction uncertainty estimation has to be continued but not as a goal in itself but as a mean to identify lacks of current modelling techniques and additional needs of process knowledge and data.

References

Andreassian, V., Perrin, C. and Michel, C., 2004. Impact of imperfect potential evapotranspiration knowledge on the efficiency and parameters of watershed models. Journal of Hydrology, 286(1-4): 19-35.

Blöschl, G., Kirnbauer, R. and Gutknecht, D., 1991. Distributed snowmelt simulations in an Alpine catchment. 1. Model evaluation on the basis of snow cover patterns. Water Resources Research, 27(12): 3171-3179.

Brath, A., Montanari, A. and Toth, E., 2004. Analysis of the effects of different scenarios of historical data availability on the calibration of a spatially-distributed hydrological model. Journal of Hydrology, 291(3-4): 232-253.

Chaubey, I., Haan, C.T., Grunwald, S. and Salisbury, J.M., 1999. Uncertainty in the model parameters due to spatial variability of rainfall. Journal of Hydrology, 220(1-2): 48-61.

Doucet, A., de Freitas, N. and Gordon, N. (Editors), 2001. Sequential Monte Carlo methods in practice. Springer, New York, 581 pp.

Fox, B.L., 1999. Strategies for quasi-Monte Carlo. Kluwer, Boston, 368 pp.

Hundecha, Y. and Bardossy, A., 2004. Modeling of the effect of land use changes on the runoff generation of a river basin through parameter regionalization of a watershed model. Journal of Hydrology, 292(1-4): 281-295.

Iba, Y., 2001. Population Monte Carlo algorithms, Transactions of the Japanese Society for Artificial Intelligence, Vol 16, No. 2, pp. 279-286.

Jasper, K., Calanca, P., Gyalistras, D. and Fuhrer, J., 2004. Differential impacts of climate change on the hydrology of two alpine river basins. Climate Research, 26(2): 113-129.

Kuczera, G., 1982. On the relationship between the reliability of parameter estimates and hydrologic time-series data used in calibration. Water Resources Research, 18(1): 146-154.

Leyland, G.B., 2002. Multi-Objective Optimisation Applied to Industrial Energy Problems. Doctoral Thesis, Swiss Institute of Technology, Lausanne, Lausanne, 188 pp.

Neal, R.M., 2001. Annealed importance sampling. Statistics and Computing, 11: 125-139.

Niederreiter, H. (Editor), 2004. Monte Carlo and Quasi-Monte Carlo methods 2002 : proceedings of a conference held at the National University of Singapore, Republic of Singapore, November 25-28, 2002. Springer, Berlin, 459 pp.

Obled, C., Wendling, J. and Beven, K., 1994. The sensitivity of hydrological models to spatial rainfall patterns - an evaluation using observed data. Journal of Hydrology, 159(1-4): 305-333.

Parlange, M.B., Eichinger, W.E. and Albertson, J.D., 1995. Regional-scale evaporation and the atmospheric boundary layer. Reviews of Geophysics, 33(1): 99-124.

Spanier, J., 1994. Quasi-MonteCarlo methods for aprticla transport problems. In: H. Niederreiter and P. Jau-Shyong Shiue (Editors), Monte Carlo and Quasi-Monte Carlo Methods in scientific Computing. Springer, University of Nevada, Las Vegas, USA, pp. 121-148.

Wang, L. and Fu, J.C., 2004. A practical sampling approach for Bayesian mixture model with unknown number of components, Department of Statistics, University of Manitoba.

Wigley, T.M.L. and Raper, S.C.B., 2001. Interpretation of High Projections for Global-Mean Warming. Science, 293(5529): 451-454.

Wilks, D.S. and Wilby, R.L., 1999. The weather generation game: Review of stochastic weather models. Progress in Physical Geography, 23(3): 329-357.

Xu, C.Y., 1999. From GCMs to river flow: a review of downscaling methods and hydrologic modelling approaches. Progress in Physical Geography, 23(2): 229-249.

Bettina Schaefli

Born on the 13th October 1976 in Aarau, Switzerland

Swiss citizen

Education

May 02 – April 05:	PhD student at the Laboratory of Hydrology and Land Improvement, Swiss Institute of Technology, Lausanne (EPFL)
	Title PhD-thesis: "Quantification of modelling uncertainties in climate change impact studies on water resources: Application to a glacier-fed hydropower production system in the Swiss Alps"
	Supervisor: Prof. A. Musy
Sept. 04 – Feb. 05	Research stay in the group of Prof. A. Bárdossy at the Institute of Hydraulic Engineering of the University of Stuttgart. *Fellowship of the Swiss National Science Foundation*
Oct. 96 – March 01	Master in Environmental Engineering, EPFL; master thesis in the area of land management in a developing country (Senegal)
	Award for best results at final exams and final research project

Professional Activities

May 01 - present	Research and teaching assistant including undergraduate and graduate teaching activities at the Laboratory of Hydrology and Land Improvement, EPFL
July 99 – Aug. 99	Training at the engineering office *Hydec* in Kuala Lumpur (Malaysia); development of a geographic information system for the analysis of soil erosion potential

Committees

Jan. 02 – present	Member of the Faculty Council of the School of Architecture, Civil and Environmental Engineering, EPFL
Oct. 96 – March 01	Member of the Department Council and the teaching commission of the Department of Rural Engineering, EPFL

Refereed publications

Schaefli, B., Hingray, B. and Musy, A., 2004. Improved calibration of hydrological models: use of a multi-objective evolutionary algorithm for parameter and model structure uncertainty estimation. In B. Webb: Hydrology: Science and Practice for the 21st Century. British Hydrological Society, London, p. 362 – 371

Schaefli B., Hingray B., Musy A., 2005. Climate change impacts on hydropower production in the Swiss Alps (accepted for publication in Hydrology and Earth System Sciences)

Schaefli, B., Hingray, B. and Musy, A., 2005. A conceptual glacio-hydrological model for high mountainous catchments. Hydrology and Earth System Sciences Discussions

Contributions to conferences & seminars

Schaefli B, Hingray B., Niggli M., Musy A., 2003a. Management of an alpine hydrological system - performance under uncertain climate change. International Workshop on Mountain Hydrology, Einsiedeln, Switzerland, 02-04 April 2003. Abstract

Schaefli B, Hingray B., Niggli M., Musy A., 2003b. Climate change impacts on a highly glacierized alpine catchment and implications for the hydropower production in the Swiss Alps. EGS - AGU - EUG Joint Assembly, Nice, France, 6 - 11 April 2003, abstract EAE03-A-01109

Schaefli B, Hingray B., Musy A., 2004a. Climate Change Impacts on Highly Glacierized Catchments in the Swiss Alps. Research seminar at the Section of Glaciology, ETH Zürich, 18. April 2004

Schaefli B, Hingray B., Musy A., 2004b. Use of the Metropolis-Hastings Algorithm for the quantification of the hydrological modelling uncertainty in climate change impact studies. EGU 1st General Assembly Nice, France, 25 - 30 April 2004, abstract EGU04-A-06322

Schaefli B, Hingray B., Musy A., 2004c. Improved calibration of hydrological models: use of a multi-objective evolutionary algorithm for parameter and model structure uncertainty estimation, BHS2004, Hydrology: Science and Practice for the 21st Century. London, 12 – 16 July 2004

Languages

German:	Mother tongue
French:	Very well spoken & written (bilingual)
English:	Very well spoken & written
Spanish:	Well spoken

Contact

bettina.schaefli@a3.epfl.ch